S. Colbeck

12

SIPRE REPORT 17

PREPARED FOR
SNOW, ICE AND PERMAFROST RESEARCH ESTABLISHMENT (SIPRE)
CORPS OF ENGINEERS, U. S. ARMY

Friction on Snow and Ice

JUNE, 1955

UNIVERSITY OF MINNESOTA
INSTITUTE OF TECHNOLOGY
MECHANICAL ENGINEERING DEPARTMENT

Mechanical Engineering Department
Institute of Technology
University of Minnesota

FRICTION ON SNOW AND ICE

Department of the Army Project 8-66-02-001 (DA-11-190-ENG-1),
Research for Investigating the Friction on Snow.

University of Minnesota
James L. Morrill, President
Institute of Technology
Athelstan F. Spilhaus, Dean
Mechanical Engineering Department
Richard C. Jordan, Head

Project Personnel

C. D. Fitz, Ph.D.
W. H. Ito, Ph.D.
H. T. Mantis, Ph.D.
G. W. McElrath, M.S.
R. G. Mokadam, Ph.D.
H. E. Staph, M.S.
W. C. Stolov, M.A.
K. P. Synestvedt, M.S.M.E.
R. C. Jordan, (Director); Ph.D.

Minneapolis, Minnesota
June, 1955

TABLE OF CONTENTS

PREFACE

This is a report of the work resulting from researches on snow and ice sponsored by the Snow, Ice and Permafrost Research Establishment of the U. S. Army Corps of Engineers in contract with the Mechanical Engineering Department of the University of Minnesota. The initial contract was begun in August 1951 and the first progress report issued in July 1952. A renewal of the contract was effected in August of that year and the second progress report issued in July 1953. A third progress report was issued in August 1954. This report is a summary of the work reported earlier together with additional information forthcoming during the past year. Although the work is far from complete this must be regarded as a final report on the current phases of the activity.

A number of persons in the Department of Mechanical Engineering have contributed to the work. Dr. Dudley Fitz, recently aided by Professor Horace Staph has been in charge of the experimental activities and together they have accomplished the major portion of the work.

Dr. Homer T. Mantis has provided valuable consultation and advice in the direction of the activities. Professor Gayle McElrath and Dr. Wallace H. Ito have directed the statistical analyses.

Mr. Walter Stolov has prosecuted the researches on electrical impedance measurement of contact area and has prepared that chapter of this report. Particularly among the students who have aided in prosecution of the experimental activities we wish to mention Mr. Verdis Erickson and Mr. Edward Zoerb.

University of Minnesota
June, 1955

Richard C. Jordan
Project Director

ABSTRACT

Frictional resistance on ice and snow was examined in terms of current frictional theories. It was concluded that a liquidlike film of some type exists or is formed on the ice surface. The basic mechanism forming this film is either the frictional heating mechanism suggested by Bowden, or is electrical in nature as suggested by Weyl.

A "Stick-Slip" friction measuring apparatus was constructed and its vibratory characteristics analyzed. Experimental measurements were made of the static and kinetic friction under various conditions of load, apparent area, slider material, temperature, humidity, time of stationary contact, and carriage velocity. Statistical analysis of experimental data indicated that time of stationary contact, temperature, humidity, apparent area and material characteristics had significant influence upon the frictional resistance. Within the range of carriage velocities investigated, the magnitude of the velocity had no appreciable influence on the kinetic friction.

Oscillographs taken of the intermittent stick-slip motion of sliders on ice provided the basis for certain deductions regarding the influence of time on frictional resistance. It was concluded that merely bringing a slider momentarily to rest is not sufficient to obtain static friction. A short but finite period of time is required to obtain static friction, the frictional resistance rising to very high values (freezedown) following fairly long periods of stationary contact.

Measurements of the electrical resistance and capacitance between a slider and an electrode frozen within the ice provided information regarding the contact area characteristics.

Radioactive studies of the frictional process indicated a maximum transfer of ice to slider during the stick portion of the stick-slip motion.

CHAPTER I

THEORY OF FRICTION ON COMPACTED SNOW

Chapter I

Theory of Friction on Compacted Snow

The experimental relations known as the classical laws of dry friction have been known for several hundred years. (Historical development of the classical laws is briefly described in Appendix A of this report.) These classical laws as stated by Coulomb are:

1. Frictional force for a constant load is independent of the apparent area of contact.
2. Frictional force is directly proportional to the load, that is, to the total force which acts normal to the sliding surface.
3. Static friction force differs from kinetic friction force; however, the kinetic friction is independent of the velocity of the slider.
4. Frictional force depends upon the nature of the materials in contact.

The second of these classical laws of dry friction may be expressed mathematically as:

$$F = \mu N \qquad (1\text{-}1)$$

where:

F = Frictional force

N = Normal load

μ = Coefficient of Friction

A subscript is often added to the symbol for the coefficient of friction to indicate the distinction between the static coefficient and the kinetic coefficient, i.e. μ_s and μ_k. These static and kinetic coefficients according to Law Four are dependent upon the nature of the materials in contact, but (Law One) are independent of the apparent area of contact.

The characteristics of hydrodynamic friction, on the other hand, are quite different. In many cases it is exactly opposite to the characteristics of dry friction. For a Newtonian fluid the force of resistance is related to the apparent area of contact, the velocity gradient, and to the viscosity according to the equation:

$$F = m A \frac{dv}{dx} \qquad (1\text{-}2)$$

where:

F = Tangential Resistance Force

m = Absolute viscosity

A = Apparent contact area

$\frac{dv}{dx}$ = Velocity gradient

The relations expressed by equations 1-1 and 1-2 would seem to indicate that the determination of the type of frictional resistance for any particular case should be comparatively simple. Measurement of the frictional force and its variation with load, apparent area, and velocity should enable the distinction between dry and fluid friction. These criteria have been applied to friction on ice. Experimental measurements do indicate that the frictional force is nearly a linear function of the load, and related to the materials of the two surfaces. The variation

of frictional force with apparent area and velocity is very small. These several relations indicate that friction of materials on ice is primarily of the dry friction variety.

Let us examine further therefore the basic mechanism of dry friction. This mechanism is undoubtedly related to the presence of asperities on the surface. Several theories have been proposed to explain this relationship. According to the so-called surface roughness theory the asperities are considered to be rigid with an average slope angle equal to Θ. The applied tangential force supposedly has a component parallel to the slope which is sufficient to lift the normal load over the rigid asperities by the relation:[1]

$$F \cos \Theta = N \sin \Theta \qquad (1\text{-}3)$$

thus:

$$\mu = \frac{F}{N} = \tan \Theta \qquad (1\text{-}4)$$

Hardy[2] pointed out in 1920 that the lifting mechanism cannot be the principal mechanism of frictional resistance since in experiments with flat clean metal surfaces friction appears practically independent of the surface roughness. Adhesion, he concluded, must be the dominant force of friction. Prandtl[3] in 1928 and Tomlinson[4] in 1929 formulated theories

---

[1] Bikerman, J. J. (1944) "Surface Roughness and Sliding Friction," Rev. Mod. Phys., Vol. 16, No. 2, pp. 53-68.

[2] Hardy, W. B. (1920) "Some Problems of Lubrication," Nature, Vol. 106, pp. 569-72.

[3] Prandtl, L. (1928) "Ein Gedankenmodell zur kinetschen Theorie der festen Korper," Z. angew. Math. und Mech., Vol. 8, pp. 85-106.

[4] Tomlinson, G. A. (1929) "A Molecular Theory of Friction," Phil. Mag., Vol. 7, pp. 905-39.

on the molecular forces causing an adhesive resistance to motion. Credit is generally given to Holm,[5,6] however, for the development of a reasonable theory of frictional resistance based on surface adhesion. Although Coulomb had considered the possibility of adhesion as a frictional mechanism, he believed that the adhesion would act over the entire surface area and therefore the frictional resistance would be proportional to the apparent area. Since this result contradicts Amonton's First Law of Friction regarding the independence of frictional force from area, Coulomb concluded that adhesion was not the source of friction.

Holm has suggested on the other hand that the adhesive force acts only over the real area of contact. As will be shown in the analysis of Chapter 2 this actual or real area of contact between a sliding body and a stationary surface composed of a single material is a function of the normal load applied. This relation may be expressed by the equation:

$$A_r = \frac{N}{p_m} \qquad (1\text{-}5)$$

in which:

A_r = Real Contact Area

N = Normal Load

p_m = Plastic mean flow pressure of the softest material.

The tangential resistive force or the friction force by Holm's Adhesion Theory equals the product of the shear stress in the contact

---

[5] Holm, R. (1938) "Uber die auf die wirkliche Beruhrungsflache bezogene Reibungskraft," Wiss. Veroff. Siemens-Werk, Vol. 17, No. 4, p. 38

[6] Holm, R. (1946) Electric Contacts, Hugo Gebers, Forlag, Stockholm, p. 203.

region times the real area of contact.

$$F = s\, A_r \tag{1-6}$$

in which:

F = Resistance or Frictional Force

A_r = Real Contact Area

s = Shear stress of weaker material

Substituting the expression for the real contact area Equation (1-5) in Equation (1-6) leads to :

$$F = s \frac{N}{p_m} \tag{1-7}$$

According to Equation 1-7 there is a linear relationship between the friction force and normal load. Thus Amonton's Second Law is obeyed by the postulated adhesion mechanism. The coefficient of friction may be derived from Equations 1-1 and 1-7 as:

$$\mu = \frac{F}{N} = \frac{s}{p_m} \tag{1-8}$$

Equation 1-8 indicates that the coefficient of friction is a function of the shear strength and the mean flow pressure and consequently to any other factor which may affect these properties.

The shear strength, s, may either be the adhesive strength between the dissimilar materials at the contact surface or it may be the cohesive strength in the interior of the weaker material. The latter concept in which s is regarded as a bulk property of the weaker material is accepted by most investigators. The mean flow pressure as previously indicated is also a bulk property of the weaker material.

McFarlane and Tabor[7] have pointed out that both s and p_m are related to the strength of the material generally expressed in terms of the tensile yield point Y.

$$f(s, p_m, Y) = 0 \qquad (1\text{-}9)$$

Thus if the functional relation of s, p_m, and Y were known for the weaker material of two surfaces in contact, the calculation of the frictional resistance should be a determinant problem. The desired functional relationship for various materials has not as yet been determined. Equations 1-8 and 1-9 however, do offer an explanation for Friction Law Four regarding the dependence of frictional force upon the nature of the materials in contact.

Factors which influence the bulk strength properties will also influence the coefficient of friction. Two factors which are well-known to affect the strength are temperature and time. The influence of temperature was recently investigated by Simon, McMahon, and Bowen.[8] These investigators reasoned that the temperature variation of the coefficient of friction should be a critical test between the surface roughness and adhesion theories. Since the geometric slope of the asperities is independent of the temperature there should be no friction change with temperature according to the surface roughness hypothesis.

---

[7] McFarlane, J. S., and D. Tabor, (1950) "Relation between Friction and Adhesion," Proc. Roy. Soc., Vol. A 202, pp. 244-53.

[8] Simon, I., H. O. McMahon, and R. J. Bowen, (1951) "Dry Metallic Friction as a Function of Temperature between 4.2° K and 600° K," J. Appl. Phys., Vol. 22, No. 2, pp. 177-84.

However, since both s and p_m are temperature sensitive, a temperature variation of the coefficient of friction would be expected by the adhesion theory. Experimental measurements indicated that the temperature variation was very similar to the ratio of the variations of s and p_m. Thus the temperature variation tended to substantiate the adhesion theory. A third factor, the triaxial stress ratio, has been shown by Bridgeman[9] and McAdam[10] to affect the tensile yield point Y and must therefore also influence s and p_m. This would indicate an effect caused by load upon the coefficient of friction.

The situation previously described was based on the assumption of contact between two surfaces having at the most only two types of material present. In many cases, however, there exists a third type of material or another phase of one of the materials in the region of interest. This third material may have considerable influence on the friction characteristics of the system. Several possible arrangements of the three materials present themselves, the two most obvious being a series arrangement and a parallel arrangement.

Let us consider the case in which a thin layer of a third material completely separates the sliding body from the stationary surface. In this situation which may be considered as a series arrangement the third material if more plastic than the other two generally serves as a lubricant to decrease the frictional resistance.

---

[9] Bridgeman, P. W. (1939) "Considerations on Rupture under Triaxial Stress," Mech. Eng., Vol. 61, pp. 107-111.

[10] McAdam, D. J., Jr. (1944) "The Technical Cohesive Strength of Metals in Terms of the Principal Stresses," Metals Tech., TP 1782.

Bowden and Tabor[11] have shown that in the separation of two hard metals by a thin layer of a soft metal, both the real area of contact and the shear stress are low. The soft intermediate material transmits the load to the substrate of hard material which carries the entire load on its asperities with only a small deformation and therefore a small area of support. Although the pressure in the soft material separating the support points may increase, the material does not necessarily rupture and allow direct contact between the harder materials. The resistance of this intermediate material to a tangential force is generally low, resulting in a low shear stress. Thus the desirable characteristics of a small shear stress are obtained. The influence of this intermediate film upon the contact area and the shear stress is a function of the film thickness. As the thickness increases the effective area of contact becomes greater as more of the load is supported by the soft material in the region surrounding the hard substrata asperities. On the other hand for thicknesses too low the film tends to breakdown allowing direct contact between the two principle materials and with this action an increase in the shear strength. As a result of these two opposing influences an optimum film thickness exists above which the contact area increases and below which the effective shear stress increases. A similar optimum load has been shown to exist with breakdown of the intermediate film occurring for excessive load and a large bearing area on the soft film for low loads. These relations are seen to closely correspond with the recognized characteristics of boundary lubrication.

---

[11] Bowden, F. P. and D. Tabor (1950) The Friction and Lubrication of Solids, Oxford Clarendon Press, pp. 111-113.

It is not always necessary, however, to introduce a liquid or soft solid film into the sliding region to obtain this low friction characteristic. As Bisson[12] has recently demonstrated, it is often possible to obtain an internally created film in the form of oxides or sulfides which produce the desired characteristics and which are also self-repairing. The creation of beneficial oxides on the cylinder walls of an automobile while breaking the automobile in at low speeds is one such example of self-created and self-repairing films.

On the other hand, if a third material as hard as, or harder than, the two principal materials is present, this third material may bite into the interior regions of the slider and the stationary surface, and may appreciably increase the shear strength. Contact area may also be increased by this action. Total result is an increase in the frictional resistance. As an example of this effect, one might consider the action of a hard abrasive in a journal.

Another possible arrangement of the three materials under consideration is a parallel arrangement in which the third material only partially separates the slider and stationary surface. This situation is the condition mentioned above when considering boundary lubrication breakdown of the separating film by decreasing the film thickness or increasing the load. In the resulting parallel arrangement the total normal load is partially supported by the third material and partially by direct contact between the two principal materials. Each load-supporting method

---

[12] Bisson, E. E. "The Influence of Solid Surface Films on the Friction and Surface Damage of Steel at High Sliding Velocities," Lubrication Engineering, Vol. 9, No. 2, April, 1953, pp. 75-77.

will have an effective contact area. This situation may be expressed by the equation:

$$N = A_{r1} p_{m1} + A_{r2} p_{m2} \qquad (1\text{-}10)$$

The frictional resistance by this arrangement may also be expressed as:

$$F = A_{r1} s_1 + A_{r2} s_2 \qquad (1\text{-}11)$$

The coefficient of friction would equal then:

$$\mu = \frac{A_{r1} s_1 + A_{r2} s_2}{A_{r1} p_{m1} + A_{r2} p_{m2}} \qquad (1\text{-}12)$$

It is therefore necessary to know the distribution of the load over the two contact areas in order to determine the total frictional resistance and the coefficient of friction. This load distribution is undoubtedly related to the relative hardness of the material as well as to the time, temperature, and loading characteristics of the materials' plasticity.

In many cases the load distribution or the relative magnitude of the two contact areas appears to be uncontrolled. This results in completely erratic frictional resistance. Tomlinson[13] noted this situation in the sliding of glass over glass with a castor oil lubricant and attributed the erratic friction to the uncontrolled load distribution between the lubricant and direct glass to glass contacts.

It has also been proposed that welding or adhesion occurs only over a fraction k of the real area of contact of the two principal materials.[14] Under this assumption the friction force may be expressed as:

$$F = ks\, A_r \qquad (1\text{-}13)$$

---

[13] Tomlinson, G. A. (1927) "Rusting of Steel Surfaces in Contact," Proc. Roy. Soc., Vol. A 115, pp. 472-83.

[14] Finnie, I., and M. C. Shaw (1954) The Friction Process in Metal Cutting, presented at the Annual Meeting of the American Society of Mechanical Engineers, New York, Nov. 1954, ASME Paper No. 54 - A - 108, p. 3.

and the coefficient of friction as:

$$\mu = \frac{k_s A_r}{p_m A_r} = \frac{k_s}{p_m} \qquad (1\text{-}14)$$

In addition to the frictional resistance created by adhesion, resistance to sliding is also encountered from the so called plowing effect. The resistance to relative motion obtained by this effect is undoubtedly caused by the frontal resistance to plastic deformation of the softer of the two surface materials. Such deformation can either be the small scale scratching created by the microscopic asperities separating nominally mating surfaces or large scale grooving as the softer material packs or flows laterally before the forward edge of a macroscopic indenter (non-mating surfaces.)

The total plowing force must equal the area of the cross section of the grooved track A' multiplied by the mean pressure, p', required to displace the material in the surface.[15]

$$F_p = A' \, p' \qquad (1\text{-}15)$$

The molecular mechanism of adhesive frictional resistance is considered to be caused by mutual attraction of atoms in the two surfaces. This attraction disturbs the neutral position or interatomic distances of the atoms in the surfaces as specified by the Morse Potential relations. Tomlinson suggests that as the atoms of the two surfaces are moved relative to each other that their mutual attraction further distorts their position. These atoms finally must choose between two force fields, the field of their original surface or the field of the opposite surface. If an atom chooses the field of the opposite surface, it may be completely transferred or it may be disengaged as a wear particle. If it chooses

---

[15] Bowden, F. P., and D. Tabor (1950) op. cit., p. 91.

to remain in its former surface, it will snap back and vibrate around its neutral position. In either case vibrational or thermal energy is created at the expense of mechanical energy.

Feng[16] has recently suggested that adhesive friction also involves mechanical interlocking in its basic mechanism. Such interlocking should have the same influence mathematically as the more conventional adhesion.

Let us next consider the application of the general theory of friction to the case of friction on ice, the end point of compacted snow. First let us examine Equation 1-8 which states that the coefficient of friction should equal the ratio of the shear stress to the plastic mean flow pressure. Values of the shear strength of ice as found by several investigators were collected and presented in the Review of Properties of Snow and Ice.[17] These include:

	Shear Strength--lb/in^2	
Experimenter	Approx. Average	Variation
Pineghin (Weinberg 1938)	100	88-117
Finlayson (1927)	110	91-115
Wilson and Horeth (1948)	95	75-115

Since 1 lb/in^2 = 70.4 gr/cm^2, a shear strength of 100 lb/in^2 will equal 7040 gr/cm^2 in the cgs system.

Smith-Johannsen[18] has since made further measurements of the shear strength between ice and certain plastics. These measurements indicate a shear strength in the order of 2000 gr/cm^2.

---

16 Feng, I. M. (1952) "Metal Transfer and Wear," J. Appl Phys., Vol. 23, p. 1011.

17 University of Minnesota, Institute of Technology, Engineering Experimental Station, July, 1951, "Review of Properties of Snow and Ice," SIPRE Report 4, Snow, Ice, and Permafrost Res. Est., Corps of Eng., U. S. Army, p. 24.

18 Smith-Johannsen, R., (1951) "Surfaces having Low adhesion to Ice," U. S. Patent No. 2,575,141.

Values of the plastic mean flow pressure may be interpreted from other data. The mean flow pressure is often taken as equal to 1.1Y where Y is the yield stress or proportional limit of the material. In the case of ice the elastic limit has been reported[19] as lying between 7 to 14 lb/in^2, or 490 to 980 gm/cm^2. Weinberg[20] reports that Fabian[21] had measured the elastic limit of ice as 500 gm/cm^2 and Pfaff[22] had found a value of 900 gm/cm^2. Thus the mean flow pressure from these measurements should vary from 550 gm/cm^2 to 1000 gm/cm^2.

Another method of determining the plastic mean flow pressure is through data on the viscosity of the material. From measurements of the viscosity of ice Weinberg[20] found as limiting figures to apply in Schwedoff's law of relaxation the quantities:

$$\lambda = 570 \text{ gm/cm}^2 \text{ Neva River Ice}$$

$$\lambda = 90 \text{ gm/cm}^2 \text{ Glacier Ice}$$

If from the above measurement data a shear strength of 7000 gr/cm^2 and a mean flow pressure equal to 700 gr/cm^2 are taken, the coefficient of friction on ice should equal approximately:

$$\mu = \frac{s}{p_m} \approx \frac{7000}{700} = 10 \qquad (1\text{-}17)$$

This calculated value of the coefficient of friction is much higher than experimentally obtained values. The low actual values of friction

---

19 University of Minnesota, op. cit., Review of Properties of Snow and Ice, p. 28.

20 Weinberg, B. (1938) "Mechanical Properties of Ice," Trans. of the Internat. Comm. of Snow and Glaciers, Internat. Assoc. of Scientific Hydrology, Bull. No. 23, Riga, pp. 509-36.

21 Fabian, O. (1877) "Über Dehnbarkert und Elastizitat des Eises", Carl's Report d Phys.,Vol. 13, pp. 447 - 452.

22 Pfaff, F. (1875) "Versuche über die plastizitat des Eises," Ann. d Phys., Vol. 155, pp. 169-174.

on ice might be interpreted as indicating errors in the measurement of the shear stress and mean flow pressure. It could also be interpreted as indicating the presence of a modifying influence such as a third lubricating material or a low proportion of adhesive welds at the junctions.

The concept of an intervening lubricant as the principal cause of low friction on ice and snow is by no means a new idea. It was surmised for many years that liquid water was probably formed at the interface of a slider on snow and ice to provide the necessary lubrication for low friction. The mechanism by which this water was formed or converted from ice was not easily explained however.

In the mid 1800's James and William Thomson presented a number of papers[23-27] regarding the possibility of ice melting due to the lowering of the melting temperature by the application of pressure. This mechanism they suggested enabled the explanation of a number of

---

[23] Thomson, J. (1849) "Theoretical Considerations on the Effect of Pressure in Lowering the Freezing Point of Water," Trans. Roy. Soc. of Edinburgh, Vol. 16, pp. 575-580.

[24] Thomson, W. (1850) "The Effect of Pressure in Lowering the Freezing Point of Water Experimentally Demonstrated," Phil. Mag. Vol. 37, pp. 123-127.

[25] Thomson, J. (1857) "On the Plasticity of Ice as Manifested in Glaciers," Proc. Roy. Soc. (London), Vol. 8, pp. 455-458.

[26] Thomson, W. (1858), "Remarks on the Interior Melting of Ice," Proc. Roy. Soc. (London), Vol. 9, pp. 141-143.

[27] Thomson, J. (1859) "On Recent Theories and Experiments Regarding Ice at or Near its Melting Point," Proc. Roy. Soc. (London), Vol. 10, pp. 152-160.

phemonenon including the flow of glaciers and the occurrence of blue lines in glacial ice.

In 1886 J. Joly[28] suggested that the low friction obtained in ice skating could be explained by Thomsons' concept of melting temperature reduction under pressure. This lower melting temperature would result in melting of a thin layer of liquid water serving as a lubricant. O. Reynolds[29] who proposed essentially the same idea in 1901 is usually credited with the "Pressure Melting" theory of low ice friction. Reynolds supported this theory by noting that several investigators had experimentally found a decrease in the slipperiness of ice at low temperatures. This fact was interpreted by Reynolds as indicating insufficient pressure available to lower the melting temperature to the low ambient temperature.

On the other hand if one examines the phenomenon quantitatively, it will be noted that approximately 100 atmospheres of pressure are required to lower the melting temperature by 1°C. Furthermore low friction conditions are obtained for a considerable temperature differential below the melting point. The tremendous pressure necessary to supply this melting temperature depression places the pressure melting mechanism in doubt as the chief source of lubricant supply.

---

28 Joly, J. (1886) "The Phenomenon of Skating and Professor J. Thomson's Thermodynamic Relation," Proc. Roy. Dublin Soc. Vol. 5, pp. 453-454.

29 Reynolds, O. (1901) "On the Slipperiness of Ice," Papers on Mechanical and Physical Subjects. Cambridge, University Press, Vol. II, pp. 734-738.

F. P. Bowden and T. P. Hughes[30] were apparently the first to note the extreme pressures necessary to fulfill the pressure melting hypothesis. They agreed however that liquid water must be the lubricant involved and suggested that this liquid is formed by frictional heating of the ice-slider interface. Depending upon the relative thermal conductivity of the slider and ice, part of the frictional heat is lost to the slider and part is used in melting ice or snow crystals. Thus, theoretically, the coefficient of friction between brass and ice should be greater than that between ebonite and ice, since brass with the higher thermal conductivity will conduct away more heat than ebonite, leaving less heat to melt the ice. Bowden and Hughes showed experimentally that ebonite did have a lower frictional resistance than brass as suggested by the theory.

G. J. Klein[31] supported the frictional melting theory as the means of providing water lubrication. Using a ski having a glass window in the bottom he experimentally studied the surface conditions while drawing the ski over snow. It was noted that the snow contacted the ski bottom at a number of small areas, each enclosed in a drop of water. The total area of contact for a unit loading of 200 lbs per sq ft was in the order of 20% and for 500 lbs per sq ft in the order of 50%. Klein further suggested that the total tangential resistance to motion was composed of the following:

---

30 Bowden, F. P., and T. P. Hughes. (1939) "The Mechanism of Sliding on Ice and Snow," Proc. Roy. Soc., Vol. A 172, pp. 280-298.

31 Klein, G. J. (1947) "The Snow Characteristics of Aircraft Skis," Nat'l Res. Council of Canada Div. of Mech Eng. Aero Rep. 2, Ottawa, 19 pp.

(a). Solid friction (resistance between solid phases) most of which occurs at the bow of a ski.

(b). Viscous resistance due to shearing in the thin film of water.

(c). Resistance due to surface tension effects.

As evidence of the surface tension resistance Klein noted that the angle of contact of the water drops to the ski bottom material was greater on the leading side than on the trailing side. This difference in contact angle evidently indicated the presence of a tangential force component.

Another Canadian investigator, Pfalzner,[32] reasoned however, that if heat from frictional action created a lubricating fluid film, direct heating of sliding runners would facilitate melting and further reduce friction. His experimental results did not indicate the expected frictional reduction and cast doubt on the friction melting theory.

Bell[33] also questioned the pressure melting and the frictional melting theories. His calculations, using skate runner data, indicated the necessity for an extremely high thermal conductivity to transfer kinetic heat from the rear of a runner to the supposed melting region at the front of the runner. Bell proposed instead a plastic flow theory in which pressure and frictional heat cause increased plasticity of the solid ice surface, rather than a complete phase change to liquid. Low resistance to motion by the plastic substance would result in a low

---

32 Pfalzner, P. M. (1947) "The Friction of Heated Sleigh Runners on Ice," Can. J. of Research, Vol. F 25, pp. 192-5, N.R.C. No. 1510.

33 Bell, A. E. (1948) "Theory of Skating," Nature, Vol. 161, pp. 391-2.

friction coefficient.

T. H. McConica[34-35] has also pointed out practical and theoretical objections to the frictional melting theory. He found that a bare magnesium ski surface was faster; i.e., had less friction, than well lacquered wood at temperatures substantially below the melting point, although the thermal conductivity of the magnesium was much higher than that of the wood. McConica conducted an extensive experimental study of the resisting frictional force of several types of sliders on ice. His experimental findings indicated, among other things, the presence of critical values of loading and velocity. Based on these experimental results and certain theoretical considerations McConica proposed that lubrication must occur through some fluid film on the ice surface which was not water, but more likely an absorbed transient layer of "water vapor".

The concept of a fluid film on an ice surface at temperatures below the melting point is also an old idea. Faraday[36-37] in 1842 had postulated the existence of such a fluid boundary region on an ice surface as the basis of the phenomenon of regelation. Considerable discussion

---

34 McConica, T. H. (1950) "Sliding on Ice and Snow," American Ski Company Report to the Research and Development Division, Office of Quartermaster General, U.S. Army, Under Contract W. 44-109-Q.M.-2113 (Mimeographed). 46 pp.

35 McConica, T. H. (1951) "Aircraft Ski Performance," American Ski Company Report, WADC Tr 52-19.

36 Faraday, M. (1933) Faraday's Diary. Bell and Sons, Ltd. London, Vol. IV p. 79.

37 Faraday, M. (1860) "Note on Regelation," Proc. Roy. Soc. London Vol. 10, pp. 440-450.

was aroused by Faraday's suggestions, particularly in connection with the thermodynamics of such a process.[38] This question has never been completely solved.

According to W.A. Weyl,[39] it is the inherent property of ice or snow to have a thin "liquid like" film in the form of an electrical dipole disturbance acting as a transition layer between the bulk solid and the surface. He postulated that the ice surface does not contain any protons. A dipole surface exists due to the ability of the anions to polarize. Therefore, the O^{2-} ions remain in the exterior layer followed by a second layer containing non-polarizable H^{+} ions. This theory is discussed in greater detain in Appendix B.

Weyl suggested that the "liquid like" film from the electrical dipole was the lubricant creating the low frictional resistance. This theory has also been subscribed to by Nakaya and Matsumoto.[40]

While the "Electrical Dipole" theory offers a number of interesting possibilities, it is by no means completely confirmed. At the same time Bowden's "Frictional Melting" theory should not be discounted in spite of the deductions of Pfalzner, Bell, and McConica.

---

[38] Thomson, J. (1861), "Note of Professor Faraday's Recent Experiments on Regelation," Proc. Roy. Soc. (London), Vol. 11, pp. 198-204.

[39] Weyl, W.A. (1951) "Surface Structure of Water and Some of its Physical and Chemical Manifestations," J. Colloid Science. Vol. 6, pp. 389-405.

[40] Nakaya, U. and Matsumoto, (1953) "Evidence of the Existence of a Liquidlike Film on Ice Surfaces," Research Paper 4, Snow, Ice, and Permafrost Res. Estab., Corps of Engr. U.S. Army, Wilmette, Illinois.

Both Holm[41] and Bowden have found that the temperatures in the immediate region of the contact points in the case of metals sliding upon each other is sufficient to melt the metallic points and form molten junctions.

It has also been determined that the necessary time to reach melting temperature is extremely short. This melting action at the contact points has recently been experimentally confirmed by Epprecht in connection with the examination of the fluctuations of the current passing through metallic sliding contacts.[42]

Dr. Bowden in presenting the 41st Hawksley Lecture of the Institution of Mechanical Engineers (January 1955 at Leicester, Eng.) again reviewed the surface temperatures developed during friction and application of the high surface temperatures to the surface melting of snow and ice. Additional experimental evidence recently obtained by Dr. Bowden indicating a surface melting mechanism was also presented.

In explanation of the experimental results of Pfalzner, it must be recalled that his electrical energy was supplied to the entire surface. This distributed energy may not result in an appreciable amount of melting over the entire surface. On the other hand the conversion of mechanical energy to thermal energy over the concentrated regions of contact is able to melt the material in the restricted point regions. Thus the application

---

[41] Holm, R. (1948) "Calculation of the Temperature Development in a Contact Surface, and Application to the Problem of the Temperature Rise in a Sliding Contact," J. Appl. Phys., Vol. 19, pp. 361-366.

[42] Epprecht, G. W. (1954) "Current Fluctuation Phenomena in Current Carrying Sliding Contacts," J. Appl. Phys., Vol. 25, pp. 1473-1480.

of external energy may be too widely distributed to appreciably affect the frictional resistance by aiding the surface meltings.

While Bell considered the large scale flow of heat from the rear to the front of a skate and demonstrated the impossibility of the rate of heat flow required, such flow may not be necessary. This heat may be retained in the immediate region in which it was produced to be utilized in the melting of asperities in this region. In this case the major amount of frictional resistance and surface melting will occur in the forward portion of the slider. This would further indicate certain benefits to be obtained from a long narrow rectangular skate or slider in which the rear portion of the slider carrying a large portion of the load would encounter lower frictional resistance due to previous melting in that region.

In reference to Dr. McConica's experimental results regarding the low friction of magnesium it is possible that the surface of the magnesium slider was so oxidized or contaminated as to result in a lower thermal conductivity than that of the pure metal.

Still another hypothesis to explain the low friction on snow is G. Seligman's[43] Ball Bearing Action Theory. According to this theory, snow particles move under the sliders providing a roller action, thus decreasing the friction coefficient. While this mechanism may apply partially in the case of motion over snow, it is doubtful whether it contributes extensively in the case of friction on ice.

The lubricant film, whatever its original source, does not appear to completely separate a slider from the basic ice surface but provides a parallel arrangement for supporting the load as described by Equation (1-10). For this reason the frictional characteristics of ice similar to the frictional characteristics of boundary lubrication are extremely erratic.

The characteristics of materials sliding on ice and snow can undoubtedly be described by Equations (1-10) and (1-11) and by functional relation of the experimental parameters including load, apparent area, time, and temperature upon terms of Equations (1-10) and (1-11).

Experimental investigations have been made of the influence of the above parameters to friction on ice and snow. W. Hopkins[44] in 1845, H. Moseley[45] in 1871, and A. Morphy[46] in 1913 performed several experimental

---

[43] Seligman, G. and F. Debenhan, (1943) "Friction on Snow Surfaces," Polar Record, Vol. 4, No. 25, pp. 2-11.

[44] Hopkins, W. (1845) "On the Motion of Glaciers," Phil. Mag. Series 6, Vol. 47, pp. 303-6.

[45] Moseley, Henry, (1871) "On the Mechanical Impossibility of the Desent of Glaciers by Their Weight Only," Phil Mag. Series 4, Vol. 42, pp. 138-49.

[46] Morphy, H. (1913) "The Influence of Pressure on the Surface Friction of Ice," Phil. Mag. Series 6, Vol. 25, pp. 113-35.

tests on ice friction although their findings were not appreciable except to note a dry friction type of relation between friction force and load.

Field studies on practical problems involved in the use of skis were made by C. Gliddon[47] in 1922 in Canada and by N. Soderberg[48] in 1932 in Sweden. Starting in 1934 G. J. Klein[31, 49] for the National Research Council of Canada carried out a systematic study of the influences of various parameters upon the performance of sliders on snow.

Klein noted from his experiments that the static and kinetic friction increased with a decrease of temperature for all ski materials. He also noted that the tangential resistance decreased with an increase in the unit loading of the ski. This would indicate a friction decrease for either an increase in the total load or a decrease in the apparent area of contact.

The material of the slider was also found by Klein to be extremely important under both static and kinetic conditions. Bakelite, various waxes, monel metal, and white ash treated with linseed oil were all found to have low kinetic friction. The bakelite also had a low static friction while the monel metal had a rather high static friction.

---

[47] Gliddon, C. (1922), "Investigation into the Effect of Weather Conditions on the Friction of Sleigh Runners on Snow," Canadian Air Force Report.

[48] Soderberg, N. (1932), "Investigations of Ski Frictions," I.V.A.'S Flygte Kriska Kommittee Rep. No. 1, Stockholm.

[49] Klein, G. J. (1938), "The Snow Performance of Aircraft Skis," Nat'l Res. Council of Canada, NRC. No. 722, Ottawa, (mimeographed). 20 pp.

Ski shape was found to influence the kinetic friction more than the static. The most important factor in ski shape was the aspect ratio or ratio of length to width of the rectangular ski; the greater this ratio, the lower the sliding resistance.

Regarding snow conditions Klein found that the highest kinetic resistance occurred when the snow was slightly wet but still retained some of its dendritic structure. Some evidence seemed to indicate that for similar snow structure the finer the structure the higher the resistance. When the snow was very wet the kinetic resistance increased with velocity and under hard packed and wet conditions the kinetic resistance was greater than static. On the other hand static resistance of all skis was low when the snow was very wet. For waxed or the bakelite surface the static friction was low at ambient temperatures above 20°F while the metal skis had high static friction in this temperature range.

McConica's experiments[34-35] as previously noted, indicated the presence of critical values of loading, velocity, and temperature. For loadings below 150 lb per sq ft in the case of bakelite sliding on smooth ice at -15°C his curves indicate a very rapid drop of the kinetic coefficient of friction. These curves also indicate a decrease in the kinetic coefficient of friction in the loading range above 150 lb per sq ft but at a lower rate. McConica also noted that the critical loading value appeared to be quite constant for different slider materials. It was further pointed out by McConica that the loading conditions on personnel skis correspond to loadings below this critical value while the loadings on skates or sleds are generally

above the critical. Thus an increase in the area or decrease in the normal load would be advantageous toward lowering the friction in ski applications, the opposite holding true for skates and sleds.

In regard to the velocity relation McConica noted that the coefficient of friction vs. velocity curves were characterized by a sharp drop in the friction from the static value with the initiation of motion. This was followed by a sharp rise above a velocity of 50 to 100 cm/sec and a later decrease of the coefficient above a velocity of 200 to 400 cm/sec. Instability in the friction was noted in the velocity range between the two critical points which could possibly have been caused by the "stick-slip" characteristics of his particular experimental apparatus as well as the characteristics of the two materials.

The optimum temperature as pointed out by McConica is not at the melting point of ice but several degrees below depending upon the nature of the runner surface, the loading, and the velocity. Above this optimum temperature a viscous drag appears to resist motion while below this optimum temperature the dry friction increases with decreased temperature.

Several other influences such as the crystalline form of the snow and other physical properties of the slider and the ice and snow surface were examined by McConica. Conclusions reached regarding these influences were tentative.

Following the introduction of synthetic rubber tires, it was noted that the synthetic rubber appeared to have lower friction (less acceleration and braking) on snow and ice surfaces than natural rubber. Several safety committees, road research groups, and tire producers set up research

programs to investigate the friction characteristics of tires on snow and ice in the hopes of improving these characteristics.

Conant, Dum, and Cox[50] (Firestone Tire and Rubber Company) in their investigation of various natural and synthetic tread compounds concluded that:

1. Both static and kinetic coefficients of friction increase with a decrease in temperature.
2. Static and kinetic coefficients of friction increased with increase in the age of the ice.
3. The kinetic coefficient decreased more than the static with an increase in the loading pressure.
4. The relation between friction on ice and the hardness, stiffness, and hysteresis of the rubber was very small.
5. Both the static and kinetic friction on ice were very sensitive to the type and amount of softener or black. The softer stock generally resulted in higher friction.
6. The pick up of ice appeared to decrease the kinetic coefficient of friction.
7. Both kinetic and static friction should be high for best performance of tires on ice.

C. S. Wilkinson, Jr.[51] in studying the problem of friction of tire treads

---

[50]Conant, F. S., J. L. Dum, and C. M. Cox. (1949), "Frictional Properties of Tread-Type Compounds on Ice," Ind. Eng. Chem. Vol. 41, No. 1, pp. 120-6.

[51]Wilkinson, C. S. Jr. (1953), "Study of the Factors Affecting the Friction of Tread Compounds on Ice," India Rubber World, Vol. 128, No. 4 pp. 475-81.

on ice for the Goodyear Tire and Rubber Co. noted the following:

1. Kinetic coefficient of friction increased with a decrease in the temperature.
2. Kinetic coefficient decreased with load and pressure. This friction decrease appeared to be proportional to the logarithm of the pressure.
3. Kinetic coefficient increased with velocity up to a velocity of 2 cm/sec above which the coefficient declined. (all loads and materials)
4. Kinetic coefficient increased if the sample surfaces were cleaned.
5. Kinetic coefficient decreased with a change of the slider sample from a solid plug to a membrane.
6. Static coefficient increased with time of stationary contact.
7. After a contact time of one minute the difference between static and kinetic friction was not appreciable.
8. Differences between tread compounds become less pronounced as the testing temperature approaches 0°C.
9. Friction decreased with an increase in the hardness of the tread compounds.

These several items of experimental evidence regarding the friction of various materials on ice and snow furnish several clues as to the basic mechanism of the friction on ice and snow. This evidence will be further considered in later chapters.

CHAPTER II

REAL AREA OF CONTACT BETWEEN ELASTIC AND PLASTIC SURFACE MATERIAL

Chapter II

Real Area of Contact between Elastic and Plastic Surface Material

All surfaces consist of innumerable humps and hollows. The height, depth, and spacings of these irregularities vary widely with the type of material and the surface treatment. Roughness or relative magnitude of the ridges may be reduced but never completely eliminated by special finishing techniques. Recognition of this circumstance leads to the conclusion that the mathematically smooth surface is unattainable.

Let us consider the consequence of placing one of these uneven surfaces upon another. Contact will first be made at a single point, the position at which an asperity of one of the surfaces happens to be the nearest to a hump or hollow of the adjacent surface. If the materials of the two surfaces are perfectly rigid, the upper surface would then tilt until contact is made at three points. This situation may be considered equivalent to the pure mathematical problem solved by J. Boussinesq for a normal force applied at a point on the boundary of a semi-infinite body. In this case the stress distribution in the semi-infinite body expressed in cylindrical coordinates was shown to be:[1,2]

---

[1] Timoshenko, S., and J. N. Goodier, (1951) Theory of Elasticity, 2nd Ed., McGraw-Hill, New York, p. 362.

[2] Boussinesq, J. "Application des Potentials," Memoirs de la Societe des Sciences de l'Agriculture et des arts de Lille, Lille, 1885.

$$\sigma_r = \frac{N}{2\pi}\left\{(1-2V)\left[\frac{1}{r^2} - \frac{z}{r^2}(r^2+z^2)^{-1/2}\right] - 3r^2 z\,(r^2+z^2)^{-5/2}\right\} \quad (2\text{-}1a)$$

$$\sigma_z = -\frac{3N}{2\pi} z^3\,(r^2+z^2)^{-5/2} \quad (2\text{-}1b)$$

$$\sigma_\theta = \frac{N}{2\pi}(1-2V)\left\{-\frac{1}{r^2} + \frac{z}{r^2}(r^2+z^2)^{-1/2} + z(r^2+z^2)^{-3/2}\right\} \quad (2\text{-}1c)$$

$$\gamma_{rz} = -\frac{3N}{2\pi} rz^2\,(r^2+z^2)^{-5/2} \quad (2\text{-}1d)$$

where:

N = applied force

V = Poisson's ratio

r, z, θ = cylindrical coordinates of point

σ_r, σ_z, σ_θ = Normal stresses

γ_{rz} = shear stress

From equations 2-1 it may be seen that the stresses become infinite at the origin or the point of contact regardless of the magnitude of the applied force. Since no actual material can withstand such stress, elastic and inelastic deformation of the contacting material must occur. This deformation produces two results:

(1) the original point contacts are squeezed out to become finite areas.

(2) the surfaces are allowed to come closer together bringing more asperities into contact.

Let us next examine the contact surface expansion of a single asperity. The problem of deformation and resulting contact area between two curved surfaces under perfectly elastic conditions was first solved

by Heinrich Hertz in 1881. Hertz's assumptions which govern the region of validity of his equations are:[3,4]

(1) Reactions must be normal to the contact surface.

(2) No tangential forces must be induced between the bodies in contact.

(3) Contact is limited to small portions of the surface.

(4) The bodies must be elastic and isotropic.

(5) The bodies must be at rest in relation to each other.

(6) Strain must be within the elastic limit.

Hertz determined that under his assumptions, spheres of radii R_1 and R_2 (Figure 2-1) when pressed together will deform starting at the point of contact to form a surface of contact approximately circular in shape. The radius of this circular contact area may be expressed as:

$$a = \left[\frac{\frac{1 - V_1^2}{E_1} + \frac{1 - V_2^2}{E_2}}{\frac{1}{R_1} + \frac{1}{R_2}} \quad \frac{3}{4} N \right]^{1/3} \qquad (2\text{-}2)$$

in which:

a = radius of circular area of contact

N = compressing force between the two spheres

R_1, R_2 = radii of spheres 1 and 2

E_1, E_2 = moduli of elasticity of bodies 1 and 2

V_1, V_2 = Poisson's ratio of bodies 1 and 2

---

[3] Hertz, H. (1882) "Ueber die Beruhung fester elasticher Korper," Journal fur die reine und angewandte Mathematik, Vol. 92, pp. 156-71.

[4] Allan, R. K. (1946) Rolling Bearings, Second Edition, Pitman and Sons, London, p. 100.

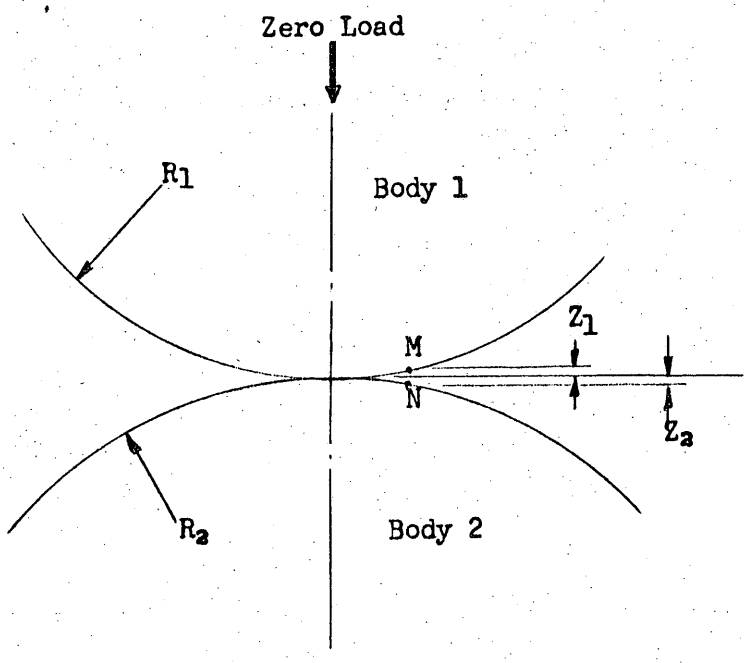

a. Contact Region Between Two Spheres, No Load

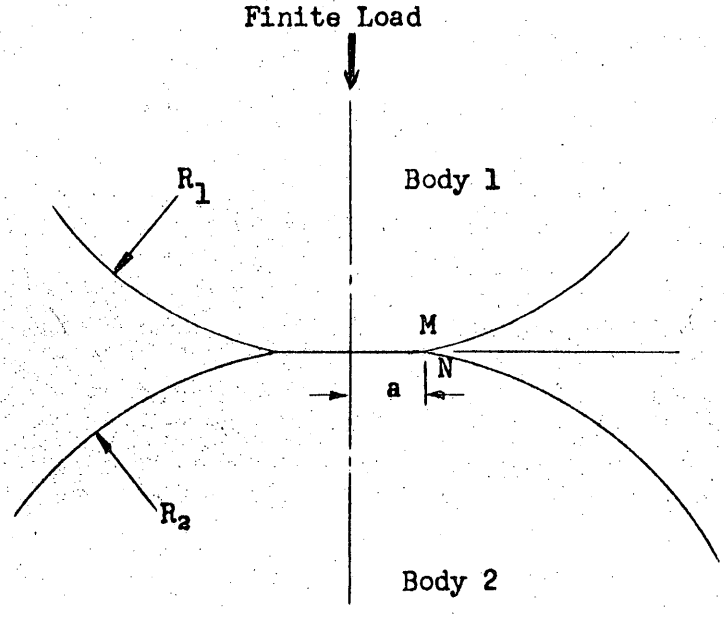

b. Contact Region Between Two Spheres, Finite Load

Figure 2-1 SPHERES IN CONTACT

Equation (2-2) also may be applied to the particular cases of a sphere in contact with a plane or with a spherical seat. For a plane, R_1 may be considered as very large approaching infinity as a limit. For a spherical seat R_1 may be taken as negative.

Hertz also developed equations for the case of generalized curvature of the contacting elastic bodies. For this case the surface of contact may be shown to approximate an ellipse with semi-axes a and b equaling:

$$a = m\left[\frac{\frac{3\pi}{4} N \left(\frac{1 - V_1^2}{\pi E_1} + \frac{1 - V_2^2}{\pi E_2}\right)}{A + B}\right]^{1/3} \qquad (2\text{-}3a)$$

$$b = n\left[\frac{\frac{3\pi}{4} N \left(\frac{1 - V_1^2}{\pi E_1} + \frac{1 - V_2^2}{\pi E_2}\right)}{A + B}\right]^{1/3} \qquad (2\text{-}3b)$$

in which:

a, b = semi-major and semi-minor axes length

N = compressing force between bodies 1 and 2

E_1, E_2 = moduli of elasticity for bodies 1 and 2

V_1, V_2 = Poisson's ratio for bodies 1 and 2

A, B = constants depending upon the magnitude of the principal curvature of the surfaces in contact and upon the angle between the planes of principal curvature of the two surfaces.

m, n = numbers depending upon the ratio of $\frac{B - A}{A + B}$

The elliptical area of contact for the generalized case reduces to other shapes for particular cases such as to a circular area for two spheres or to a rectangle for two parallel cylinders in contact.

The pressure distribution over the area of contact was shown by Hertz to be semi-ellipsoidal in shape with the maximum pressure occurring at the center, the pressure reducing to zero magnitude on the outer boundary. The maximum pressure at the center was found to equal 3/2 the average pressure or:

$$q_o = \frac{3}{2}\frac{N}{\pi ab} \tag{2-4}$$

for the body of generalized curvature.

Equation (2-4) reduces for the particular case of two spherical bodies in contact to:

$$q_o = \frac{3}{2}\frac{N}{\pi a^2} \tag{2-5}$$

and substituting for a from Equation (2-2):

$$q_o = \frac{6^{1/3}}{\pi} N^{1/3} \left[\frac{\frac{1}{R_1} + \frac{1}{R_2}}{\frac{1-V_1^2}{E_1} + \frac{1-V_2^2}{E_2}} \right] \tag{2-6}$$

As can well be imagined the deformations and the stresses engendered in the contacting bodies are very complex. The Boussinesq stresses (Equations 2-1) resulting from each differential area in the contact surface must be summed or integrated to obtain the total stress at a point. Numerical determination of the resulting stresses may be performed in several ways usually involving the summation of various infinite series.

Morton and Close,[5] for example, applied the method of expansion in zonal harmonics to the evaluation of stresses arising from the contact of two spherical surfaces. Due to the complexity of the resulting equations it is much easier to study the results in graphical form. Morton and Close have constructed stress diagrams for the stresses along lines running from the center of contact in directions making angles of 0°, 30°, 60°, and 90° with the normal. Figure 2-2 copied from Foppl[6] illustrates the stress distribution along the z axis for the case of a sphere in contact with a plane, both bodies having a Poisson ratio equal to 0.3.

From the graphed relations the following may be noted regarding the stresses within an elastic sphere:

(1) The compressive axial stress, σ_z, is greatest at the surface, equaling at this point the maximum loading q_o. This stress slowly decreases in the interior of the body equaling approximately 1/2 q_o at a depth equal to the radius of the circular area of contact.

(2) The radial and tangential stresses, σ_r and σ_t, equal approximately 0.8 q_o at the center of the contact surface. These stresses decrease rapidly equaling only about 0.05 q_o at $z = a$.

(3) The shear stress γ_{rz} has a value of 0.1 q_o on the surface but increases in the interior rising to a maximum of 0.31 q_o at a depth of $z = 0.47$ a. After this point the shear stress again decreases.

---

5 Morton, W. B., and L. J. Close. "Notes on Hertz's Theory of the Contact of Elastic Bodies," Phil. Mag., Vol. 43, pp. 320-29.

6 Foppl, L. "Der Spannungszustand und die Anstrengung des Werkstoffes bei der Beruhrung zweir Korper," Forschung auf dem Gebeite des Ingenieurwesens, Bd. 7, No. 5, p. 215.

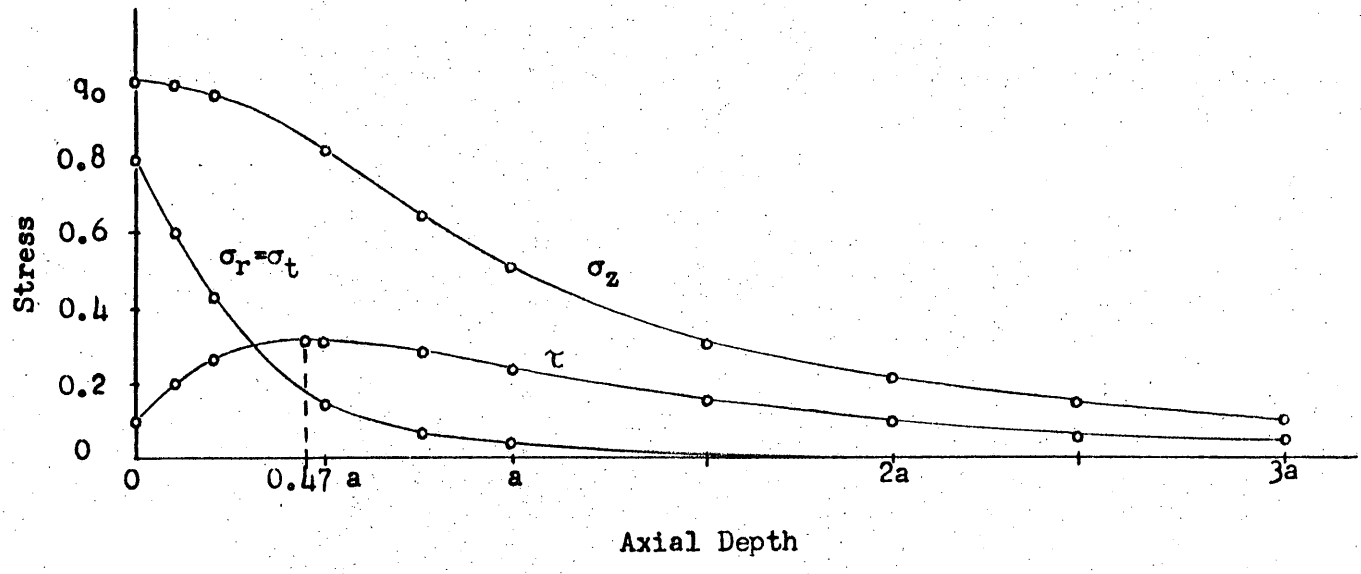

Stress distribution along the axis of symmetry in a sphere

σ_z = axial stress

σ_r = radial stress

σ_t = tangential stress

τ = shear stress

q_o = maximum pressure at center of surface of contact

a = radius of surface of contact

Extracted from Foppl, L. "Der Spannungszustand und die Anstrengung des Werkstoffes bei der Beruhrung Zweir Korper" Forschung auf dem Gabeite des Ingenieurwesens, Bd.7, (1936) Nr. 5, P. 215

Figure 2-2

Examining the stresses along the surface of the elastic body it has been found that[7]

(1) The axial compressive stress decreases to zero at the boundary of the contact surface.

(2) The radial and tangential stresses decrease more slowly having values of

$$\sigma_r = -\sigma_t = \frac{(1 - 2V)}{3} q_o \qquad (2\text{-}7a)$$

at the circular boundary of the surface of contact.

(3) The shear stress increases from the center to a value equal to the radial stress on the circular boundary or:

$$\tau_{rz} = \sigma_r = \frac{(1 - 2V)}{3} q_o \qquad (2\text{-}7b)$$

For the region at a slight distance from the actual contact region the stress relations (2-1) determined by Boussinesq apply.

Experimental investigations have verified Hertz's relations for materials having macroscopic dimensions which follow Hooke's law and in which the stresses are within the elastic limit.

For materials which fail in shear the critical region is the point of maximum shear occurring as previously mentioned for spherical contacts at a depth of 0.47 a below the surface. If a surface pressure is applied which results in the maximum shear exceeding the elastic limit, an irreversible deformation occurs. This deformation is plastic if the material is ductile in nature, or splintering if the material is brittle.

---

[7] Timoshenko and Goodin, op. cit., pp. 376-77.

The resulting deformation is generally plastic in nature. This plastic deformation enables the material to spread out under the contact region and results in a greater area of contact. Over the contact area the pressure distribution becomes more uniform as the nose of the semi-ellipsoid becomes flattened. As additional load is applied the average pressure over the contact surface becomes a greater proportion of the maximum pressure.

The plasticity of materials is known to be related to temperature and to time, as well as to the stress applied. Also the deformation produced is generally of a permanent nature.

In spite of a considerable amount of effort in this field in recent years, there still exist wide gaps in the understanding of the performance of real materials. Due to the lack of knowledge and to the complexity of the problem, it is impossible at present to develop an analysis of the stress and strain conditions in the generalized plastic material. Analysis based on certain simplifying assumptions is possible, however. The assumption of perfect elasticity is one such approximation to the actual case. Bypassing for the present the effects of time and temperature, let us consider for the second approximation to the real material, the plastic or St. Venant material. This material has a stress strain relationship defined as:

$$\sigma = Ee \quad \text{for } \sigma < f(Y_o) \tag{2-8}$$

$$\sigma = f(Y_o) \qquad \text{(at higher levels)}$$

where:

σ = stress

e = strain

E = Modulus of Elasticity

Y_o = Yield Point

This definition merely means that the deformation of the material is elastic below the yield point, Y_o, but is a function of the yield point above this stress condition. It is possible to further restrict and simplify the definition of the plastic material by assuming that $f(Y_o)$ equals a constant which may be arbitrarily taken as the mean flow pressure, p_m. In terms of this plastic constant the load applied between two spherical plastic bodies results in an area of contact expressed as:

$$A = \frac{N}{p_m} \qquad (2\text{-}9)$$

in which:

A = Contact Area

N = Normal Load

p_m = Mean Flow Pressure

The previous discussion of elastic and plastic deformation is fundamental for the understanding of the behavior of surface asperities. Let us assume that an asperity is conical or pyramidal in shape with a perfectly smooth spherical tip. The area of contact under elastic conditions for the i^{th} asperity is:

$$A_i = \pi a^2 = \pi \left[\frac{\frac{1 - v_1^2}{E_1} + \frac{1 - v_2^2}{E_2}}{\frac{1}{R_1} + \frac{1}{R_2}} \frac{3}{4} N_i \right]^{2/3} \qquad (2\text{-}10)$$

Under plastic conditions the contact area of the i^{th} asperity is:

$$A_i = \pi a^2 = \frac{N_i}{p_m} \qquad (2\text{-}11)$$

Equations (2-10) and (2-11) indicate that the contact area of a single asperity is proportional to the 2/3 power of the load under elastic conditions and to the first power of the load under plastic conditions.

It is also possible to relate the contact area and the applied load to the vertical deformation of the bodies in contact. Archard[8] has proposed the model illustrated in Figure 2-3 for the analysis of this relation in the case of a plastic material. This model postulates a spherical deformable surface having a radius R in contact with a flat non-deformable surface. As an approximation to the actual situation it is assumed that no lateral expansion of the material occurs. The area of contact resulting from a vertical deformation, x, is assumed to equal the circular slice of the spherical body at the depth x. The radius of this contact area may be determined by trigonometry as:

$$a^2 = R^2 - (R - x)^2 \qquad (2\text{-}12a)$$

$$= R^2 - R^2 + 2Rx - x^2 \qquad (2\text{-}12b)$$

$$= 2Rx - x^2$$

If x is a small quantity relative to R the equation of the radius of the contact area may be approximated as:

---

[8] Archard, J. F. (1953) "Contact and Rubbing of Flat Surfaces," J. Appl. Phys., Vol. 24, No. 8, pp. 981-88.

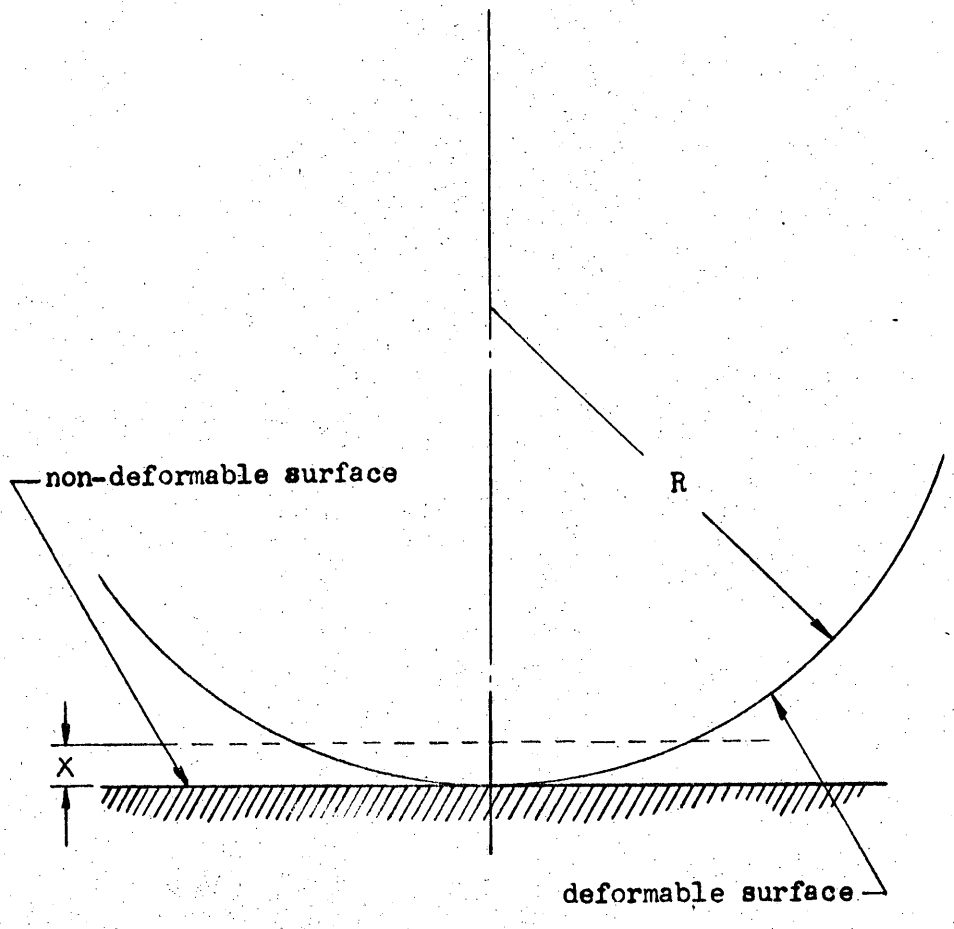

Figure 2-3 ARCHARD'S MODEL OF A SINGLE ASPERITY IN CONTACT WITH A PLANE SURFACE.

$$a^2 \approx 2\,Rx \tag{2-13}$$

The total area of contact then becomes:

$$A_i = \pi a^2 \approx 2\,\pi\,Rx \tag{2-14}$$

Equation 2-14 indicates a linear relationship between the area of contact and the deformation.

A similar linear relationship may be drawn between the load and vertical deformation as follows:

$$N_i = A_i\,p_m \approx 2\,\pi\,Rx\,p_m \tag{2-15}$$

Equations (2-14) and (2-15) may be generalized in the form:

$$A = bx \tag{2-16}$$

$$N = cx^m \tag{2-17}$$

For the plastic material under consideration the constants of these generalized equations are:

$$b = 2\,\pi r \tag{2-18a}$$

$$c = 2\,\pi r\,p_m \tag{2-18b}$$

$$m = 1 \tag{2-18c}$$

For two elastic spheres in contact a similar set of linear relations are found to hold. The constants for the elastic bodies may be determined as:

$$b = \frac{2\pi}{\frac{1}{R_1} + \frac{1}{R_2}} \tag{2-19a}$$

$$c = \frac{\frac{4}{3}\left[\frac{1}{R_1} + \frac{1}{R_2}\right]}{\left[\frac{1 - V_1^2}{E_1} + \frac{V_2^2}{E_2}\right]} \tag{2-19b}$$

$$m = 3/2 \tag{2-19c}$$

For the particular case of a single elastic sphere on a flat surface the constants of Equations (2-19) reduce to:

$$b = 2\pi R_1 \tag{2-20a}$$

$$c = \frac{\frac{4}{3} R^{-1/2}}{\left[\frac{1 - V_1^2}{E_1} + \frac{1 - V_2^2}{E_2}\right]} \tag{2-20b}$$

$$m = 3/2 \tag{2-20c}$$

Eliminating x between Equations (2-16) and (2-17):

$$A = b \left(\frac{N}{c}\right)^{1/m} \tag{2-21}$$

and introducing the values of b, c, and m given by Equations (2-19) and (2-20), it may again be seen that the area of contact of a single asperity is proportional to the 2/3 power of the load for elastic conditions and to the first power of the load for plastic conditions.

Let us next consider the multiple areas of contact actually existing between mating rough surfaces. Archard has suggested for this problem the model illustrated in Figure 2-4.

This model consists of a perfectly flat non-deformable surface and a nominally flat deformable surface containing a large number of spherical asperities of equal radii of curvature. The assumption is made that the asperities are evenly distributed in depth (the x direction). There is thus one asperity at each of the x coordinates x = 0, h, 2h, 3h, ... where $h \ll R$. These levels are termed the zero, first, second, third ... etc. levels respectively. The assumed asperity distribution may be plotted graphically as indicated in Figure 2-5.

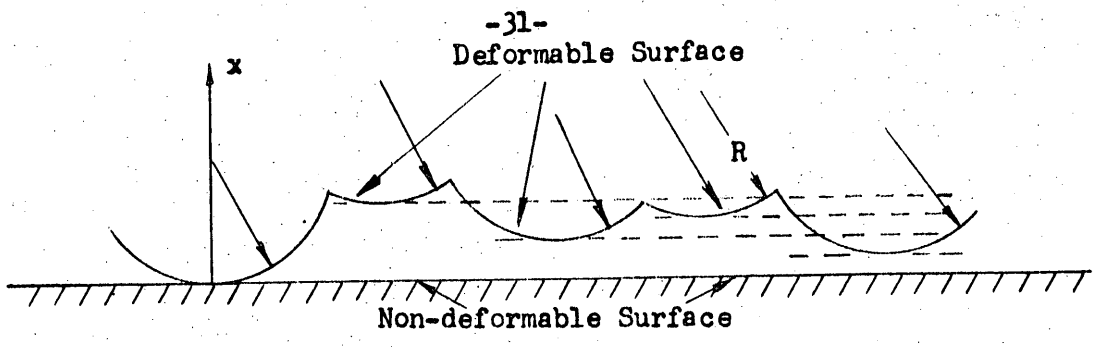

Figure 2-4 ARCHARD'S SURFACE MODEL FOR MULTIPLE CONTACT AREAS

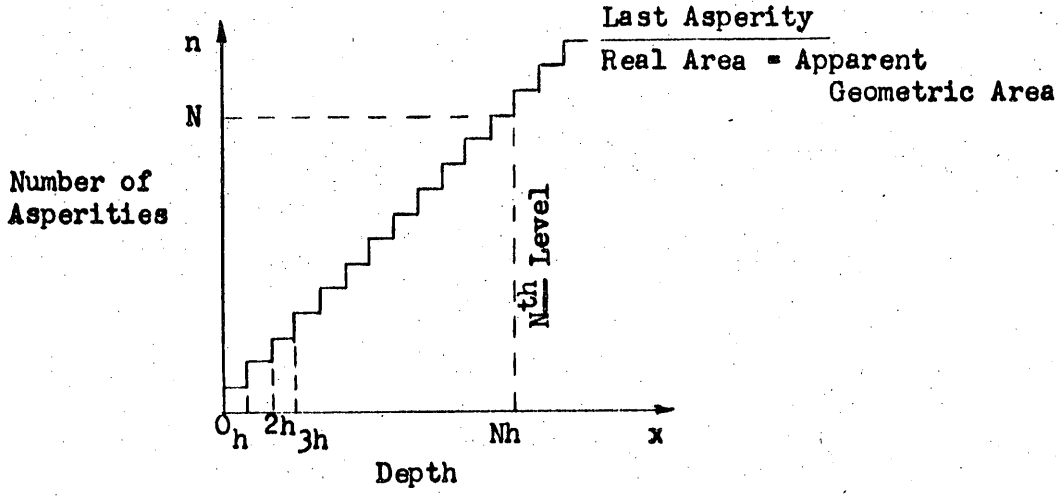

Figure 2-5 STEPWISE ASPERITY DISTRIBUTION WITH DEPTH FOR ARCHARD'S MODEL

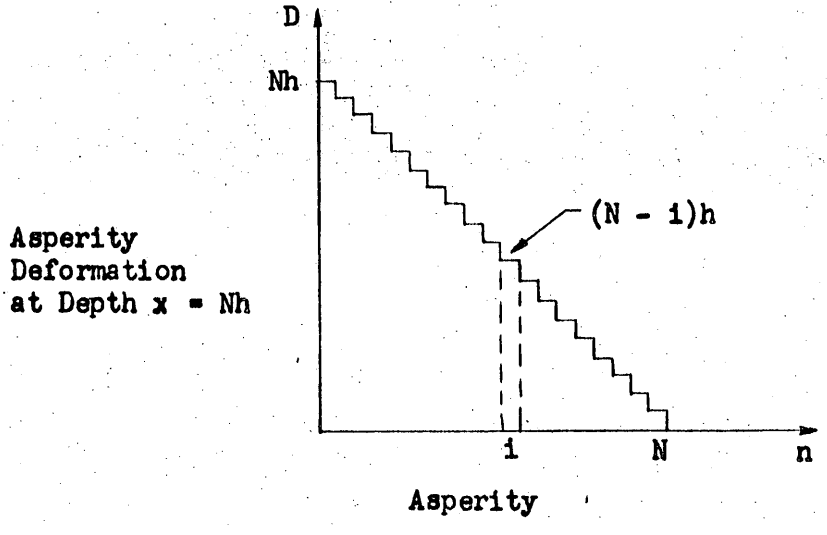

Figure 2-6 DEFORMATION OF INDIVIDUAL ASPERITIES FOR ARCHARD'S MODEL

Movement of the deformable surface closer to the non-deformable surface not only increases the total number of asperities but also increases the area contribution from asperities previously contacted. Recalling that the area of each individual asperity by Equation (2-16) is:

$$A_1 = b\,x \tag{2-16}$$

and that the deformation of the $i^{\underline{th}}$ asperity at depth Nh is (N - i)h, (Figure 2-6) the contribution to the total area by this asperity is therefore:

$$\delta A_i = b\,(N - i)h \tag{2-21}$$

The total contact area at depth $x = Nh$ equals the sum of the individual contributions.

$$A_M = \sum_{i=0}^{N-1} b\,(N - i)\,h \tag{2-22}$$

For large values of N this summation equals approximately:

$$A_M = 1/2\ bh\ N^2 \tag{2-23}$$

or substituting

$$x = Nh \tag{2-24}$$

then:

$$A_M = \frac{1}{2}\frac{b}{h}\,x^2 \tag{2-25}$$

Equation (2-25) indicates that the total area resulting from multiple point contact between a rough deformable surface and a flat non- deformable surface increases as the square of the depth. For comparison the contact area between single point contacts increases only as the first power of the distance, x.

Relation (2-25) can also be derived using the methods of integral calculus if the step relation between the number of asperities, N, and the depth, x, is approximated by the continuous function Nh = x. The deformation of the asperity originally contacted at depth x resulting from a total deformation to the depth y then equals: (Figure 2-7)

$$D = y - x_1 \tag{2-26}$$

The area differential of this same asperity is:

$$dA_M = \frac{b}{h}(y - x)\frac{dx}{h} \tag{2-27}$$

which may be integrated over the limits of interest to obtain:

$$A_M = \int_0^y \frac{b}{h}(y - x)\,dx \tag{2-28a}$$

$$= \frac{b}{h}\left(yx - \frac{x^2}{2}\right)\Big|_0^y \tag{2-28b}$$

$$= \frac{b}{h}\frac{y^2}{2} \tag{2-28c}$$

resulting in the same expression previously obtained in (2-25).

Next consider the relation of the applied load to the number of asperities contacted and to the deformation of the surface. Since an individual asperity deformed a distance (N - i)h will carry a load P_i in which:

$$P_i = c\left[(N - i)h\right]^m \tag{2-29}$$

the total load will equal:

$$P_M = \sum_{i=0}^{N-1} c\left[(N - i)h\right]^m \tag{2-30}$$

In terms of integral calculus this sum may be determined more easily using the approximation

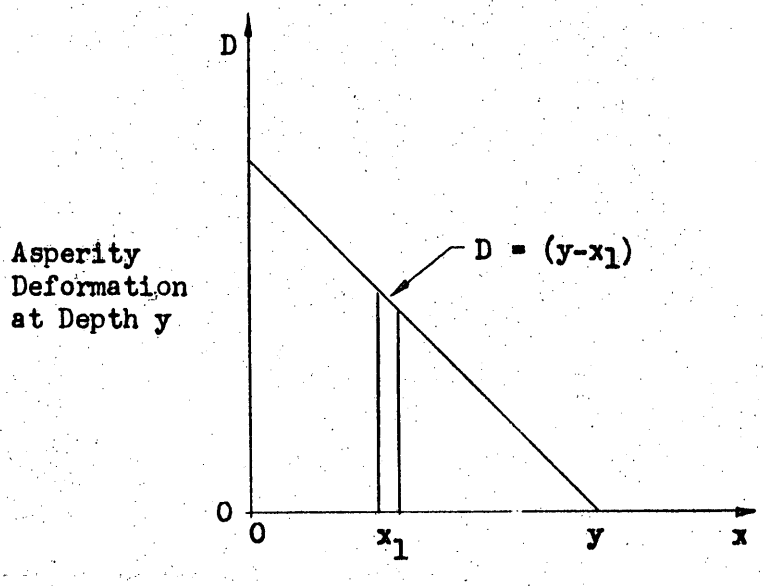

Figure 2-7 DEFORMATION OF ASPERITIES FOR CONTINUOUS DISTRIBUTION OF ASPERITIES WITH DEPTH

$$d P_M = c[y - x]^m \, dN \tag{2-31}$$

$$= c[y - x]^m \frac{dx}{h} \tag{2-32}$$

Integrated over limits 0 to y:

$$P_M = \int_o^y \frac{c}{h} [y - x]^m \, dx \tag{2-33a}$$

$$= -\frac{c}{h} \frac{(y - x)^{m+1}}{m + 1} \Bigg]_o^y \tag{2-33b}$$

$$P_M = \frac{c}{h} \frac{y^{m+1}}{m + 1} \tag{2-33c}$$

Total area of multiple contact can also be related to the total load as follows:

$$A_M = \frac{1}{2} \frac{b}{h} y^2 \tag{2-28c}$$

$$P_M = \frac{c}{h} \frac{1}{m + 1} y^{m+1} \tag{2-33c}$$

$$y = P_M^{1/m+1} \left[\frac{h}{c}^{m+1} \right]^{1/m+1} \tag{2-34}$$

$$A_M = \frac{1}{2} \frac{b}{h} \left[\frac{h}{c}^{m+1} \right]^{2/m+1} P_M^{2/m+1} \tag{2-35}$$

Archard's model of the multiple areas of contact could be considerably improved by assuming both surfaces as deformable surfaces with spherical asperities uniformly distributed in depth. The radii of the spherical asperities of the two surfaces need not be the same. Similarly the distribution interval of the asperities of the two surfaces may have different values.

In this model illustrated in Figure 2-8, the zero level or peak of the highest asperity on each surface will be considered the reference

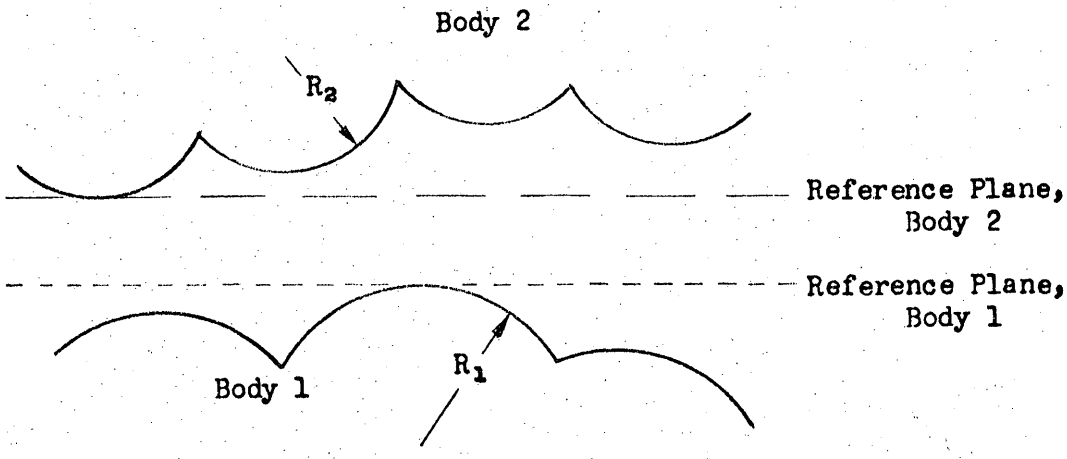

Figure 2-8 MODEL OF SURFACES WITH ASPERITIES ON BOTH BODIES LINEARLY DISTRIBUTED

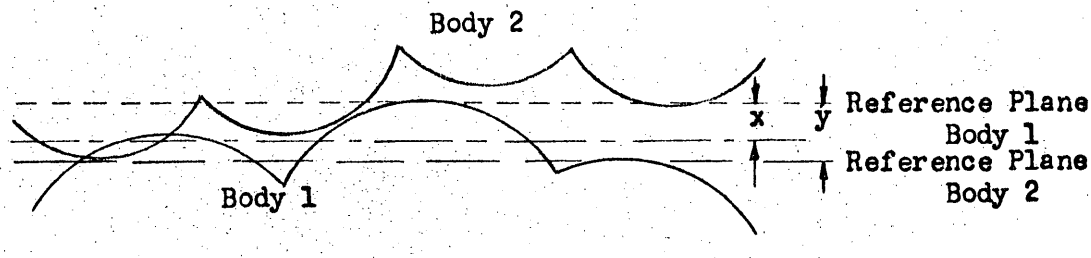

Figure 2-9 INTERPENETRATION OF SURFACES EACH WITH LINEARLY DISTRIBUTED ASPERITIES

plane of that surface. Bringing the two reference planes into coincidence does not necessitate that the highest asperities of the two bodies come into contact. Actually the probability is vanishingly small that the highest asperity of each body should occur at the identical surface location.

The reference planes of the two bodies must therefore penetrate each other some distance before contact is actually made. Further penetration is required to bring sufficient area into contact to support the applied load.

Consider the situation illustrated in Figure 2-9 in which the reference planes of bodies 1 and 2 have penetrated each other to a depth y. Consider further the status of point x in the penetration region between the two reference planes. The probability of this point being on or within Body 1 is evidently related to the real area subtended by a plane slicing through the asperities of Body 1 parallel to Reference Plane 1, and at the depth x. Let us define this probability as equaling the ratio of the real area at this level to the apparent area or the maximum area at the depth of the lowest asperity.

$$B_1 = \frac{A_{R1}}{A_{A1}} \tag{2-36}$$

Further for mathematical convenience let us consider the apparent area as equaling unity. The probability of point x being on or within body 1 is then equal to the real area of Body 1 at this level.

$$B_1 = A_{R1} \tag{2-37}$$

This real area as expressed by equation (2-25) is proportional to the square of the depth.

$$A_{R1} = \frac{1}{2} \frac{b_1}{h_1} x^2 \tag{2-38}$$

Similarly the probability of point x being on or within body 2 is:

$$B_2 = A_{R2} = \frac{1}{2} \frac{b_2}{h_2} (y - x)^2 \tag{2-39}$$

The probability of the point x being on or within both bodies equals the product of the separate probabilities.

$$B_{12} = A_{R1} A_{R2} = \frac{1}{2} \frac{b_1}{h_1} x^2 \frac{1}{2} \frac{b_2}{h_2} (y - x)^2 \tag{2-40a}$$

$$= \frac{1}{4} \frac{b_1 b_2}{h_1 h_2} x^2 (y - x)^2 \tag{2-40b}$$

Examining equation (2-40b) it may be noted that the probability of being on or within both bodies at a depth $x = 0$ is zero since there is zero probability of contacting Body 1. Similarly the probability drops to zero at $x = y$ where the probability of touching Body 2 is zero.

The probabilities expressed in Equation (2-40b) are only the probabilities of contact existing over a plane at a particular level. The area of interest is the area resulting from contact of all possible asperities through the entire depth of penetration. This total area is not merely equal to the sum of the contact areas at the individual levels since these areas are often duplicated over several levels. The cumulative total area may be determined by considering the additional area contribution from each level. At level x the real area of Body 2 available

for contact equals:

$$A_{R2} = \frac{1}{2} \frac{b_2}{h_2} (y - x)^2 \qquad (2\text{-}39)$$

The area increment supplied by the body 1 asperity originally contacted at point x equals:

$$\delta A = b_1 (y - x) \qquad (2\text{-}41)$$

The number of additional body 1 asperities subtended by motion through the distance dx is:

$$dN_1 = \frac{dx}{h_1} \qquad (2\text{-}42)$$

Combining these three relations the total real area increment from level x is:

$$dA_M = \frac{1}{2} \frac{b_2}{h_2} (y - x)^2 b_1 (y - x) \frac{dx}{h_1} \qquad (2\text{-}43)$$

Integrating over the limits 0 to y

$$A_M = \int_o^y \frac{1}{2} \frac{b_2}{h_2} \frac{b_1}{h_1} (y - x)^3 \, dx \qquad (2\text{-}44a)$$

$$= -\frac{1}{2} \frac{b_2 b_1}{h_2 h_1} \frac{(y - x)^4}{4} \Bigg]_o^y \qquad (2\text{-}44b)$$

$$= \frac{1}{8} \frac{b_2 b_1}{h_2 h_1} y^4 \qquad (2\text{-}44c)$$

The total load carried by multiple point contact may be similarly computed.

Area of Body 2 available for contact:

$$A_{R2} = \frac{1}{2} \frac{b_2}{h_2} (y - x)^2 \qquad (2\text{-}39)$$

Load increment carried by body 1 asperity contacted at point x:

$$P = c_1 (y - x)^m \tag{2-45}$$

Number of additional body 1 asperities subtended by motion through the distance dx

$$dN_1 = \frac{dx}{h_1} \tag{2-42}$$

Combining:

$$dP_m = \frac{1}{2} \frac{b_2}{h_2} (y - x)^2 \, c_1 (y - x)^m \, \frac{dx}{h_1} \tag{2-46}$$

and integrating

$$P_m = \frac{1}{2} \frac{b_2}{h_2} \frac{c_1}{h_1} \int_o^y (y - x)^{m+2} \, dx \tag{2-47a}$$

$$= -\frac{1}{2} \frac{b_2}{h_2} \frac{c_1}{h_1} \frac{(Y - x)^{m+3}}{m + 3} \Bigg]_o^y \tag{2-47b}$$

$$= \frac{1}{2} \frac{b_2}{h_2} \frac{c_1}{h_1} \frac{1}{m + 3} \, y^{m+3} \tag{2-47c}$$

The direct relation between contact area and load for the second assumed model of multiple contact may be determined as follows:

$$A_M = \frac{1}{8} \frac{b_2}{h_2} \frac{b_1}{h_1} \, y^4 \tag{2-44c}$$

$$P_M = \frac{1}{2} \frac{b_2}{h_2} \frac{c_1}{h_1} \frac{1}{m + 3} \, y^{m+3} \tag{2-47c}$$

$$y = P_M^{1/m+3} \left[\frac{2h_2h_1 (m+3)}{b_2c_1} \right]^{1/m+3} \tag{2-48}$$

$$A_M = \frac{1}{8} \frac{b_2b_1}{h_2h_1} \left[\frac{2 \, h_2h_1 (m+3)}{b_2c_1} \right]^{4/m+3} P_M^{4/m+3} \tag{2-49}$$

A review of the contact area vs. load relation for the various assumed models indicates an interesting trend.

For single point contacts the area was shown to vary directly as the 2/3 power of the load for elastic material and directly as the first power for plastic material. Intermediate values of the power sometimes found experimentally were thought to indicate a combination of elastic and plastic region influences.

Multiple point contacts on first thought might be expected to have the same relationships between area and load as single point contacts. This would be true if all the asperities had exactly the same height. Archard's model in which the asperities on one surface are assumed to be linearly distributed, leads however to the conclusion that the area varies directly as the 4/5 power of the load for elastic material and as the first power for plastic material. In a similar fashion the second model approximation in which asperities on both surfaces are linearly distributed concludes that the area varies directly as the 8/9 power of the load for elastic material and once again as the first power for plastic material.

Table 2-1

Values of Power k in equation $A_M = P_M^{\,k}$ for assumed models of surface roughness.

Multiple Point Contact in which	All Asperities same height	Asperities one Surface Linearly Distributed	Asperities both Surfaces Linearly Distributed
Elastic Material	2/3	4/5	8/9
Plastic Material	1	1	1

It is thus seen that as the multiple contact area model is improved the area relationship to load for the elastic material becomes successively closer to a linear relationship. Further improvements on the model, such as assumption of conical asperities in which the cross-section area of the individual asperity increases as the square of the depth, brings the relationship even closer.

It is reasonable to assume, therefore, that for multiple point contact of actual surfaces, the area will vary directly as the first power of the applied load for both elastic and plastic conditions.

The resulting contact area is generally designated as the real contact area, A_r, to distinguish this area from the apparent area, A_a, measured by standard geometric methods. If the mean flow pressure of the surface material is much greater than the average apparent pressure over the geometric apparent area, the real contact area will be practically independent of the apparent area. This does not necessarily imply that the number of asperities is independent of the apparent area. For a large apparent area there will probably be a large number of individual support points, each undergoing a comparatively small deformation. A smaller apparent area will probably have a smaller number of individual support points, but these points will be deformed a greater amount to obtain the same real contact area.

For a low ratio of the loading or average apparent pressure to the mean flow pressure, therefore, the real contact area may be considered as:

(1) Independent of the apparent area.

(2) Directly proportional to the first power of the normal applied load.

and is thus in agreement with the first two classical laws of friction.

At higher ratios of the loading to the mean flow pressure, however, the real area of contact becomes an appreciable portion of the apparent area.

Since the real area of contact obviously cannot exceed the apparent area, it may be seen that the ratio of A_r/A_a must approach a limiting value of unity at extreme loads. Finnie and Shaw[9] have suggested that the functional relation of the real area to the normal load must be in the manner illustrated in Figure 2-10. This behavior, as also suggested by Finnie and Shaw, may be represented analytically as:

$$\frac{A_r}{A_a} = 1 - e^{-BN} \qquad (2\text{-}50)$$

where:

A_r = Real area of contact
A_a = Apparent area
N = Normal load
B = Constant

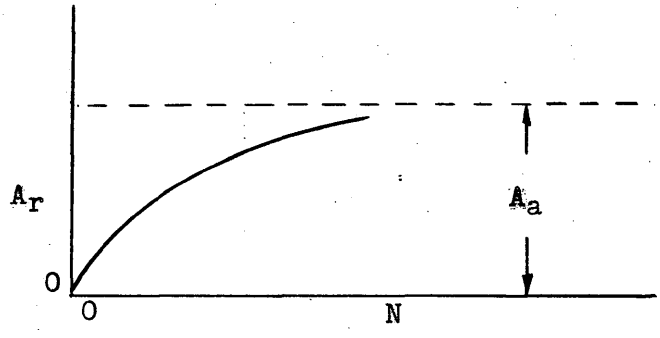

FIGURE 2-10

[9] Finnie, I., and M. C. Shaw (1954)"The Friction Process in Metal Cutting," presented at the Annual Meeting of the American Society of Mechanical Engineers, New York, Nov. 1954, ASME Paper No. 54-A-108, pp. 5.

It may be noted that the end conditions of Equation 2-50 satisfy the physical situation, i.e.

As: $N \rightarrow 0$, $A_r \rightarrow 0$

As: $N \rightarrow \infty$, $A_r \rightarrow A_a$

Furthermore for low values of the normal load the expression e^{-BN} in Equation 2-50 may be expressed as:

$$e^{-BN} \cong 1 - BN \qquad (2\text{-}51)$$

Therefore:

$$\frac{A_r}{A_a} \cong 1 - (1 - BN) = BN \qquad (2\text{-}52)$$

and the real area of contact becomes a linear function of the normal load as required by the Second Classical Law of Dry Friction.

The constant B according to the above approximation should be at low values of the normal load:

$$B = \frac{A_r}{A_a} \frac{1}{N} \qquad (2\text{-}53)$$

or substituting from Equation 1-5:

$$p_m = \frac{N}{A_r} \qquad (1\text{-}5)$$

$$B = \frac{1}{A_a p_m} \qquad (2\text{-}54)$$

While the real area - load relation suggested by Finnie and Shaw has not been confirmed experimentally over the entire loading range, it does appear to approximate the general situation.

CHAPTER III

HYPOTHESIZED INFLUENCE OF CERTAIN EXPERIMENTAL PARAMETERS UPON THE FRICTION OF SLIDERS ON COMPACTED SNOW

CHAPTER III

Hypothesized Influence of Certain Experimental Parameters Upon the Friction of Sliders on Compacted Snow

If the normal load between a slider and compacted snow is distributed in a parallel fashion between rigid asperities and a liquid-like film as was suggested in Chapter I, the load distribution and the frictional force could conceivably be influenced by several experimental parameters. Let us consider a few of these possible influences.

In equation 1-10 the normal load was assumed to be distributed over the two materials by the relation:

$$N = A_{r1}\, p_{m1} + A_{r2}\, p_{m2} \qquad (3\text{-}1)$$

The adhesive frictional resistance was also assumed as equaling:

$$F = A_{r1}\, s_1 + A_{r2}\, s_2 \qquad (3\text{-}2)$$

where:

N = Normal Load

F = Frictional Force

A_{r1}, A_{r2} = Real area of contact of solid asperities and film respectively.

p_{m1}, p_{m2} = Mean flow pressure of solid asperities and film.

s_1, s_2 = Shear stress of solid asperities and film.

Let us next assume that the area of direct contact between the slider and the solid asperities of the compacted snow or ice equals a certain proportion α of the apparent contact area. Let us also assume that the area of influence of the film equals the proportion β of the apparent

contact area.

Next, if we hypothesize that the ratio of the two areas α/β is very small for a short time interval but grows with time, then we might deduce that the friction force for a short time interval is basically:

$$F_{\text{short time}} = s_2 \beta A_a \tag{3-3}$$

while the friction force for a medium interval equals:

$$F_{\text{medium time}} = s_1 \alpha A_a + s_2 \beta A_a \tag{3-4}$$

For the short time interval the load might be considered as being supported entirely by the film. In this case Equation 3-1 becomes:

$$N = p_{m2} \beta A_a \tag{3-5}$$

After the medium time interval, the direct contact points may be supporting some of the load. In this situation the load equals:

$$N = p_{m1} \alpha A_a + p_{m2} \beta A_a \tag{3-6}$$

The coefficients of friction for the short and medium time situations become:

$$\mu_{\text{short time}} = \frac{s_2}{p_{m2}} \tag{3-7}$$

$$\mu_{\text{medium time}} = \frac{s_1 \alpha + s_2 \beta}{p_{m1} \alpha + p_{m2} \beta} \tag{3-8}$$

The hypothesis upon which these conclusions are based is quite logical. In the short time period case, the slider may be considered as riding on a low resistance film which is continually self-repairing. If the slider is allowed to remain stationary for any period of time the slider sinks through the film and establishes direct contact with the main ice structure.

The short time period coefficient may be the friction obtained under kinetic conditions while the medium time period may apply to static friction.

It has been experimentally noted that the static coefficients are considerably more erratic than the kinetic. This static erraticness might be explained as due to the uncontrolled distribution of load over high and low shear strength areas.

For very long stationary time periods, such as many hours, it has also been noted that the static coefficient of friction rises to large values often above unity. This phenomenon may be caused by the load being completely supported by direct contact with ice asperities. In this case the coefficient of friction should be:

$$\mu \text{ long time} = \frac{s_1}{p_{m1}} \qquad (3\text{-}9)$$

It is also possible that under long contact conditions the film may change its characteristics. This change may take the form of a greater adhesion over the film or a freezedown. This would also result in the much larger frictional force found experimentally.

The long time period static coefficients may be expected to approach the theoretical values predicted by the substitution of values of s and p_m of ice in Equation 1-8.

In addition to the possible time effect on the contact area, time also has considerable influence on the basic shear strength and mean flow pressure properties.

These characteristics are related to the so called ductility of the material. Although ductility and its opposite quality, brittleness, are applied rather loosely to the plastic and fracture characteristics of a material, a few experimental relationships have been noted. Zener and

others have suggested that two factors affect the ductile characteristics of a material:[1-3]

1. Rate of strain.

   A more rapid application of strain decreases ductility.

2. Temperature.

   A rise in temperature increases the ductility.

These two factors may be mathematically combined as a single parameter through an equation suggested by Zener:

$$Z = \overline{\nu} e^{Q/RT} \tag{3-9}$$

where

Z = Parameter of ductility

$\overline{\nu}$ = Rate of strain

T = Temperature

Q = Heat of activation

R = Gas constant

The influence of slider velocity upon the friction may undoubtedly be interpreted in terms of the influence of time upon the distribution of load over the solid asperities and the film.

---

[1] Zener, C. (1945) "Fracture Stress of Steel," Rev. Mod. Phys., Vol. 17, pp. 20.

[2] Holloman, H. H. and C. Zener (1944) "Conditions of Fracture of Steel," Metals Tech., TP 1782.

[3] Taylor, N. W. (1947) "Mechanism of Fracture of Glass and Similar Brittle Solids," J. App. Phys., Vol. 18, pp. 943.

High velocities would correspond to very short contact time intervals and, as previously indicated, would probably result in the load being supported almost entirely by the film. If the film is viscous in nature and the resistance force is created by a shearing action in the film, the friction force may be expected to increase with velocity. If, on the other hand, the resisting force occurs at the interface of the slider with the film, the friction force would probably be independent of the velocity, a function only of the contact area with the film. If some resistance is also obtained from contact with solid asperities and if the amount of contact increases with time, the friction should decrease with an increase in velocity.

The influence of the apparent area of contact upon frictional resistance is undoubtedly related to the normal load and to the time of contact. For low values of the normal load and comparatively short time of contact, the real area of contact between the solid asperities of the compacted snow or ice and the slider is practically independent of the apparent area. Thus the adhesive resistance of the solid asperities should also be nearly independent of the apparent area. On the other hand, the area of contact of the film which is the chief support of the load under short contact time conditions could be expected to be directly related to the apparent area.

Under longer contact times, such as the time available under static and freezedown conditions, either the slider sinks through the film to form additional contacts with the solid asperities or the film changes

to a solid form. In such cases, particularly so for the freezedown case, the adhesive frictional resistance would be directly related to the apparent area of contact.

Under heavier loads, the slider sinks further through the film and establishes a greater region of real contact with the solid asperities. This real contact area increases with the load but is limited in its upper value by the magnitude of the apparent area. It would appear, therefore, that the adhesive friction would also approach an upper limit. On the other hand, under high loading conditions as the real area approaches the apparent area, excessive penetration of the ice or compacted snow occurs. This results in an increased plowing effect. As the total frictional resistance is the sum of the adhesive and plowing resistances, the minimum total friction should occur at an apparent area sufficient to support the load without excessive penetration and still not so large as to create unnecessary adhesive friction of the film.

The load on the slider also has a complex influence upon the frictional force. This influence is basically related to the influence of the load upon the real contact area. At low loads, the real contact area as previously described is approximately a linear function of the load and, therefore, the frictional force is approximately directly related to the load. At high loads the adhesive friction should no longer increase linearly with the load due to the approach of the magnitude of the real area to the apparent area. Under these conditions, however, the plowing resistance rapidly increases.

The influence of slider material upon the frictional resistance lies mainly in its mechanical properties of hardness and shear strength and in

its electrical and chemical effects upon the surface film. A material which assists the formation of a surface film on the ice should have a lower frictional resistance.

Temperature is able to affect frictional resistance through its influence upon the properties of the solid asperities and the film. It is reasonable to expect a larger surface film at higher temperatures. Thus, at low temperatures, a greater share of the load will be carried by the solid surface asperities and the frictional resistance will be fairly low. This frictional resistance should decrease with an increase in temperature and an increase in the amount of film until an excessive amount of film is present. If the film is too thick, hydrodynamic resistance increases. Thus there should be an optimum temperature for minimum frictional resistance.

A high relative humidity is also conducive to the formation and retention of a liquid-like film on the surface of ice or compacted snow. Thus a high relative humidity should be accompanied by a decreased frictional resistance.

Other gases in the atmosphere which might collect on the ice surface and form a low shear strength film should also result in low frictional resistance.

In addition to the properties of the slider surface material, certain bulk properties of the slider material, such as the flexibility and the thermal conductivity should be able to affect the frictional resistance. The flexibility of the slider regulates the distribution of the total load over the slider surface and, therefore, is able to affect the real area - apparent area relation. A high thermal conductivity enables a rapid flow of heat away from the contact surface and decreases the opportunity for film formation.

Although the shape of the slider and the magnitude of the slider perimeter should have no influence upon the adhesive frictional resistance, these characteristics should have a large effect upon compaction and the plowing resistance.

CHAPTER IV

A METHOD FOR THE DETERMINATION OF FRICTION CONSTANTS FROM THE ANALYSIS OF THE MOTION OF A SLIDER

Chapter IV

A Method for the Determination of Friction Constants from the Analysis of the Motion of a Slider

If the motion of a slider drawn by a flexible member over a stationary surface is closely examined, it will be noted that the motion generally consists of a series of forward jerks. This intermittent motion has been called "stick-slip" motion and is a form of self excited vibrations or relaxation oscillations. Several investigators including Kaidanovskii[1,2], Papenhuyzen[3], Blok[4], Bowden et al[5-8], Tomlinson[9], Sampson, Morgan, Reed, and Muskat[10-12], Thomas[13], Bristow[14], and Dudley and Swift[15] have noted and examined this type of motion.

---

[1] Kaidanovskii, N. L., and S. E. Haykin. (1933), "Mechanical Relaxation Oscillations," Zhurnal Tech. Phys. USSR, Vol. 3, No. 1, pp. 91-109.

[2] Kaidanovskii, J. L. (1949), "The Nature of the Mechanical Autovibrations Produced in Dry Friction," Zhurnal Technicheskai Fisiki, Vol. 19, pp. 985-96.

[3] Papenhuyzen, P. J. (1938), "Wrijvingsproeven in Verband met het slippen van autobanden," De Ingenieur, Vol. 53, pp. v75-v81.

[4] Blok, H. (1940), "Fundamental Mechanical Aspects of Boundary Lubrication," J. Soc. Aut. Eng., Vol. 46, pp. 54-68.

[5] Bowden, F. P., and K. E. W. Ridler. (1936), "The Surface Temperature of Sliding Metals, the Temperature of Lubricated Surfaces," Proc. Roy. Soc., Vol. A154, pp. 640-56.

[6] Bowden, F. P., (1939), "The Nature of Sliding and the Analysis of Friction," Proc. Roy. Soc., Vol. A 169, pp. 371-91.

[7] Bowden, F. P., L. Leben, and D. Tabor. (1939), "The Sliding of Metals, Frictional Fluctuations, and Vibration of Moving Parts," The Engineer, Vol. 168, pp. 214-217.

The fundamental characteristics of the intermittent "stick-slip" motion may be demonstrated through the analysis of the simple spring-mass-friction system having a single degree of freedom represented by the model sketched in Figure 4-1.

In this model a slider resting on a stationary base is attached through a spring to a carriage. The position of the slider relative to the carriage is designated by x, and relative to the stationary base by x'. If the carriage is moving with a velocity, v, the relation between x and x' may be expressed as:

$$x' = \int v dt - x \qquad (4\text{-}1)$$

---

[8] Bowden, F. P. and D. Tabor. (1950), The Friction and Lubrication of Solids, Oxford: Clarendon Press, 337 pp.

[9] Tomlinson, G. A. (1927), "The Rusting of Steel Surfaces in Contact," Proc. Roy. Soc. Vol. A 115, pp. 472-483.

[10] Morgan, F., M. Muskat, and D. W. Reed. (April, 1949), "Friction of Dry and Lubricated Surfaces," Lubrication Eng., Vol. 5, No. 2, pp. 75-82, 103.

[11] Morgan, F., M. Muskat, and D. W. Reed. (1941), "Studies in Lubrication X, Friction Phenomenon and the Stick-Slip Process," J. Appl. Phys., Vol. 12, pp. 743-752.

[12] Sampson, J. B., F. Morgan, D. W. Reed, and M. Muskat. (1943), "Friction Behavior during the Slip Portion of the Stick-Slip Process," J. Appl. Phys., Vol. 14, p. 696.

[13] Thomas, S. (1930), "Vibrations Damped by Solid Friction," Phil. Mag., Series 7, Vol. 9, pp. 329-45.

[14] Bristow, J. R. (1949), "Measurement of Kinetic Boundary Friction on Experimental Investigation of Oiliness," Proc. Inst. Mech. Eng., Vol. 160, No. 3, pp. 384-92.

[15] Dudley, B. R., and H. W. Swift. (1949), "Frictional Relaxation Oscillations," Phil. Mag., Vol. 40, No. 307, pp. 849-61.

FIGURE 4 - 1

MODEL OF SPRING-MASS-FRICTION SYSTEM

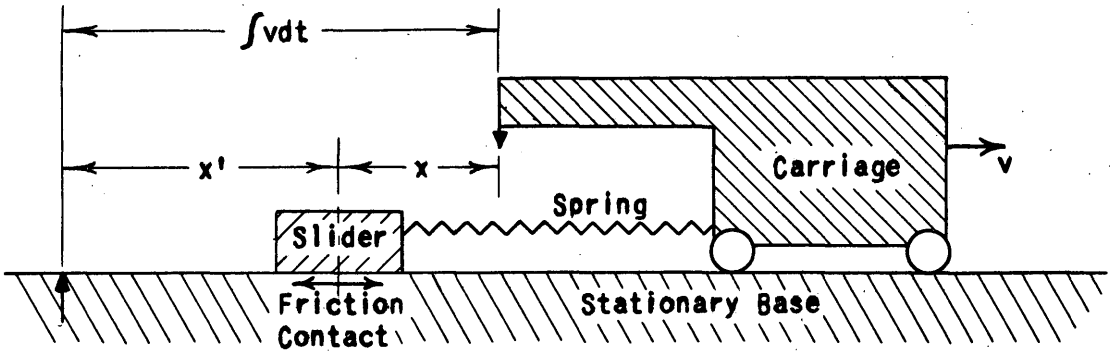

For situations in which the carriage is moving with a constant velocity equal to v_o the relation between the two positions reduces to:

$$x' = v_o t - x \qquad (4\text{-}2)$$

The motion of the slider is governed by three forces, the inertial force of the slider mass, the force of the spring attaching the slider to the carriage, and the friction force between the slider and the stationary base. These forces combine to form the basic equation of motion:

$$m\ddot{x} + kx + f(F) = 0 \qquad (4\text{-}3)$$

in which

$m\ddot{x}$ = Inertial Force

kx = Spring Force

$f(F)$ = Frictional Force

For convenience the direction of positive force in Equation (4-3) is chosen in the same direction as increasing x' values or decreasing x values.

Let us next consider several possible functions for the frictional force function and the resulting slider motion corresponding to zero carriage velocity and to a constant carriage velocity.

Case A

First if the friction function is zero, the slider will oscillate sinusoidally around the spring mid-position whether the carriage is stationary or moving with a constant velocity.

Case B

The second possible friction function is a frictional resistance equal to a constant quantity, $f(F) = F_k$. Let us consider the resulting motion under the conditions of zero carriage velocity. This case is commonly known as Coulomb damped free vibration. Since the friction force for this case is independent of the displacement and its derivatives, a single algebraic sign of the damping force cannot be assigned which would truly represent the friction over an entire cycle of motion. Considering the frictional force as a retarding force, it is therefore necessary to assign an algebraic sign corresponding to the direction of travel. This further necessitates writing two sets of equations of motion, one for each direction of travel. These equations are:

$$m\ddot{x} + kx - F_k = 0 \qquad (4\text{-}4a)$$

$$m\ddot{x} + kx + F_k = 0 \qquad (4\text{-}4b)$$

The first of these equations applies to the situation in which the slider of Figure 4-1 is moving to the right and the second equation to motion of the slider toward the left.

Dividing all terms by m and transferring the friction term to the right hand side, equation (4-4a) becomes:

$$\ddot{x} + \frac{k}{m}x = \frac{F_k}{m} \qquad (4\text{-}5)$$

the solution of which can be shown to equal:

$$x = A \sin\sqrt{\frac{k}{m}}\,t + B \cos\sqrt{\frac{k}{m}}\,t + \frac{F_k}{k} \qquad (4\text{-}6)$$

Assuming that the slider motion started from zero velocity and an initial displacement of x_o, the particular solution of the first motion equation becomes:

$$x = (x_o - \frac{F_k}{k}) \cos\sqrt{\frac{k}{m}}\, t + \frac{F_k}{k} \qquad (4\text{-}7)$$

Taking the initial conditions of the second motion equation from the final conditions of the first, the particular solution of the second equation becomes:

$$x = (x_o - \frac{3F_k}{k}) \cos\sqrt{\frac{k}{m}}\, t - \frac{F_k}{k} \qquad (4\text{-}8)$$

Motion of the slider will proceed in this manner alternating between solutions of Equations (4-4a) and (4-4b) as illustrated in Figure 4-2. During each half cycle the amplitude of motion is diminished by $2\frac{F_k}{k}$. Thus a total amplitude decay equaling $4\frac{F_k}{k}$ occurs each cycle.

It is interesting to note that over the first half cycle the midpoint of the oscillation occurs at the displacement equal to $\frac{F_k}{k}$.

$$x_{m1} = x_o \cos\sqrt{\frac{k}{m}}\,(\sqrt{\frac{m}{k}}\,\frac{\pi}{2}) + \frac{F_k}{k}\left[1 - \cos\sqrt{\frac{k}{m}}\,(\sqrt{\frac{m}{k}}\,\frac{\pi}{2})\right] \qquad (4\text{-}9a)$$

$$x_{m1} = \frac{F_k}{k} \qquad (4\text{-}9b)$$

Similarly, the midpoint of the second half cycle occurs at:

$$x_{m2} = -\frac{F_k}{k} \qquad (4\text{-}10)$$

This midpoint of oscillation continues to alternate from $+\frac{F_k}{k}$ to $-\frac{F_k}{k}$. Meanwhile the amplitude of motion decreases by $2\frac{F_k}{k}$ during each half cycle. Motion will finally terminate when the displacement at the end of a slide lies within the range $-\frac{F_k}{k} \leqslant x \leqslant +\frac{F_k}{k}$. At this point

FIGURE 4 - 2

ZERO CARRIAGE VELOCITY

COULOMB DAMPED FREE VIBRATION OF SLIDER RELATIVE TO CARRIAGE

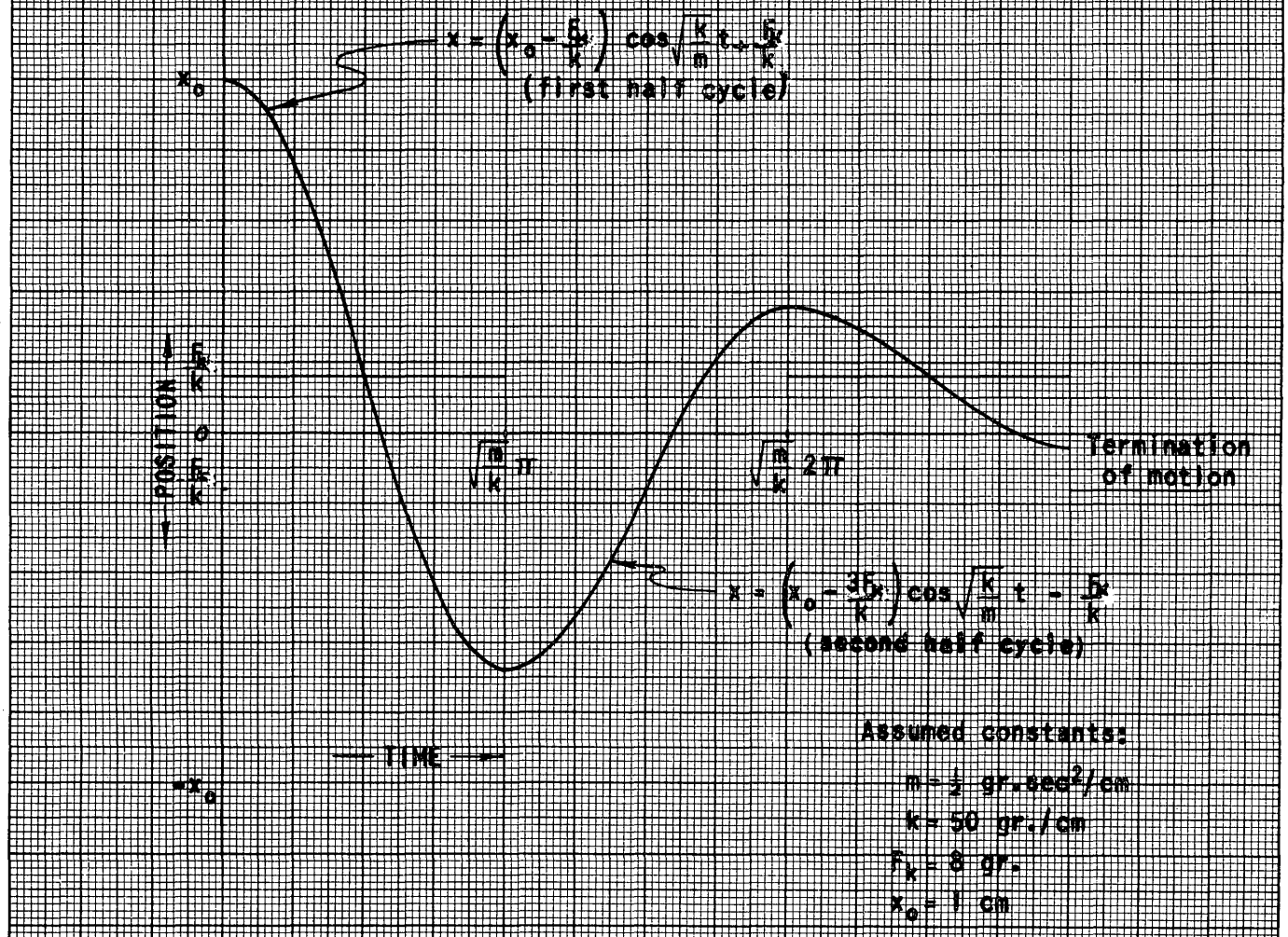

the spring force no longer exceeds the friction force and the slider cannot move.

Next consider the influence of a constant friction function in the situation in which the carriage is moving at a constant velocity relative to the base. The friction function for this case must be defined as:

$$\text{for } \dot{x}' > 0, \quad f(F) = -F_k$$

$$\text{for } \dot{x}' < 0, \quad f(F) = +F_k$$

$$\text{for } \dot{x}' = 0, \quad f(F) = k\,(x' - v_o t)$$

$$-F_k \leqslant k(x' - v_o t) \leqslant +F_k$$

The friction function specified in the zero velocity case, it should be recalled, changed algebraic signs when the velocity of the slider relative to the carriage, $\dot{x}$, was reduced to zero. In the present situation the algebraic sign of the friction term changes when the slider velocity relative to the stationary base, $\dot{x}'$, becomes zero.

Due to the peculiarities in this change of algebraic sign, it is most convenient to analyze the motion with reference to the stationary base. This shift to x' coordinates has no effect on the inertial force term since the carriage is assumed as moving at a constant velocity. The spring force on the other hand depends upon the position of the slider relative to the carriage, thus requiring a suitable transformation in the spring force term.

The equations of motion of the slider for the constant friction case are therefore:

$$-m\ddot{x}' + k(v_o t - x') - F_k = 0 \qquad (4\text{-}11a)$$

$$-m\ddot{x}' + k(v_o t - x') + F_k = 0 \qquad (4\text{-}11b)$$

in which equation (4-11a) applies to motion of the slider toward the right, and (4-11b) to motion toward the left.

Equation (4-11a) may be reduced to

$$m \ddot{x}' + k x' = k v_o t - F_k \qquad (4\text{-}12)$$

the general solution os which may be shown to equal

$$x' = v_o t - A \sin\sqrt{\frac{k}{m}}\, t - B \cos\sqrt{\frac{k}{m}}\, t - \frac{F_k}{k} \qquad (4\text{-}13)$$

Choosing again as the initial conditions the position and velocity such that at

$$t = 0, \quad (x')_{t=0} = - x'_o \quad \text{and} \quad (\dot{x}')_{t=0} = 0$$

then the integration constants become:

$$A = \sqrt{\frac{m}{k}}\, v_o \qquad (4\text{-}14a)$$

$$B = (x'_o - \frac{F_k}{k}) \qquad (4\text{-}14b)$$

Combining the trigonometric terms the position of the slider relative to the base may be expressed as:

$$x' = v_o t - \sqrt{\frac{m}{k} v_o^2 + (x'_o - \frac{F_k}{k})^2}\, \cos\left(\sqrt{\frac{k}{m}}\, t - \tan^{-1}\frac{\sqrt{\frac{m}{k}}\, v_o}{x'_o - \frac{F_k}{k}}\right) - \frac{F_k}{k} \qquad (4\text{-}15)$$

Equation (4-2) may be used to transform the slider position relative to the base to the slider position relative to the carriage.

The slider positions relative to the base as specified by Equation (4-12) and relative to the carriage are plotted in Figures(4-3) and (4-4). Examination of the position equations and figures reveals several interesting facts regarding the motion under the assumed condition of constant friction resistance.

FIGURE 4 - 3

CONSTANT CARRIAGE VELOCITY
COULOMB DAMPED VIBRATION OF SLIDER RELATIVE TO BASE

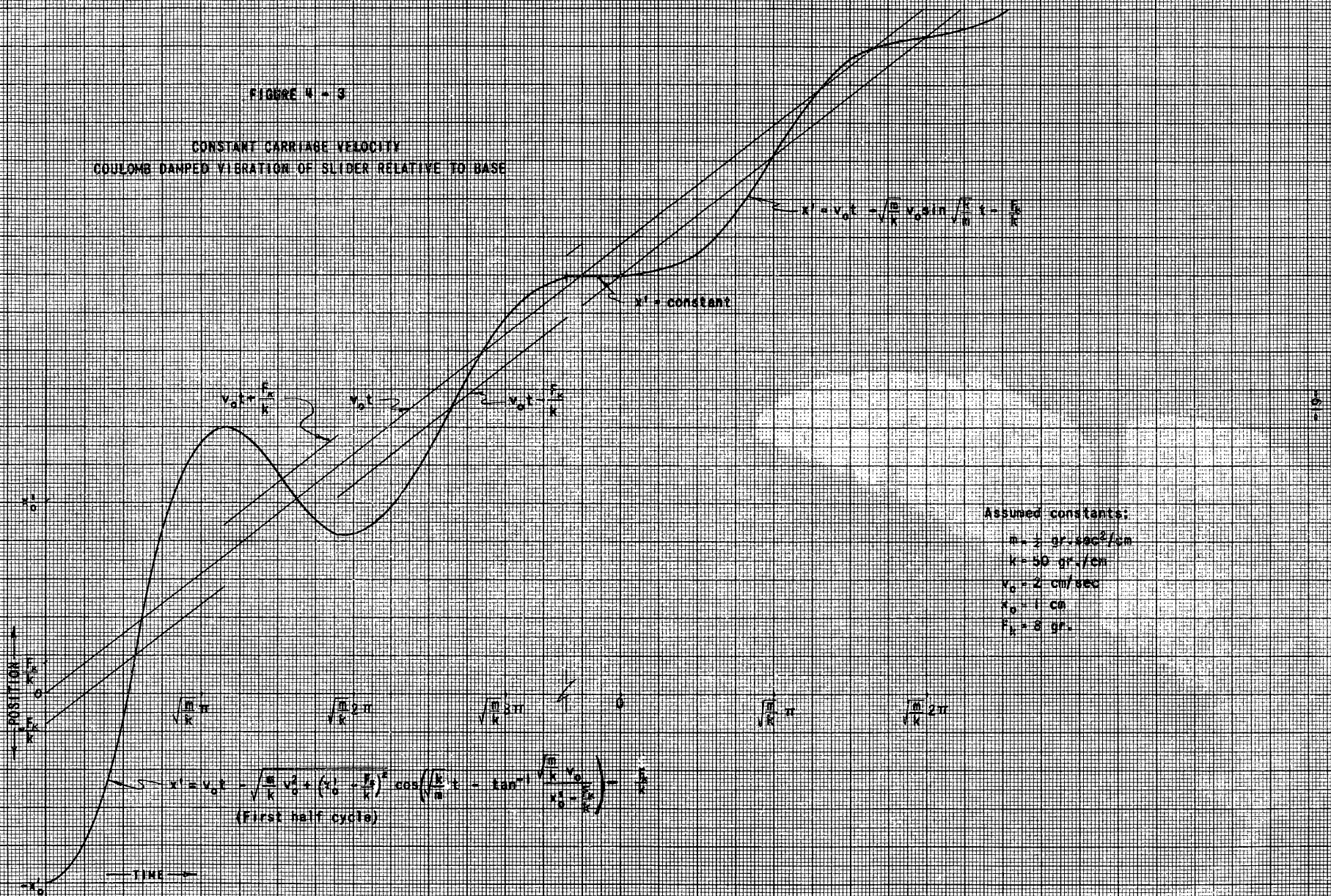

Assumed constants:

$m = \frac{1}{2}$ gr-sec^2/cm
$k = 50$ gr./cm
$v_0 = 2$ cm/sec
$x_0' = 1$ cm
$F_k = 8$ gr.

FIGURE 5 - 6

CONSTANT CARRIAGE VELOCITY
COULOMB DAMPED VIBRATION OF SLIDER RELATIVE TO CARRIAGE

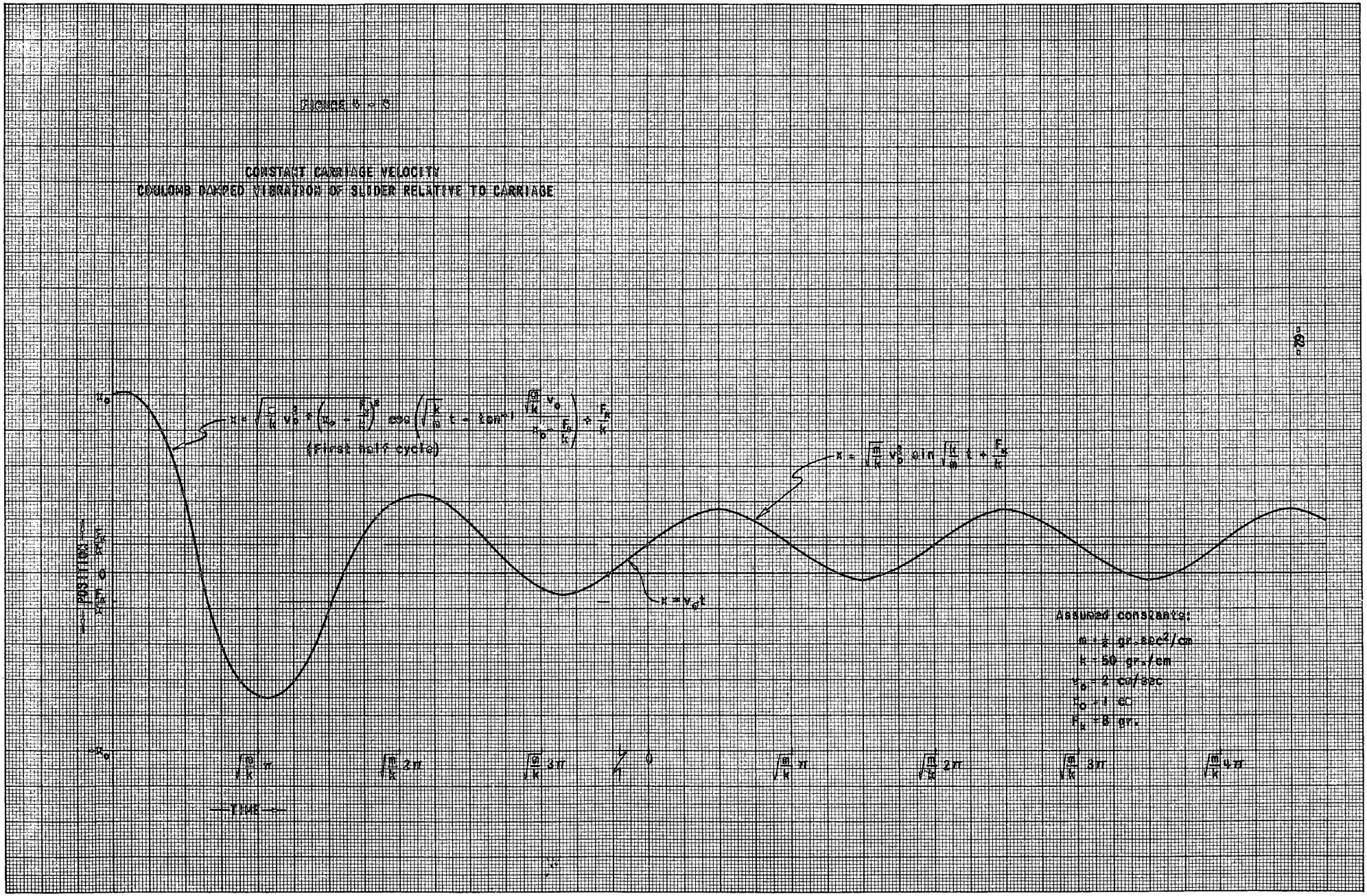

At the initial instant the slider, while at rest relative to the base, is still moving to the left or rearward relative to the carriage. In the first time interval it continues this rearward motion relative to the carriage, reaching an extreme position when the velocity relative to the carriage equals zero at the time:

$$t = \sqrt{\frac{m}{k}} \tan^{-1} \frac{\sqrt{\frac{m}{k}}\, v_o}{x'_o - \frac{F_k}{k}} = \sqrt{\frac{m}{k}}\, \phi_1 \qquad (4\text{-}16a)$$

During this first time interval the friction force is being exerted toward the left due to the motion of the slider toward the right. The inertial force is acting toward the left and the spring force is opposed by both the inertial force and the friction force. This force arrangement continues as the slider slips forward relative to both base and carriage.

At the instant at which the slider position relative to the carriage equals the ratio of the friction force to the spring constant, $x = \frac{F_k}{k}$, the spring force exactly equals the friction force. However, since the slider approaches this position at a velocity somewhat above the carriage velocity, it slips on past the neutral position. The vectorial direction of the inertial force and the spring force changes at this neutral position. In the following time interval the inertial force is to the right while the spring force and friction force are to the left.

At the time

$$t = \sqrt{\frac{m}{k}}\, (\pi + \phi_1) \qquad (4\text{-}16b)$$

the slider comes to rest relative to the carriage but continues forward

relative to the base. The slider finally stops at the time instant:

$$t = \sqrt{\frac{m}{k}}\,(\pi + 2\,\phi_1) \qquad (4\text{-}16c)$$

and reverses its motion relative to the base. With a reversal in the direction of motion relative to the base there occurs a reversal in the direction of the friction force and Equation (4-11b) becomes applicable.

The initial conditions upon Equation (4-11b) are similar to the conditions placed upon Equation (4-11a) in that the velocity $\dot{x}' = 0$. The initial position, however, has been increased by the movement of the carriage and decreased by frictional drag to the value:

$$x'_1 = v_o\sqrt{\frac{m}{k}}\left(\pi + 2\,\tan^{-1}\frac{\sqrt{\frac{m}{k}}\,v_o}{x'_o - \frac{F_k}{k}}\right) + \left(x'_o - \frac{F_k}{k}\right) - \frac{F_k}{k} \qquad (4\text{-}17)$$

A particular solution of (4-11b) may be determined using the above initial conditions which will hold during the period in which the slider is moving rearward relative to both carriage and stationary base. This solution ceases to apply at time

$$t = \sqrt{\frac{m}{k}}\left(2\,\pi + 2\,\tan^{-1}\frac{\sqrt{\frac{m}{k}}\,v_o}{\left(x'_o - \frac{F_k}{k}\right)} - 2\,\tan^{-1}\frac{\sqrt{\frac{m}{k}}\,v_o}{\left(x'_o - \frac{3F_k}{k}\right)}\right) \qquad (4\text{-}18)$$

when the slider again comes to rest on the stationary base.

Over the entire cycle the amplitude of motion of the slider relative to the carriage decreased by $4\,\frac{F_k}{k}$ similar to the attenuation described in the zero carriage velocity situation. This amplitude decrease continues with each oscillation until the slider displacement relative to the

carriage no longer exceeds $\frac{F_k}{k}$ at the end of a slip. The slider then becomes stationary on the base held by the friction force.

It is interesting to note that in addition to the decrease in the amplitude of motion over the cycle there is also an increase in the phase angle. As the difference between the initial spring force of a particular slip and the kinetic friction force becomes smaller, the phase angle grows, reaching a value of $\frac{\pi}{2}$ for a zero difference.

In the period following the stickdown of the slider, the carriage continues to move forward at a constant velocity. This produces an effective displacement of the slider relative to the carriage equal to:

$$x = x_p + v_o (t - t_p) \qquad (4\text{-}19)$$

in which:

x_p = position of the slider relative to the carriage upon coming to rest.

v_o = velocity of the carriage

t = time

t_p = time instant at which slider becomes stationary

At the time, t_q, the carriage has moved forward to such an extent that the slider displacement relative to the carriage and thus the spring force has become sufficient to overcome the friction force. The slider will start to move, but due to its inertia will be unable to immediately assume the finite velocity of the carriage. There is thus a period following the initiation of slider motion in which the slider is being accelerated and in which the spring force is further increased. When the

slider velocity finally reaches the carriage velocity the spring force is considerably greater than the friction force leaving an excess force which operates to further accelerate the slider. The slider therefore slips forward increasing in velocity until the spring force is again reduced to a value equal to the friction force.

At this stage the high speed and the inertia of the slider causes the slider to slip past the neutral point. Beyond this point the friction force must be partially balanced by the inertial force, resulting in a decrease of slider velocity. The slider again slows down, decreasing to the magnitude of the carriage velocity by the time the spring deflection or slider position relative to the carriage has dropped to zero. In the following period the slider velocity decreases further, but since the carriage is moving faster than the slider the spring starts to deflect. At the instant at which the slider velocity relative to the base has reduced to zero, the spring force has increased to equal the constant friction force. This condition is identical with the condition found at t_q and the cycle will be repeated. Thus an oscillatory motion is set up and sustained by the friction force coupled with the carriage velocity.

Case C

Let us next consider the case in which the stationary resistance or static friction is greater than the kinetic friction. The friction function may be defined for zero carriage velocity as:

$$f(F) = F_s \quad \text{for } \dot{x} = 0$$

$$f(F) = F_k \quad \text{for } \dot{x} \neq 0$$

The addition of a high constant static friction force term to the low constant kinetic friction in the zero carriage velocity subcase has very little effect upon the resulting motion. If the spring force at the beginning or the end of a slide is greater than the static friction force, the slider will break away and move as predicted by Case B across to its opposite zero velocity position. During this half cycle the amplitude of motion will be decreased by $2\frac{F_k}{k}$. Oscillatory motion will continue until the amplitude at the end of a slip is less than $\frac{F_s}{k}$. Since the spring force at this point is less than the static friction force, the slider will remain stationary.

For a constant carriage velocity however the presence of a static friction force higher than the kinetic force is a key factor in the generation and maintenance of frictional vibrations. The friction function for this sub case may be defined as

$$f(F) = \pm F_s \quad \text{for } \dot{x}' = 0$$

$$f(F) = \pm F_k \quad \text{for } \dot{x}' \neq 0$$

If a slider is initially released from a displacement considerably greater than $\frac{F_s}{k}$, the slider will slip forward relative to the base as described by Equation (4-15) and illustrated by Figures 4-3 and 4-4. During this slip the amplitude of motion is decreased by $2\frac{F_k}{k}$. If the spring force at the end of the first slip is again greater than the static friction force, the slider will slip in the reverse direction. This oscillation will continue until the static friction force exceeds the available spring force. The slider will then remain stationary upon

the base. The carriage, however will continue moving forward further deflecting the spring until the spring force again balances the static friction force. Similar to the situation described under the constant kinetic case, the slider will start to move at this balance point, but will be unable to immediately assume the velocity of the carriage. The spring is consequently further deflected while the slider is accelerating until the slider velocity reaches the magnitude of the carriage velocity. This additional deflection is much less than the amount obtained in the constant friction case since after the initiation of slider motion the entire spring force above F_k is available for acceleration of the slider mass. The slider continues to accelerate forward, slips past the kinetic friction force level and proceeds to decelerate. By the time the slider velocity has dropped to zero the action of the kinetic friction force has attenuated the motion amplitude considerably below $\frac{F_s}{k}$. The spring force therefore cannot overcome the static friction force and the slider is unable to start its return slip. The slider must thus remain stationary while the carriage moves forward at its uniform velocity, decreasing and then increasing the spring deflection in the opposite direction. When the spring force again equals the static friction force the slider will slip ahead and the cycle will be repeated.

The slider motion therefore consists of two portions, a "slip" portion and a "stick" portion. The "slip" motion corresponds to the motion described by Equations (4-11) through (4-15) under the constant kinetic case. In these equations the initial displacement x'_o may

be replaced by $\frac{F_s}{k}$ to obtain equations applying particularly to this case.

The position of the slider relative to the stationary base during slip is therefore:

$$x' = v_o t - \sqrt{\frac{m}{k} v_o^2 + \left(\frac{F_s - F_k}{k}\right)^2} \cos\left(\sqrt{\frac{k}{m}}\, t - \tan^{-1} \frac{\sqrt{\frac{m}{k}}\, v_o}{\frac{F_s - F_k}{k}}\right) - \frac{F_k}{k} \qquad (4\text{-}20)$$

The phase angle

$$\phi_1 = \tan^{-1} \frac{\sqrt{\frac{m}{k}}\, v_o}{\left(\frac{F_s - F_k}{k}\right)}$$

is again seen to depend upon the ratio of the carriage velocity to the difference in static and kinetic friction. As the kinetic friction approaches the value of the static friction, this difference becomes smaller and the phase angle increases.

After slipping ahead the slider finally comes to rest upon the base at the time:

$$t_p = \sqrt{\frac{m}{k}} \left(\pi + 2 \tan^{-1} \frac{\sqrt{\frac{m}{k}}\, v_o}{\frac{F_s - F_k}{k}}\right) = \sqrt{\frac{m}{k}} \left(\pi + 2\, \phi_1\right) \qquad (4\text{-}21)$$

In the next time interval the slider remains stationary on the base. During this "stick" portion of the cycle the position of the slider relative to the stationary base is given by:

$$x' = v_o t_p = v_o \sqrt{\frac{m}{k}} \left(\pi + 2\, \phi_1\right) \qquad (4\text{-}22)$$

FIGURE V - 5

CONSTANT CARRIAGE VELOCITY

STATIC PLUS CONSTANT KINETIC DAMPED VIBRATIONS OF SLIDER RELATIVE TO BASE

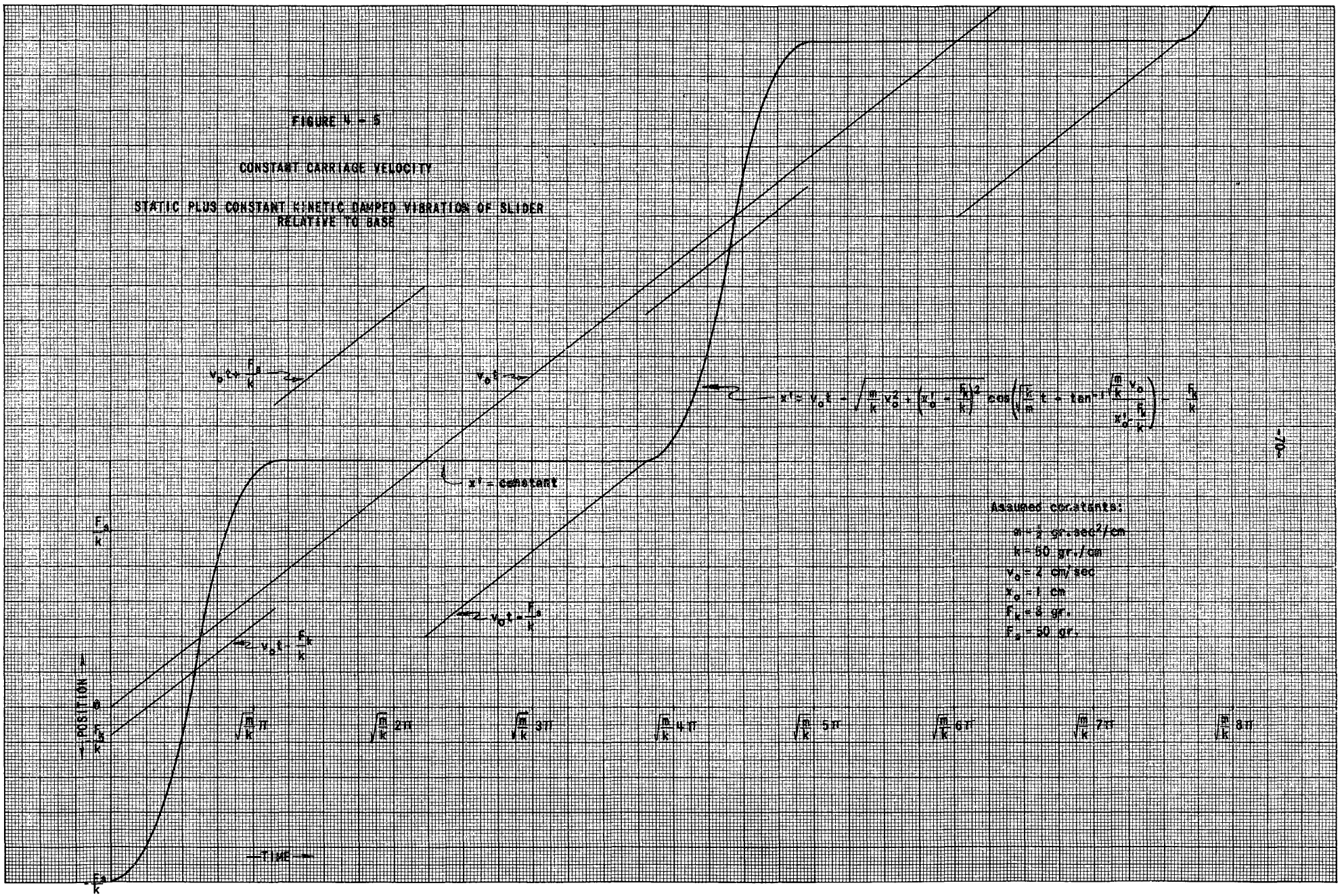

FIGURE 4 - 6

CONSTANT CARRIAGE VELOCITY

STATIC PLUS CONSTANT KINETIC DAMPED VIBRATION OF SLIDER RELATIVE TO CARRIAGE

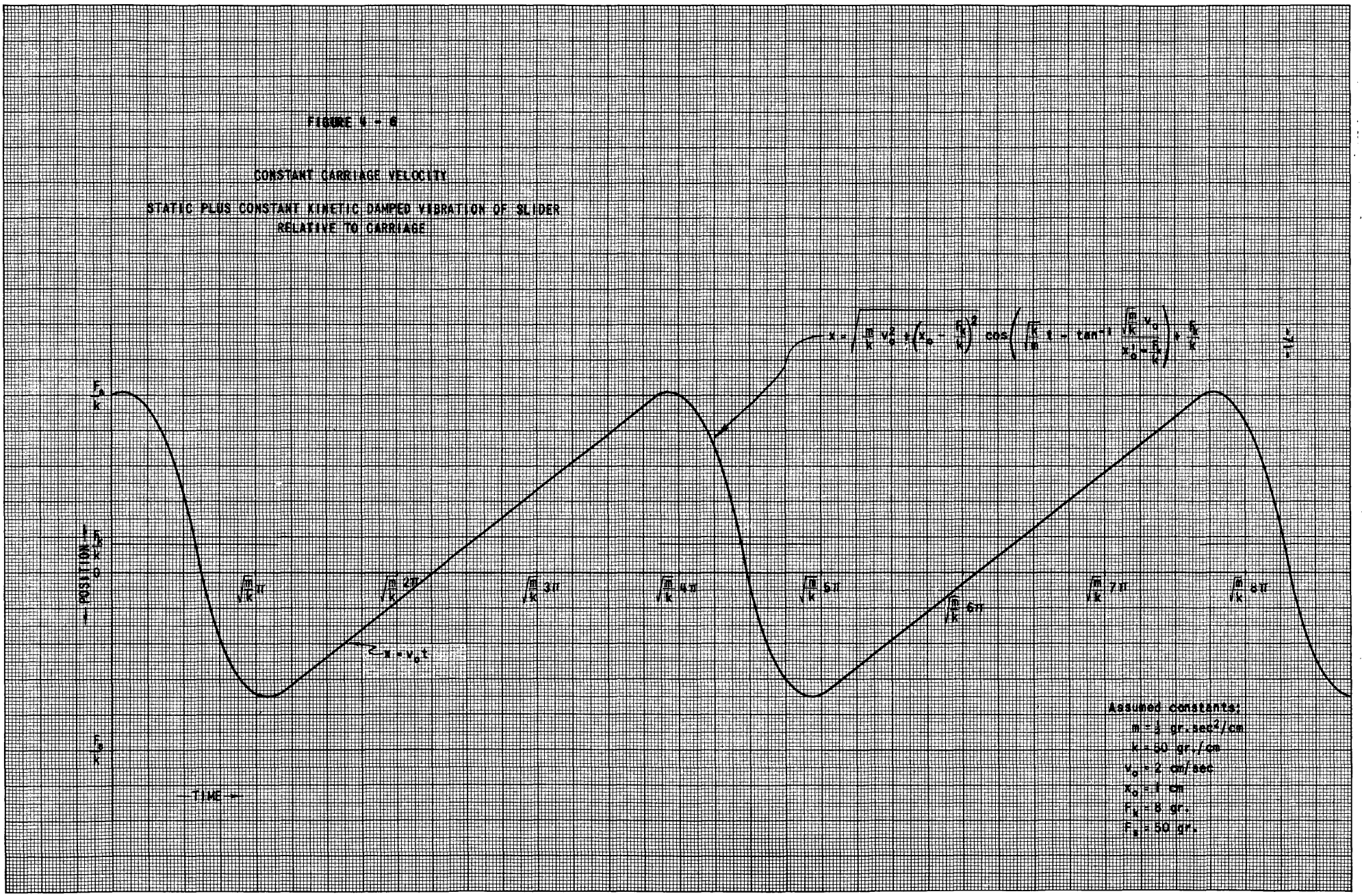

Relative to the carriage the slider position is:

$$x = v_o \Delta t - v_o \sqrt{\frac{m}{k}} (\pi + 2 \phi_1) \qquad (4\text{-}23)$$

where:

$$\Delta t = t - t_p$$

The velocity of the slider during this portion of the motion equals zero relative to the base and v_o relative to the carriage.

The slider therefore moves down the stationary base with a series of jerks. Relative to the carriage, however, this motion appears to be an intermittent type of oscillation. This motion relative to base and to carriage is illustrated in Figures 4-5 and 4-6.

Case D

A friction force which is proportional to the velocity results in the well-known situation of viscous damping. Setting $f(F) = c \dot{x}$ and assuming no driving force, the equation of motion for viscous damped free vibration takes the form:

$$m \ddot{x} + c \dot{x} + k x = 0 \qquad (4\text{-}24)$$

General solution of this differential equation may be written as:

$$x = e^{-\frac{c}{2m} t} \left(A e^{+\sqrt{(\frac{c}{2m})^2 - \frac{k}{m}}\, t} + B e^{-\sqrt{(\frac{c}{2m})^2 - \frac{k}{m}}\, t} \right) \qquad (4\text{-}25)$$

The presence of the exponential multiplying factor, $e^{-\frac{c}{2m} t}$, indicates that as long as the viscous damping constant, c, is positive, the amplitude of motion will be continually decreasing. If the damping constant should happen to be negative, this multiplying factor would result in an increase of amplitude. This situation is physically possible through

only a small region of amplification. For the present, therefore, only positive values of c will be considered.

The actual motion of the system having positive damping depends upon the radical in the exponents. Three types of motion can occur corresponding to real, imaginary, or zero values of this radical. In investigating these types of motion it has been found expedient to introduce a second set of parametric constants defined by the expressions:

$$w = \sqrt{\frac{k}{m}} \quad \text{(Free Vibration Radial Velocity)} \tag{4-26}$$

$$s = \frac{c}{2\sqrt{mk}} = \text{(Damping Ratio)} \tag{4-27}$$

Type 1 motion (Large Damping) occurs for damping in which $s \gg 1$. The radical for this case is real and has a value which is always less than s. The displacement is therefore made up of the sum of two decaying exponentials:

$$x = e^{-swt}\left(Ae^{\sqrt{s^2-1}\,wt} + Be^{-\sqrt{s^2-1}\,wt}\right) \tag{4-28}$$

This nonvibratory or aperiodic motion enables the displaced body to slowly creep back to the equilibrium position.

Assuming the same initial conditions previously used, the constants of integration become:

$$A = \left(\frac{+s + \sqrt{s^2-1}}{2\sqrt{s^2-1}}\right) x_o \tag{4-29a}$$

$$B = \left(\frac{-s + \sqrt{s^2-1}}{2\sqrt{s^2-1}}\right) x_o \tag{4-29b}$$

Type 2 motion (Light Damping) occurs for values of $0 < \varepsilon < 1$. In this type of motion the radical is imaginary and the general solution of the equation of motion is

$$x = e^{-\varepsilon\omega t}\left[Ae^{i\sqrt{1-\varepsilon^2}\,\omega t} + Be^{-i\sqrt{1-\varepsilon^2}\,\omega t}\right] \qquad (4\text{-}30)$$

or expressed in trigonometric terms and condensed:

$$x = e^{-\varepsilon\omega t} C' \left(\cos\sqrt{1-\varepsilon^2}\;\omega t - \phi\right) \qquad (4\text{-}31)$$

Type 2 motion is thus seen to have a displacement which is oscillatory with diminishing amplitude.

Comparison of Equation (4-31) with the equation of motion for undamped free vibration indicates the following differences:

(1) Amplitude of motion in the damped case is decreased by the factor $e^{-\varepsilon\omega t}$.

(2) Frequency of oscillation of the damped case is less than that of the undamped by the factor $\sqrt{1-\varepsilon^2}$.

This type of motion is seen to differ from motion under Coulomb friction in that the midpoint of oscillation is always at the center rather than alternating from $-\frac{F_k}{k}$ to $+\frac{F_k}{k}$. Also in Coulomb friction damping, the amplitude of motion decreased by a constant amount each cycle and the frequency of oscillation equalled the frequency of the undamped case.

If the initial conditions previously considered are utilized then

FIGURE 4 - 7

ZERO CARRIAGE VELOCITY
VISCOUS DAMPED FREE VIBRATION RELATIVE TO CARRIAGE

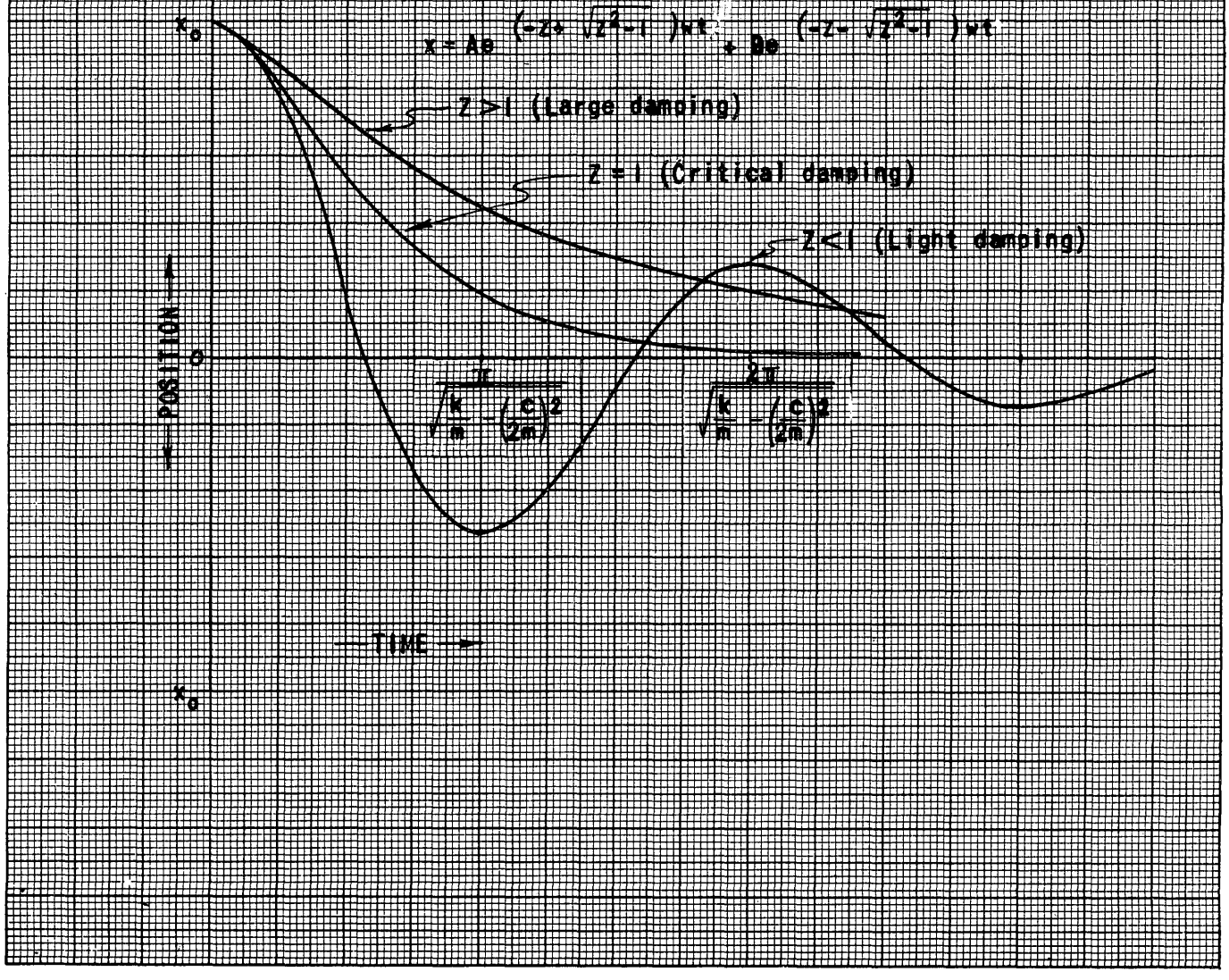

the constants of Equation (4-31) become:

$$C' = \frac{x_o}{\sqrt{1 - \varepsilon^2}} \tag{4-32a}$$

$$\phi = \tan^{-1} \frac{\varepsilon}{\sqrt{1 - \varepsilon^2}} \tag{4-32b}$$

Type 3 motion (Critical Damping) represents the condition intermediate to oscillatory and non-oscillatory motion corresponding to $\varepsilon = 1$. For this value of ε the radical reduces to zero and the solution of the equation of motion becomes:

$$x = (A + Bt)\, e^{-wt} \tag{4-33}$$

The constants determined from the initial conditions previously used become:

$$A = x_o \tag{4-34a}$$

$$B = w\, x_o \tag{4-34b}$$

The three types of motion obtained under viscous resistance and zero carriage velocity are illustrated in Figure 4-7.

Under a constant velocity of the carriage the viscous resistance again dampens the motion of a slider. It should be borne in mind, however, that the resistance is proportional to the relative velocity between the slider and the stationary base rather than between the slider and carriage.

Defining the friction function therefore as:

$$f(F) = c\, \dot{x}'$$

the equation of motion relative to the stationary base for constant carriage velocity with viscous damping becomes:

$$-m\ddot{x}' - c\,\dot{x}' - k\,(x' - v_o t) = 0 \tag{4-35}$$

the general solution of which may be shown to equal:

$$x' + v_o t = - A\, e^{s_1 t} \pm B\, e^{s_2 t} - \frac{c\, v_o}{k} \qquad (4\text{-}36)$$

in which:

$$s_{1,2} = w\,(- g \pm \sqrt{g^2 - 1} \qquad (4\text{-}37)$$

Under conditions of light damping the general solution may be expressed as:

$$x' = v_o t - \frac{c\, v_o}{k} - e^{-\frac{c}{2m} t}\, C' \cos\left(\sqrt{\frac{k}{m} - \left(\frac{c}{2m}\right)^2}\; t - \phi_1\right) \qquad (4\text{-}38)$$

If the slider has the initial conditions:

$$(x')_{t=0} = - x'_o, \quad (\dot{x}')_{t=0} = 0$$

the constants of Equation (4-38) become:

$$C' = \sqrt{\frac{\frac{k}{m}\left(x'_o - \frac{c\, v_o}{k}\right)^2 + \frac{c\, v_o}{m}\left(x'_o - \frac{c\, v_o}{k}\right) + v_o^2}{\frac{k}{m} - \left(\frac{c}{2m}\right)^2}} \qquad (4\text{-}39a)$$

$$\phi_1 = \tan^{-1} \frac{\frac{c}{2m}\; \frac{v_o}{x'_o - \frac{c\, v_o}{k}}}{\sqrt{\frac{k}{m} - \left(\frac{c}{2m}\right)^2}} \qquad (4\text{-}39b)$$

The positions of the slider relative to the base and to the carriage under the condition of light viscous damping are illustrated in Figures 4-8 and 4-9. These figures describe a vibration having the following characteristics:

FIGURE 4 - 8

CONSTANT CARRIAGE VELOCITY

VISCOUS DAMPED VIBRATION OF SLIDER RELATIVE TO BASE

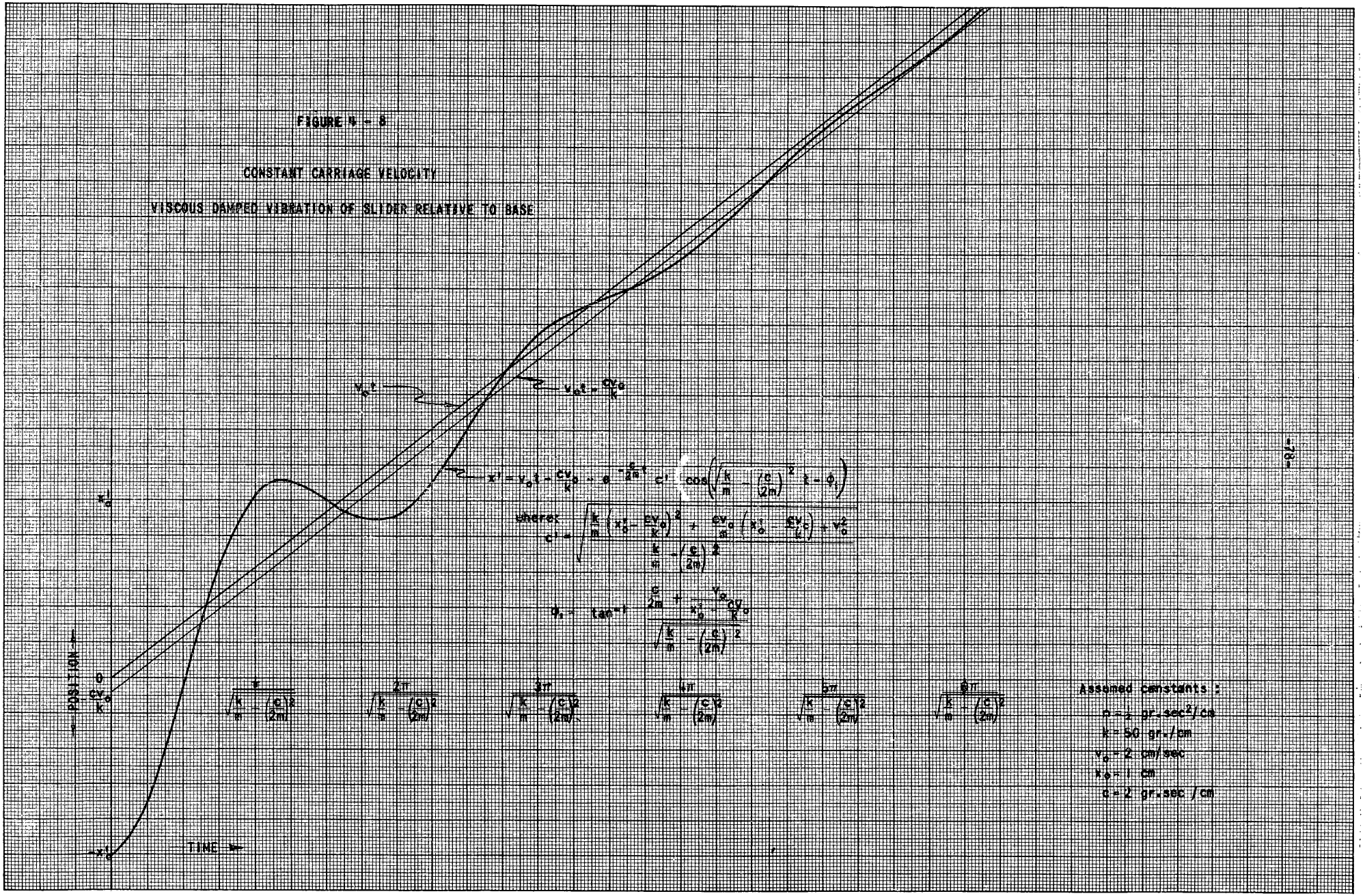

$$x' = v_o t - \frac{cv_o}{k} - e^{-\frac{c}{2m}t} c' \cos\left(\sqrt{\frac{k}{m}-\left(\frac{c}{2m}\right)^2}\, t - \phi_1\right)$$

where:

$$c' = \sqrt{\frac{\frac{k}{m}\left(x_o' - \frac{cv_o}{k}\right)^2 + \frac{cv_o}{m}\left(x_o' - \frac{cv_o}{k}\right) + v_o^2}{\frac{k}{m}-\left(\frac{c}{2m}\right)^2}}$$

$$\phi_1 = \tan^{-1}\frac{\frac{c}{2m} + \frac{v_o - \frac{cv_o}{k}}{x_o' - \frac{cv_o}{k}}}{\sqrt{\frac{k}{m}-\left(\frac{c}{2m}\right)^2}}$$

Assumed constants :

n = 2 gr. sec²/cm

k = 50 gr./cm

v_o = 2 cm/sec

x_o' = 1 cm

c = 2 gr.sec /cm

FIGURE 4 - 8

CONSTANT CARRIAGE VELOCITY

VISCOUS DAMPED VIBRATION OF SLIDER RELATIVE TO CARRIAGE

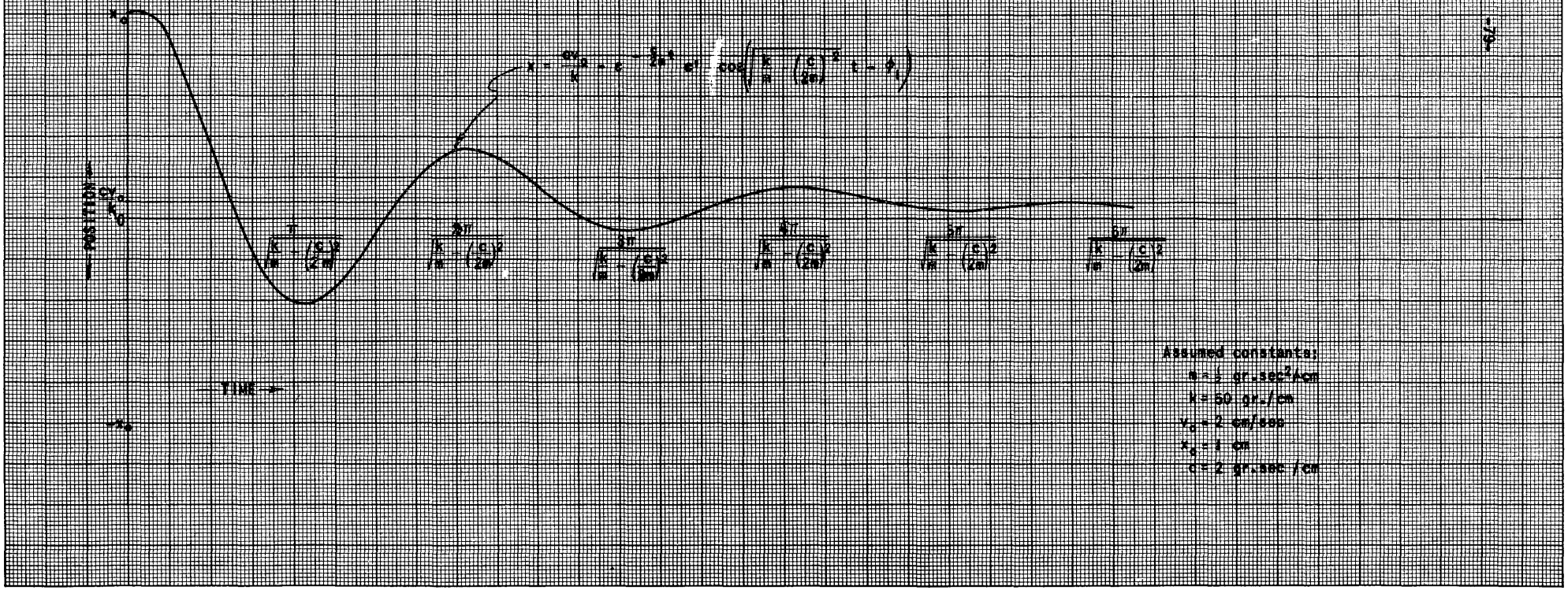

Assumed constants:

$m = .5$ gr.sec^2/cm

$k = 50$ gr./cm

$v_0 = 2$ cm/sec

$x_0 = 1$ cm

$c = 2$ gr.sec/cm

1. Amplitude of oscillation decreases exponentially by the factor $e^{-\frac{c}{2m}t}$.

2. The center of the oscillatory motion is shifted due to the carriage velocity. This displacement amounts to $x_m = \frac{c\,v_o}{k}$ relative to the carriage.

3. The vibrating wave is shifted on the time axis through a phase angle equal to ϕ_1 due to the initial conditions, namely, starting at the arbitrary deflection with a zero velocity.

Case E

Let us next examine the motion resulting from a combination of static friction force with both a constant kinetic friction force and a viscous resistance. Since the zero carriage velocity situation may be easily derived from the constant carriage velocity case let us consider this case.

The friction function for the combination of forces may be expressed as:

$$f(F) = \pm F_s \quad \text{for} \quad \dot{x}' = 0$$

$$f(F) = \pm F_k + c\,\dot{x}' \quad \text{for} \quad \dot{x}' \neq 0$$

Under this frictional resistance a slider initially at rest on the stationary base will be held by the static friction until the forward motion of the carriage causes the spring force to equal the friction force. At this point the slider will start to slip ahead. During a forward slip the equation of motion is:

$$-m\ddot{x}' - c\dot{x}' - k(x' - v_o t) - F_k = 0 \qquad (4\text{-}40)$$

The resulting equation for the position relative to the stationary base becomes:

$$x' = v_o t - e^{-\frac{c}{2m} t} C' \cos\left(\sqrt{\frac{k}{m} - \left(\frac{c}{2m}\right)^2}\, t - \phi_1\right) - \frac{F_k + c\, v_o}{k} \qquad (4\text{-}41)$$

in which the constants for a slider starting from the static friction displacement are:

$$C' = \sqrt{\frac{\frac{k}{m}\left(\frac{F_s - F_k - c\, v_o}{k}\right)^2 + \frac{c\, v_o}{m}\left(\frac{F_s - F_k - c\, v_o}{k}\right) + v_o^2}{\frac{k}{m} - \left(\frac{c}{2m}\right)^2}} \qquad (4\text{-}42a)$$

and:

$$\phi_1 = \tan^{-1} \frac{\frac{c}{2m} + \frac{k\, v_o}{F_s - F_k - c\, v_o}}{\sqrt{\frac{k}{m} - \left(\frac{c}{2m}\right)^2}} \qquad (4\text{-}42b)$$

The resulting motion is again a series of oscillations of the "stick-slip" variety. The slider, after breaking away from the static friction, slips ahead to come to rest again beyond the neutral spring position. Damping caused by the constant kinetic friction and the viscous resistance attenuates the motion so that the maximum deflection at the end of slip will not again equal the static friction/spring constant ratio. Static friction comes into action at the zero velocity position and holds the slider while the carriage moves ahead to deflect the spring again.

The slider position relative to the base (Equation 4-41) with the constants defined by (4-42a) and (4-42b) may be seen to be the generalized relation covering all previous cases. The particular equations of the

former cases may be obtained from this by setting the appropriate variables equal to zero. Motion of this generalized case relative to the stationary base and relative to the carriage is illustrated in Figures 4-10 and 4-11.

The previously-examined cases point out the important influence of the friction function on the amplitude, frequency, and wave form of oscillations. In order to predict the characteristics of expected vibrations in any particular situation it is therefore necessary to know the form of this friction function, the magnitude of the constants, and the influence upon this function of other environmental factors. Conversely, analysis of the oscillations generated under laboratory conditions may aid in the determination of the friction function and in turn lead to a better understanding of the friction mechanism. Examination of laboratory-induced frictional vibrations should also confirm the physical reality of the motion characteristics predicted by the analysis of this chapter.

Let us next consider methods by which the equations developed for the several assumed friction functions might be utilized in the determination of the constants of the assumed functions.

First let us examine the equations developed for Coulomb or constant kinetic friction under the conditions of zero carriage velocity. It was shown that in this case the total attenuation of the vibration amplitude over a half cycle equals $2\frac{F_k}{k}$. Thus the mean of the two extreme positions over this half cycle equals exactly $\frac{F_k}{k}$. The point of inflection for this half cycle also occurs at $+\frac{F_k}{k}$. This inflection point, however, is more difficult to determine experimentally than the extreme displacement positions.

FIGURE 9 - 10

CONSTANT CARRIAGE VELOCITY

STATIC PLUS COULOMB PLUS VISCOUS DAMPED VIBRATION OF SLIDER RELATIVE TO BASE

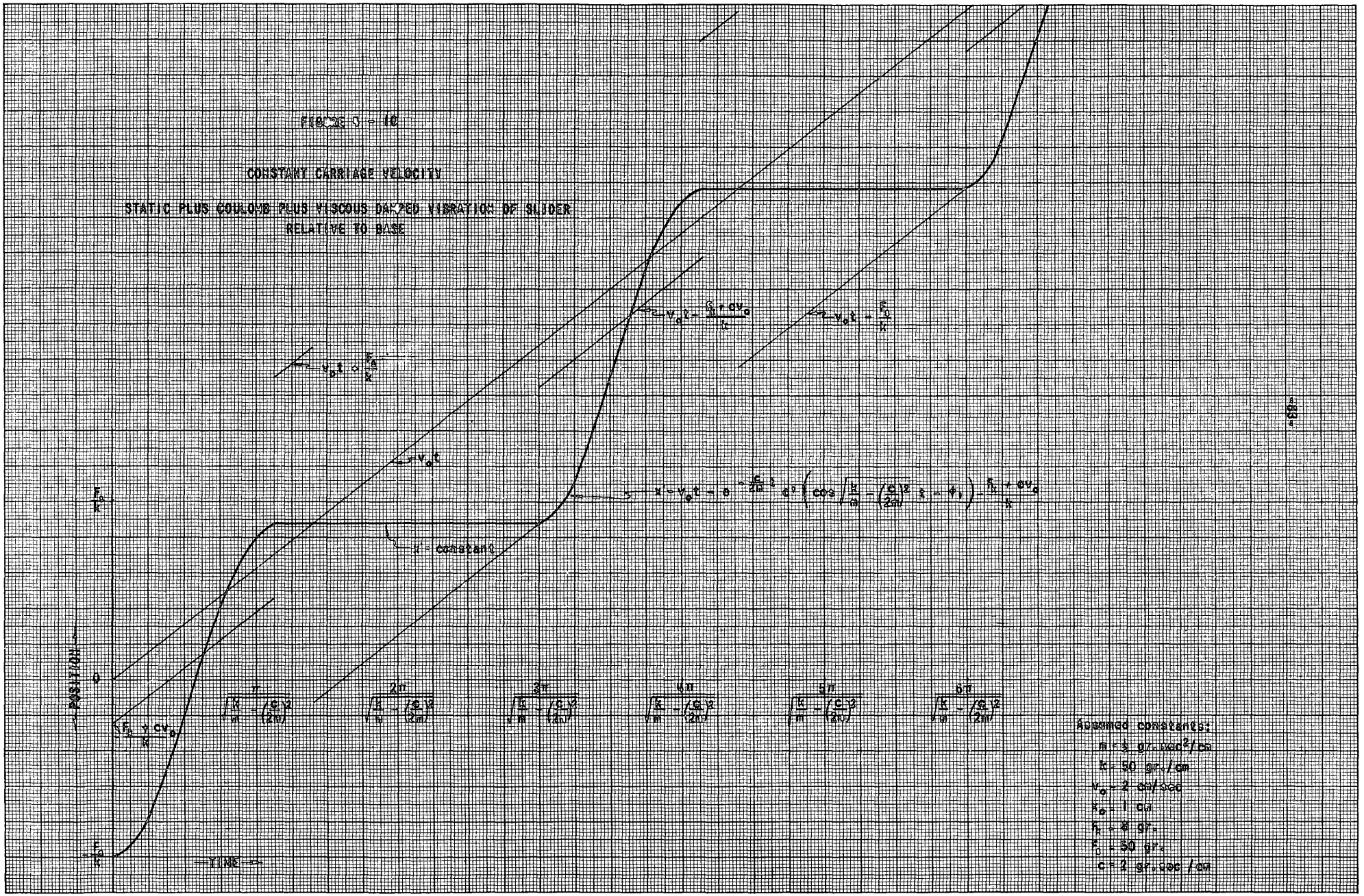

Assumed constants:

$m = 3$ gr. sec^2/cm
$k = 50$ gr./cm
$v_0 = 2$ cm/sec
$x_0 = 1$ cm
$F_h = 8$ gr.
$F_0 = 50$ gr.
$c = 2$ gr. sec/cm

FIGURE V - 11

CONSTANT CARRIAGE VELOCITY

STATIC PLUS COULOMB PLUS VISCOUS DAMPED VIBRATION OF SLIDER RELATIVE TO CARRIAGE

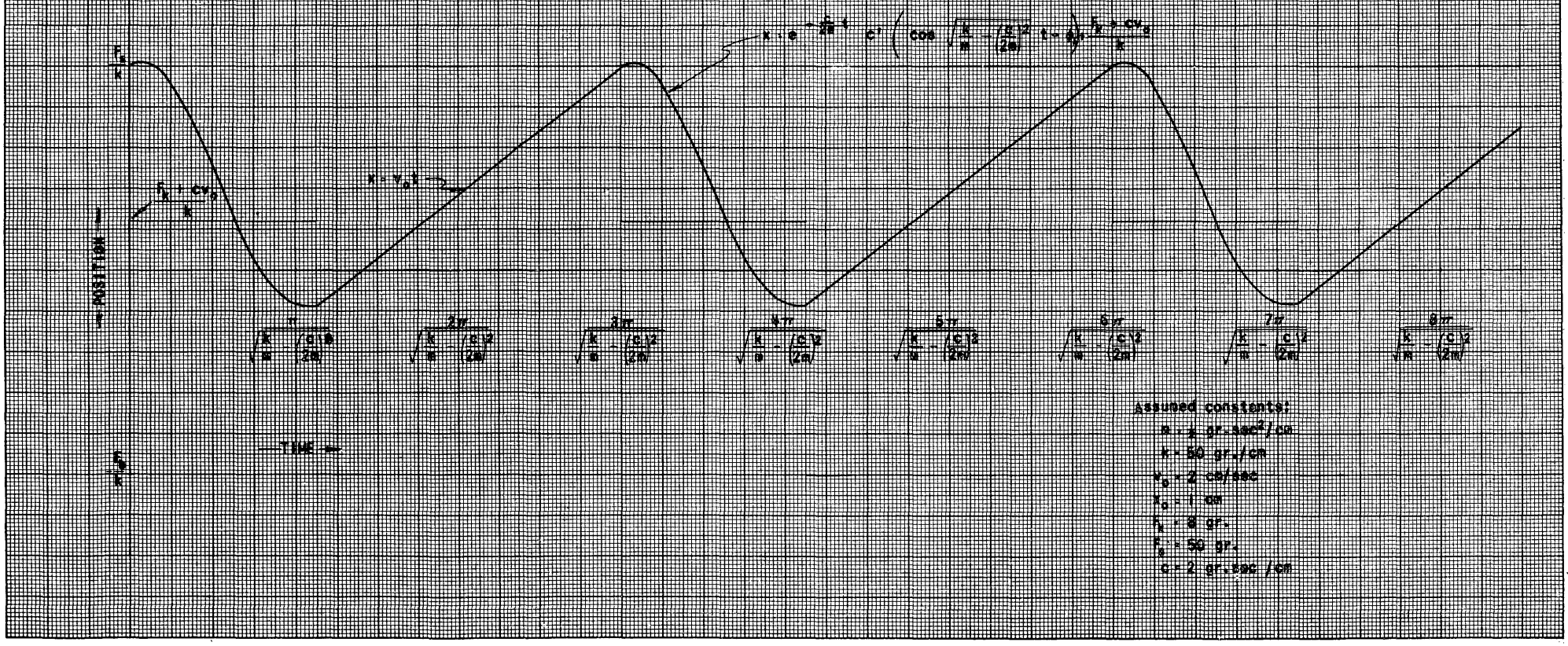

Assumed constants:

$m = .2$ gr.-sec^2/cm
$k = 50$ gr./cm
$v_o = 2$ cm/sec
$x_o = 1$ cm
$F_k = 8$ gr.
$F_s = 50$ gr.
$c = 2$ gr.-sec/cm

A constant carriage velocity has only minor effects upon the slider motion relative to the carriage under Coulomb damping. The mean of the extreme displacements and the point of inflection of the first half cycle still occurs at $\frac{F_k}{k}$. The motion amplitude is slightly increased if the slider starts from rest due to its inertia. Also the phase angle of this maximum displacement becomes

$$\phi_1 = \tan^{-1} \frac{\sqrt{\frac{m}{k}}\, v_o}{x_o - \frac{F_k}{k}}$$

The time during which the slider oscillates around $+\frac{F_k}{k}$ becomes a greater portion of the entire cycle period as the velocity is increased or as the initial displacement is decreased.

If the slider is held stationary upon the base by the constant Coulomb friction while the carriage moves forward to deflect the spring and overcome the frictional force, the resulting sinusoidal motion will be centered throughout the entire period upon $+\frac{F_k}{k}$ with an amplitude proportional to the velocity. Therefore, both the mean of the two extreme displacements and the point of inflection will remain at $\frac{F_k}{k}$.

The determination of the functional constants encountered in viscous damping is generally performed through an auxiliary quantity entitled the logarithmic decrement. This quantity is defined as the natural logarithm of the ratio of any two successive amplitudes. It may be recalled that the position of the slider at any time t is:

$$x = e^{-\frac{c}{2m} t}\, C' \left(\cos \sqrt{\frac{k}{m} - \left(\frac{c}{2m}\right)^2}\, t - \phi_1\right) \qquad (4\text{-}43)$$

Thus if x_n equals the maximum amplitude of the n^{th} vibration and x_{n+1} is the maximum amplitude of the $n+1^{st}$ vibration; from Equation (4-43):

$$x_{n+1} = x_n e^{-\frac{c}{2m} T} \tag{4-44}$$

in which T is the period of the entire cycle. This period of damped oscillation may also be shown to equal:

$$T = \frac{2\pi}{w\sqrt{1-g^2}} = \frac{2\pi}{\sqrt{\frac{k}{m}}\sqrt{1-\frac{c^2}{4mk}}} \tag{4-45}$$

Substituting this value of T in Equation (4-44):

$$x_{n+1} = x_n e^{-\frac{c}{2m}\frac{2\pi}{\sqrt{\frac{k}{m}}}\frac{1}{\sqrt{1-\frac{c^2}{4mk}}}} \tag{4-46}$$

From the definition of the logarithmic decrement therefore, it follows that:

$$d = \ln\frac{x_n}{x_{n+1}} = \frac{c\pi}{\sqrt{mk}}\frac{1}{\sqrt{1-\frac{c^2}{4mk}}} \tag{4-47}$$

For small values of d the series expansion of e^{-d} may be shown to equal approximately:

$$e^{-d} \approx 1 - d + \frac{d^2}{2} \tag{4-48}$$

then:

$$\frac{x_{n+1}}{x_n} = e^{-d} \approx 1 - d + \frac{d^2}{2} \tag{4-49}$$

and:

$$\frac{x_n - x_{n+1}}{x_n} = d - \frac{d^2}{2} \tag{4-50}$$

The experimental measurement of the displacements specified on the left hand side of Equation (4-50) enables the determination of the logarithmic decrement and consequently the evaluation of the component quantities.

In many cases, however, it is difficult or impossible to obtain the trace of an entire cycle. In this situation the amplitude decrease over a half cycle may be determined by measurement of the two extreme positions. Since the time of the half cycle equals half the total cycle period the power of the exponential factor will equal exactly half the logarithmic decrement of the entire cycle. Thus over a half cycle:

$$\frac{x_{n+1/2}}{x_n} = -e^{-\frac{d}{2}} \qquad -1 + \frac{d}{2} - \frac{d^2}{8} \tag{4-51}$$

and:

$$\frac{x_n + x_{n+1/2}}{x_n} = \frac{d}{2} - \frac{d^2}{8} \tag{4-52}$$

Setting:

$$x_{mean} = \frac{x_n + x_{n+1/2}}{2} \tag{4-53}$$

Equation (4-51) becomes:

$$\frac{x_{mean}}{x_n} = \frac{d}{4} - \frac{d^2}{16} \tag{4-54}$$

or substituting for the logarithmic decrement the relation given by Equation (4-47)

$$\frac{x_{mean}}{x_n} = \frac{\pi c}{4\sqrt{mk}} \frac{1}{\sqrt{1 - \frac{c^2}{4mk}}} - \left[\frac{\pi c}{4\sqrt{mk}} \frac{1}{\sqrt{1 - \frac{c^2}{4mk}}} \right]^2 \qquad (4\text{-}54b)$$

By experimental measurement of the initial displacement and the extreme position a half cycle later, it is possible to determine the approximate value of the logarithmic decrement.

It should also be noted that the point of inflection of this half cycle for zero carriage velocity occurred at zero displacement.

For a constant carriage velocity and viscous damping the point of inflection is shifted to $x_i = \frac{c\, v_o}{k}$ and the attenuation over a half cycle increased by $2\,\frac{c\, v_o}{k}$. Since the mean of the extreme displacements is therefore increased by $\frac{c\, v_o}{k}$, the equations for the experimental determination of the logarithmic decrement should be corrected for this quantity.

Thus:

$$\frac{x_{mean} - \frac{c\, v_o}{k}}{x_n} = \frac{d}{4} - \frac{d^2}{16} \qquad (4\text{-}55)$$

The amplitude of motion is again slightly increased due to the inertia of the slider if the slider is suddenly pulled from a rest condition by the moving carriage. Similarly the phase position of the maximum spring deflection is shifted slightly by the constant velocity

condition. The viscous damping condition differs from the Coulomb damping, however, in that the point of inflection does not shift with direction of motion, but always remains at $\frac{c\ v_o}{k}$. After a period of time the amplitude of motion will be completely dampened by the viscous resistance and the slider will move continuously at a deflection equal to $\frac{c\ v_o}{k}$.

If Coulomb friction is present as well as viscous damping the numerator on the left hand side of Equation (4-55) must be further modified to:

$$\frac{x_{mean} - \frac{c\ v_o}{k} - \frac{F_k}{k}}{x_n} = \frac{d}{4} - \frac{d^2}{16} \qquad (4\text{-}56)$$

The point of inflection of the first half cycle for this combination of resistances now occurs at $\frac{F_k + c\ v_o}{k}$.

Since static friction has no influence on the resistance during slider motion, it does not affect the mean position of the slider. It does, however, influence the deflection at which the slider starts to move. Motion of the slider previously held by static friction starts therefore at the position:

$$x = \frac{F_s}{k}$$

This position on the other hand is not the extreme displacement. It may be shown that the maximum displacement for combined static and constant kinetic friction equals:

$$x_{mean} = \sqrt{\frac{m}{k} v_o^2 + \left(\frac{F_s - F_k}{k}\right)^2} + \frac{F_k}{k} \qquad (4\text{-}57)$$

Equation (4-57) may be transformed to:

$$x_{max} = \left(\frac{F_s - F_k}{k}\right) \left[1 + \left(\frac{\frac{m}{k} v_o}{\frac{F_s - F_k}{k}}\right)^2\right]^{1/2} + \frac{F_k}{k} \qquad (4\text{-}58)$$

The second factor of the first term above may be expanded by means of the Binomial Theorem to form an infinite series of the type:

$$(1 + x)^{1/2} = 1 + 1/2\, x - 1/8\, x^2 + \ldots. \qquad (4\text{-}59)$$

This alternating series is known to be convergent for $x<1$.

Therefore if:

$$\frac{F_s - F_k}{k} > \sqrt{\frac{m}{k}}\, v_o \qquad (4\text{-}60)$$

Equation (4-58) may be expanded as:

$$x_{max} = \left(\frac{F_s - F_k}{k}\right) \left[1 + \frac{1}{2}\left(\frac{\sqrt{\frac{m}{k}}\, v_o}{F_s - F_k}\right)^2 - \frac{1}{8}\left(\frac{\sqrt{\frac{m}{k}}\, v_o}{\frac{F_s - F_k}{k}}\right)^4 + \ldots\right] + \frac{F_k}{k} \qquad (4\text{-}61)$$

and reduced to:

$$x_{max} = \frac{F_s}{k} + \frac{m\, v_o^2}{2(F_s - F_k)} + \triangle \qquad (4\text{-}62)$$

where $\triangle$ refers to negligible higher order terms. The displacement at the next extremum a half cycle later is:

$$x_{min} = -\sqrt{\frac{m}{k} v_o^2 + \left(\frac{F_s - F_k}{k}\right)^2} + \frac{F_k}{k} \qquad (4\text{-}63)$$

This equation also may be reduced through use of the Binomial Theorem if:

$$\frac{F_s - F_k}{k} > \sqrt{\frac{m}{k}}\, v_o \qquad (4\text{-}64)$$

Equation (4-63) then becomes:

$$x_{min} = -\left(\frac{F_s - F_k}{k}\right)\left[1 + \frac{1}{2}\left(\frac{\frac{m}{k} v_o}{\frac{F_s - F_k}{k}}\right)^2 + \ldots\right] + \frac{F_k}{k} \qquad (4\text{-}65)$$

which reduces to:

$$x_{min} = -\left(\frac{F_s - 2F_k}{k}\right) - \frac{m v_o^2}{2(F_s - F_k)} + \Delta \qquad (4\text{-}66)$$

The mean position of the maximum and minimum points for static plus constant kinetic friction reduces as previously indicated to:

$$x_{mean} = \frac{x_{max} + x_{min}}{2} \qquad (4\text{-}67)$$

Substituting for x_{max} and x_{min} from Equations (4-62) and (4-66):

$$x_{mean} = \frac{F_s}{k} + \frac{m v_o^2}{2(F_s - F_k)} - \left(\frac{F_s - 2F_k}{k}\right) - \frac{m v_o^2}{2(F_s - F_k)} \qquad (4\text{-}68)$$

$$x_{mean} = \frac{F_k}{k} \qquad (4\text{-}69)$$

Equation (4-69) verifies the statement that the static friction has no influence on the mean slider position for this particular combination of frictional resistance.

The maximum deflection for a combination of static friction plus Coulomb plus viscous resistance may be shown in a fashion similar to the above analysis to equal approximately:

$$x_{max} = \frac{F_s}{k} + \frac{m v_o^2}{2(F_s - F_k - c v_o)} + \Delta \qquad (4\text{-}70)$$

Examination of Equations (4-56) and (4-70) indicates that the values of the friction constants F_s, F_k, and c may be experimentally determined by measurement of the maximum displacement and the mean displacement. Assuming the x_n of Equation (4-56) to equal the maximum displacement the mean position of the slider equals approximately:

$$x_{mean} = \frac{F_k}{k} + \frac{c\, v_o}{k} + x_{max} \frac{\pi c}{4\sqrt{mk}} \frac{1}{\sqrt{1 - \frac{c^2}{4\ mk}}} \qquad (4\text{-}71)$$

It may be noted that the second term on the right hand side of Equation (4-71) is dependent upon the velocity, while the other two terms are velocity independent. This provides a means of distinguishing between the influences of the Coulomb resistance and the viscous resistance. If the mean position is determined over a range of carriage velocities, the slope of the functional relation to velocity or $\frac{d\, x_{mean}}{d\, v_o}$ will equal $\frac{c}{k}$, and the intercept on the mean displacement axis will become

$$\frac{F_k}{k} + x_{max} \frac{\pi c}{4\sqrt{mk}} \frac{1}{\sqrt{1 - \frac{c^2}{4\ mk}}}$$

Thus through measurement of the slope and a separate determination of the spring constant, the value of c may be determined. Knowledge of c will than enable the determination of the constant kinetic friction force.

Another method of experimentally distinguishing between the Coulomb and the viscous resistance is based upon the variation of the load upon

the slider. If the second classical law of friction is accepted, then the static and constant kinetic friction forces may be expressed as:

$$F_s = \mu_s Mg \tag{4-72}$$

$$F_k = \mu_k Mg \tag{4-73}$$

where:

F_s = Static Friction Force

F_k = Constant Kinetic Friction Force

μ_s = Static Coefficient of Friction

μ_k = Kinetic Coefficient of Friction

Mg = Total load on the slider

Further if the second term on the right hand side of Equation (4-70) is ignored, the maximum deflection equals:

$$x_{max} = \frac{F_s}{k} = \frac{\mu_s Mg}{k} \tag{4-74}$$

The mean deflection may therefore be expressed as:

$$x_{mean} = \frac{\mu_k Mg}{k} + \frac{c\, v_o}{k} + \frac{\mu_s Mg}{k} \frac{\pi c}{4\sqrt{mk}} \frac{1}{\sqrt{1 - \frac{c^2}{4mk}}} \tag{4-75}$$

It should be noted that the total inertial mass of the slider expressed by the symbol m differs somewhat from the M of the total load. The total inertial mass includes both the mass of the load and any effective mass of the apparatus under zero load conditions.

Thus:

$$m = M + M_{eff} \tag{4-76}$$

Combining Equations (4-75) and (4-76):

$$x_{mean} = \frac{\mu_k Mg}{k} + \frac{c\, v_o}{k} + \frac{\mu_s Mg}{k} \frac{\pi c}{4\sqrt{(M + M_{eff})\, k}} \frac{1}{\sqrt{1 - \frac{c^2}{4\,(M + M_{eff})\, k}}} \qquad (4\text{-}77)$$

It may be noted that the second term of Equation (4-77) is independent of the load while the first is directly dependent upon the load and the third term depends approximately upon the square root of the load. A plot of the mean displacement versus the load should therefore enable the separation of the Coulomb and viscous resistances.

The above analysis indicates that through experimental measurement of the maximum and the mean positions of a slider for a range of values of the velocity parameter, it should be possible to determine the constants of the several assumed friction functions.

CHAPTER V

FRICTIONAL FORCE EXPERIMENTAL APPARATUS

Chapter V

Frictional Force Experimental Apparatus

Experimental apparatus has been designed and constructed for the investigation of the factors affecting friction on ice and snow. This apparatus has been described in detail in the Progress Reports on Friction on Snow and Ice.

The following sections present a brief review of the principal friction measuring apparatus and the procedures followed in calibrating these apparatus.

A. Linear Path Friction Force Dynamometer

A linear path dynamometer has been utilized for static and low velocity kinetic friction force measurements. This machine enables a test slider to be drawn in a linear path over an ice surface while providing means for detecting and recording the tangential force between the slider and stationary surface. This same detection equipment also indicates the instantaneous position of the slider relative to a moving frame.

A 14-ft. lathe and a carriage sliding on the lathe ways are used as the stationary and moving frames (Fig. 5-1). These units provide a firm base with accurate linear motion of the moving frame of reference. Placed between the lathe ways and supported on the cross webs of the lathe base is a tray for the stationary test material.

Source of power for the carriage motion is supplied by a 1/4 hp. 1800 RPM AC electric motor. This motor is coupled to the input shaft of a hydraulic torque converter which in turn is able to supply output power

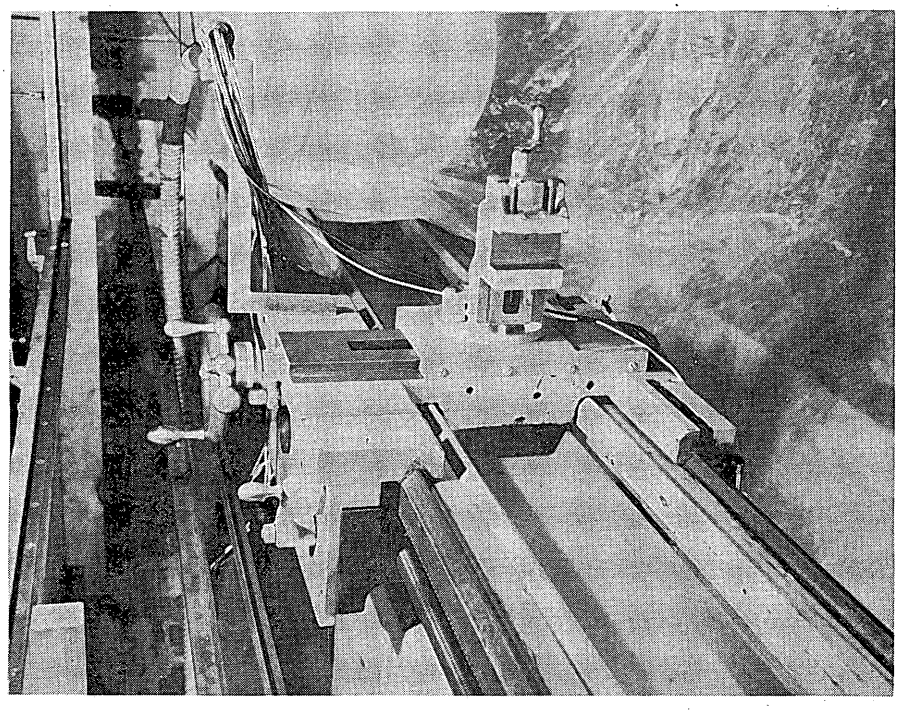

Fig. 5-1 Lathe Base And Carriage.

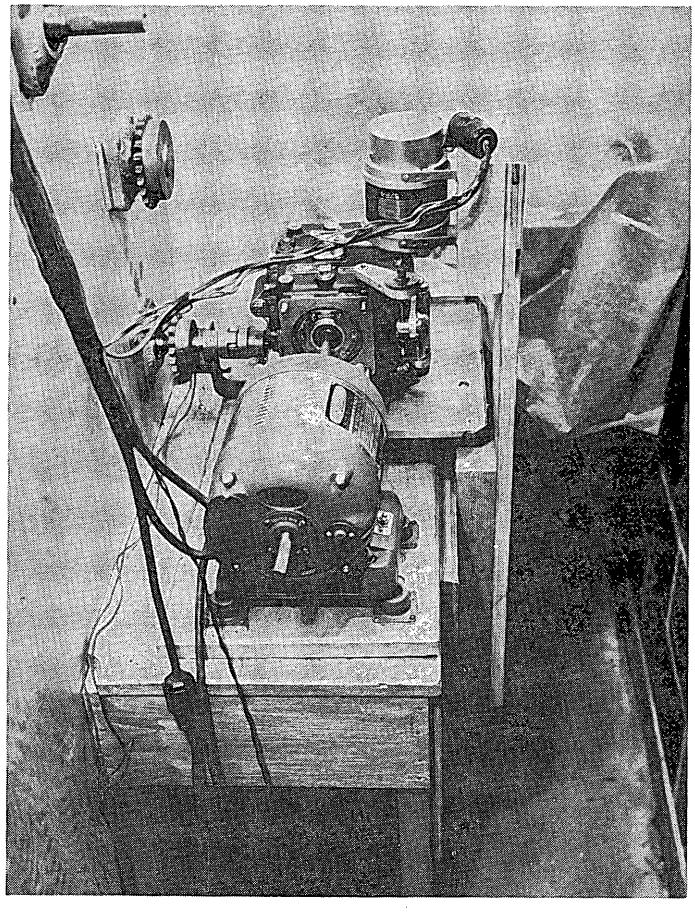

Fig. 5-2 Power And Speed Control Units.

at speeds ranging from 600 RPM in the clockwise direction to 600 RPM in the counterclockwise direction. A fine screw adjustment is connected to the speed control mechanism on the torque converter to enable close control of the speed. This fine screw mechanism is also attached to a synchro unit for remote control of the speed adjustment. A lead screw transmits power from the output shaft on the torque converter to the carriage. Figure 5-2 illustrates these power and speed control units.

In addition to the original carriage cross feed, a vertical column milling clamp is attached to the cross slide block. This permits both lateral and vertical movement of the apparatus for ice surface preparation and force testing. The individual preparation and test devices are connected to the carriage by means of the cross slot vice on the vertical column milling unit.

Figure 5-3 illustrates the apparatus arrangement with the loading and tangential resistance measuring device installed on the carriage. This test device was designed to apply and measure both normal and tangential forces upon a machinist scriber. The point of this scriber in turn transmits the forces to the conical socket on a slider holder (Fig. 5-4). In this manner it is possible to apply the desired forces at a point very close to the surface of interest and thus to reduce the influence of moment arms.

The scriber is supported vertically at one end of a loading arm. The other end is connected to a double set of pivot points which allow motion of the arm assembly in both the vertical and the tangential direction but prevent a twisting motion. Thus, the scriber is always held in a vertical position regardless of the direction of motion.

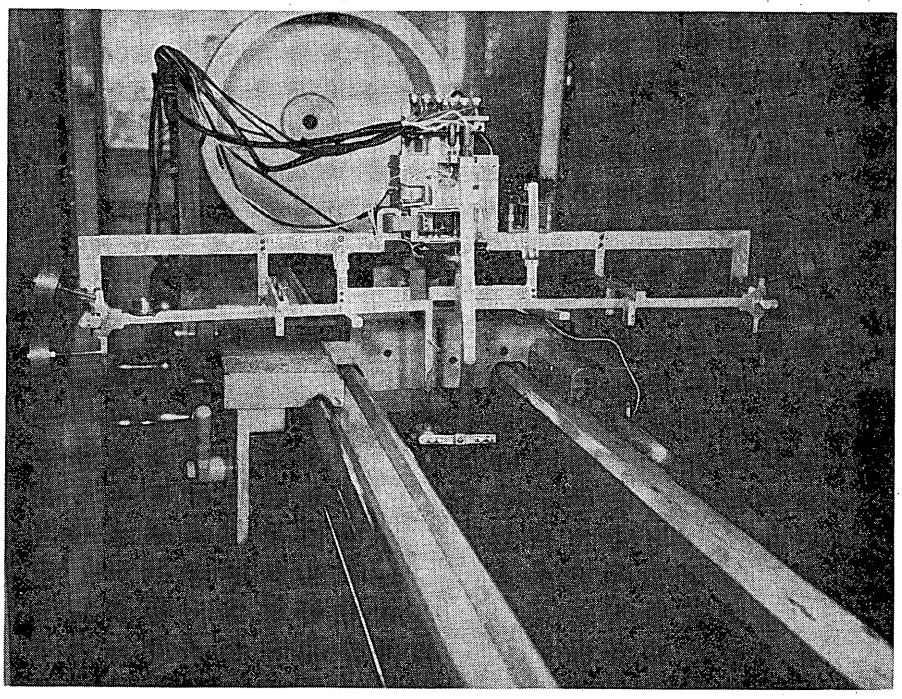

Fig. 5-3 Tangential Resistance Measuring Apparatus Installed On Carriage.

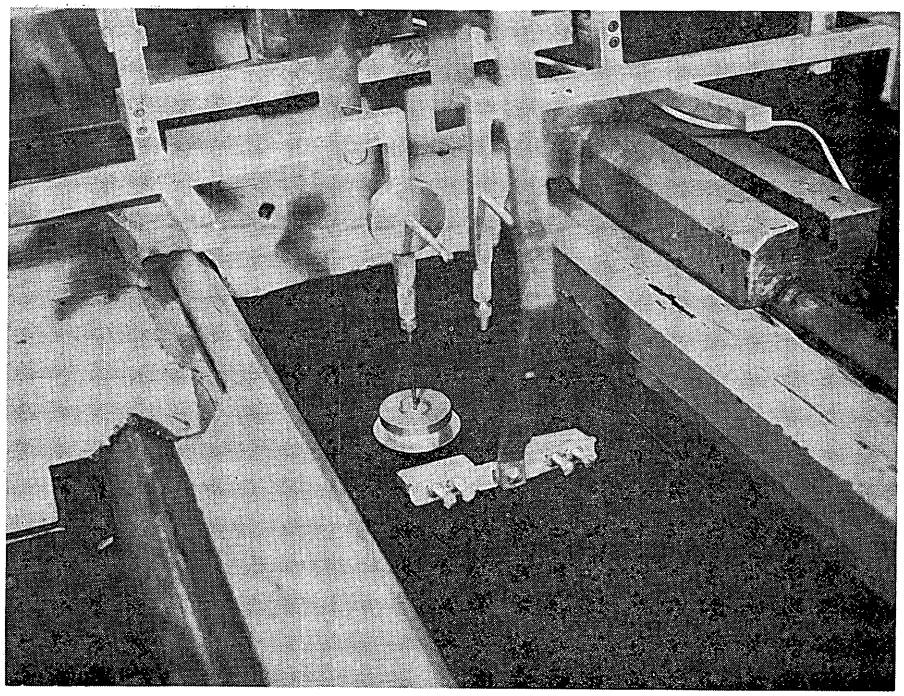

Fig. 5-4 Slider Attachment To Measuring Apparatus.

Load is applied to the slider by means of ring weights slipped over a pin on the loading arm. A cantilever beam connected to the scriber and arm by means of a wire supplies the tangential force. The cantilever beam, constructed of heat treated beryllium copper, is clamped between two beam blocks which in turn attach to a plate on the test device frame. It is possible to vary the length of the cantilever beam and, therefore, the spring constant by varying the vertical position of the beam blocks on the plate. Strain gauges on the cantilever beams detect any beam deflection and transmit this information in the form of a resistance change to Brush Universal Analyzers outside the test cell. The analyzers in turn place a signal upon an oscillograph which finally records the position upon the oscillograph tape.

Through a cam and electric breaker system attached to the leadscrew of the carriage drive it is possible to actuate an event marker on the oscillograph. In this way a mark is placed on the oscillograph tape corresponding to each revolution of the leadscrew. Knowing the pitch of the leadscrew and the speed of the oscillograph tape, it is possible to determine the position and velocity of the moving frame. This information together with the position-time trace of the slider relative to the carriage enables the determination of the position and velocity of the slider relative to the stationary ice sheet.

The test equipment is located within a cold room whose temperature may be controlled within a few degrees down to -65° F. The major portion of the test work has been performed at +15° F. since this temperature

may be obtained and controlled fairly economically. Figure 5-7a illustrates the cold room and the low temperature refrigeration equipment.

In the preliminary test series the several manipulative operations were manually performed by an investigator within the test region. Since the presence of this operator within the temperature cell tended to disturb the thermal control and since the manipulations were difficult to perform, especially at low temperatures, several remote control devices were installed. These devices aided considerably in the temperature control and the ease and speed of operation.

Included amoung these devices were methods for nudging the slider forward and lifting the slider from the ice sheet. Means were also provided for automatically stopping the carriage at the end of the ice sheet through the use of limit switches (Fig. 5-5), for bypassing the limit switches when restarting, for reversing the carriage motion by changing the motor polarity thus eliminating the necessity of adjusting the speed control mechanism, and for remote adjustment of the carriage velocity. Except for the process of changing sliders on the test device all the necessary manipulation operations of the slider and carriage were concentrated at a test station outside the test cell. Figure 5-6 illustrates the remote control equipment and data recording equipment at the test station.

A humidity chamber has been constructed which encloses

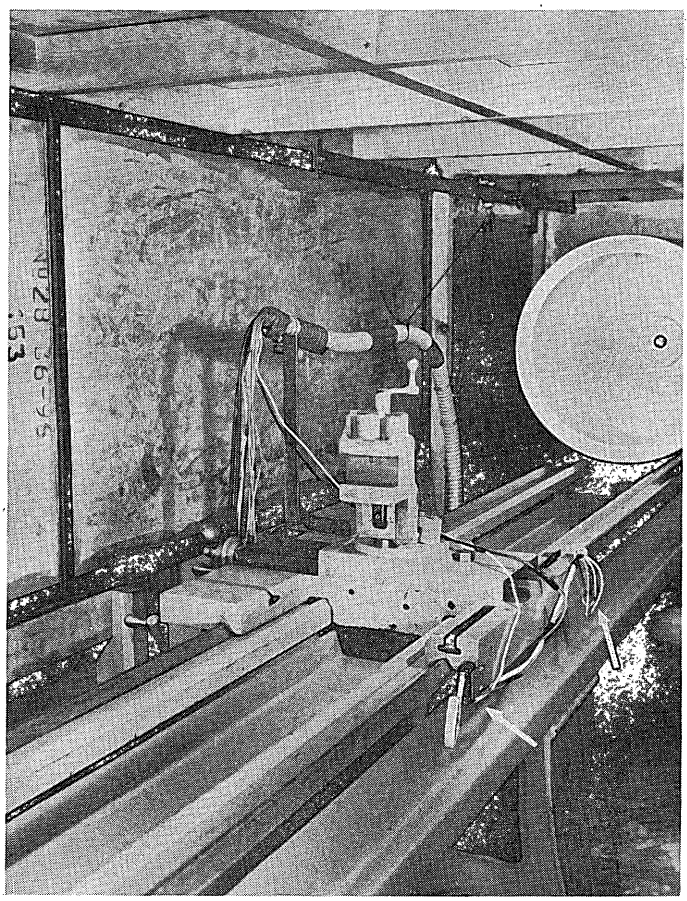

Fig. 5-5 Carriage Limit Switches (arrows).

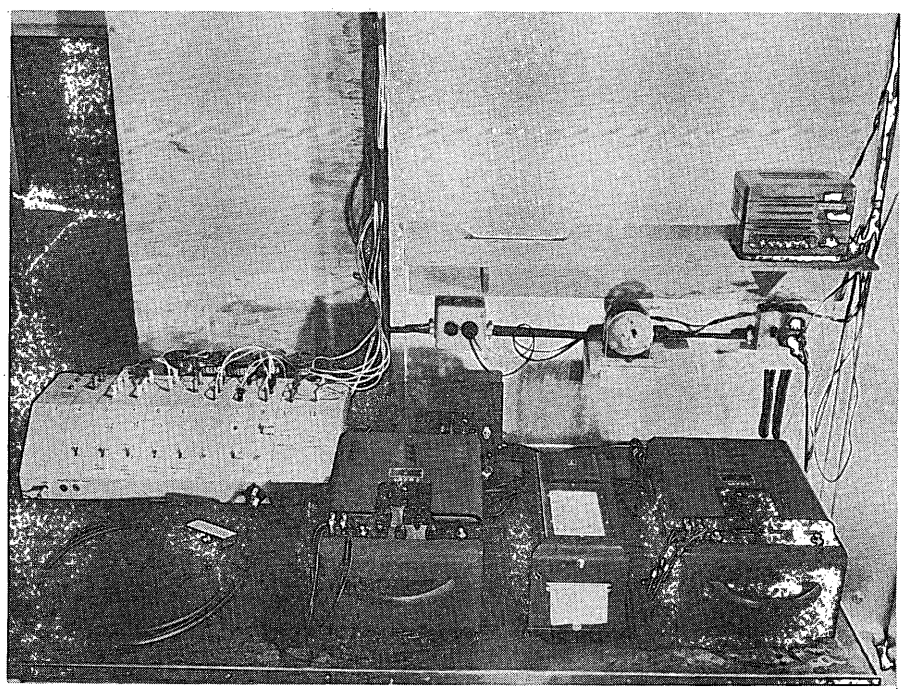

Fig. 5-6 Remote Controls And Recording Equipment At Test Station.

the test region. It had been noted during certain aging and area measuring tests that excessive sublimation occurred on the ice surface unprotected by a stationary slider. This sublimation amounting sometimes to nearly 0.015 inch per day made it impossible to maintain the same uniform surface for each material-load-apparent area slider combination over a given test series. Since the continued loss of ice surface must affect the friction characteristics steps were taken to prevent or reduce the sublimation.

The principal cause of the ice sublimation was found to be the temperature difference between the ice and the evaporation coils of the cooling unit. With this temperature difference there naturally existed a vapor pressure difference which in turn caused the sublimation from the ice and deposition of frost on the coils.

One solution to the sublimation problem would be to place a second cooling unit directly in contact with the ice tray. This would make the ice surface itself cooler than the air and thus reduce the transfer of water molecules from the solid to the gaseous state. On the other hand such a procedure would make equilibrium temperature conditions on the ice surface difficult to obtain. Control of the second cooling unit in such a way as to prevent frost formation on the ice surface would also be a difficult procedure.

A second solution would be to place more evaporation surface in the test region and thereby reduce the temperature differential. While this reduction in temperature differential would reduce the vapor pressure

differential, some difference would still exist and sublimation would continue on a smaller scale.

It was concluded, therefore, that a means of completely isolating the atmosphere of the test region from the atmosphere of the cooling coils was required. A vapor tight box completely surrounding the test apparatus could serve as a barrier to moisture transfer. Furthermore, if such a box were constructed of high thermal conductivity material, such as metal, the ambient temperature of the cold room would be readily transmitted to the interior of the chamber. If the metal chamber had no direct contact with the evaporator coils, the entire surface of the chamber would have the same temperature and there would be no cold spots on the interior and, therefore, no region for the preferred collection of frost.

Several other advantages were noted for the humidity chamber solution including the isolation of the test region from undesired vapors and the shielding of the ice from radiant energy.

Based on the third proposed solution for the sublimation problem, a humidity chamber was designed and constructed. This chamber is illustrated in Figures 5-7b, 5-8, and 5-5. The framework of this chamber is covered with galvanized sheet steel with all corners and joints soldered. A 10 ft. 9 in. x 2 ft. 5 in. door is provided on both sides of the chamber for access to the ice tray and equipment. Windows were placed at strategic points to enable observation of the equipment. Rubber gloves with rubber arm extensions were also attached in such a way as to enable manipulation of certain equipment within the chamber without opening it. (Fig. 5-8)

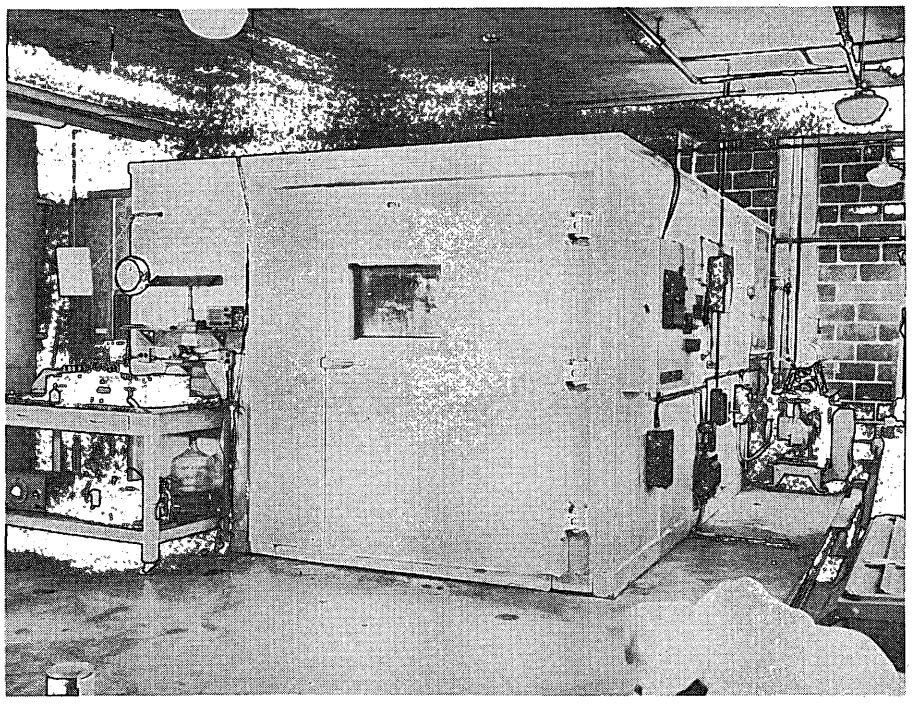

Fig. 5-7a Cold Room And Low Temperature Refrigeration Equipment.

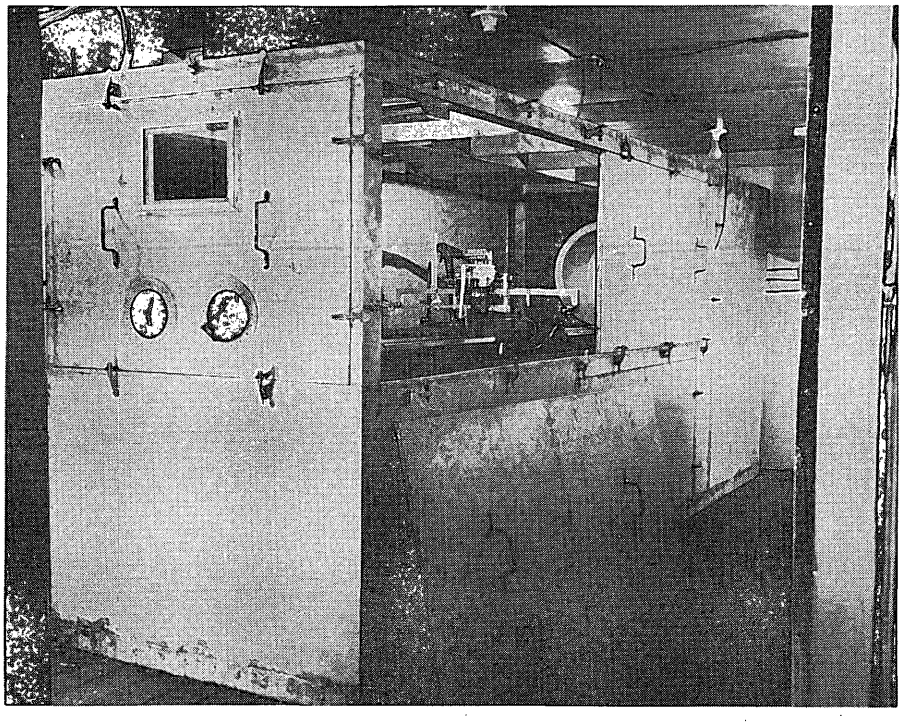

Fig. 5-7b Humidity Chamber

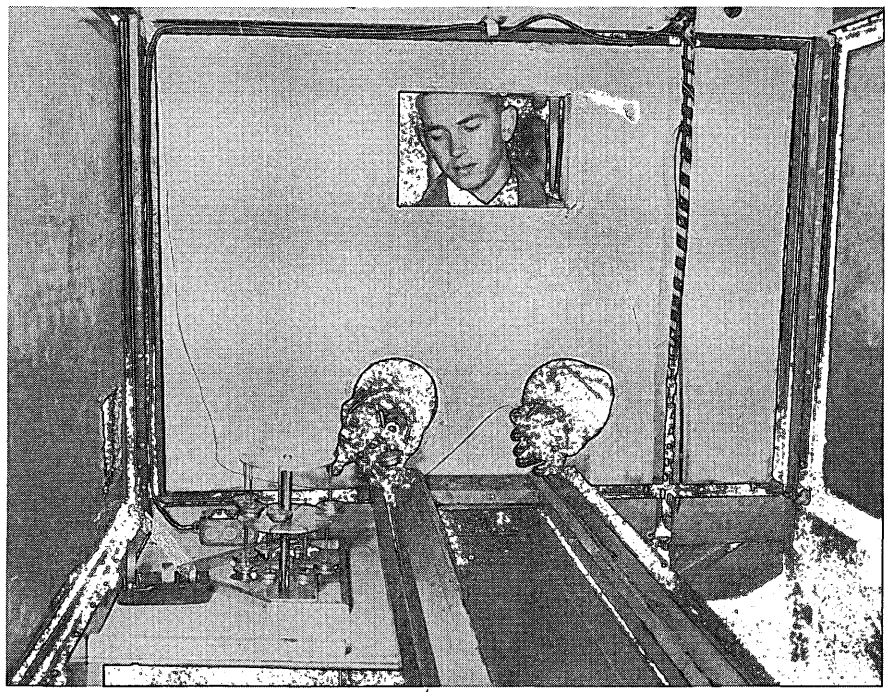

Fig. 5-8 Rubber Gloves In Humidity Chamber.

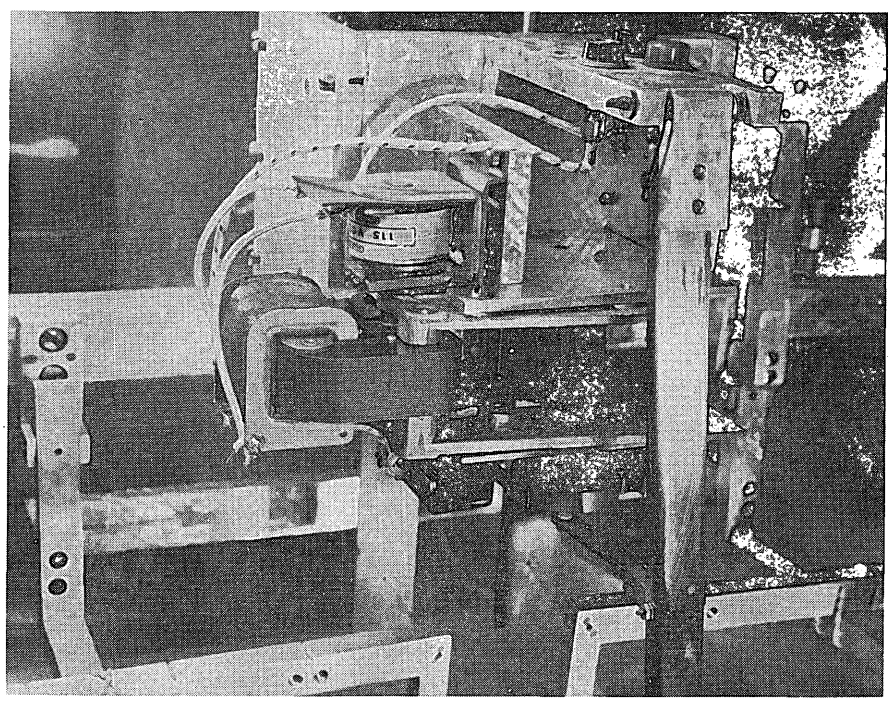

Fig. 5-9 Top View Of Nudger Motor And Brake.

To raise the humidity inside the chamber with a negligible amount of sublimation from the studied ice surface, ice shavings from the machining operation are placed in trays at the bottom of the chamber. The greater surface area of the shavings supplies the water vapor for raising the humidity when the chamber is closed.

Measurement of the humidity within the chamber has been accomplished by means of a National Bureau of Standards Gas Dew Point Tester. A rubber tube and pump connects the atmosphere of the chamber to the dew point tester.

Enclosure of the test equipment within the temperature and humidity chamber required certain modifications of the friction measuring equipment to obtain complete remote control of all operations.

The original design of the nudger, whose function is to push the sliders ahead to a new arbitrary test position, was not entirely satisfactory. In this first design, in which a solenoid was used to actuate the nudging motion, a small dashpot was required to dampen the motion and prevent excessive slider motion. In cold temperature operations the dashpot had to be heated to function correctly. These several difficulties indicated a necessity for redesigning the unit. To provide a more reliable remote nudging system, a 24 RPM Motoresearch gearmotor is now used to power the nudger arm as shown in Fig. 5-9.

A limit switch and cam arrangement (Fig. 5-10) permits the operator to stop the nudger in the nudged position by depressing a push button switch on the control panel. Releasing the switch causes the nudger arm

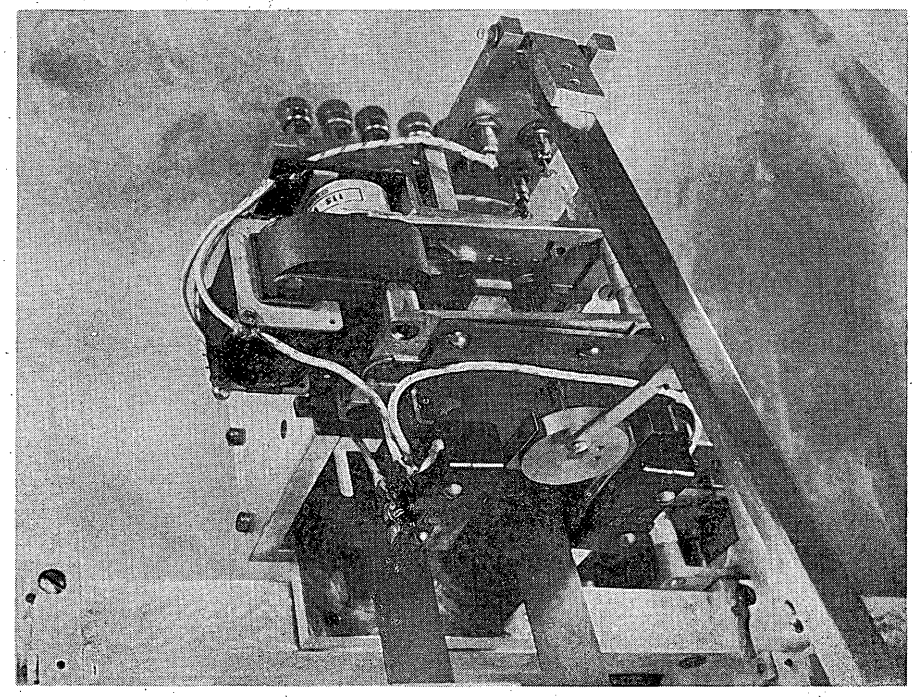

Fig. 5-10 Bottom View Of Nudger Motor Showing Limit Switches And Cam.

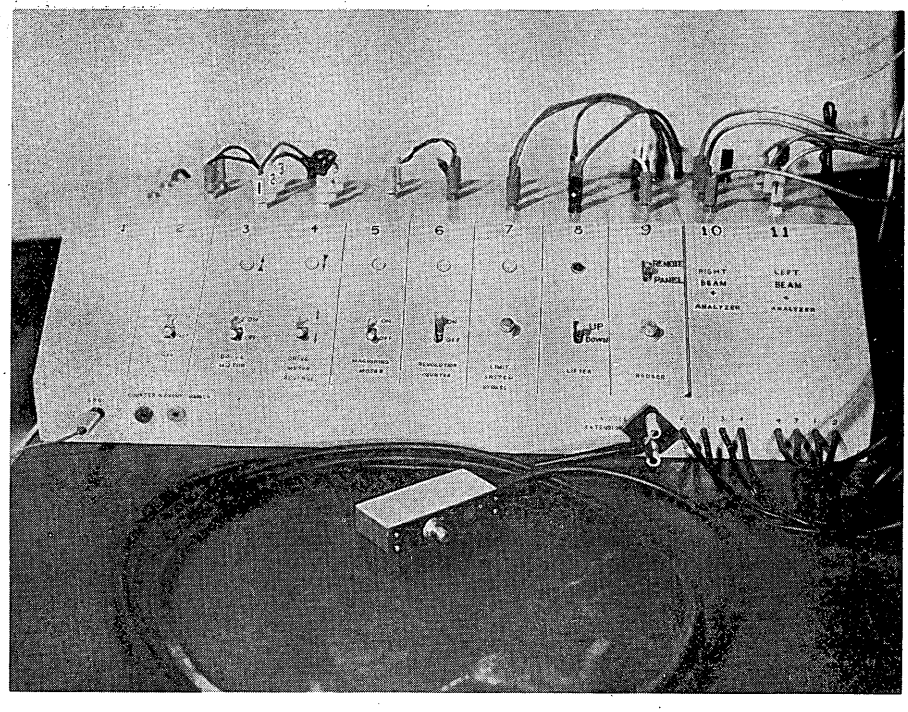

Fig. 5-11 Control Panel With Extension Nudger.

to return to its retracted position and stop. Since the motor tends to coast after the power is cut off, a brake is necessary to stop the motor rapidly at a predetermined position of the nudger. This brake is activated by a Guardian relay coil connected in parallel with the motor terminals as shown in Figure 5-10. The nudger extension cord switch shown in Fig. 5-11 permits one operator to control the nudger while observing and marking the oscillograph chart.

Limit switches were also installed on the lifting mechanism to enable remote and invisible operation of the lifting process (Fig. 5-12). Previously it had been necessary for the operator to observe the lifting process as he actuated the lifter. These limit switches automatically stop the lifter in either up or down position depending upon the position of the control panel lifter switch.

The controls wiring diagram including the above modifications is given in Fig. 5-14.

Another operation which was found difficult to perform in the humidity chamber was changing the individual sliders on the test arm. The method used previously consisted of screwing a slider on a slider holder which in turn was semi-permanently connected to the scriber point. With hands enclosed in the rubber gloves at cold temperatures, the manipulation of the sliders on and off the slider holder was extremely unwieldy. This problem was reduced, however, by construction of individual slider holders and scribers for each test slider. The combined units were then hung from a swiveling "Lazy Susan" in such a way that the desired test slider

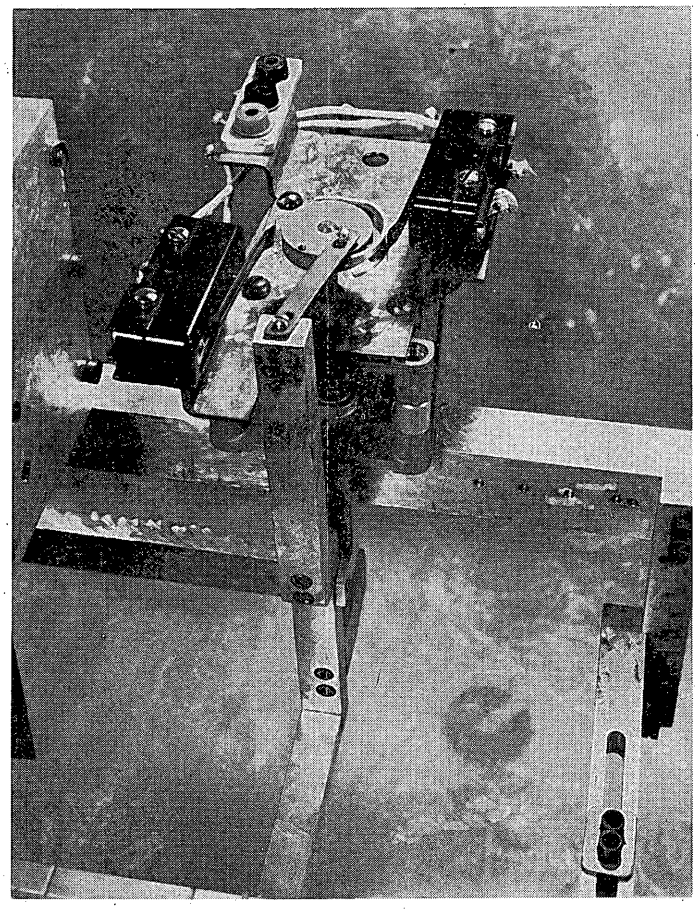

Fig. 5-12 Slider Lifter Motor.

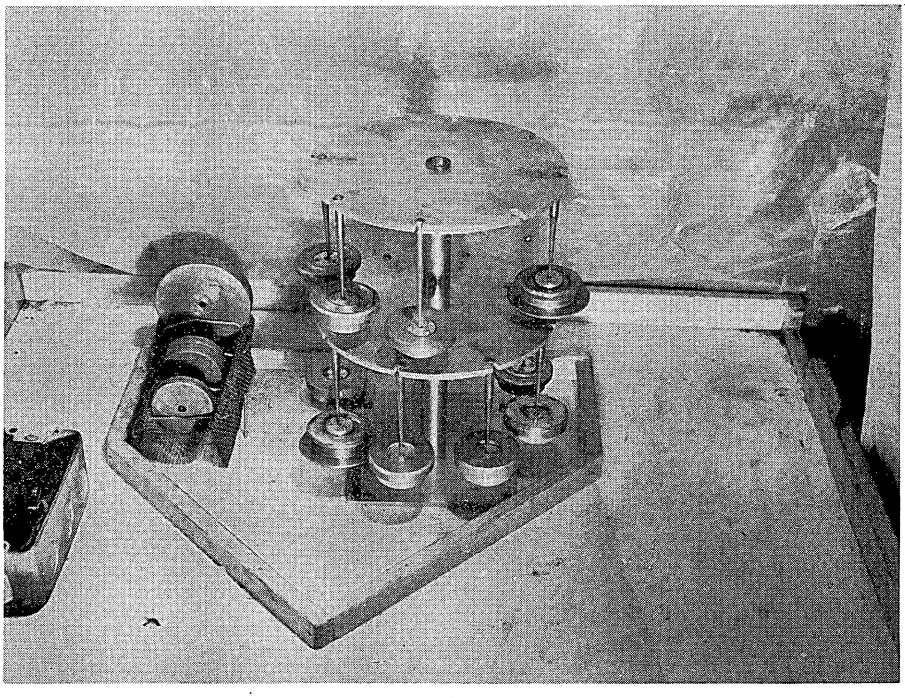

Fig. 5-13 Lazy Susan And Loading Weights.

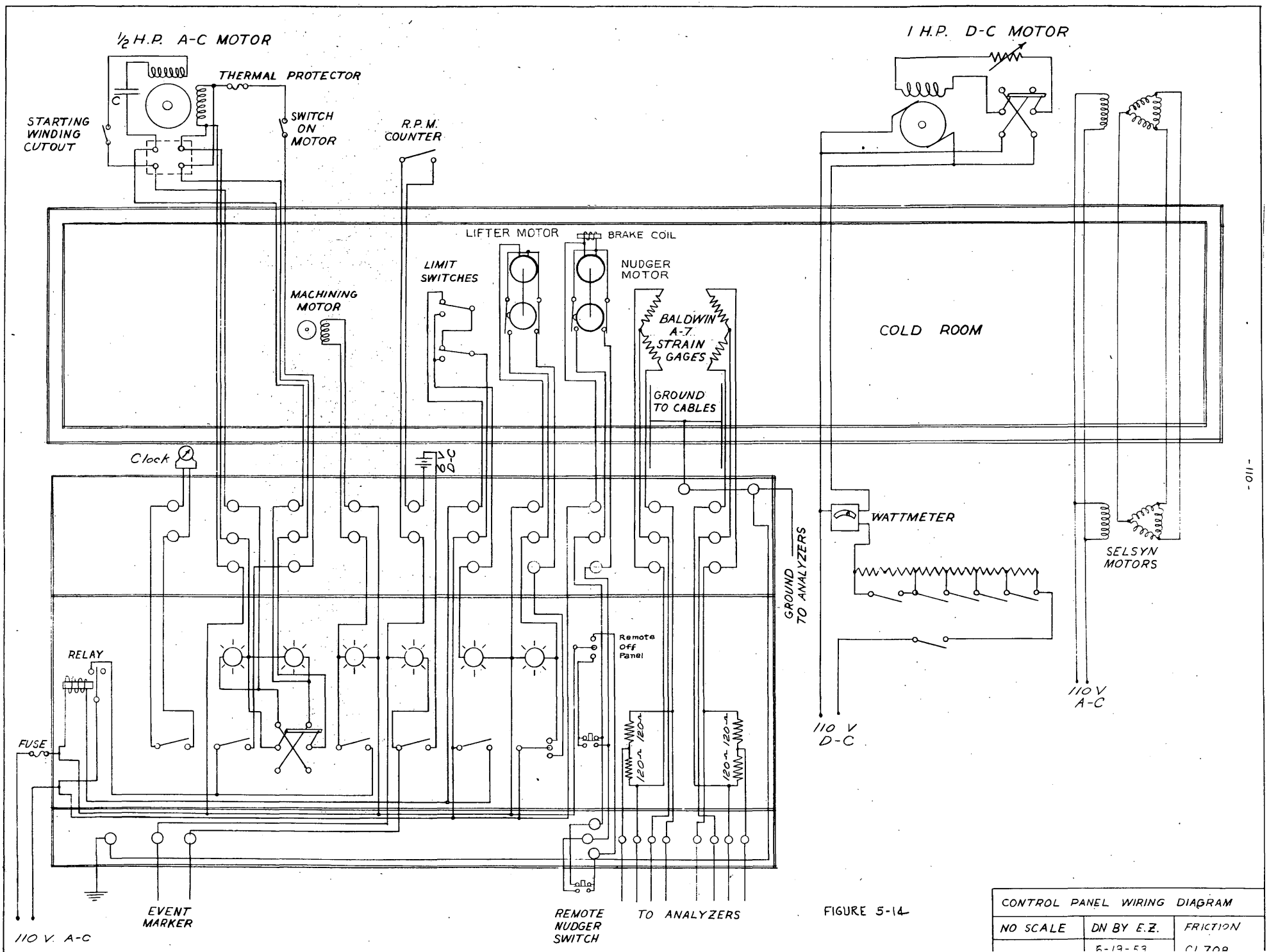

FIGURE 5-14

CONTROL PANEL WIRING DIAGRAM		
NO SCALE	DN BY E.Z.	FRICTION
	5-19-53	CLTOR

could be easily selected and installed by pushing the scriber into a chuck. This technique decreased considerably the time required to change the test slider. The Lazy Susan and suspended test sliders may be seen in Fig. 5-13.

For ease in obtaining the selected test loads, balance weights were added to each slider and holder combination to bring the total initial load on the slider surface to 80 grams. Additional ring weights of 80, 160, and 320 grams were constructed to provide higher test loads at 160, 320, and 640 grams. These ring weights are installed on a loading pin directly above the slider as illustrated in Figure 5-4. A spring clip holds the weights secure while the towing apparatus is in motion but still allows the operator to easily remove and replace the individual weights.

C. Apparatus Calibration

The spring force corresponding to a unit chart deflection of the oscillograph pen was calibrated directly through the use of a sensitive milligram spring balance. This calibration balance was mounted on a second carriage upon the lathe bed and connected through a system of levers and threads to the scriber point on the test arm. A pre-selected force was set up on the left pan of the balance and the balance carriage moved ahead deflecting the cantilever beam. The chart or pen deflection corresponding to the null position on the spring balance was noted. This process was repeated over a range of calibration spring force values for several attenuation settings of the Universal Analyzer. Figure 5-15

FIGURE 5 - 15

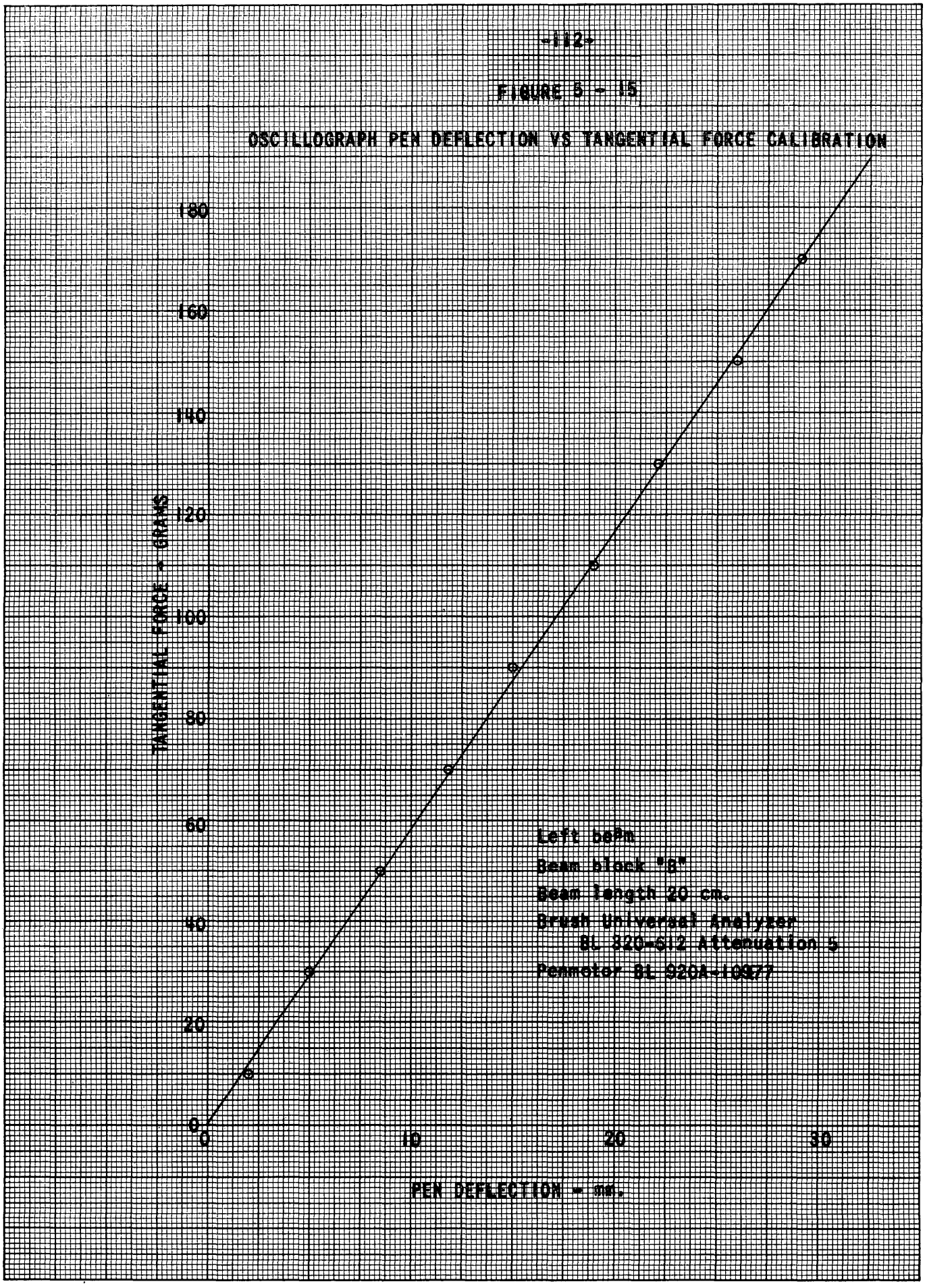
OSCILLOGRAPH PEN DEFLECTION VS TANGENTIAL FORCE CALIBRATION
TANGENTIAL FORCE - GRAMS
180
160
140
120
100
80
60
40
20
0
0
10
20
30
PEN DEFLECTION - mm.
Left beam
Beam block "B"
Beam length 20 cm.
Brush Universal Analyzer
BL 320-612 Attenuation 5
Pennotor BL 920A-10877

illustrates one of the resulting calibration curves. These calibration curves provided a means for the direct interpretation of the slider motion oscillograms in terms of the spring force.

The deflected position of the cantilever spring may also be determined from the oscillograms. An event mark was caused to be placed on the oscillograph tape by an interrupter attached to the lead screw of the lathe. Since the pitch of the lead screw equaled six threads/inch the interval between each event mark represents 1/6 in. or 0.423 cm. of carriage travel. During the stick portion of a stick-slip cycle the slider is held stationary while the carriage moves forward. The resulting trace on the oscillogram is a rising line as though the slider were moving rearward relative to the carriage. The vertical rise of this stick line between two even marks thus equals 0.423 cm. of slider and cantilever beam deflection. This slider position data together with the previously discussed force calibration data shows that the spring constant of this particular cantilever beam equals approximately 52 gr/cm.

Analysis of the slider motion also requires the determination of the effective mass of the test arm and cantilever spring combination. This mass is the equivalent inertial mass which coupled with the spring determines the normal frequency of the system under the zero load on slider condition. It is possible to determine the effective mass by measurement of the normal frequency in the following manner. The normal frequency of undamped vibration may be shown to equal:

$$f = \frac{1}{2\pi}\sqrt{\frac{k}{M + m_e}} \qquad (5\text{-}1)$$

in which:

f = normal frequency

k = spring constant

M = added mass

m_e = effective mass of arm and beam

Thus the measurement of the natural frequency for a series of added known loads enables the calculation of the effective mass and a check on the spring constant.

Frequency measurements on the left beam corresponding to several added loads were taken. For these loads the frequency equalled 172 cyc/min. for 80 gram load and 140 cyc/min. for 160 gram load. Inserting this data in Equation (5-1), the spring constant was found to equal 52 gr/cm and the effective mass to be 77 grams. It may be noted that the spring constant calculated by this method agrees with the value determined by more direct measurements.

Horizontal Cylindrical Path Friction Force Dynamometer

Measurements made of the kinetic friction force on ice and compacted snow using the linear path friction force dynamometer are restricted to a low range of relative velocities by the finite length of the lathe bed. The continuous path available on a turntable or on the surface of a cylinder provides an infinite distance available for acceleration and deceleration. Use of a continuous path of this nature enables a considerable extension of the range of velocities for friction measurements.

Several combinations of continuous ice surface and slide mechanisms are possible.

Four such combinations are:

Type 1. Stationary slider -- horizontal flat revolving surface (turntable);

2. Stationary ice surface -- horizontal revolving slider and allied equipment;

3. Rotating cylindrical ice surface on vertical axis -- rotating slider mechanism in vertical axis;

4. Rotating cylindrical ice surface on horizontal axis -- stationary slider mechanism;

Of the above types, number four was considered to be the best arrangement for higher velocity measurements. The advantages and disadvantages of this arrangement include:

1. Advantages:
   a. Mechanism may be brought to speed before tests are initiated.
   b. High rotative speeds of drum provide high relative velocities between ice surface and sliders.
   c. Continuous ice surface enables possibility of long runs.
   d. Ice will not be thrown off by centrifugal action.
   e. Small space requirement.
   f. Entire unit may be enclosed to permit temperature, pressure, and humidity variation control, and to exclude foreign materials.
2. Disadvantages:
   a. Snow or ice surface undergoes compression due to centrifugal force.
   b. Snow or ice surface is subjected to "wind".
   c. Contraction of drum with decreased temperature sets up stresses in ice surface.
   d. Apparatus is difficult to use for static measurements.
   e. An extremely low velocity is hard to maintain.
   f. Vibration of component parts becomes appreciable.
   g. Special curved sliders are required for surface contact.

A horizontal cylindrical path friction force dynamometer (Figure 5-16) was constructed using the lathe bed and headstock as a base. A drum formed from a 24 inch diameter 1/2 inch thick steel pipe is mounted on the spindle of the lathe headstock. To obtain accurate alignment of the

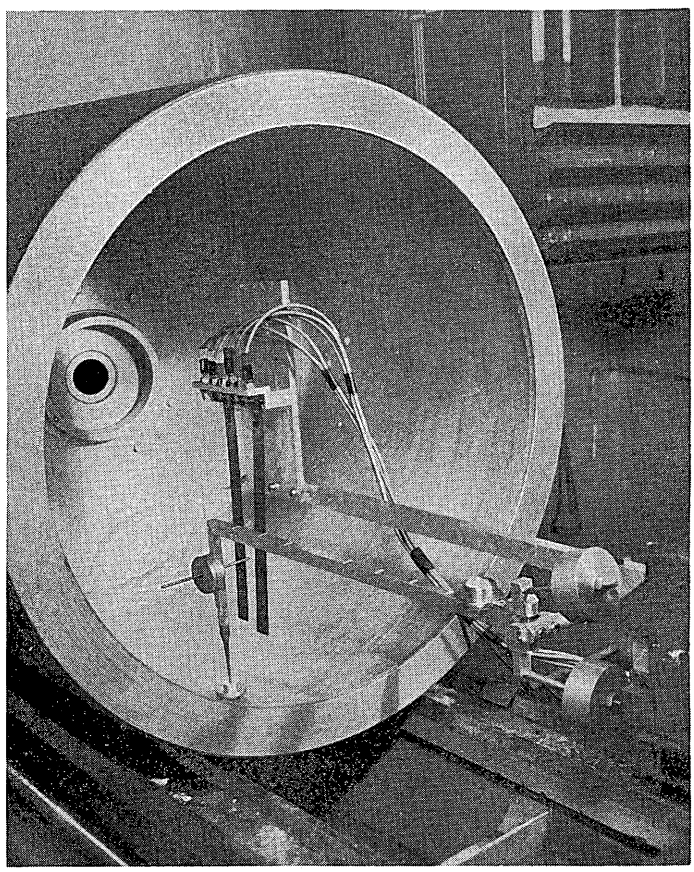

Fig. 5-16 Horizontal Cylindrical Path
Friction Force Dynamometer

drum a hub and flange were constructed in a fashion such that the drum can be shimmed to less than 0.001" eccentricity. A rim on the outside edge of the drum retains water within the drum during the freezing process.

The drum is powered by one of two sources depending upon the speed desired. An A.C motor coupled to a hydraulic torque converter supplies a range of low speeds. For high speeds a DC motor with a rheostat control may be coupled to the spindle.

The same loading and tangential friction measuring device developed for the linear path dynamometer is used with a few modifications for the cylindrical path apparatus. This device is mounted on the lathe carriage. Movement of this carriage in the direction of the cylinder axis simultaneous with cylinder rotation enables a spiral path to be taken by the slider relative to the ice surface. These motions may be synchronized such that the slider is traveling over a fresh surface during a frictional test.

The same calibrated cantilever beams, strain gages, Brush analyzers, and oscillographs used in the linear path apparatus were used in measuring and recording the frictional resistance in the cylindrical path apparatus.

The sliders used in the cylindrical path apparatus are of necessity slightly different than the sliders used in the linear path. This difference lies in the curvature of the lower surface. To maintain a surface region of contact, the slider surface must have the same curvature as the material surface in the drum. The curvature of this material surface depends upon the size of the drum and the thickness of the ice

or snow layer. Drum dimensions and possible ice or snow layer suggested an inside diameter of the material drum in the range between 56 to 58 cm. Fabrication of the sliders dictated the dimension finally chosen. Since it was necessary to obtain the final machining and polishing of the sliders in an optician's laboratory, it was also necessary to specify the curvature in diopters, the optician's curvature units. The curvature in diopters is defined as the reciprocal of the diameter of the sphere in meter length units. The nearest standard grinding and polishing plate to the desired drum surface curvature has a curvature of 1.75 diopters or 57.14 cm. Sliders were therefore ground and polished to this curvature. Templates were also made from standards to facilitate drum surfacing to this same curvature.

CHAPTER VI

STATIC FRICTION MEASUREMENTS

Chapter VI

Static Friction Measurements

Data Collection Approach

The friction measuring apparatus was not alone in requiring changes and modifications during the course of the investigation of static friction on ice. As the project matured and as additional information was gathered, it was necessary to modify the philosophy of the data collection.

In the first stage of data collection it was expected that a single tangential resistance value and a single coefficient of friction could be measured at each matrix cross-setting of the several parameters affecting the friction. It was soon learned however that individual measurements often varied by several hundred per cent. Improvement of the apparatus and standardization of the measuring techniques reduced the variation considerably, but an appreciable variation still existed.

In the Series Three measurements in which the percentage of "pullaways" corresponding to a preselected tangential test force was measured it was found that the static friction force has approximately a normal distribution. This finding was further confirmed by the measurements of Series Four in which a large number of individual measurements of the static friction were obtained using the cantilever beam - strain gauge - analyzer - recording oscillograph apparatus. It was then felt that the mean value of the normally distributed individual measurements would provide the desired single value for the matrix cross setting of the studied parameters. To provide a measure of the spread of individual values from the mean, the

standard deviation of the values at each setting was also determined.

Static friction measurements were taken corresponding to this approach for a number of parametric settings of load, apparent area, slider material, and ambient temperature. In these series of measurements, Series Five through Seven, the measurements were taken in the most advantageous order for ease in obtaining the desired experimental conditions. As an example, having selected and installed a particular slider on the test apparatus, the entire series of friction measurements would be obtained from this slider before changing to the next slider. By the time the desired measurements could be made on the second slider, unknown changes may have occurred in the ice. Plots of the mean values plus or minus a standard deviation against values of the studied parameters indicated erratic tendencies.

It was next decided to adopt the conventional engineering approach in which only one variable is examined at a time, all other parameters being held constant. A set of readings corresponding to various settings of this single parameter such as apparent contact area, would be taken during a single experiment time period. In this way data variations due to aging, wear, and other unknown influences related to the ice or slider history are reduced. By this experimental approach a repetition of the friction measurements is required of a particular combination of the experimental parameter settings for each variable separately investigated. Each replicate is applicable however only to the study of the single parameter under inspection.

The Eighth Series of friction force measurements on ice were made following this experimental approach.

To provide a better basis for the comparison of the influence of the individual parameters the basic experimental approach was again modified. For this comparison the statistical methods of the Theory of Variance were adopted. A brief description of this theory and the method of application to actual problems are given in Appendix D of this report.

One of the requirements for the application of the Theory of Variance is that the individual measurements must be taken in a random order. Each individual measurement may therefore be utilized in the examination of all the parameters under investigation, but due to the randomization of order the influence of uncontrolled variables will not introduce a trend which may be falsely attributed to some other factor. The randomization of order requirement was fulfilled by assigning to each individual combination of parameter settings a particular card. The collection of cards for all the combinations was gathered together and thoroughly shuffled. Cards were then withdrawn from the pack and the parameter settings made as dictated by the randomized cards.

A second requirement of the Theory of Variance is the collection of replicates of the entire set of measurements. For each replicate set the order of performance was randomized using the above described card technique.

Series Ten through Fourteen Friction Measurements were made following the Theory of Variance approach and analyzed using the technique described in Appendix D.

Data and Results

The experimental measurements and results of the first seven series of static friction measurements have been previously reported in Progress Reports I and II.

In the Series Eight Friction Force Measurements an attempt was made to concentrate on the individual influence upon the static friction on ice of load, area, and the combination of these two factors in the form of pressure. The influence of these factors upon sliders of several materials and at several temperature settings was to be obtained. Figures 6-1 through 6-10 graphically present the results of these measurements. Each plotted point on these graphs represents the mean of fifty individual measurements. The line on either side of the plotted points extends a distance equal to the standard deviation of the fifty values.

Load test results covering a load range of 40 grams to 960 grams for sliders having a 4 cm^2 apparent contact area made from steel, magnesium, brass, bakelite, and hickory materials and taken at temperatures of + 15° F., - 25° F., - 40° F., and - 60° F. are presented in Figures 6-1 through 6-5. These graphs indicate the following trends:

1. The variation with load does not appear to be appreciable. The changes which do occur are not consistent.
2. Of the slider materials the English bakelite slider appeared to have the highest static coefficient of friction with a value of approximately 0.4 at + 15° F. Magnesium had the second highest static coefficient with a value of approximately 0.3 at + 15° F

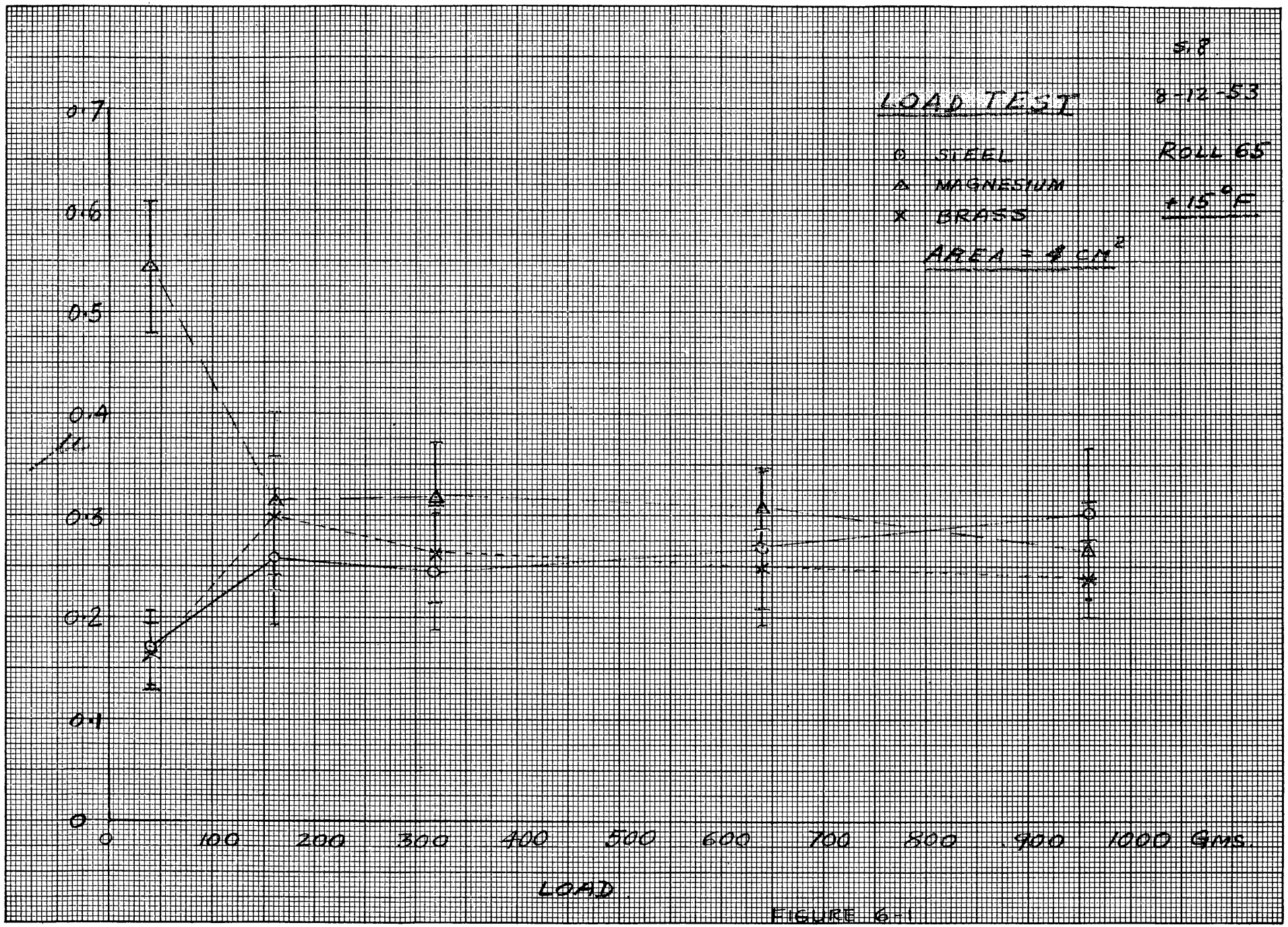
LOAD TEST
8-12-53
ROLL 65
±15°C
o STEEL
Δ MAGNESIUM
× BRASS
AREA = 4 cm²
0·7
0·6
0·5
0·4
0·3
0·2
0·1
0
100
200
300
400
500
600
700
800
900
1000 Gms.
LOAD

FIGURE 6-1

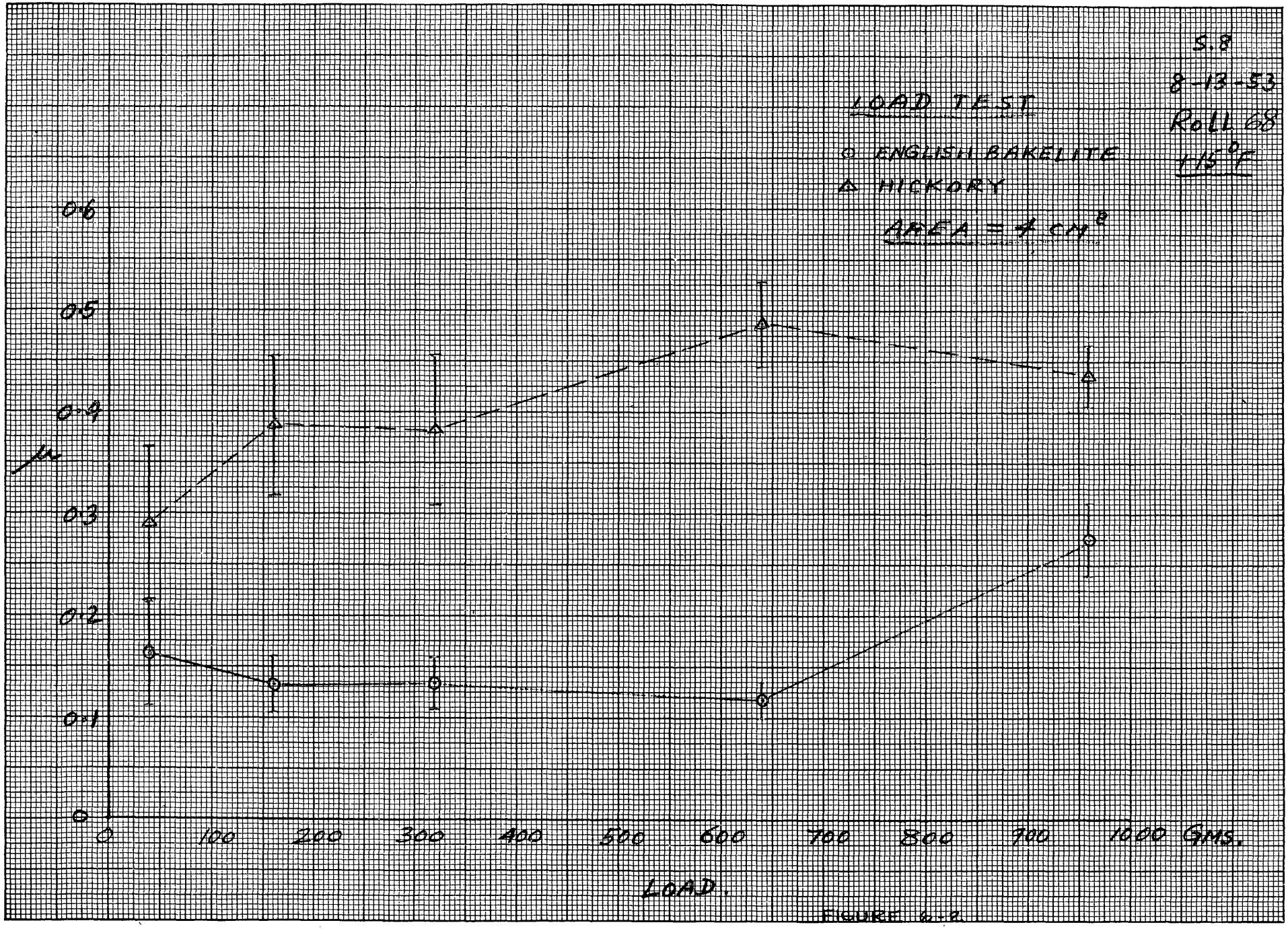
S.8
8-13-53
Roll 68
LOAD TEST
○ ENGLISH BAKELITE
△ HICKORY
AREA = 1 cm²
0.6
0.5
0.4
0.3
0.2
0.1
0
0
100
200
300
400
500
600
700
800
900
1000 GMS.
LOAD.

FIGURE 6.2

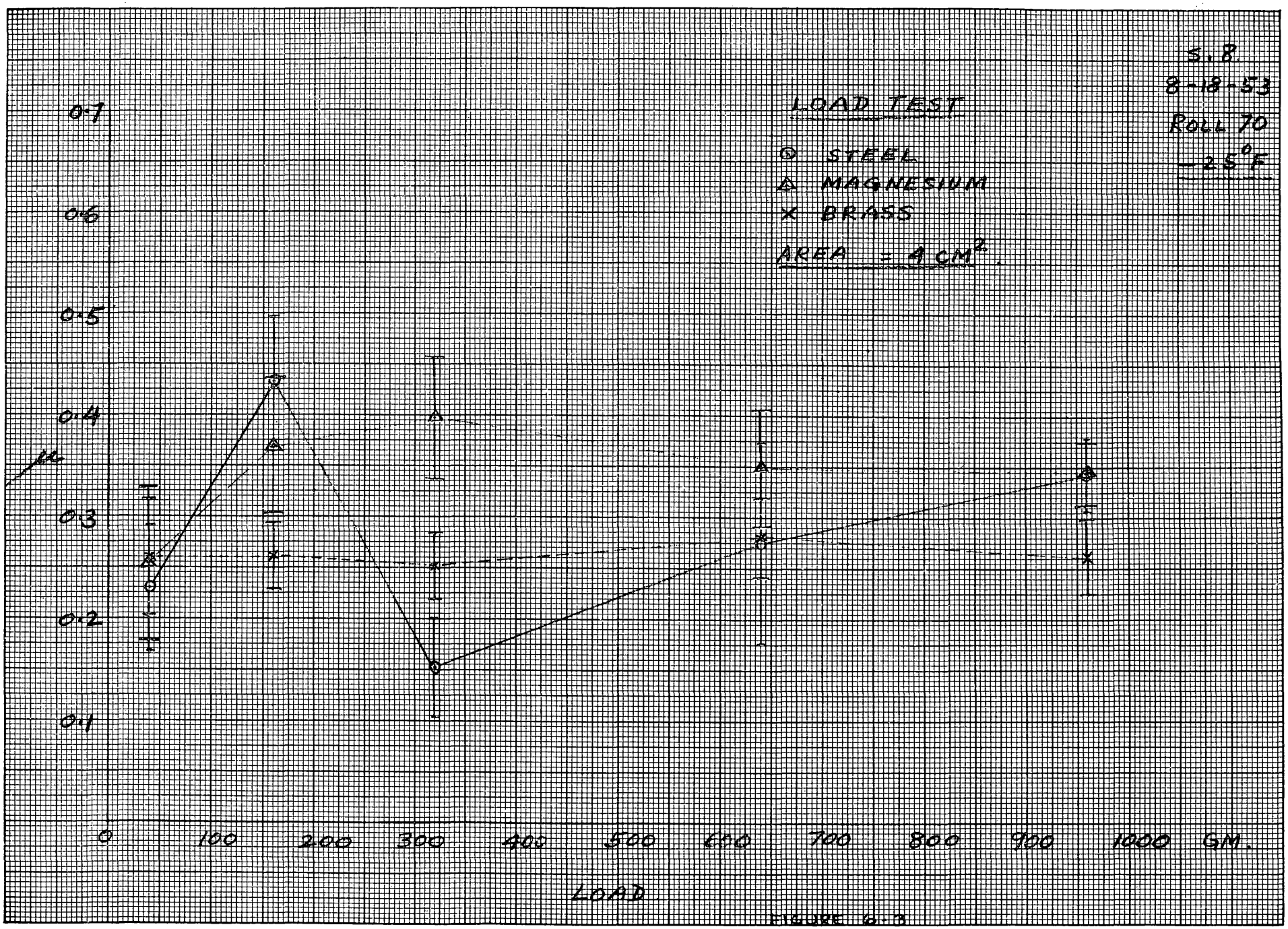
S.8
8-18-53
ROLL 70
-25°F
LOAD TEST
⊙ STEEL
△ MAGNESIUM
× BRASS
AREA = 4 CM².
0·7
0·6
0·5
0·4
0·3
0·2
0·1
0
100
200
300
400
500
600
700
800
900
1000
GM.
LOAD

FIGURE 6-3

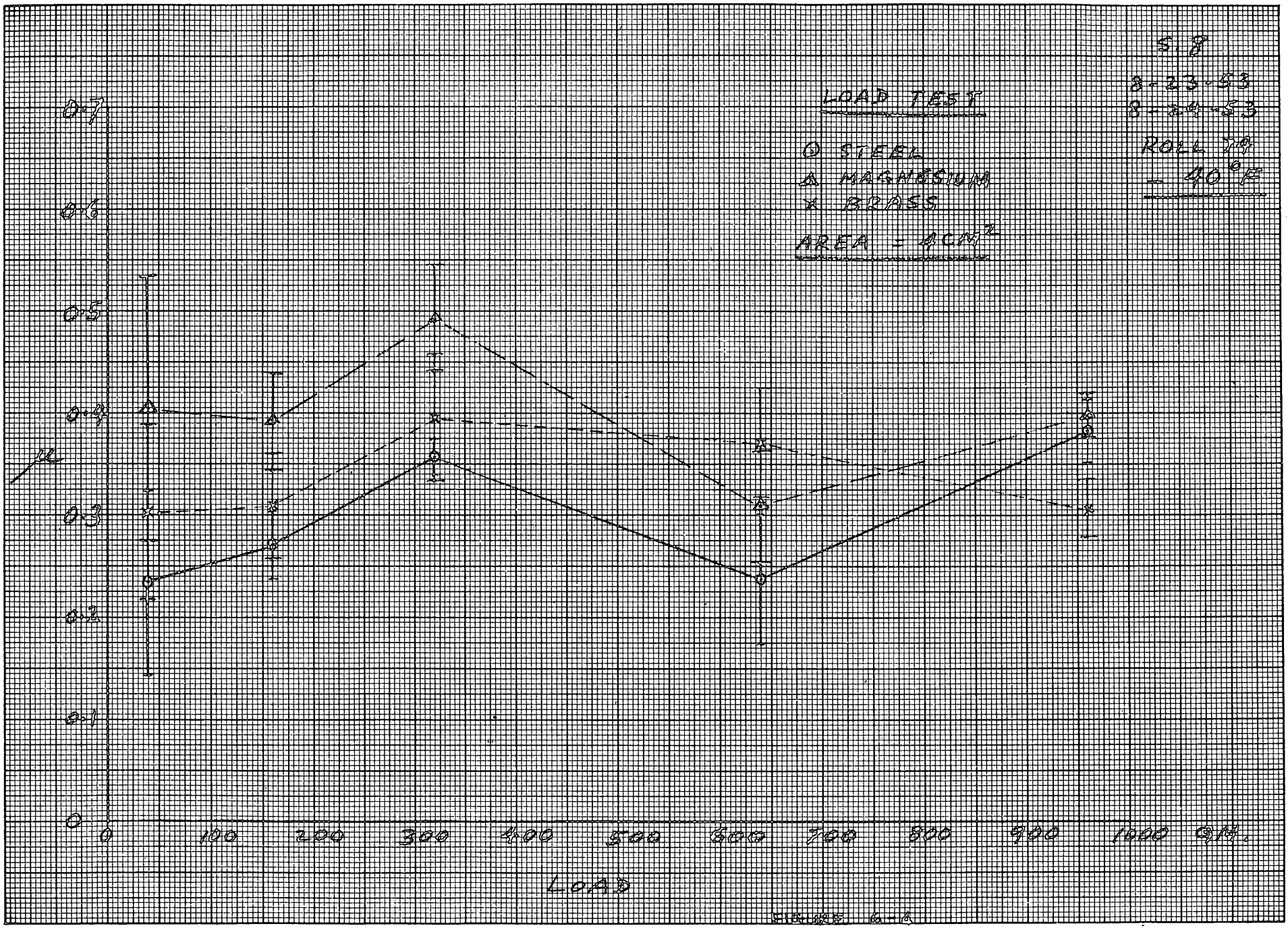
LOAD TEST
○ STEEL
△ MAGNESIUM
× BRASS
AREA = 4 CM²
S B
8-23-53
8-24-53
ROLL 20
40 PSI
0·7
0·6
0·5
0·4
0·3
0·2
0·1
0
0
100
200
300
400
500
600
700
800
900
1000
GM.
LOAD

FIGURE 6-4

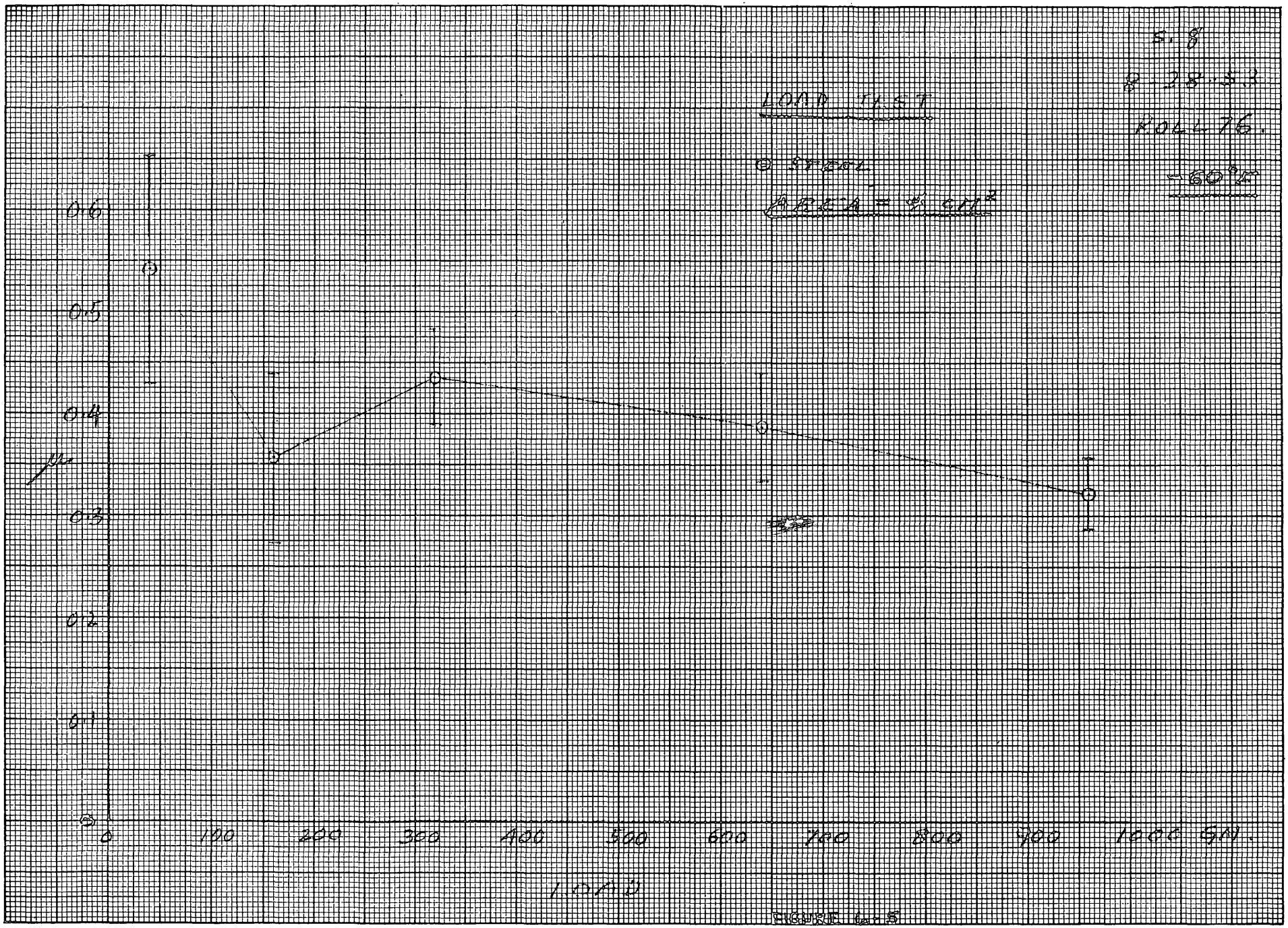
S. 6
8 - 28 - 53
R04476.
-60°F
LOAD TEST
0.6
0.5
0.4
μ
0.3
0.2
0.1
0
100
200
300
400
500
600
700
800
900
1000 PSI.
LOAD (#)

FIGURE 6.5

rising to approximately 0.4 at - 40° F. Brass and steel were next with practically the same static resistance. These materials had static coefficients of about 0.25 at + 15° F which rose to above 0.3 at - 40° F. and in the case of steel to values in the neighborhood of 0.4 at - 60° F. Hickory indicated the lowest static coefficient of friction with values of approximately 0.15 at + 15° F.

3. A decrease in temperature appeared to consistently increase the static friction force of all materials tested.

Area test results for sliders having apparent contact areas of 1/4, 1, 4, and 16 square centimeters under a constant load of 160 grams are plotted for slider materials of steel, magnesium, and brass and for ambient temperatures of + 15° F., - 30° F., and - 47° F. in Figures 6-6 through 6-8. These graphs apparently indicate:

1. Static friction force increases slightly with an increase in the apparent contact area.
2. A decrease in the temperature appeared to increase the static friction force.

Results of the pressure tests are plotted in Figures 6-9 and 6-10. In this set of experiments both the area and the load were changed at each test in such a way as to hold the pressure or ratio of load over apparent area at a constant value of 40 gms/cm^2. Sliders of steel, magnesium, and brass were tested in this fashion at + 15° F. and - 32° F. In order to agree with the predictions of other investigators the static coefficient should remain constant for a particular pressure. It is difficult to judge from the actual curves of Figures 6-9 and 6-10 whether this constancy is correct.

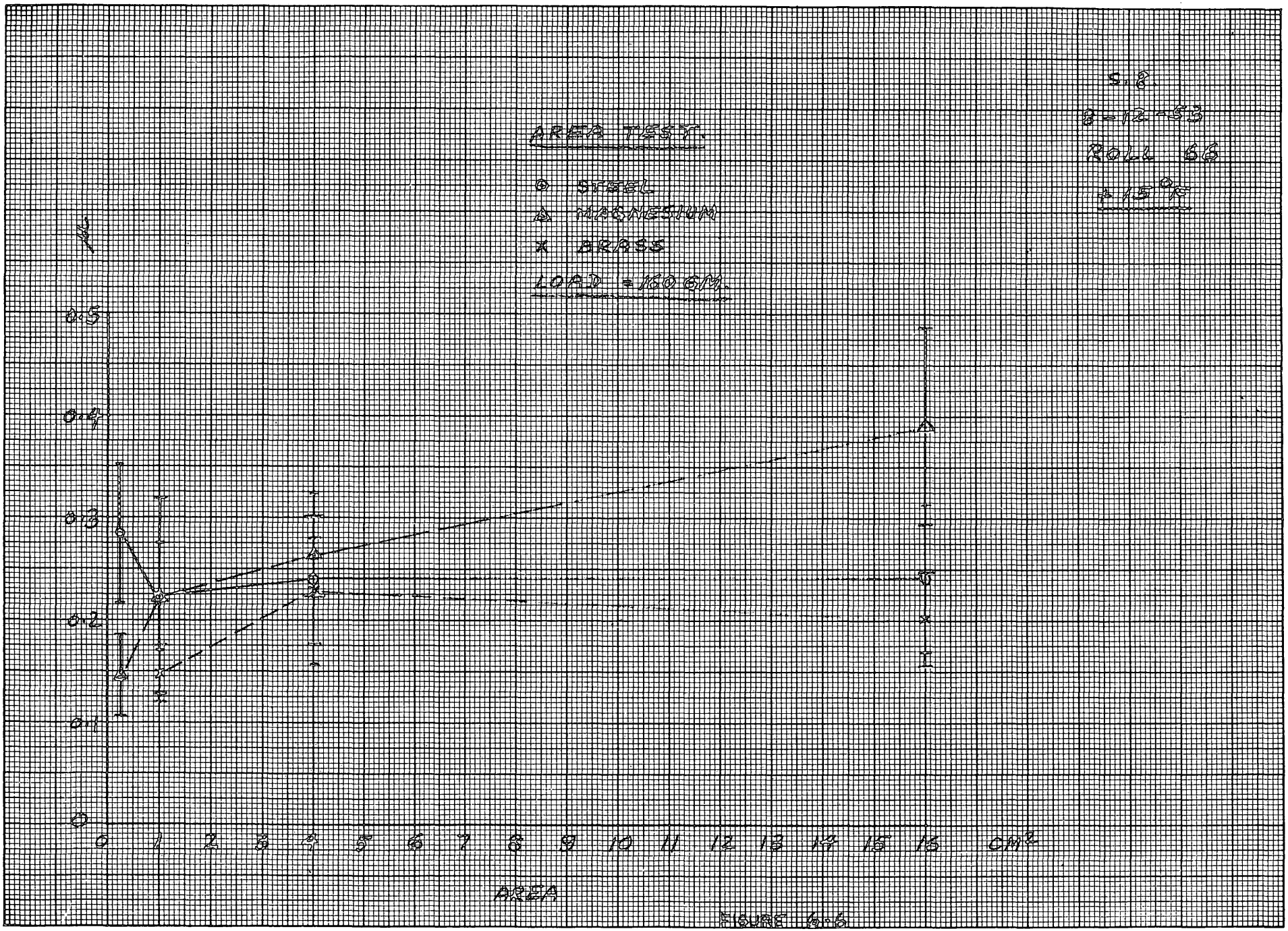
AREA TEST
○ STEEL
△ MAGNESIUM
× BRASS
LOAD = 1500 KM.
S.G.
8-12-53
ROLL 66
415 °K
0.5
0.4
0.3
0.2
0.1
0
0 1 2 3 4 5 6 7 8 9 10 11 12 13 14 15 16 CM²
AREA

FIGURE 6-6

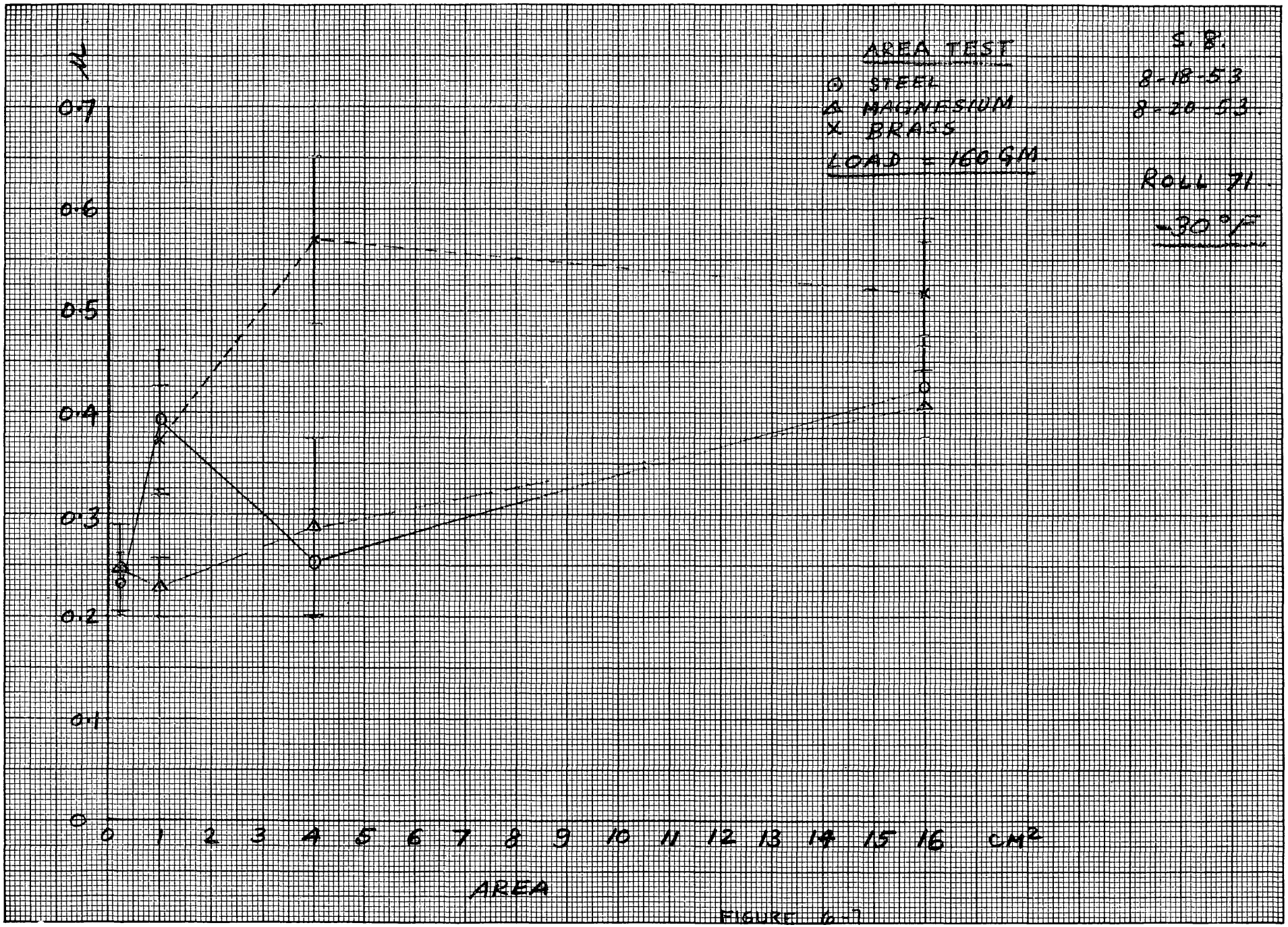
AREA TEST
⊙ STEEL
Δ MAGNESIUM
× BRASS
LOAD = 160 GM
S. B.
8-18-53
8-20-53
ROLL 71
-30°F
R
0.7
0.6
0.5
0.4
0.3
0.2
0.1
0
0 1 2 3 4 5 6 7 8 9 10 11 12 13 14 15 16 CM²
AREA

FIGURE 6-7

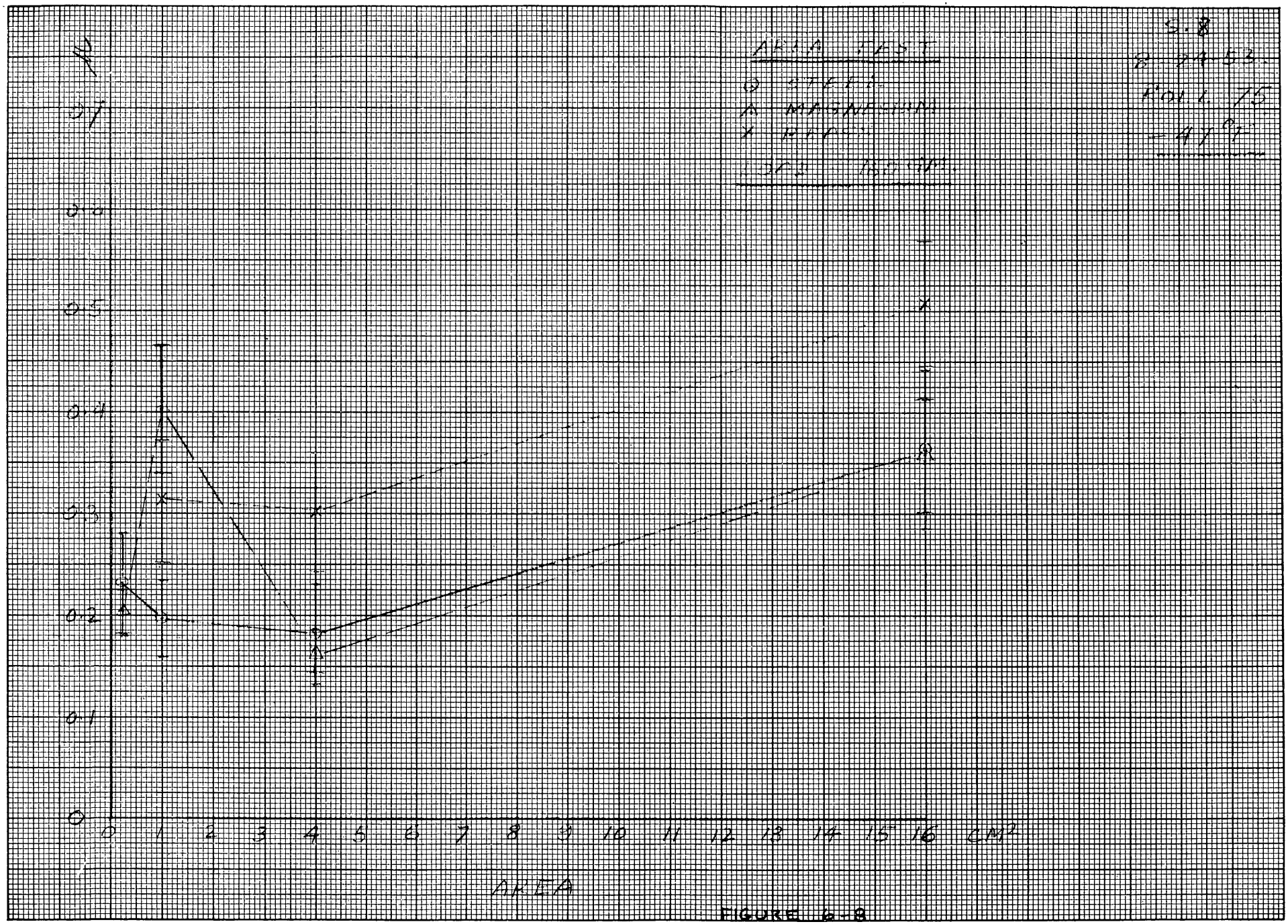

FIGURE 6-8

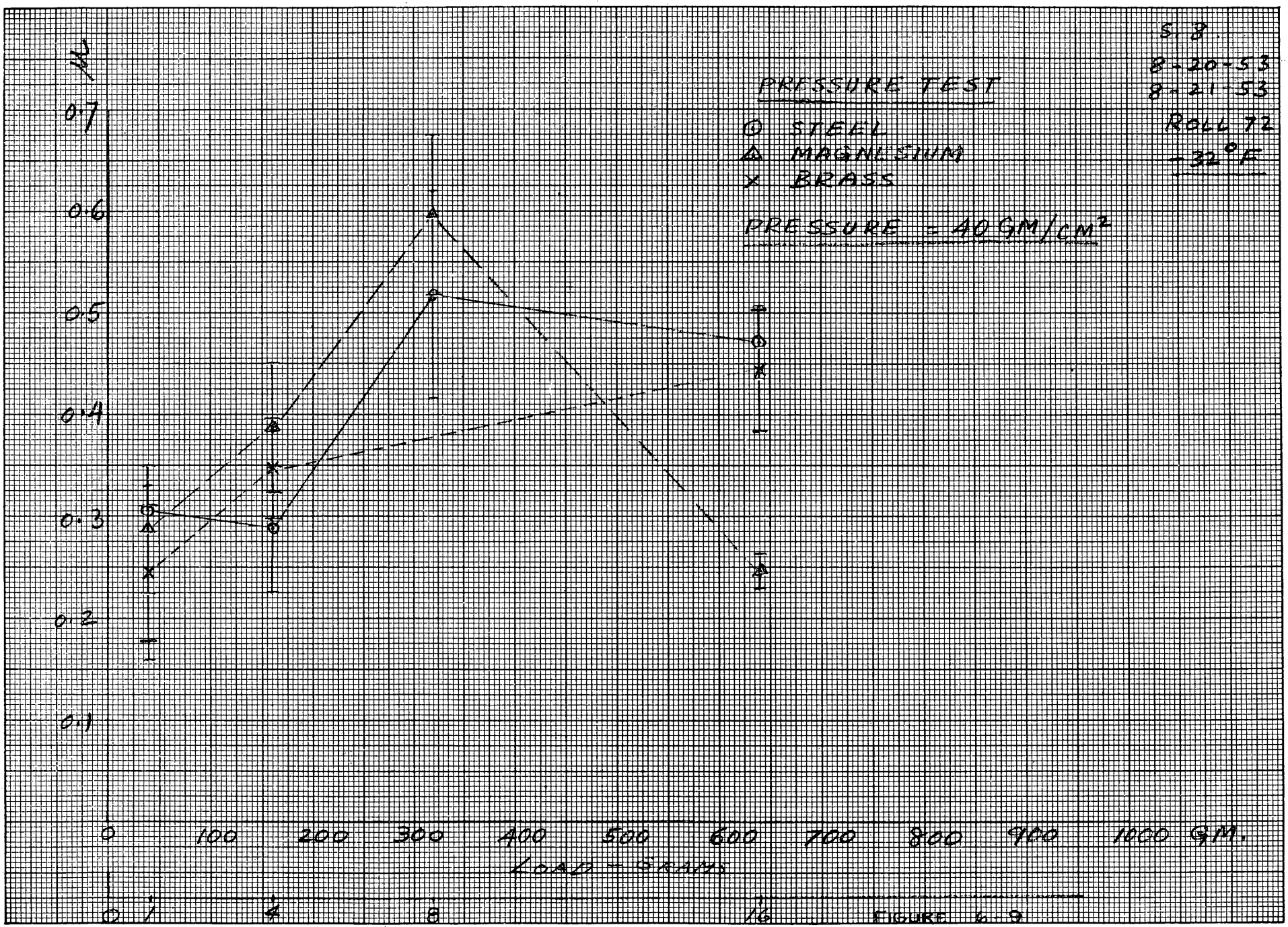
PRESSURE TEST
○ STEEL
△ MAGNESIUM
× BRASS
PRESSURE = 40 GM/CM²
S 8
8-20-53
8-21-53
ROLL 72
-32° F
P
0.7
0.6
0.5
0.4
0.3
0.2
0.1
0
100
200
300
400
500
600
700
800
900
1000 GM.
LOAD - GRAMS
0
4
8
16

FIGURE 6.9

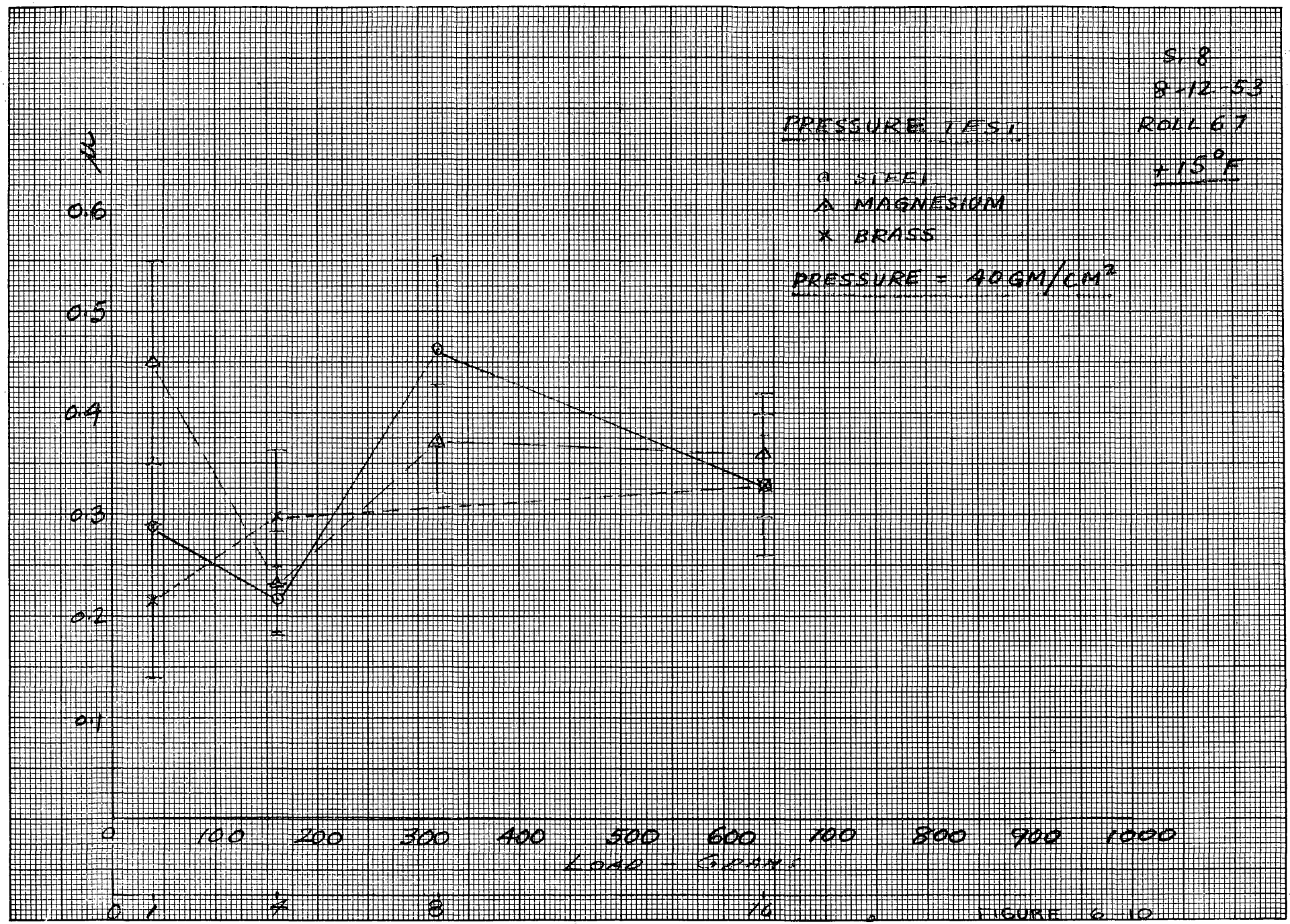
S, 8
8-12-53
ROLL 67
+15°F
PRESSURE TEST
○ STEEL
△ MAGNESIUM
× BRASS
PRESSURE = 40 GM/CM²
0.6
0.5
0.4
0.3
0.2
0.1
0
100
200
300
400
500
600
700
800
900
1000
LOAD - GRAMS

FIGURE 6.10

The Tenth Series of Friction Force Measurements was the first of the test series in which the Theory of Variance was to be applied as the basis of judging the relative influence of the several variables. In this series the following question was posed: "Is the influence of slider material, apparent contact area, load, or any combination of these variables more significant than any of the unknown or uncontrolled variables present in the test?"

An experiment was planned and performed in which three slider materials, four areas, and four loads were to be investigated. The sliders used were the same sliders previously studied in earlier test series. These sliders had a circular shape with a flat contact area. The slider materials were of steel, magnesium, and brass; the apparent contact areas equaled 1/4, 1, 4, and 16 cm^2. Loads to be applied to the slider equaled 80, 160, 320, and 640 grams.

Three replicate sets of measurements of all combinations of the studied variables were obtained. In each replicate set the friction measurement for a particular combination of variables was made in a different random order. Since there were $3 \times 4 \times 4 = 48$ combinations of the parameter settings, a total of 144 values of the coefficient of friction were determined. Each of these values incidentally represented the mean of fifty separate measurements. Unfortunately certain discrepancies in the resulting data at three combination points in one of the replicate sets, required the elimination of these points and consequently the elimination of the entire replicate set. The data obtained in the

remaining two replicate sets are tabulated in Table 6-1. This data was numerically processed using the methods of the Theory of Variance to provide the results tabulated in Table 6-2. The fifth column of this table lists the ratio of the mean squares corresponding to the parameter of interest over the mean squares of the random and triple cross product. The sixth column lists the so called "F" numbers for a 5% and a 1% significance level for the particular combination of degrees of freedom of the studied variable and the random variables. According to Variance Theory if the ratio listed in the fifth column has a numerical value less than the 5% "F" number, the parameter is most likely insignificant in its effect. At least it is possible to place a 95% confidence in this decision. On the other hand if the ratio is greater than the 5% "F" number, the corresponding parameter is possibly significant, and if the ratio exceeds the 1% "F" number, the parameter is undoubtedly quite significant.

The conclusions which may be drawn from the variance analysis of the Series Ten measurements are therefore:

1. Apparent Contact Area under the imposed conditions is very significant.
2. Slider material is significant.
3. Load is not significant.
4. The cross product of material and area is significant while all other cross products including the triple cross product of material times area times load are not significant.

Table 6-1

Series Ten Measurements of the Static Coefficient

of Friction on Ice for Material, Area, and Load Parameters

Material	Steel				Magnesium				Brass			
Area-cm^2	1/4	1	4	16	1/4	1	4	16	1/4	1	4	16
Load-gm												
80	.234	.422	.216	.234	.191	.203	.253	.175	.141	.266	.134	.216
	.097	.303	.266	.021	.097	.141	.269	.219	.131	.262	.216	.181
160	.253	.144	.347	.231	.112	.175	.481	.219	.119	.162	.138	.147
	.100	.162	.219	.421	.119	.159	.381	.303	.100	.228	.241	.247
320	.119	.178	.456	.219	.062	.288	.396	.338	.261	.247	.238	.191
	.214	.131	.343	.325	.078	.119	.492	.402	.112	.133	.142	.235
640	.244	.206	.397	.309	.209	.175	.547	.347	.078	.206	.178	.280
	.116	.209	.244	.325	.126	.109	.462	.369	.071	.191	.259	.225

Table 6-2

Variance Analysis of Series Ten Measurements of Static Friction on Ice versus Material, Area, and Load Parameters

Variable	Degrees of Freedom	Sum of Squares	Mean Squares	Ratio	"F" Number 5%	1%	Significance
M	2	.0752	.0376	4.04	3.14	4.95	barely significant at 5%
W	3	.0262	.0087	.936	2.75	4.09	not significant
A	3	.3615	.1205	13.0	2.75	4.09	very significant
M x W	6	.0235	.0039	.420	2.32	3.09	not significant
M x A	6	.1694	.0282	3.03	2.32	3.09	barely significant at 5%
W x A	9	.1272	.0141	1.52	2.02	2.69	not significant
random	67	.6219	.0093				

M = Material

W = Load

A = Apparent Area

Note:

Second order interaction insignificant, hence was pooled with the original random to give the tabulated random.

A further visual examination of the friction coefficients tabulated in Table 6-1 reveals that:

1. The static coefficient rises with an increase in the apparent area of contact.
2. Magnesium appeared to have the highest static coefficient followed in turn by steel and then brass.

Although the results of the variance analysis of the Series Ten measurements appear to definitely indicate a significance in the area and material parameters, this significance may possibly have been incorrectly assigned by the method of parameter description. For example the experimental study of the variation of area and material requires the use of completely separate sliders while load values may be varied over the same slider. There is thus the possibility that the significance attributed to area and material is actually a significance caused by other factors in the manufacture of the slider. It is possible therefore that the significance found in the Series Ten Measurements is due to a difference in individual sliders rather than to a difference in the material or area.

A new experiment was planned to test the reproducibility of the material variation. For this experiment four sliders were manufactured identical in all respects except for material. Two sliders of the group were made from steel and two made from brass. The following question was then posed: "Does the slider material cause a more significant variation of the friction than exists between individual sliders?"

Series Twelve friction measurements were made to compare the influence of slider material versus the influence of individual sliders.

Four replicate measurements were made in random order of the static friction coefficient of the four sliders. The experimental results of these measurements are tabulated in Table 6-3, and the variance analysis results in Table 6-4.

The variance analysis of Series Twelve measurements indicates that material is a very significant factor while the individual slider is not. Thus greater static friction was found to occur between sliders of dissimilar materials than between sliders of the same material.

While the significance of material was definitely established by the Series Twelve measurements, the proper interpretation of the significance attributed to area is still in question. Since the sliders were circular in shape an increase in slider area between separate sliders was accompanied by an increase in outside perimeter. It is possible that the variation assigned to slider area is actually caused by an "edge" effect. To investigate this possibility, an experiment has been proposed in which the sliders will have a ring shape with an outer and inner edge. If the sliders are constructed with a comparatively large outside diameter and perimeter, the variation of the inside diameter accompanying the variation of the contact area will not greatly change the inner and total perimeters. The performance of this experiment has been planned to accompany other investigations regarding the side or groove effect in frictional resistance.

Table 6-3

Series Twelve Measurement of the Reproducibility of the Static Coefficient of Friction on Ice for Two Materials over two Sliders of Each Material.

Material	Steel	Brass
	0.275	0.234
	0.266	0.212
Slider	0.234	0.203
One	0.338	0.191
	Avg. = 0.278	Avg. = 0.210
	0.359	0.191
	0.303	0.209
Slider	0.325	0.159
Two	0.272	0.184
	Avg. = 0.314	Avg. = 0.187

Table 6-4

Variance Analysis of Series Twelve Measurements of the Reproducibility of the Static Coefficient of Friction on Ice for Two Materials over Two Sliders of each Material

Variable	Degrees of Freedom	Sum of Squares	Mean Squares	Ratio	"F" Number 5%	"F" Number 1%	Significance
Material	1	0.0395	0.0395	32.6	4.67	9.07	Very Significant
Slider	1	0.0003	0.0003	0.248	4.67	9.07	Not Significant
M x S	1	0.0037	0.0037	3.7	4.75	9.33	Not Significant
Random	12	0.012	0.001				

Since considerable data had been collected in previous test series an attempt was made to reexamine this data using the methods of the Theory of Variance. In particular it was hoped to be able to establish the significance of temperature. It was possible to collect from previous measurements sufficient data for an analysis based on three materials, three areas, and three temperatures. The static coefficient of friction data for these three parameters are tabulated in Table 6-5. Results of the variance analysis of these parameters are given in Table 6-6. From this analysis the following conclusions may be drawn:

1. Temperature has the greatest effect.
2. Area has a large effect but less than that of temperature.
3. Material also has an effect but less than that of area.

Table 6-5

Static Coefficient of Friction on Ice for

Three Materials, Three Areas, and Three Temperatures

	M_1			M_2			M_3		
	T_1	T_2	T_3	T_1	T_2	T_3	T_1	T_2	T_3
A_1	.241	.425	.363	.390	.406	.360	.202	.517	.506
A_2	.240	.254	.181	.263	.288	.163	.229	.569	.301
A_3	.223	.394	.197	.222	.228	.403	.149	.372	.313

Where: M_1 = steel, M_2 = magnesium, M_3 = brass

A_1 = 16 cm^2, A_2 = 4 cm^2, A_3 = 1 cm^2

T_1 = +15° F., T_2 = -30° F., T_3 = -47° F.

Load = 160 grams

TABLE 6-6

Variance Analysis of Influence on Static Friction on Ice of Three Materials, Three Areas, and Three Temperatures

Variable	Degrees of Freedom	Sum of Squares	Mean Squares	"F" Number Ratio	5%	1%	Significance
Material (M)	2	.024	.012	2.22	3.88	5.85	Not Significant
Area (A)	2	.063	.0315	5.83	3.88	5.85	Significant
Temperature (T)	2	.093	.0415	7.67	3.88	5.85	Significant
M x T	4	.095	.0238	3.97	3.84	7.01	Barely at 5%
A x T	4	.094	.0235	3.92	3.84	7.01	Barely at 5%
Residual and M x A x T and M x A *	12	.065	.0054				

* M x A interaction not significant, hence pooled with residual and 2nd order interaction.

The friction measurements made through Series Twelve were taken under uncontrolled humidity conditions. Since the evaporator providing refrigeration for the test region was necessarily at a temperature below ambient, a temperature gradient and vapor pressure differential existed in the cold room. This vapor pressure differential acted to remove water vapor from the atmosphere. Thus a low relative humidity existed and ice surface sublimation occured. This ice sublimation and changing surface characteristics were considered particularly undesirable. A humidity chamber was therefore constructed within the cold room as described in Chapter Five. By placing quantities of snow and ice shavings in the humidity chamber it was possible to raise the humidity to values above 90% R. H.

Static friction measurements were first taken under the higher humidity conditions for packed snow. Over the range of the variables studied in the snow measurements it was not possible to determine any significance of the controlled variables with respect to random effects. It was found however that at individual parameter settings the deviation of individual measurements was less than the deviation under low humidity conditions. Undoubtedly the increased magnitude of the random effects was due to penetration and "digging in" of highly loaded sliders into the snow structure. This action caused grooves which affected later measurements. To insure against exceeding the bearing strength of the snow it is necessary to use only large lightly loaded sliders in friction on snow measurements.

Static friction on ice under high humidity conditions was also investigated. For purposes of comparison the same sliders and parameter settings used in the low humidity measurements of Series Ten were employed. Table 6-7 lists the results of the static friction on ice measurements under high humidity conditions (Series Fourteen). Table 6-8 presents the statistical results and deductions of these measurements. Contrary to the results of the low humidity conditions it was found that:

1. Load which had a negligible influence under low humidity has the greatest influence on the static coefficient under high humidity conditions.
2. Area has the next most significant effect under high humidity.
3. Material also has a significant effect.

An explanation of these friction characteristics under low and high humidity conditions in terms of the assumed frictional mechanism has not as yet been deduced.

Table 6-7

Analysis of Variance for Coefficient of Friction of Sliders on Ice.

Three Materials, Three Loads, Four Areas, and Three Replicates

Material	Steel (A)				Magnesium (B)				Brass (C)			
Area-cm^2	1/4	1	4	16	1/4	1	4	16	1/4	1	4	16
Load	.123	.335	.274	.298	.143	.196	.170	.419	.175	.197	.181	.214
80 grams	.210	.225	.273	.516	.119	.323	.328	.286	.175	.108	.463	.128
	.160	.200	.425	.420	.120	.253	.299	.205	.135	.185	.381	.356
	.154	.213	.209	.375	.140	.269	.226	.219	.141	.169	.422	.148
	.106	.303	.226	.297	.139	.234	.270	.233	.156	.195	.148	.220
160 grams	.114	.250	.483	.228	.138	.116	.343	.273	.147	.178	.153	.306
	.099	.086	.150	.138	.138	.083	.137	.092	.106	.049	.186	.071
	.125	.034	.195	.148	.072	.084	.100	.084	.128	.053	.098	.096
320 grams	.194	.100	.097	.137	.115	.068	.108	.134	.108	.120	.116	.124
Σ	1.285	1.746	2.332	2.557	1.124	1.626	1.981	1.945	1.271	1.254	2.148	1.663

Table 6-8

Material (M)	2	.043	.0215	4.89	3.10	4.85	Significant
Load (W)	2	.392	.196	44.6	3.10	4.85	Very Significant
Area (A)	3	.191	.06366	14.5	2.71	4.01	Very Significant
M x W	4	.002	.0005				
M x A	6	.027	.045	10.2	2.20	3.02	Very Significant
W x A	6	.092	.0153	3.48	2.20	3.02	Significant
M x W x A	12	.039	.00325	.00440			
Random	72	.346	.00480				

3rd order interaction not significant. Pool with random. M x W is not Significant. Pool with random and 3rd order interaction.

CHAPTER VII

INVESTIGATION OF STATIC AND KINETIC FRICTION ON ICE THROUGH EXAMINATION OF THE OSCILLATORY MOTION OF SLIDERS

Chapter VII

Investigation of Static and Kinetic Friction on Ice Through Examination of the Oscillatory Motion of Sliders

An experimental study has been made of the oscillatory motion of several bodies sliding on ice. The purpose of this study included:

1. Verification of the occurrence of "stick-slip" oscillations under predicted conditions.
2. Qualitative determination of the type of kinetic friction function encountered in the cases investigated.
3. Application of the oscillatory characteristics of the cantilever beam towing apparatus to the quantitative determination of the magnitude of the resistance constants obtained under several experimental conditions.

The experimental parameters which may be varied using the apparatus described in Chapter V include:

1. Material of the stationary surface
2. Relative roughness of the stationary surface
3. Material of the slider
4. Relative roughness of the slider
5. Curvature of Surface
6. Flexibility of slider
7. Shape of slider surface
8. Apparent area of slider surface

9. Ambient temperature

10. Normal load between slider and stationary surface

11. Spring constant of towing apparatus

12. Relative velocity of moving frame of reference

Due to limitations on the time and durability of the stationary surface only a few of the parameters were varied in this investigation. Experimental settings chosen for the first series of tests are listed in Table 7-1.

TABLE 7-1

PARAMETER SETTING FOR KINETIC TEST SERIES ONE

1.	Stationary surface -- clear bubble free ice frozen in the material tray
2.	Stationary surface smoothness -- ice machined and honed
3.	Slider materials -- Steel, Magnesium, Brass, Hickory, Plastic (English Bakelite)
4.	Slider surface -- honed
5.	Curvature of surface -- flat
6.	Flexibility of slider -- rigid block
7.	Shape of slider -- circular
8.	Apparent area of slider = four square centimeters
9.	Ambient temperature = - 45° F., - 30° F., + 15° F.
10.	Normal load between slider and stationary surface = 160 gram.
11.	Spring constant = 52 grams/centimeter
12.	Relative velocity = 2.54, 12.7, 25.4, 50.8, 101.6 cm/min.

For this first series of tests the usual engineering approach was followed in which only one variable was taken at a time and varied over its range while holding the associated variables at constant values. A second independent variable was then chosen and a new set of runs made. In conformance with this test approach the experimental procedure consisted of the following steps.

1. Ice surface prepared.
2. Test cell cooled to a selected temperature and held while other parameters varied through all settings.
3. Slider of desired material installed on test apparatus and loaded to 160 grams.
4. Carriage velocity adjusted to each desired setting and an oscillogram taken of resulting slider motion relative to the carriage.
5. Slider of second material installed and velocity again varied through all settings.
6. Ambient temperature adjusted to second temperature setting, and previous test procedure for slider materials and relative velocities repeated.

In this manner test runs were made for each of the experimental parameter combinations listed in Table 7-1. Examples of the resulting oscillograms for various materials, velocities, and temperatures are illustrated in Figures 7-1 through 7-4.

Steel on Ice 160 gram load
4 cm^2 Apparent Contact Area
Flat Honed Circular Slider Surface
15°F Low Humidity

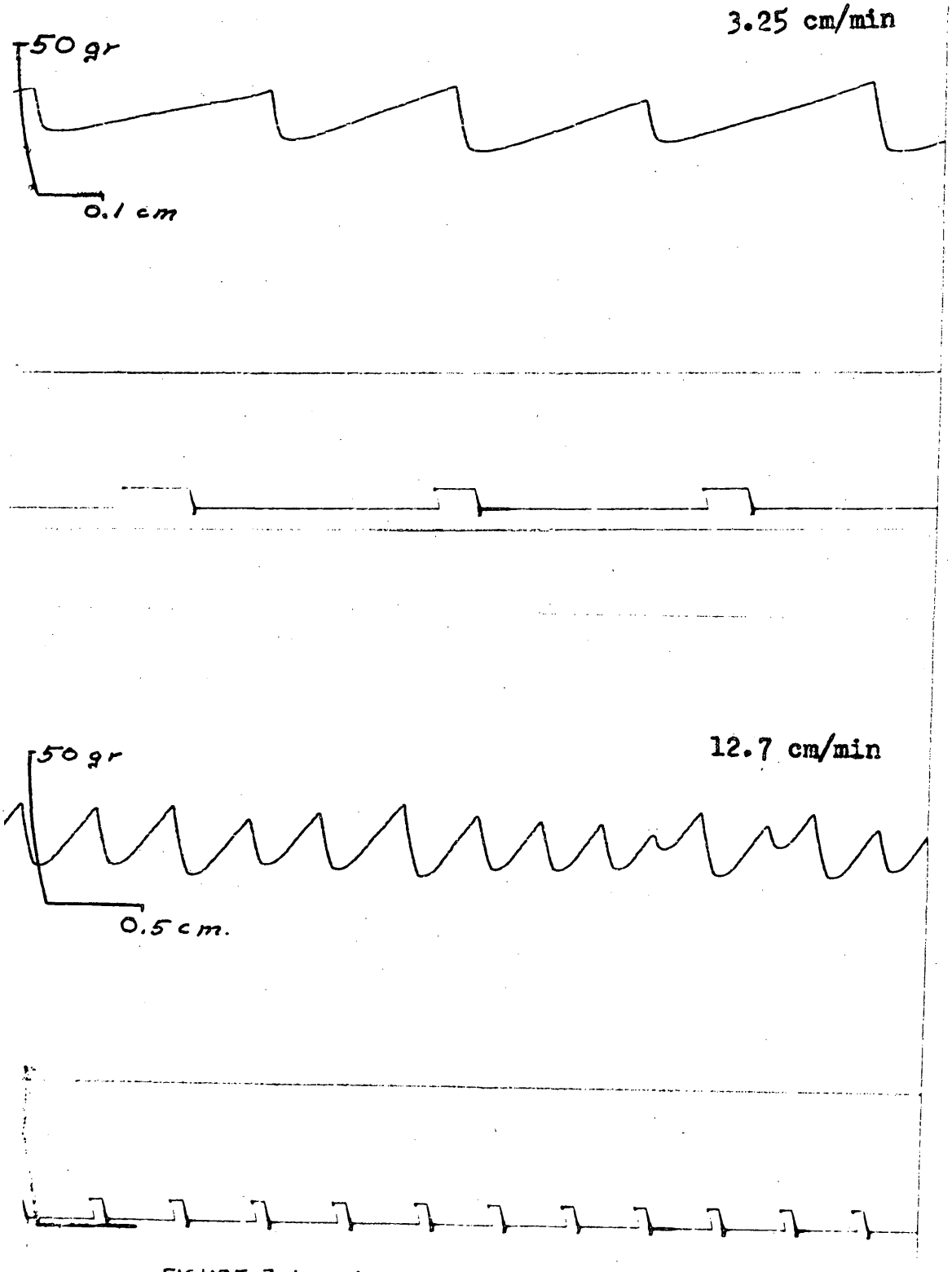

FIGURE 7-1a KINETIC OSCILLOGRAM

Steel on Ice 160 gram load
4 cm^2 Apparent Contact Area
Flat Honed Circular Slider Surface
15°F Low Humidity

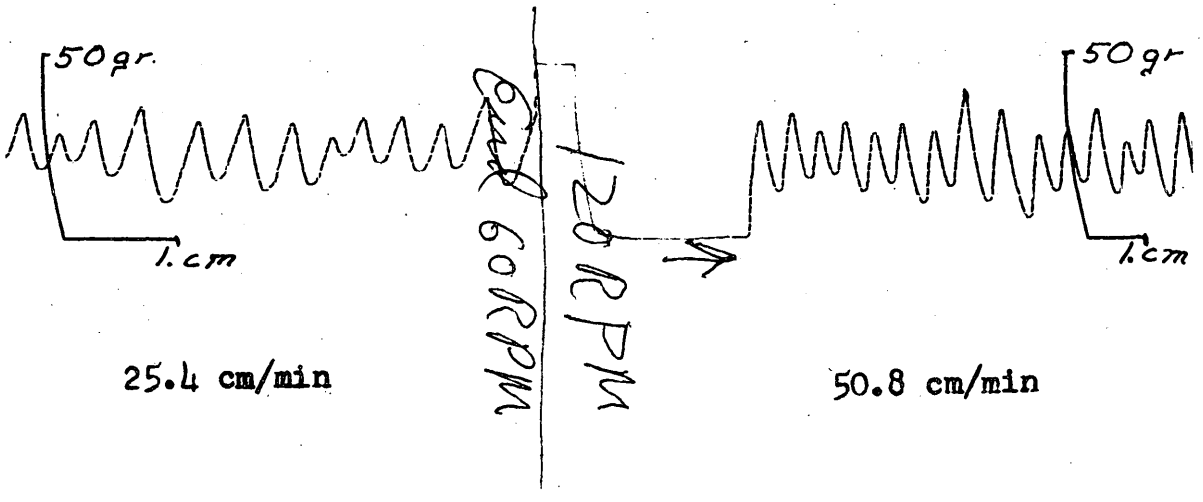

25.4 cm/min

50.8 cm/min

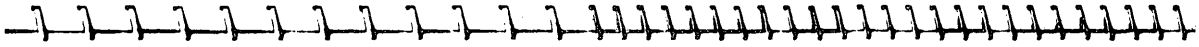

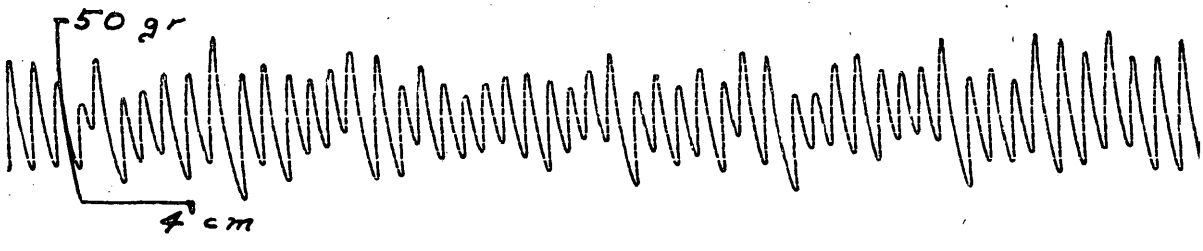

101.6 cm/min

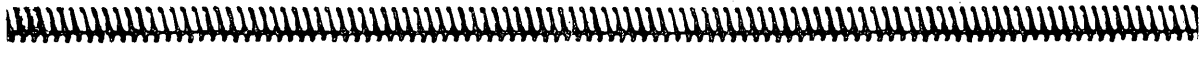

FIGURE 7-16 KINETIC OSCILLOGRAM

Magnesium on Ice 160 gram load
4 cm^2 Apparent Contact Area
Flat Honed Circular Slider Surface
15°F Low Humidity

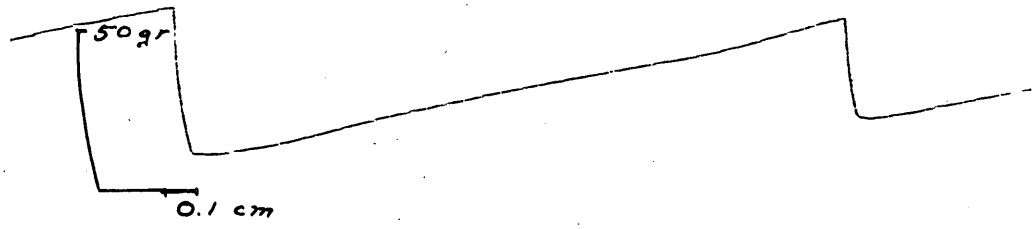

2.3 cm/min

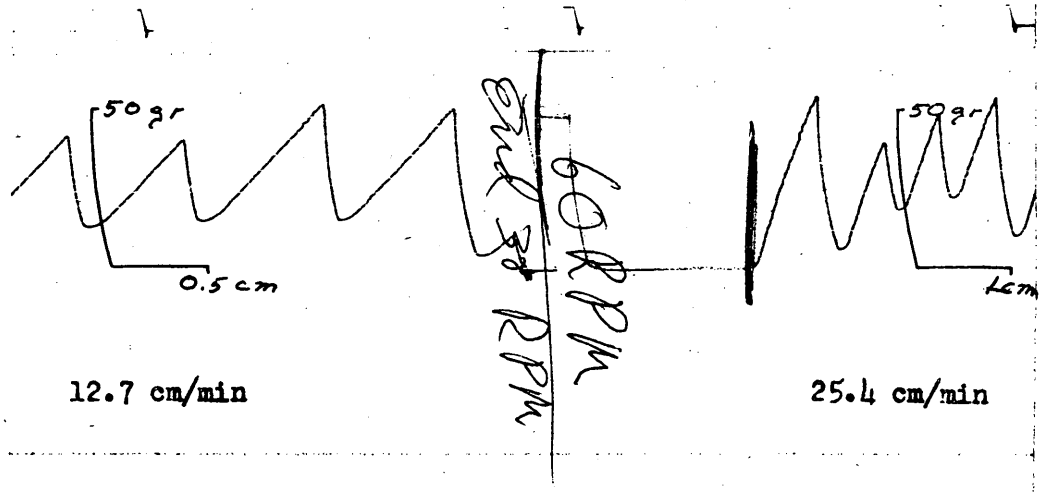

12.7 cm/min

25.4 cm/min

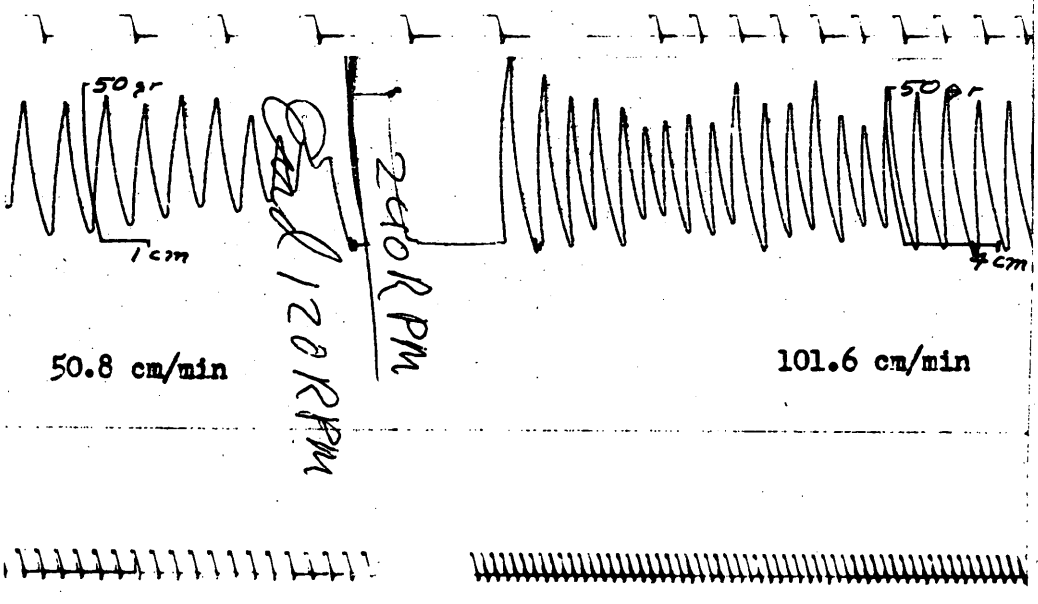

50.8 cm/min

101.6 cm/min

FIGURE 7-2 KINETIC OSCILLOGRAM

Brass on Ice 160 gram load
4 cm^2 Apparent Contact Area
Flat Honed Circular Slider Surface
15°F Low Humidity

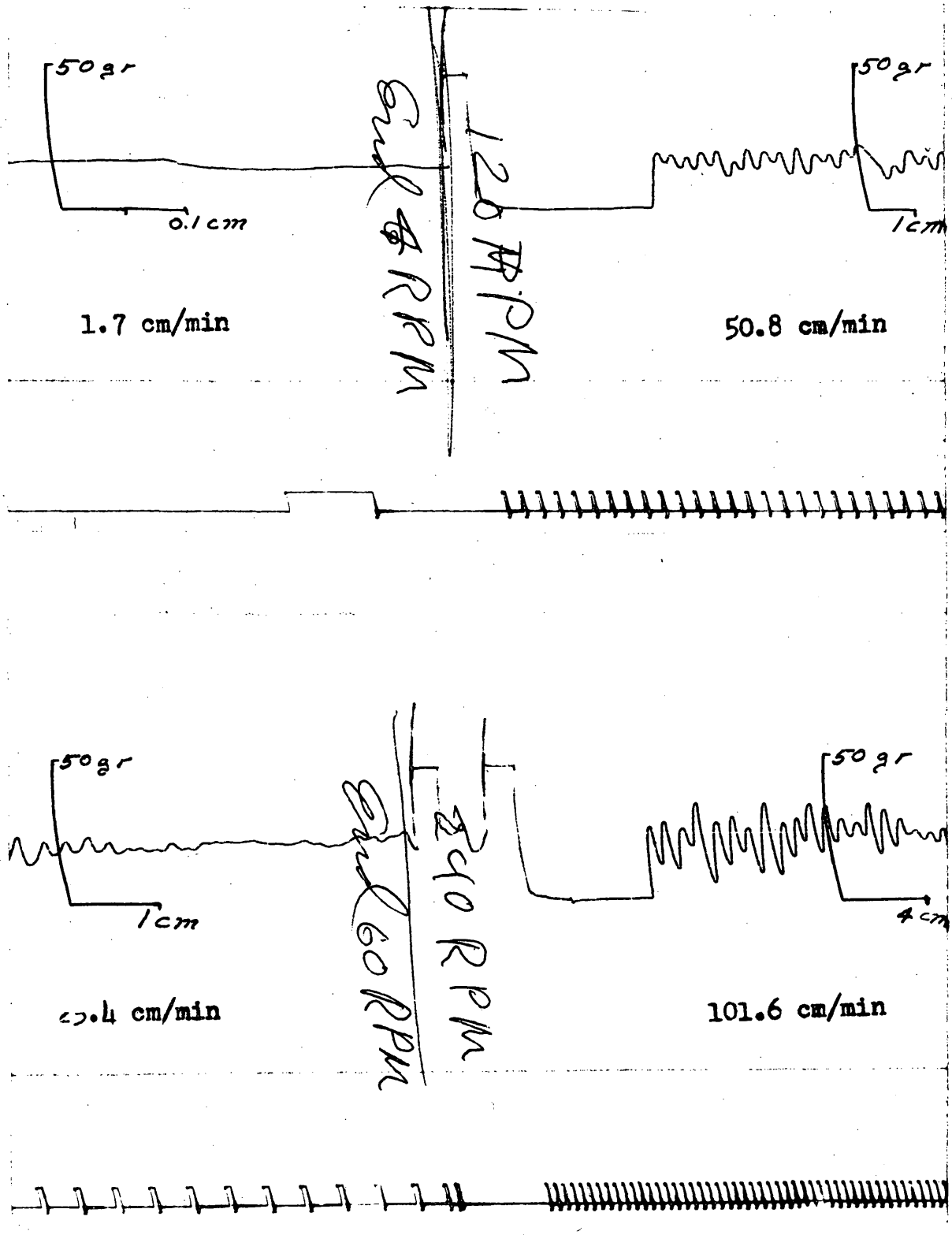

FIGURE 7-3 KINETIC OSCILLOGRAM

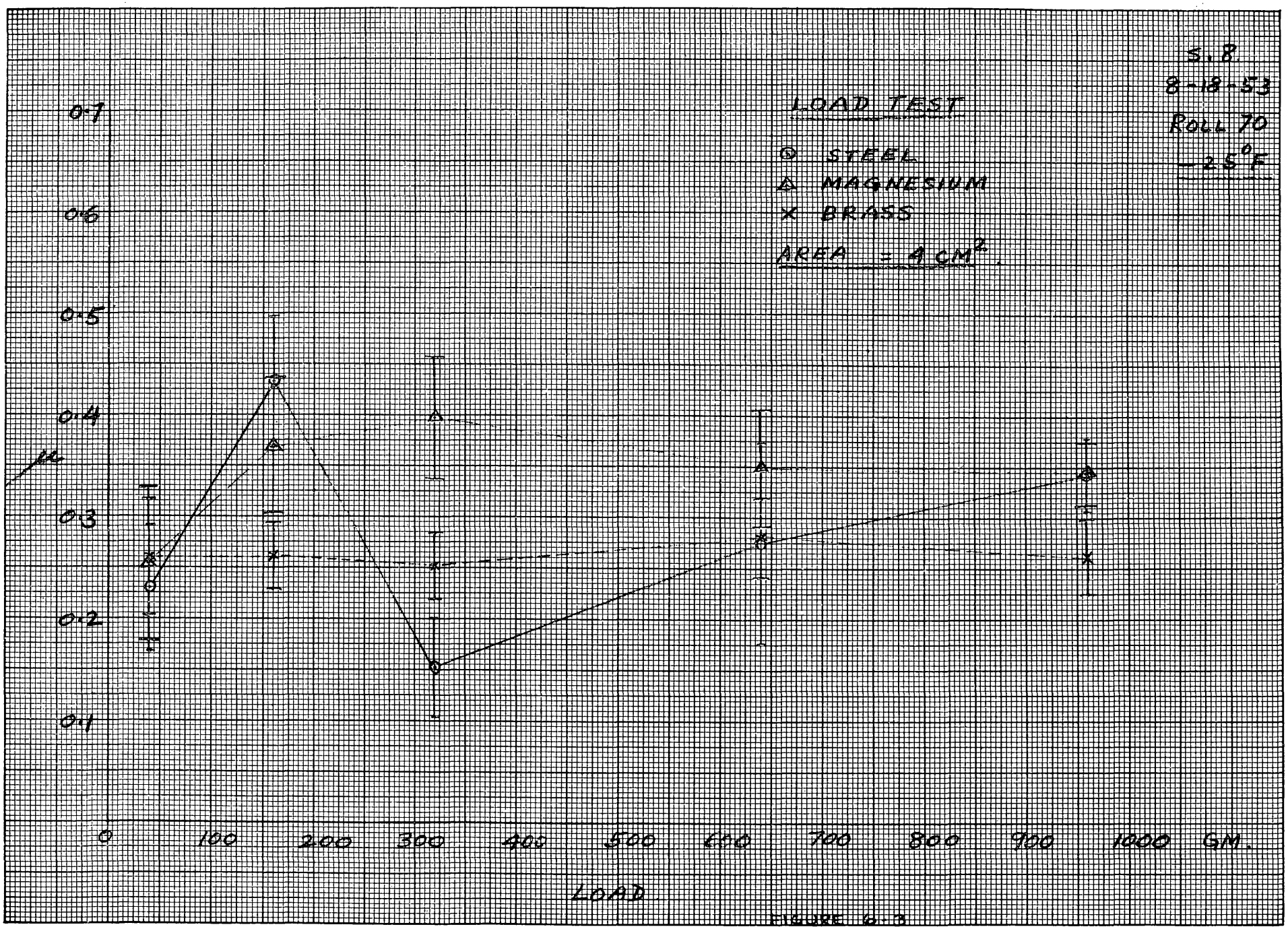
S.8
8-18-53
ROLL 70
-25°F
LOAD TEST
⊙ STEEL
△ MAGNESIUM
× BRASS
AREA = 4 CM².
0·7
0·6
0·5
0·4
0·3
0·2
0·1
0
100
200
300
400
500
600
700
800
900
1000
GM.
LOAD

FIGURE 6-3

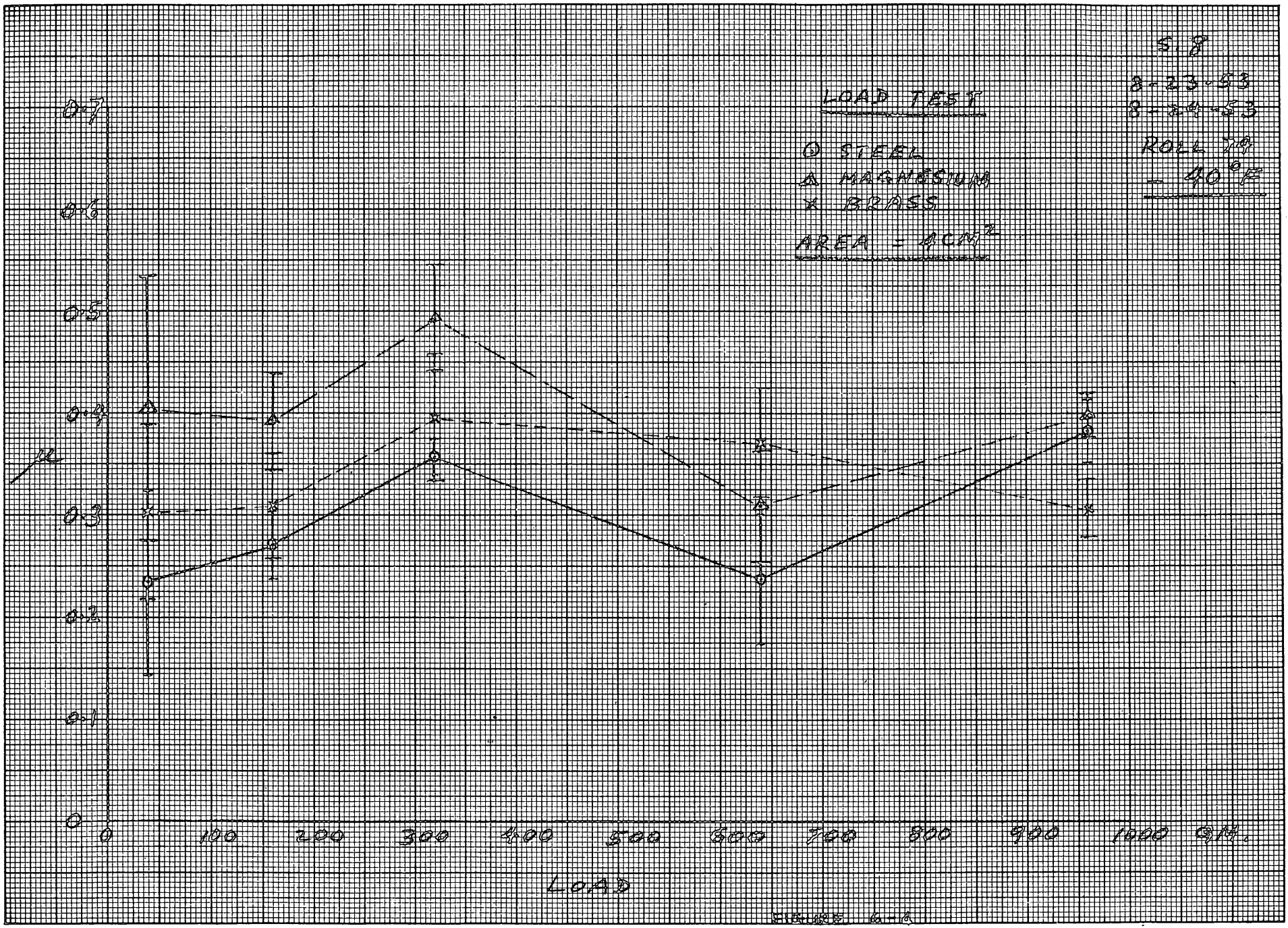
LOAD TEST
○ STEEL
△ MAGNESIUM
× BRASS
AREA = 4 CM²
S B
8-23-53
8-24-53
ROLL 20
40 PSI
0·7
0·6
0·5
0·4
0·3
0·2
0·1
0
0
100
200
300
400
500
600
700
800
900
1000
GM.
LOAD

FIGURE 6-4

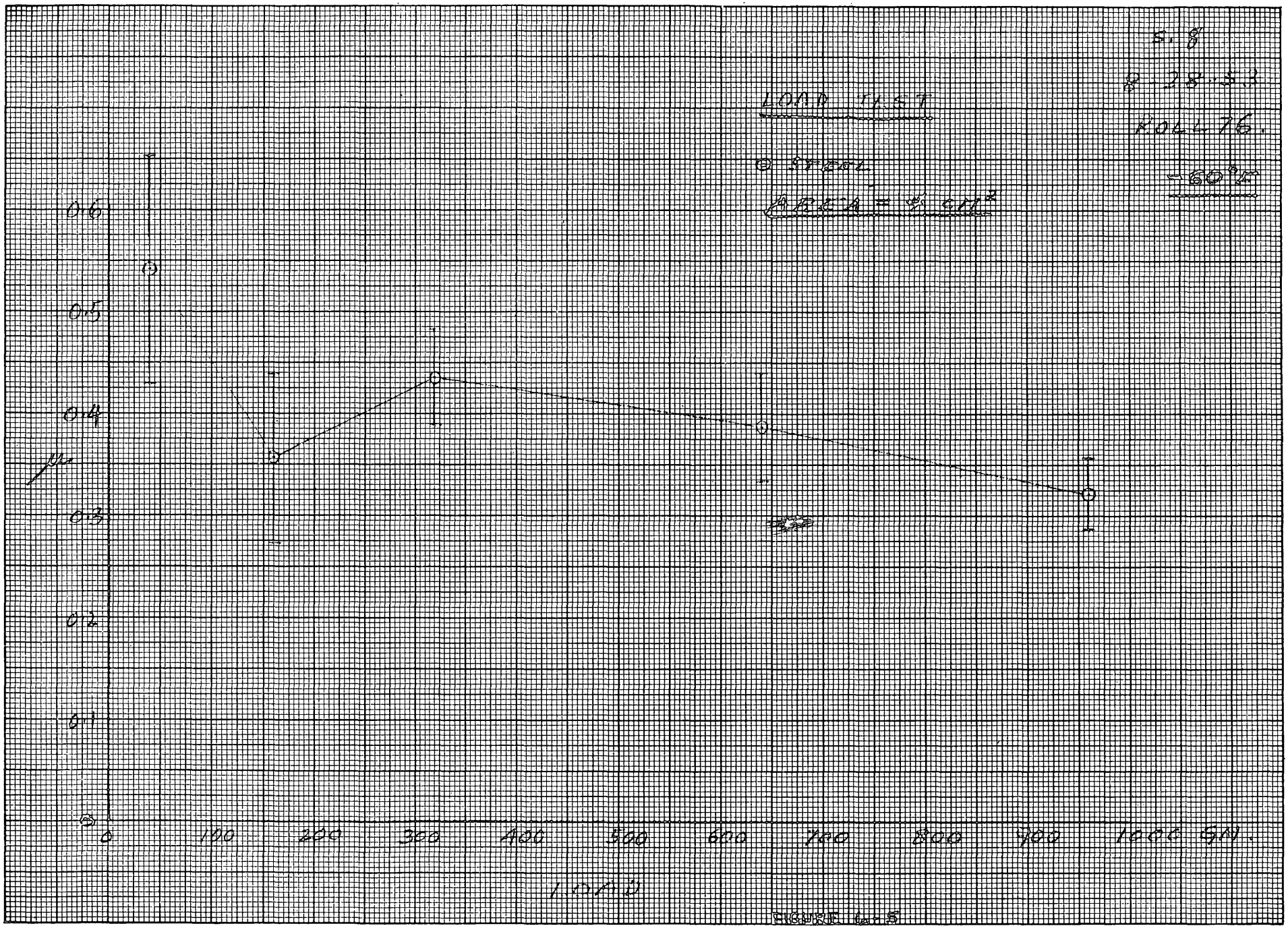
S. 6
8 - 28 - 53
R04476.
-60°F
LOAD TEST
0.6
0.5
0.4
μ
0.3
0.2
0.1
0
100
200
300
400
500
600
700
800
900
1000 PSI.
LOAD (#)

FIGURE 6.5

rising to approximately 0.4 at - 40° F. Brass and steel were next with practically the same static resistance. These materials had static coefficients of about 0.25 at + 15° F which rose to above 0.3 at - 40° F. and in the case of steel to values in the neighborhood of 0.4 at - 60° F. Hickory indicated the lowest static coefficient of friction with values of approximately 0.15 at + 15° F.

3. A decrease in temperature appeared to consistently increase the static friction force of all materials tested.

Area test results for sliders having apparent contact areas of 1/4, 1, 4, and 16 square centimeters under a constant load of 160 grams are plotted for slider materials of steel, magnesium, and brass and for ambient temperatures of + 15° F., - 30° F., and - 47° F. in Figures 6-6 through 6-8. These graphs apparently indicate:

1. Static friction force increases slightly with an increase in the apparent contact area.
2. A decrease in the temperature appeared to increase the static friction force.

Results of the pressure tests are plotted in Figures 6-9 and 6-10. In this set of experiments both the area and the load were changed at each test in such a way as to hold the pressure or ratio of load over apparent area at a constant value of 40 gms/cm^2. Sliders of steel, magnesium, and brass were tested in this fashion at + 15° F. and - 32° F. In order to agree with the predictions of other investigators the static coefficient should remain constant for a particular pressure. It is difficult to judge from the actual curves of Figures 6-9 and 6-10 whether this constancy is correct.

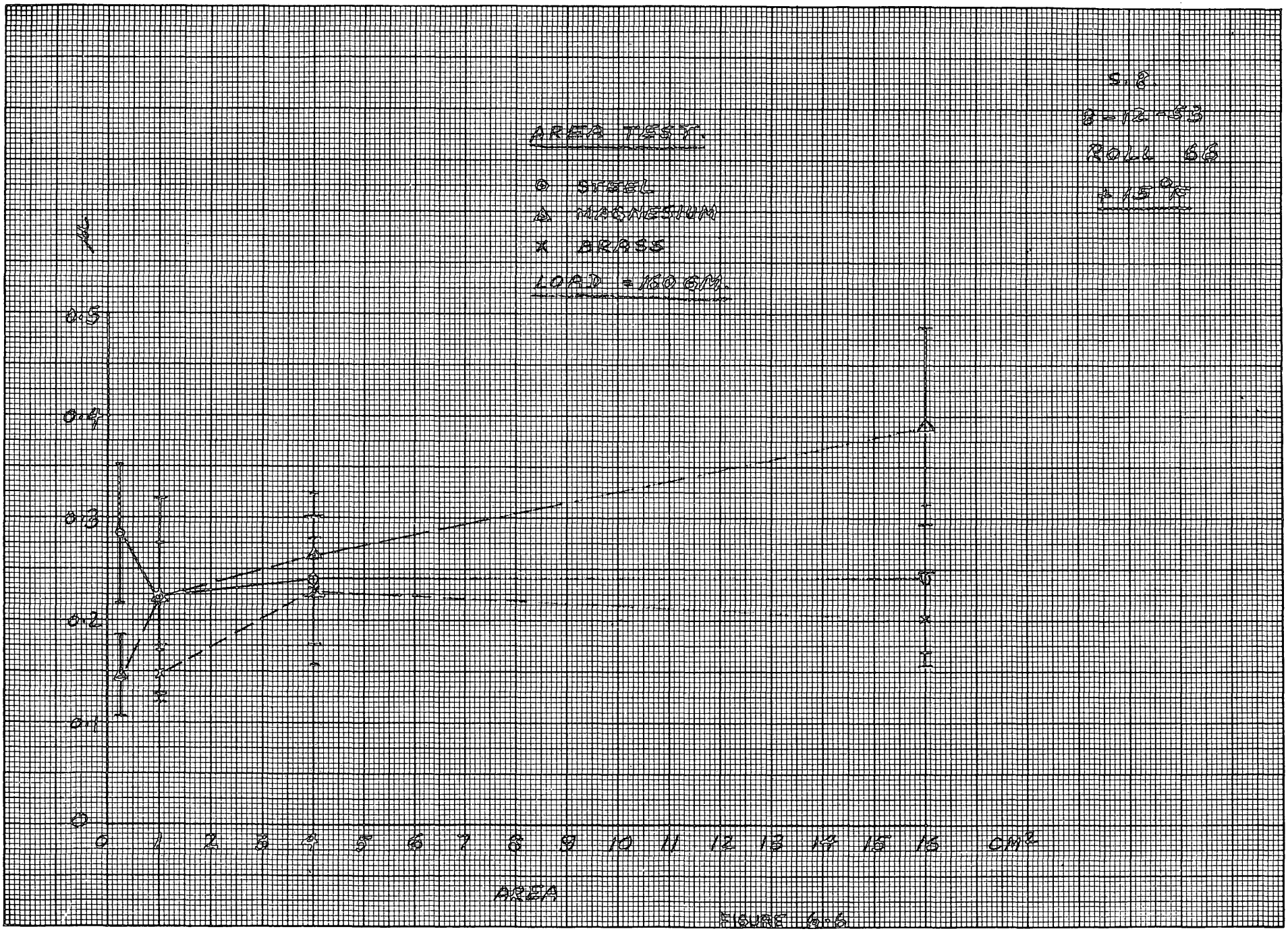
AREA TEST
○ STEEL
△ MAGNESIUM
× BRASS
LOAD = 1500 KM.
S.G.
8-12-53
ROLL 66
415 °K
0.5
0.4
0.3
0.2
0.1
0
0 1 2 3 4 5 6 7 8 9 10 11 12 13 14 15 16 CM²
AREA

FIGURE 6-6

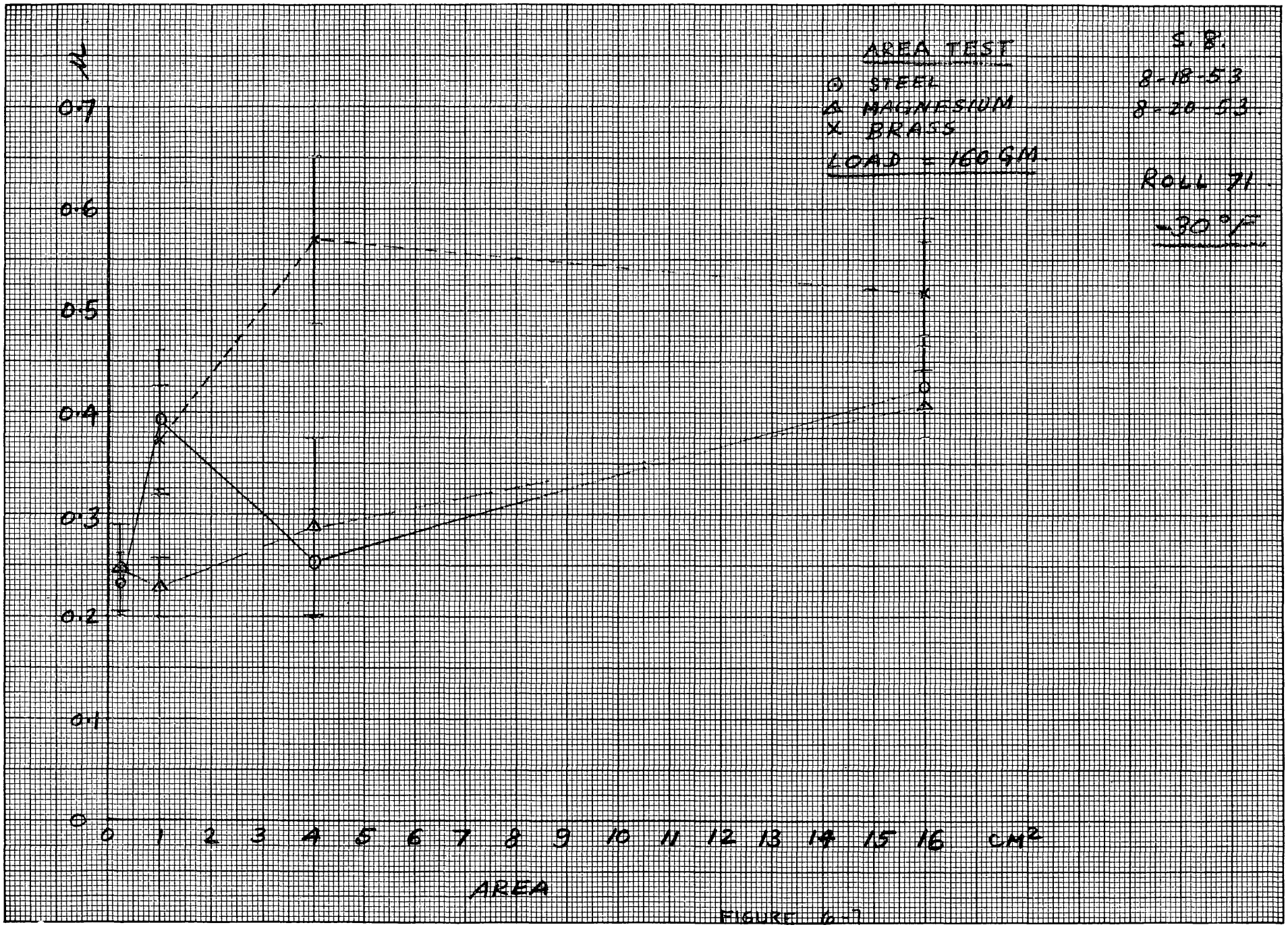
AREA TEST
⊙ STEEL
Δ MAGNESIUM
× BRASS
LOAD = 160 GM
S. B.
8-18-53
8-20-53
ROLL 71
-30°F
R
0.7
0.6
0.5
0.4
0.3
0.2
0.1
0
0 1 2 3 4 5 6 7 8 9 10 11 12 13 14 15 16 CM²
AREA

FIGURE 6-7

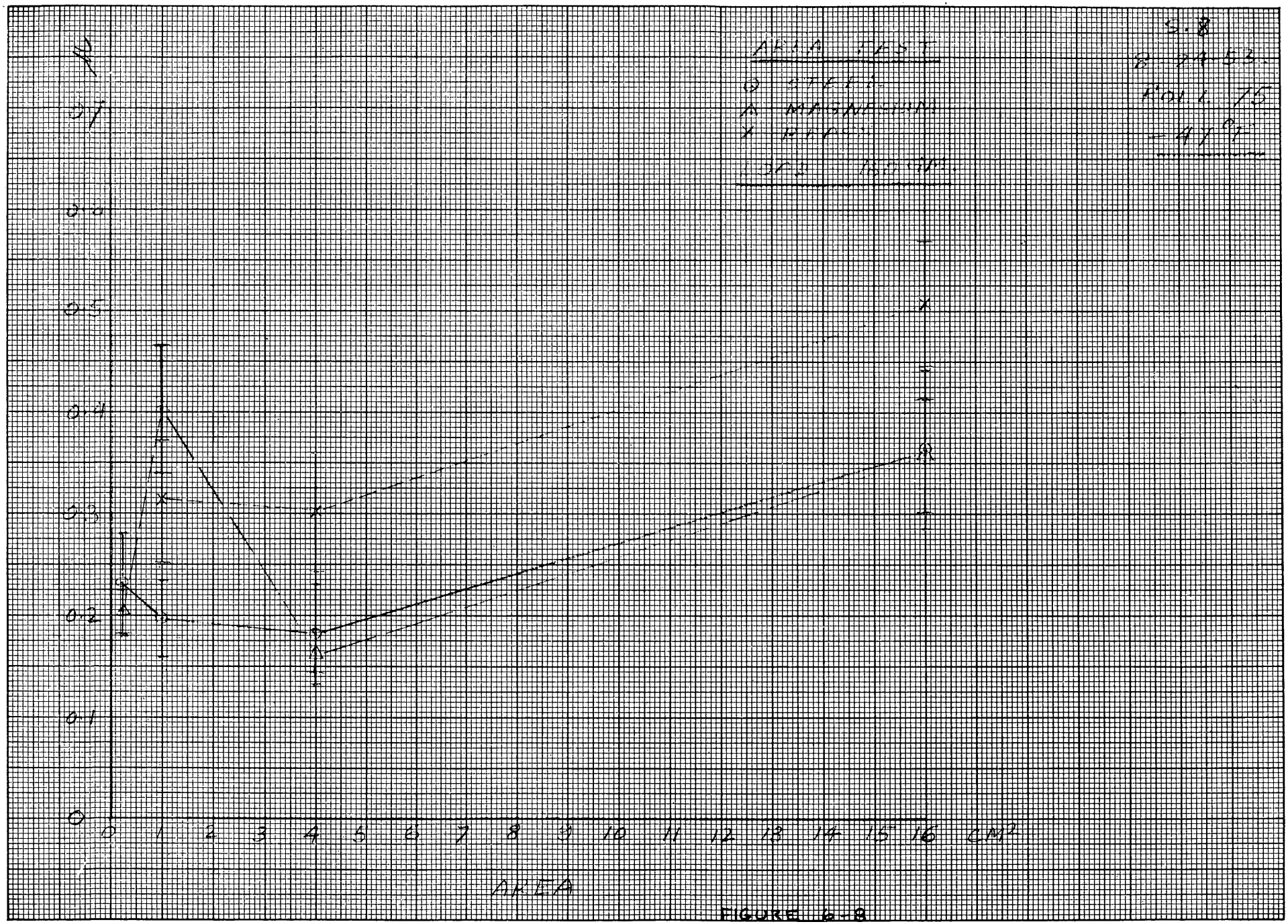

FIGURE 6-8

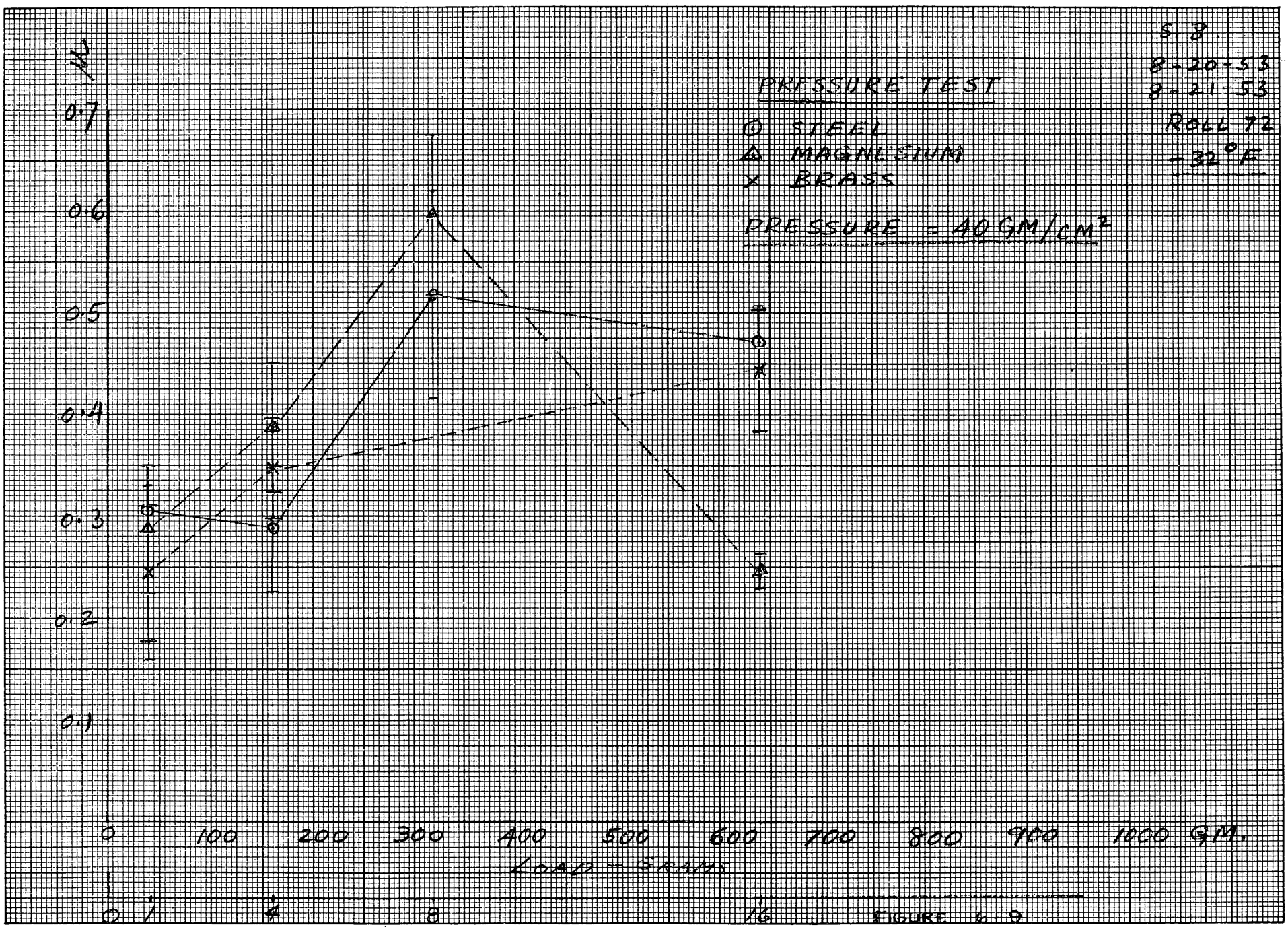
PRESSURE TEST
○ STEEL
△ MAGNESIUM
× BRASS
PRESSURE = 40 GM/CM²
S 8
8-20-53
8-21-53
ROLL 72
-32° F
P
0.7
0.6
0.5
0.4
0.3
0.2
0.1
0
100
200
300
400
500
600
700
800
900
1000 GM.
LOAD - GRAMS
0
4
8
16

FIGURE 6.9

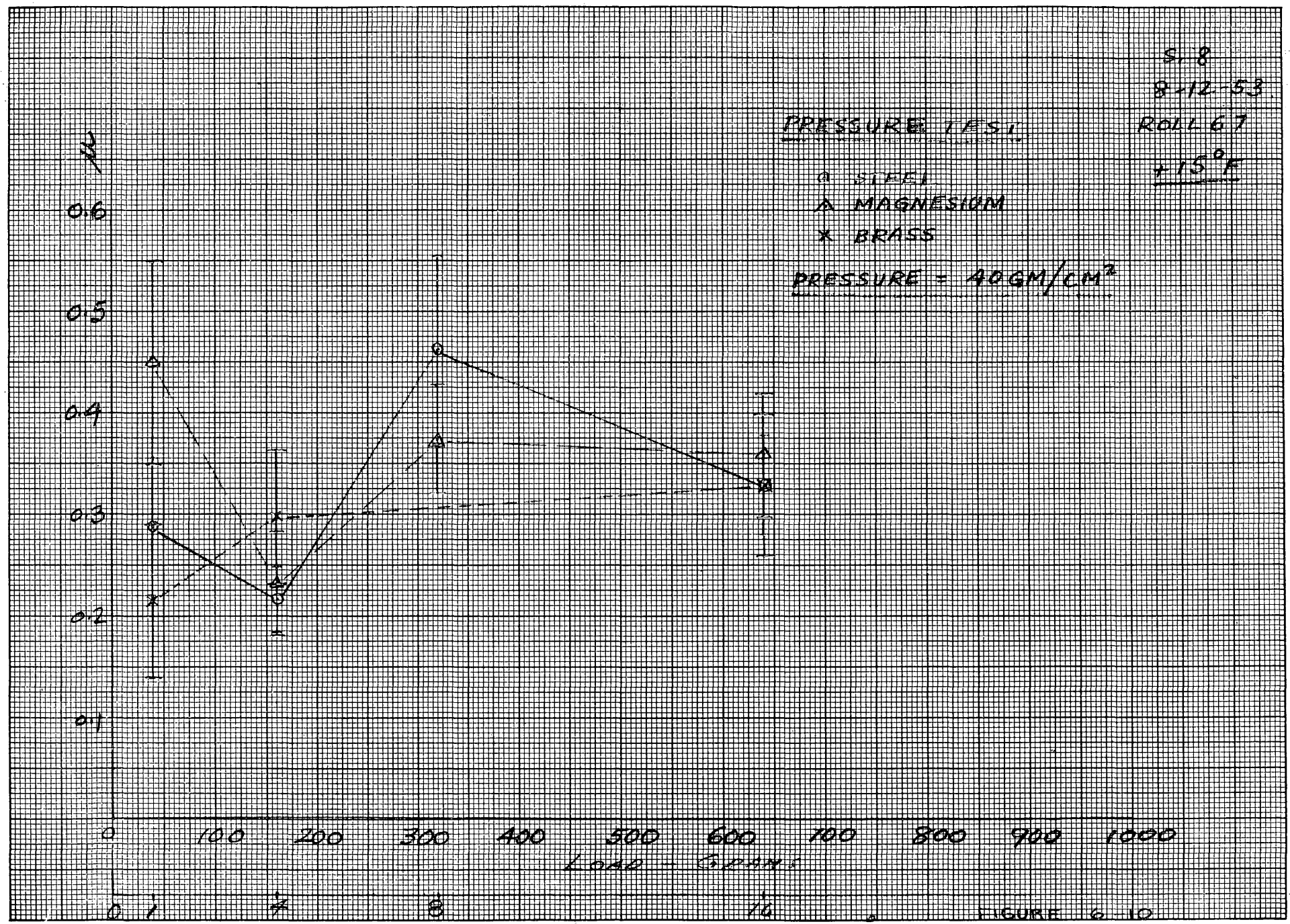
S, 8
8-12-53
ROLL 67
+15°F
PRESSURE TEST
○ STEEL
△ MAGNESIUM
× BRASS
PRESSURE = 40 GM/CM²
0.6
0.5
0.4
0.3
0.2
0.1
0
100
200
300
400
500
600
700
800
900
1000
LOAD - GRAMS

FIGURE 6.10

The Tenth Series of Friction Force Measurements was the first of the test series in which the Theory of Variance was to be applied as the basis of judging the relative influence of the several variables. In this series the following question was posed: "Is the influence of slider material, apparent contact area, load, or any combination of these variables more significant than any of the unknown or uncontrolled variables present in the test?"

An experiment was planned and performed in which three slider materials, four areas, and four loads were to be investigated. The sliders used were the same sliders previously studied in earlier test series. These sliders had a circular shape with a flat contact area. The slider materials were of steel, magnesium, and brass; the apparent contact areas equaled 1/4, 1, 4, and 16 cm^2. Loads to be applied to the slider equaled 80, 160, 320, and 640 grams.

Three replicate sets of measurements of all combinations of the studied variables were obtained. In each replicate set the friction measurement for a particular combination of variables was made in a different random order. Since there were $3 \times 4 \times 4 = 48$ combinations of the parameter settings, a total of 144 values of the coefficient of friction were determined. Each of these values incidentally represented the mean of fifty separate measurements. Unfortunately certain discrepancies in the resulting data at three combination points in one of the replicate sets, required the elimination of these points and consequently the elimination of the entire replicate set. The data obtained in the

remaining two replicate sets are tabulated in Table 6-1. This data was numerically processed using the methods of the Theory of Variance to provide the results tabulated in Table 6-2. The fifth column of this table lists the ratio of the mean squares corresponding to the parameter of interest over the mean squares of the random and triple cross product. The sixth column lists the so called "F" numbers for a 5% and a 1% significance level for the particular combination of degrees of freedom of the studied variable and the random variables. According to Variance Theory if the ratio listed in the fifth column has a numerical value less than the 5% "F" number, the parameter is most likely insignificant in its effect. At least it is possible to place a 95% confidence in this decision. On the other hand if the ratio is greater than the 5% "F" number, the corresponding parameter is possibly significant, and if the ratio exceeds the 1% "F" number, the parameter is undoubtedly quite significant.

The conclusions which may be drawn from the variance analysis of the Series Ten measurements are therefore:

1. Apparent Contact Area under the imposed conditions is very significant.
2. Slider material is significant.
3. Load is not significant.
4. The cross product of material and area is significant while all other cross products including the triple cross product of material times area times load are not significant.

Table 6-1

Series Ten Measurements of the Static Coefficient

of Friction on Ice for Material, Area, and Load Parameters

Material	Steel				Magnesium				Brass			
Area-cm^2	1/4	1	4	16	1/4	1	4	16	1/4	1	4	16
Load-gm												
80	.234	.422	.216	.234	.191	.203	.253	.175	.141	.266	.134	.216
	.097	.303	.266	.021	.097	.141	.269	.219	.131	.262	.216	.181
160	.253	.144	.347	.231	.112	.175	.481	.219	.119	.162	.138	.147
	.100	.162	.219	.421	.119	.159	.381	.303	.100	.228	.241	.247
320	.119	.178	.456	.219	.062	.288	.396	.338	.261	.247	.238	.191
	.214	.131	.343	.325	.078	.119	.492	.402	.112	.133	.142	.235
640	.244	.206	.397	.309	.209	.175	.547	.347	.078	.206	.178	.280
	.116	.209	.244	.325	.126	.109	.462	.369	.071	.191	.259	.225

Table 6-2

Variance Analysis of Series Ten Measurements of Static Friction on Ice versus Material, Area, and Load Parameters

Variable	Degrees of Freedom	Sum of Squares	Mean Squares	Ratio	"F" Number 5%	1%	Significance
M	2	.0752	.0376	4.04	3.14	4.95	barely significant at 5%
W	3	.0262	.0087	.936	2.75	4.09	not significant
A	3	.3615	.1205	13.0	2.75	4.09	very significant
M x W	6	.0235	.0039	.420	2.32	3.09	not significant
M x A	6	.1694	.0282	3.03	2.32	3.09	barely significant at 5%
W x A	9	.1272	.0141	1.52	2.02	2.69	not significant
random	67	.6219	.0093				

M = Material

W = Load

A = Apparent Area

Note:

Second order interaction insignificant, hence was pooled with the original random to give the tabulated random.

A further visual examination of the friction coefficients tabulated in Table 6-1 reveals that:

1. The static coefficient rises with an increase in the apparent area of contact.
2. Magnesium appeared to have the highest static coefficient followed in turn by steel and then brass.

Although the results of the variance analysis of the Series Ten measurements appear to definitely indicate a significance in the area and material parameters, this significance may possibly have been incorrectly assigned by the method of parameter description. For example the experimental study of the variation of area and material requires the use of completely separate sliders while load values may be varied over the same slider. There is thus the possibility that the significance attributed to area and material is actually a significance caused by other factors in the manufacture of the slider. It is possible therefore that the significance found in the Series Ten Measurements is due to a difference in individual sliders rather than to a difference in the material or area.

A new experiment was planned to test the reproducibility of the material variation. For this experiment four sliders were manufactured identical in all respects except for material. Two sliders of the group were made from steel and two made from brass. The following question was then posed: "Does the slider material cause a more significant variation of the friction than exists between individual sliders?"

Series Twelve friction measurements were made to compare the influence of slider material versus the influence of individual sliders.

Four replicate measurements were made in random order of the static friction coefficient of the four sliders. The experimental results of these measurements are tabulated in Table 6-3, and the variance analysis results in Table 6-4.

The variance analysis of Series Twelve measurements indicates that material is a very significant factor while the individual slider is not. Thus greater static friction was found to occur between sliders of dissimilar materials than between sliders of the same material.

While the significance of material was definitely established by the Series Twelve measurements, the proper interpretation of the significance attributed to area is still in question. Since the sliders were circular in shape an increase in slider area between separate sliders was accompanied by an increase in outside perimeter. It is possible that the variation assigned to slider area is actually caused by an "edge" effect. To investigate this possibility, an experiment has been proposed in which the sliders will have a ring shape with an outer and inner edge. If the sliders are constructed with a comparatively large outside diameter and perimeter, the variation of the inside diameter accompanying the variation of the contact area will not greatly change the inner and total perimeters. The performance of this experiment has been planned to accompany other investigations regarding the side or groove effect in frictional resistance.

Table 6-3

Series Twelve Measurement of the Reproducibility of the Static Coefficient of Friction on Ice for Two Materials over two Sliders of Each Material.

Material	Steel	Brass
	0.275	0.234
	0.266	0.212
Slider	0.234	0.203
One	0.338	0.191
	Avg. = 0.278	Avg. = 0.210
	0.359	0.191
	0.303	0.209
Slider	0.325	0.159
Two	0.272	0.184
	Avg. = 0.314	Avg. = 0.187

Table 6-4

Variance Analysis of Series Twelve Measurements of the Reproducibility of the Static Coefficient of Friction on Ice for Two Materials over Two Sliders of each Material

Variable	Degrees of Freedom	Sum of Squares	Mean Squares	Ratio	"F" Number 5%	"F" Number 1%	Significance
Material	1	0.0395	0.0395	32.6	4.67	9.07	Very Significant
Slider	1	0.0003	0.0003	0.248	4.67	9.07	Not Significant
M x S	1	0.0037	0.0037	3.7	4.75	9.33	Not Significant
Random	12	0.012	0.001				

Since considerable data had been collected in previous test series an attempt was made to reexamine this data using the methods of the Theory of Variance. In particular it was hoped to be able to establish the significance of temperature. It was possible to collect from previous measurements sufficient data for an analysis based on three materials, three areas, and three temperatures. The static coefficient of friction data for these three parameters are tabulated in Table 6-5. Results of the variance analysis of these parameters are given in Table 6-6. From this analysis the following conclusions may be drawn:

1. Temperature has the greatest effect.
2. Area has a large effect but less than that of temperature.
3. Material also has an effect but less than that of area.

Table 6-5

Static Coefficient of Friction on Ice for

Three Materials, Three Areas, and Three Temperatures

	M_1			M_2			M_3		
	T_1	T_2	T_3	T_1	T_2	T_3	T_1	T_2	T_3
A_1	.241	.425	.363	.390	.406	.360	.202	.517	.506
A_2	.240	.254	.181	.263	.288	.163	.229	.569	.301
A_3	.223	.394	.197	.222	.228	.403	.149	.372	.313

Where: M_1 = steel, M_2 = magnesium, M_3 = brass

A_1 = 16 cm^2, A_2 = 4 cm^2, A_3 = 1 cm^2

T_1 = +15° F., T_2 = -30° F., T_3 = -47° F.

Load = 160 grams

TABLE 6-6

Variance Analysis of Influence on Static Friction on Ice of Three Materials, Three Areas, and Three Temperatures

Variable	Degrees of Freedom	Sum of Squares	Mean Squares	"F" Number Ratio	5%	1%	Significance
Material (M)	2	.024	.012	2.22	3.88	5.85	Not Significant
Area (A)	2	.063	.0315	5.83	3.88	5.85	Significant
Temperature (T)	2	.093	.0415	7.67	3.88	5.85	Significant
M x T	4	.095	.0238	3.97	3.84	7.01	Barely at 5%
A x T	4	.094	.0235	3.92	3.84	7.01	Barely at 5%
Residual and M x A x T and M x A *	12	.065	.0054				

* M x A interaction not significant, hence pooled with residual and 2nd order interaction.

The friction measurements made through Series Twelve were taken under uncontrolled humidity conditions. Since the evaporator providing refrigeration for the test region was necessarily at a temperature below ambient, a temperature gradient and vapor pressure differential existed in the cold room. This vapor pressure differential acted to remove water vapor from the atmosphere. Thus a low relative humidity existed and ice surface sublimation occured. This ice sublimation and changing surface characteristics were considered particularly undesirable. A humidity chamber was therefore constructed within the cold room as described in Chapter Five. By placing quantities of snow and ice shavings in the humidity chamber it was possible to raise the humidity to values above 90% R. H.

Static friction measurements were first taken under the higher humidity conditions for packed snow. Over the range of the variables studied in the snow measurements it was not possible to determine any significance of the controlled variables with respect to random effects. It was found however that at individual parameter settings the deviation of individual measurements was less than the deviation under low humidity conditions. Undoubtedly the increased magnitude of the random effects was due to penetration and "digging in" of highly loaded sliders into the snow structure. This action caused grooves which affected later measurements. To insure against exceeding the bearing strength of the snow it is necessary to use only large lightly loaded sliders in friction on snow measurements.

Static friction on ice under high humidity conditions was also investigated. For purposes of comparison the same sliders and parameter settings used in the low humidity measurements of Series Ten were employed. Table 6-7 lists the results of the static friction on ice measurements under high humidity conditions (Series Fourteen). Table 6-8 presents the statistical results and deductions of these measurements. Contrary to the results of the low humidity conditions it was found that:

1. Load which had a negligible influence under low humidity has the greatest influence on the static coefficient under high humidity conditions.
2. Area has the next most significant effect under high humidity.
3. Material also has a significant effect.

An explanation of these friction characteristics under low and high humidity conditions in terms of the assumed frictional mechanism has not as yet been deduced.

Table 6-7

Analysis of Variance for Coefficient of Friction of Sliders on Ice.

Three Materials, Three Loads, Four Areas, and Three Replicates

Material	Steel (A)				Magnesium (B)				Brass (C)			
Area-cm^2	1/4	1	4	16	1/4	1	4	16	1/4	1	4	16
Load	.123	.335	.274	.298	.143	.196	.170	.419	.175	.197	.181	.214
80 grams	.210	.225	.273	.516	.119	.323	.328	.286	.175	.108	.463	.128
	.160	.200	.425	.420	.120	.253	.299	.205	.135	.185	.381	.356
	.154	.213	.209	.375	.140	.269	.226	.219	.141	.169	.422	.148
	.106	.303	.226	.297	.139	.234	.270	.233	.156	.195	.148	.220
160 grams	.114	.250	.483	.228	.138	.116	.343	.273	.147	.178	.153	.306
	.099	.086	.150	.138	.138	.083	.137	.092	.106	.049	.186	.071
	.125	.034	.195	.148	.072	.084	.100	.084	.128	.053	.098	.096
320 grams	.194	.100	.097	.137	.115	.068	.108	.134	.108	.120	.116	.124
Σ	1.285	1.746	2.332	2.557	1.124	1.626	1.981	1.945	1.271	1.254	2.148	1.663

Table 6-8

Material (M)	2	.043	.0215	4.89	3.10	4.85	Significant
Load (W)	2	.392	.196	44.6	3.10	4.85	Very Significant
Area (A)	3	.191	.06366	14.5	2.71	4.01	Very Significant
M x W	4	.002	.0005				
M x A	6	.027	.045	10.2	2.20	3.02	Very Significant
W x A	6	.092	.0153	3.48	2.20	3.02	Significant
M x W x A	12	.039	.00325	.00440			
Random	72	.346	.00480				

3rd order interaction not significant. Pool with random. M x W is not Significant. Pool with random and 3rd order interaction.

CHAPTER VII

INVESTIGATION OF STATIC AND KINETIC FRICTION ON ICE THROUGH EXAMINATION OF THE OSCILLATORY MOTION OF SLIDERS

Chapter VII

Investigation of Static and Kinetic Friction on Ice Through Examination of the Oscillatory Motion of Sliders

An experimental study has been made of the oscillatory motion of several bodies sliding on ice. The purpose of this study included:

1. Verification of the occurrence of "stick-slip" oscillations under predicted conditions.
2. Qualitative determination of the type of kinetic friction function encountered in the cases investigated.
3. Application of the oscillatory characteristics of the cantilever beam towing apparatus to the quantitative determination of the magnitude of the resistance constants obtained under several experimental conditions.

The experimental parameters which may be varied using the apparatus described in Chapter V include:

1. Material of the stationary surface
2. Relative roughness of the stationary surface
3. Material of the slider
4. Relative roughness of the slider
5. Curvature of Surface
6. Flexibility of slider
7. Shape of slider surface
8. Apparent area of slider surface

9. Ambient temperature

10. Normal load between slider and stationary surface

11. Spring constant of towing apparatus

12. Relative velocity of moving frame of reference

Due to limitations on the time and durability of the stationary surface only a few of the parameters were varied in this investigation. Experimental settings chosen for the first series of tests are listed in Table 7-1.

TABLE 7-1

PARAMETER SETTING FOR KINETIC TEST SERIES ONE

1.	Stationary surface -- clear bubble free ice frozen in the material tray
2.	Stationary surface smoothness -- ice machined and honed
3.	Slider materials -- Steel, Magnesium, Brass, Hickory, Plastic (English Bakelite)
4.	Slider surface -- honed
5.	Curvature of surface -- flat
6.	Flexibility of slider -- rigid block
7.	Shape of slider -- circular
8.	Apparent area of slider = four square centimeters
9.	Ambient temperature = - 45° F., - 30° F., + 15° F.
10.	Normal load between slider and stationary surface = 160 gram.
11.	Spring constant = 52 grams/centimeter
12.	Relative velocity = 2.54, 12.7, 25.4, 50.8, 101.6 cm/min.

For this first series of tests the usual engineering approach was followed in which only one variable was taken at a time and varied over its range while holding the associated variables at constant values. A second independent variable was then chosen and a new set of runs made. In conformance with this test approach the experimental procedure consisted of the following steps.

1. Ice surface prepared.
2. Test cell cooled to a selected temperature and held while other parameters varied through all settings.
3. Slider of desired material installed on test apparatus and loaded to 160 grams.
4. Carriage velocity adjusted to each desired setting and an oscillogram taken of resulting slider motion relative to the carriage.
5. Slider of second material installed and velocity again varied through all settings.
6. Ambient temperature adjusted to second temperature setting, and previous test procedure for slider materials and relative velocities repeated.

In this manner test runs were made for each of the experimental parameter combinations listed in Table 7-1. Examples of the resulting oscillograms for various materials, velocities, and temperatures are illustrated in Figures 7-1 through 7-4.

Steel on Ice 160 gram load
4 cm^2 Apparent Contact Area
Flat Honed Circular Slider Surface
15°F Low Humidity

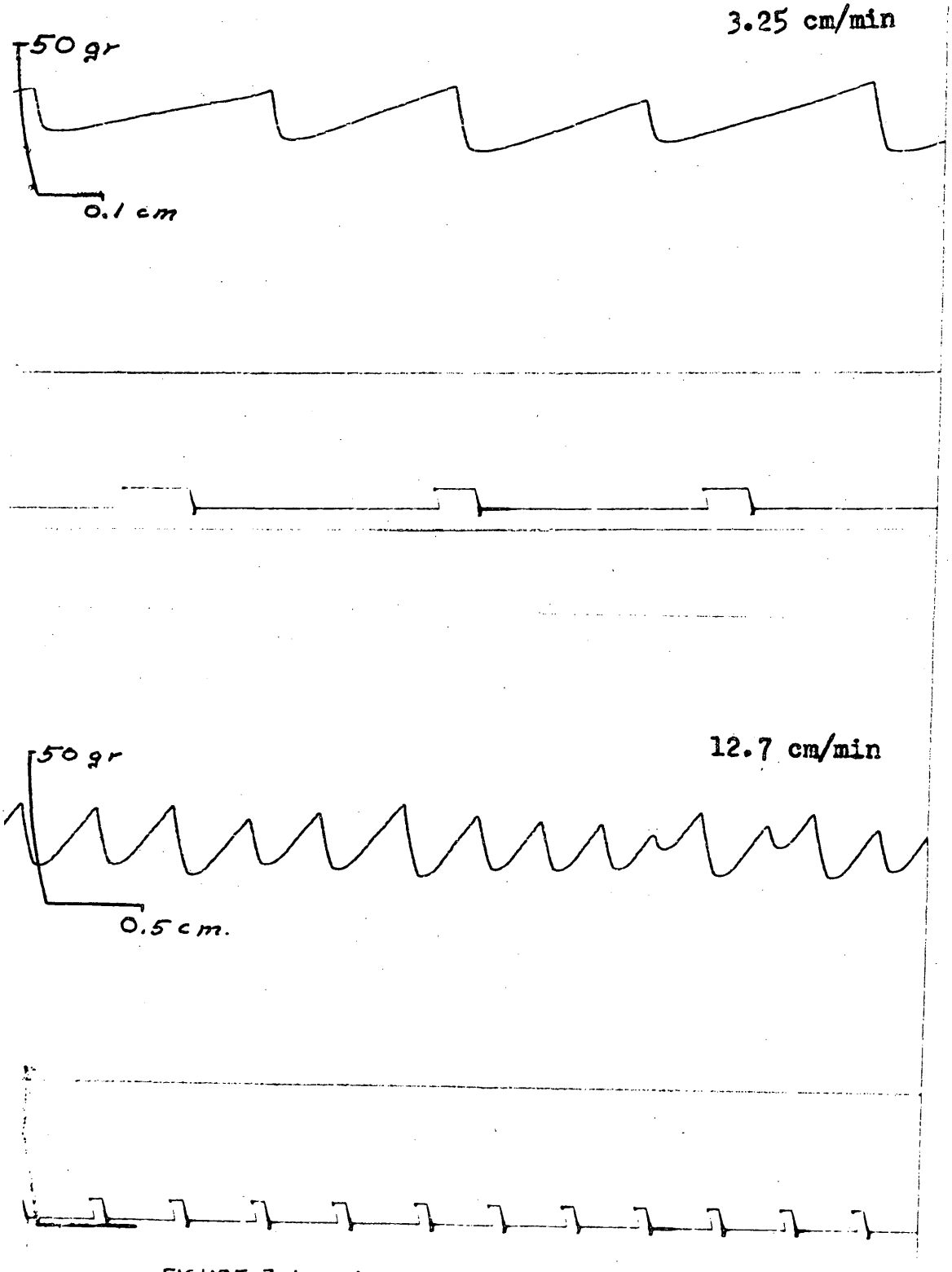

FIGURE 7-1a KINETIC OSCILLOGRAM

Steel on Ice 160 gram load
4 cm^2 Apparent Contact Area
Flat Honed Circular Slider Surface
15°F Low Humidity

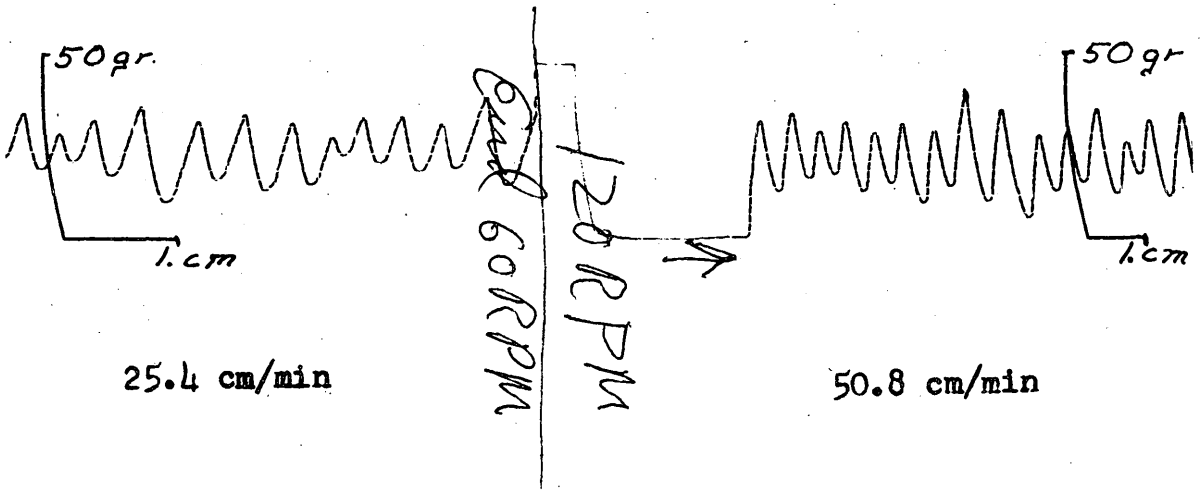

25.4 cm/min

50.8 cm/min

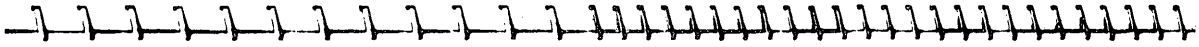

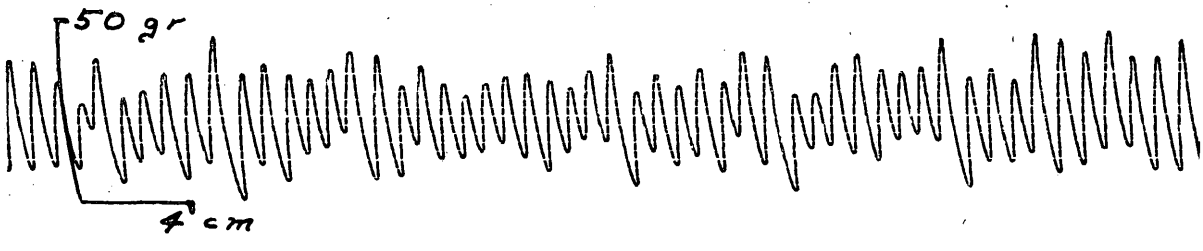

101.6 cm/min

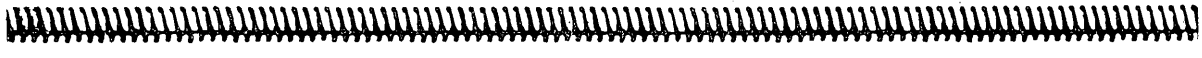

FIGURE 7-16 KINETIC OSCILLOGRAM

Magnesium on Ice 160 gram load
4 cm^2 Apparent Contact Area
Flat Honed Circular Slider Surface
15°F Low Humidity

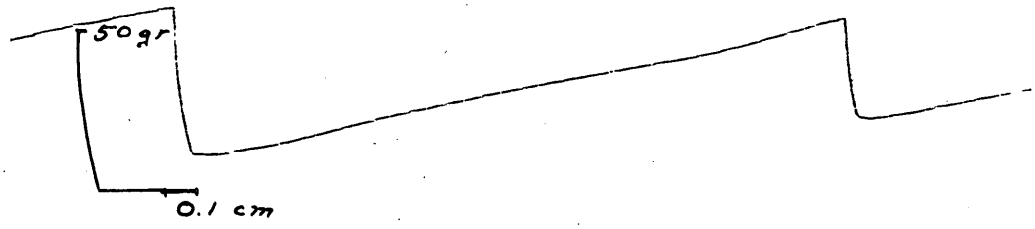

2.3 cm/min

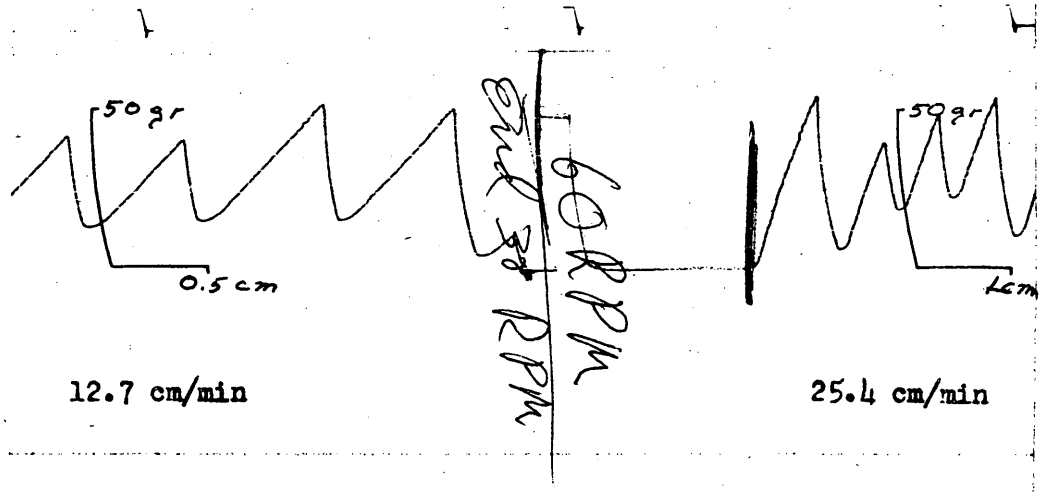

12.7 cm/min

25.4 cm/min

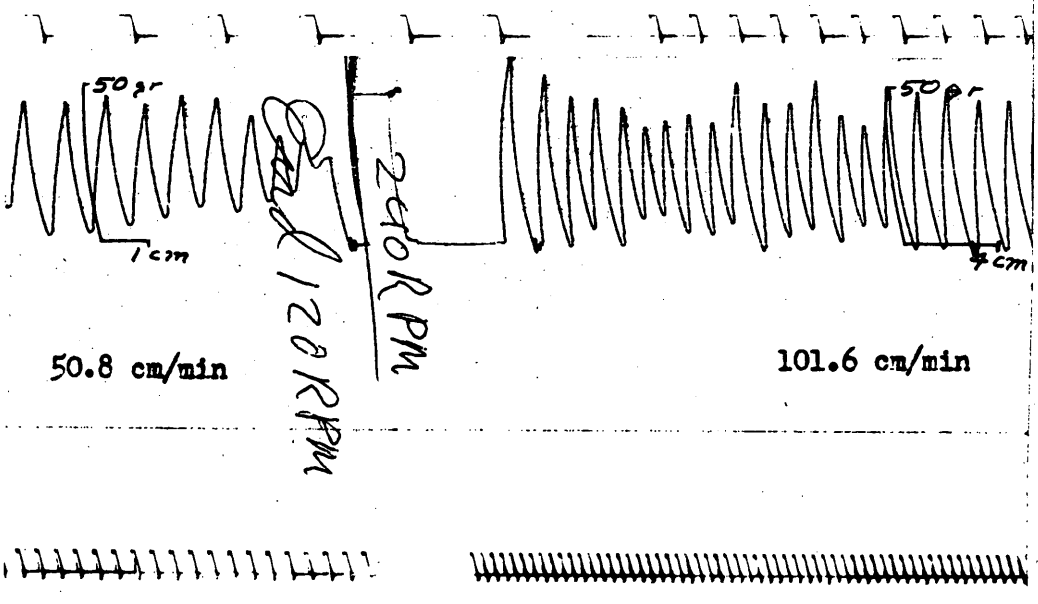

50.8 cm/min

101.6 cm/min

FIGURE 7-2 KINETIC OSCILLOGRAM

Brass on Ice 160 gram load
4 cm^2 Apparent Contact Area
Flat Honed Circular Slider Surface
15°F Low Humidity

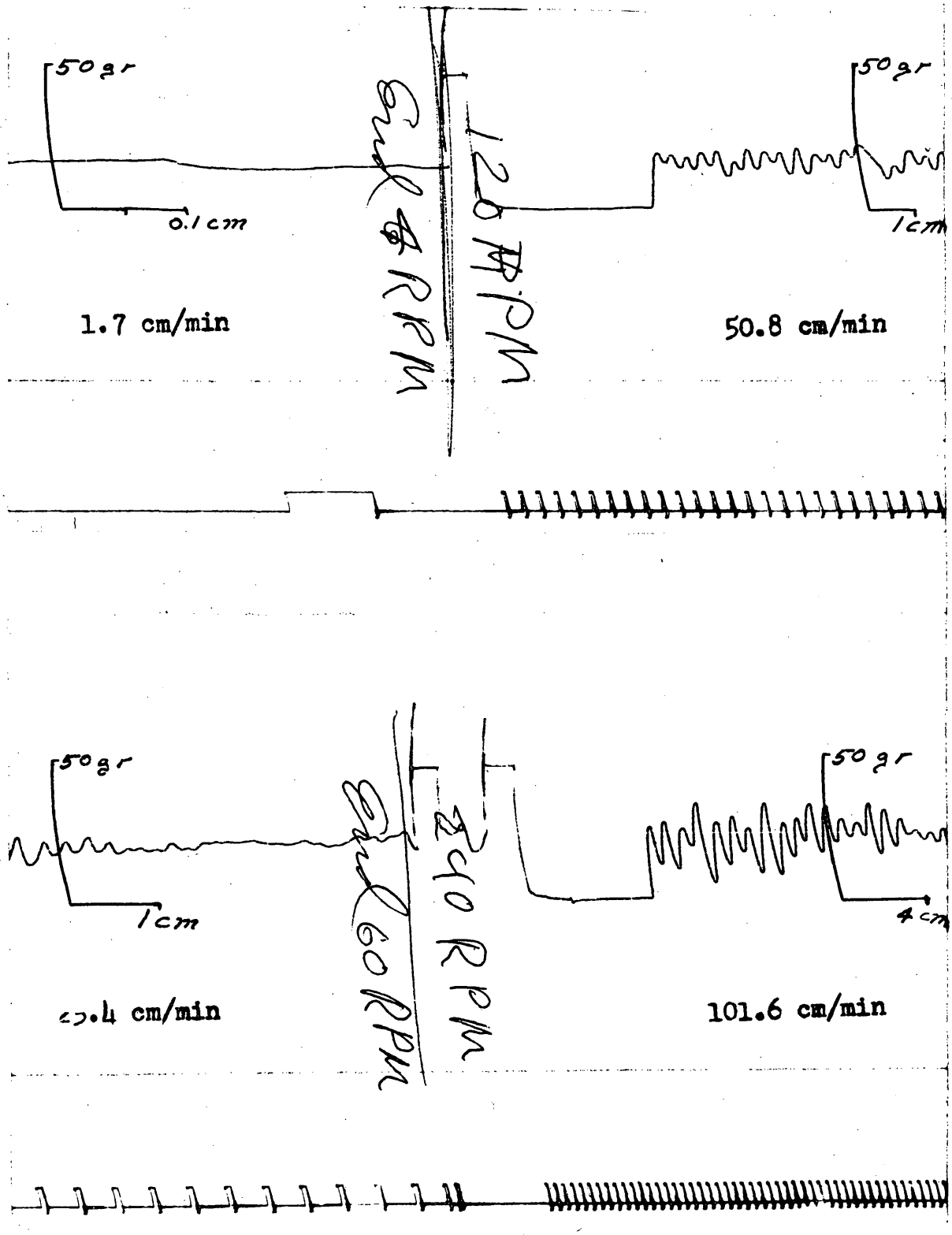

FIGURE 7-3 KINETIC OSCILLOGRAM

Brass on Ice 160 gram load
4 cm^2 Apparent Contact Area
Flat Honed Circular Slider Surface
-28°F Low Humidity

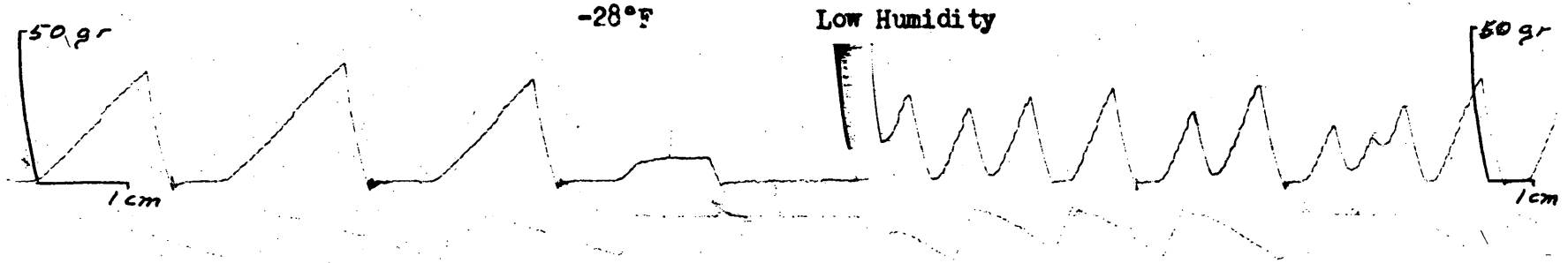

25.4 cm/min

50.8 cm/min

Steel on Ice 160 gram load
4 cm^2 Apparent Contact Area
Flat Honed Circular Slider Surface
-28°F Low Humidity

FIGURE 7-4 KINETIC OSCILLOGRAM

In these oscillograms the upper saw-toothed trace indicates the slider position. The square shaped trace on the lower line of each oscillogram marks the individual revolutions of the leadscrew and thus the distance of slider travel. An axis has been drawn on each oscillogram to indicate the relative force and distance. These traces were taken at a constant oscillograph tape speed of 5 mm/sec.

Examination of the oscillograms indicates the close correspondence of the position-time traces with the "stick-slip" motion predicted in Chapter IV. The linear slowly-rising line represents the stick period in which the slider is held stationary on the ice surface by static friction. The more rapid falling line is the period of slip. As the carriage velocity is increased the slope of the stick line is seen to have a corresponding increase.

The point at which slip motion is initiated corresponds to the static frictional force. This initial motion point is very close but not identical to the maximum deflection. As shown in Chapter IV the maximum deflection equals the sum of $\frac{F_s}{k}$ and an inertial term equal to $\frac{m v_o^2}{2 (F_s - F_k)}$ if $F_s - F_k > \sqrt{mk}\, v_o$. It is thus necessary to correct the maximum point for the inertial term to determine the true static friction.

As was also shown in Chapter IV the presence of the inertial term in both the maximum and minimum points enables this factor to be cancelled out of the mean deflection point considerations. The analysis of Chapter IV further brought out the relation of this mean deflection point to the kinetic constants of the assumed friction functions.

A quantitative analysis was made of the maximum and mean deflection points on the collected oscillograms to determine the friction function constants. Each individual cycle on the position-time oscillogram may be considered an individual experiment. Since a series of cycles were obtained at each setting of the experimental parameters, it is possible to smooth the variations between the individual cycles by averaging the values obtained from a number of cycles. To prevent the possibility of biasing the data from choice of only certain cycles, the cycles analyzed always were in consecutive order. Thus the maximum and mean positions of twenty-five consecutive cycles at each setting combination of the experimental parameters were examined and tabulated. Table 7-2 and 7-3 illustrate this tabulation for the steel slider at 15° F. temperature having velocity settings of 12.7 cm/min. and 25.4 cm/min. The maximum and mean positions of the twenty-five cycles at each test setting were also plotted on frequency diagrams. Figures 7-5a, 7-5b, 7-6a, and 7-6b are the frequency diagrams for the data of Tables 7-2 and 7-3. These sample frequency diagrams indicate qualitatively a close proximity to a normal distribution of the individual values.

The mean value and the standard deviation of each set of values were next calculated and through use of the calibration diagrams converted to force values. Table 7-4 summarizes the results of these calculations for the several parametric settings. The resulting mean values are also plotted against the carriage velocity in Figures 7-7 through 7-11. In these diagrams the mean value is indicated as a cross composed of a short horizontal line and a vertical line equal to the computed standard deviation.

TABLE 7-2

KINETIC FRICTION ON ICE

Stat. Surface Matl. - Ice	Sliding Surface	Load 160 grams
Temperature + 15° F.	Material - 1040 Steel	Velocity 12.7 cm/min.
Humidity Low	Curvature - Flat	Beam Data L20B, Att 2
	Plan Shape - Round	Date 8/13/53
	Smoothness - Honed	0905
	Appt. Area - 4 cm^2	

Maximum Pen Def. mm	Midpoint Pen. Def. mm	Minimum Pen. Def. mm
14	10	5
13	10	6
14	10	6
15	10	5
14	10	6
13	10	6
13	10	6
11	10	9
14	10	6
12	11	10
14	10	6
12	9	6
13	11	7
15	9	3
12	9	6
12	9	7
15	10	4
13	9	5
13	10	6
15	10	5
15	11	7
14	11	7
15	11	7
12	11	10
11	9	7

TABLE 7-3

KINETIC FRICTION ON ICE

Stat. Surface Matl. - Ice	Sliding Surface	Load	160 grams
Temperature + 15° F.	Material - 1040 Steel	Velocity	25.4 cm/min.
Humidity Low	Curvature - Flat	Beam Data	L20B, Att 2
	Plan Shape - Round	Date	8/13/53
	Smoothness - Honed		0910
	Appl. Area - 4 cm^2		

Maximum Pen Def. mm	Midpoint Pen Def. mm	Minimum Pen Def. mm
15	11	6
17	11	5
14	11	7
15	11	7
13	10	7
15	12	8
14	12	9
15	10	5
15	10	4
14	10	6
15	10	5
14	11	7
13	10	7
11	11	10
12	10	8
11	10	9
12	10	7
11	11	10
13	11	8
14	11	8
13	10	7
14	10	6
12	10	8
13	9	5
10	10	10

FRICTION ON COMPACTED SNOW

Code No. IA4 +15F
Date, Time 8/13/53 0905

1040 STEEL SLIDER
KINETIC MAXIMUM

Frequency

Load 160 Roll 68
C.W. 0 Att 2
Vel. 12.7 cm/min B.P. 20-LB

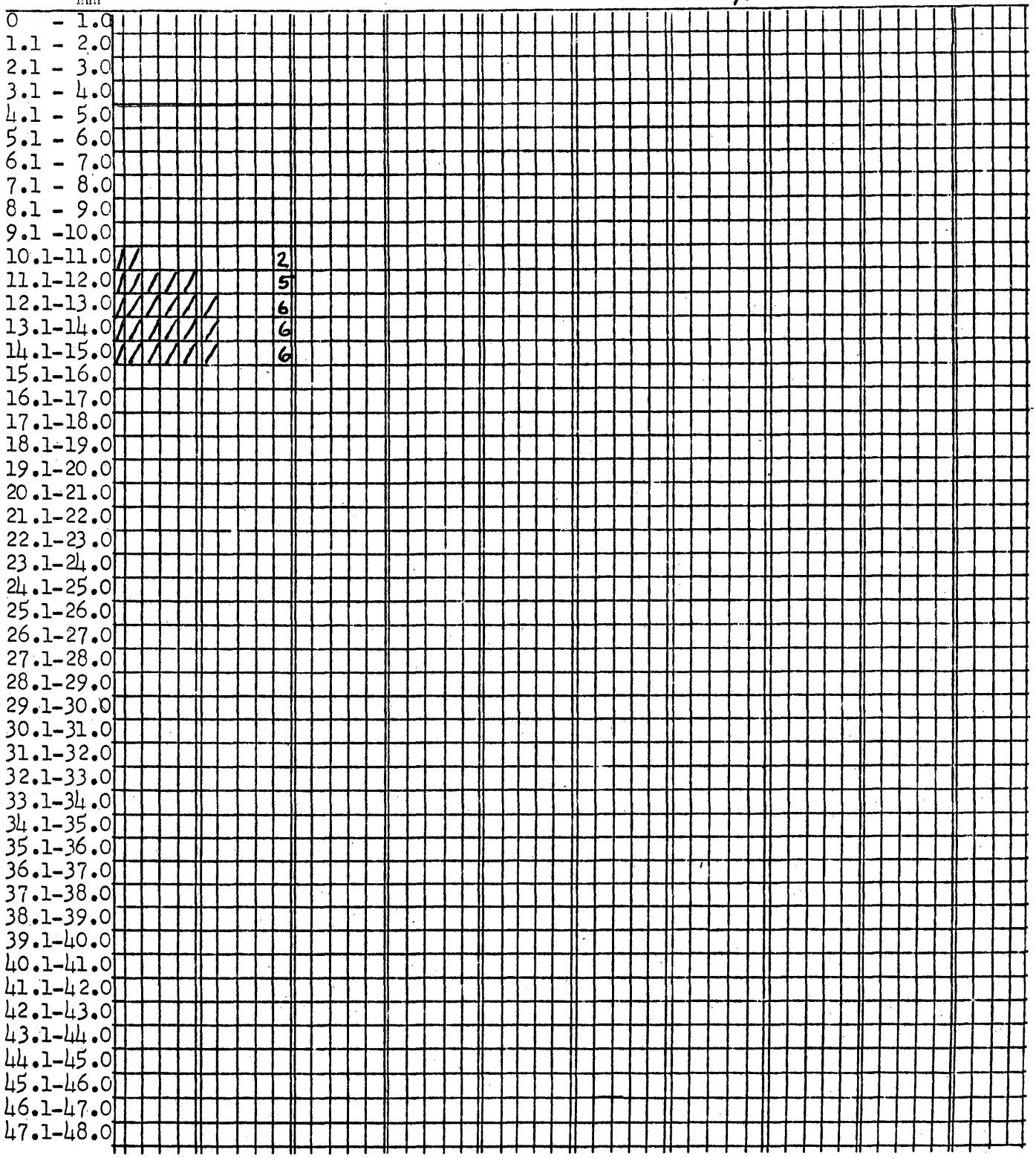

Number Readings 25

Mean Graph Def. Gd 12.86 mm

Std. Dev.^{2} 1.6 mm

Std. Dev. 1.2649

Fric. Force
Mean 29.5 gr
Std. Dev. 3.5 gr

Coef. of Fric.
Mean .184
Std.Dev. .022

FIGURE 7-5a HISTOGRAM

FRICTION ON COMPACTED SNOW

Code No. IA4 +15F
Date, Time 8/13/53 0905

Load 160 Roll 68
C.W. 0 Att 2
Vel. 12.7 cm/min B.P. 20 LB

1040 STEEL SLIDER
KINETIC MIDPOINT

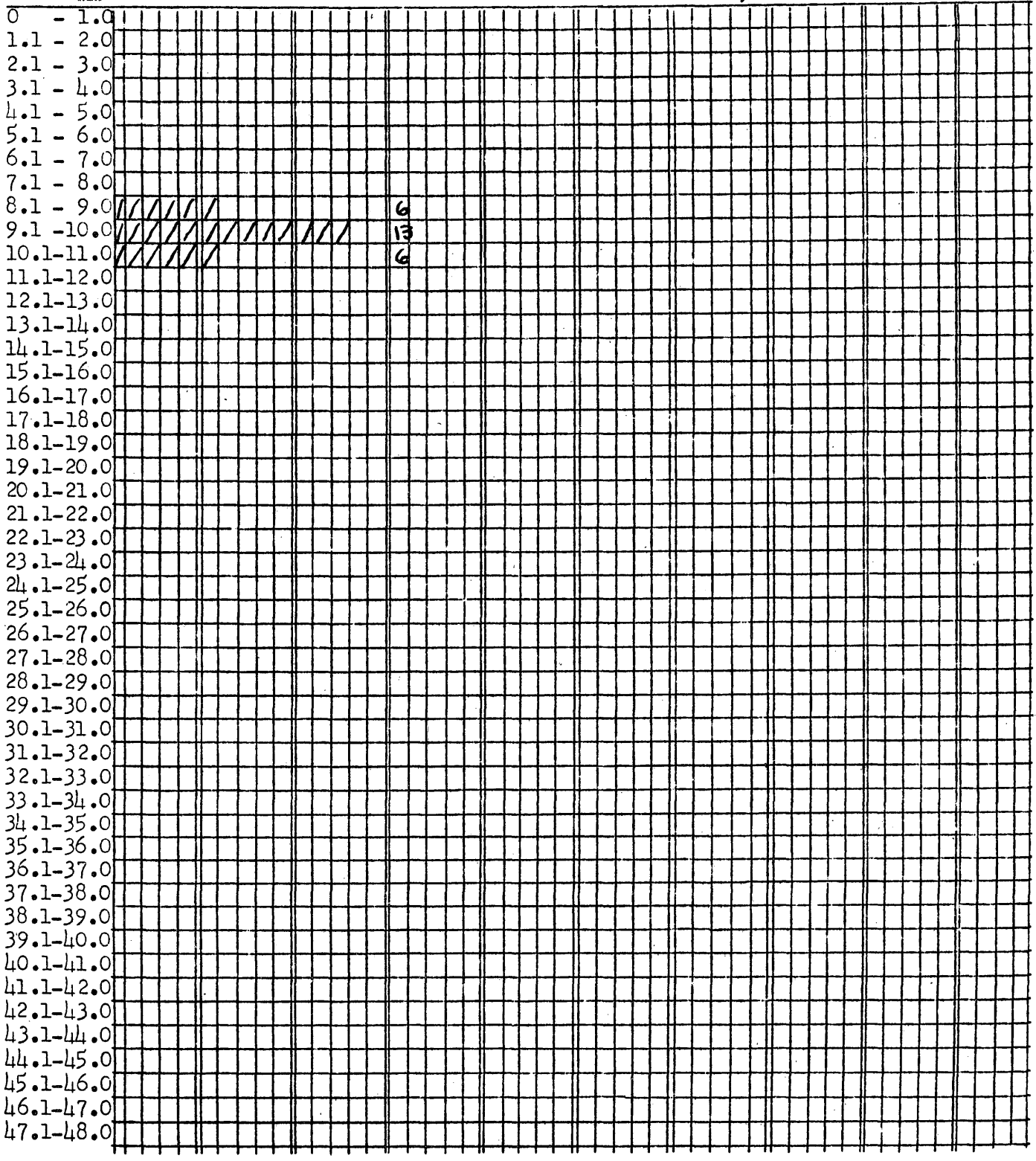

Number Readings 25

Mean Graph Def. Gd 9.5 mm

Std. Dev.^{2} .48 mm

Std. Dev. .69282

Fric. Force
Mean 22 gr
Std. Dev. 2 gr

Coef. of Fric.
Mean .138
Std.Dev. .012

FIGURE 7-56 HISTOGRAM

FRICTION ON COMPACTED SNOW

Code No. LA4 +15F
Date, Time 8/13/53 0910
Load 160 Roll 68
C.W. 0 Att 2
Vel. 25.4 cm/min B.P. 20 LB

Graph Deflection mm — 1040 STEEL SLIDER KINETIC MAXIMUM — Frequency

Deflection mm	Frequency
0 - 1.0	
1.1 - 2.0	
2.1 - 3.0	
3.1 - 4.0	
4.1 - 5.0	
5.1 - 6.0	
6.1 - 7.0	
7.1 - 8.0	
8.1 - 9.0	
9.1 -10.0	1
10.1-11.0	3
11.1-12.0	3
12.1-13.0	5
13.1-14.0	6
14.1-15.0	6
15.1-16.0	
16.1-17.0	1
17.1-18.0	
18.1-19.0	
19.1-20.0	
20.1-21.0	
21.1-22.0	
22.1-23.0	
23.1-24.0	
24.1-25.0	
25.1-26.0	
26.1-27.0	
27.1-28.0	
28.1-29.0	
29.1-30.0	
30.1-31.0	
31.1-32.0	
32.1-33.0	
33.1-34.0	
34.1-35.0	
35.1-36.0	
36.1-37.0	
37.1-38.0	
38.1-39.0	
39.1-40.0	
40.1-41.0	
41.1-42.0	
42.1-43.0	
43.1-44.0	
44.1-45.0	
45.1-46.0	
46.1-47.0	
47.1-48.0	

Number Readings 25

Mean Graph Def. Gd 12.9 mm

Std. Dev.^{2} 2.64 mm

Std. Dev. 1.6248

Fric. Force
Mean 28 gr
Std. Dev. 4.5 gr

Coef. of Fric.
Mean .175
Std.Dev. .028

FIGURE 7-6a HISTOGRAM

FRICTION ON COMPACTED SNOW

Code No. IA4 +15F
Date, Time 8/13/53 0910

Load 160 Roll 68
C.W. 0 Att 2
Vel. 25.4 cm/min. B.P. 20 LB

1040 STEEL SLIDER
KINETIC MIDPOINT

Graph Deflection mm	Frequency
0 - 1.0	
1.1 - 2.0	
2.1 - 3.0	
3.1 - 4.0	
4.1 - 5.0	
5.1 - 6.0	
6.1 - 7.0	
7.1 - 8.0	
8.1 - 9.0	1
9.1 -10.0	13
10.1-11.0	9
11.1-12.0	2
12.1-13.0	
13.1-14.0	
14.1-15.0	
15.1-16.0	
16.1-17.0	
17.1-18.0	
18.1-19.0	
19.1-20.0	
20.1-21.0	
21.1-22.0	
22.1-23.0	
23.1-24.0	
24.1-25.0	
25.1-26.0	
26.1-27.0	
27.1-28.0	
28.1-29.0	
29.1-30.0	
30.1-31.0	
31.1-32.0	
32.1-33.0	
33.1-34.0	
34.1-35.0	
35.1-36.0	
36.1-37.0	
37.1-38.0	
38.1-39.0	
39.1-40.0	
40.1-41.0	
41.1-42.0	
42.1-43.0	
43.1-44.0	
44.1-45.0	
45.1-46.0	
46.1-47.0	
47.1-48.0	

Number Readings 25

Mean Graph Def. Gd 9.98 mm

Std. Dev.^{2} .49 mm

Std. Dev. .70

Fric. Force
Mean 23 gr
Std. Dev. 2.5 gr

Coef. of Fric.
Mean .144
Std.Dev. .016

FIGURE 7-66 HISTOGRAM

TABLE 7-4

SLIDER POSITION DATA SUMMARY FOR VELOCITY, MATERIAL, AND TEMPERATURE PARAMETERS

Series 1 Data
Force in grams

M = Mean
SD = Standard Deviation

Flat Circular Shaped Sliders
4 cm^2 Apparent Area
160 grams Load
Ice Stationary Surface

Velocity	-45° F.				-30° F.				+ 15° F.			
	Max.		Mid.		Max.		Mid.		Max.		Mid.	
cm/min.	M	SD	M	SD	M	SD	M	SD	M	SD	M	SD
Steel												
2.54	46 ±	6.5	29.5	2					37	7	23	2
12.7	47 ±	6.5	29.0	4					30	3.5	22	2
25.4	38	18	28.5	4					28	4.5	23	3
50.8	33	4	28.5	2					30	4.5	23	3
101.6	32	4	29	3					34	5	22	3
Magnesium												
12.7	50	19	35	6					42	7.5	29 ±	4
25.4	47	22	35	9					44	6.5	28 ±	4
50.8	53	22	38	7					48	8	24	3
101.6	41	13	38	10					41	5	23	3
Brass												
2.54					28.5	.8	25.5 ±	.8				
12.7					29.5	.8	26.2 ±	.7	21	2.7	18.2	1.7
25.4					29.5	1.2	25.8	.6	21.5	2.3	18.3	1.8
50.8									18.7	1.8	16.5	1.4
101.6									24	7	17.5	1.2
Plastic												
2.54					47	4	26	2	21	4	20	3
12.7					42	4	26	3	17	2	17	2
25.4					38	4	26	4	36	4	36	4
50.8					30	6	24	2	20	3	20	2
101.6					27	4	23	1.5	22	5	22	4

TABLE 7-4 (Continued)

Velocity	- 45° F.				- 30° F.				+ 15° F.			
	Max.		Mid.		Max.		Mid.		Max.		Mid.	
cm/min.	M	SD	M	SD	M	SD	M	SD	M	SD	M	SD
					Hickory							
12.7					44	13	28	4	66	6	34	3
25.4					35	9	25	3	72	8	36	4
50.8					50	10	28	3	46	10	24	6
101.6					46	13	28	4				

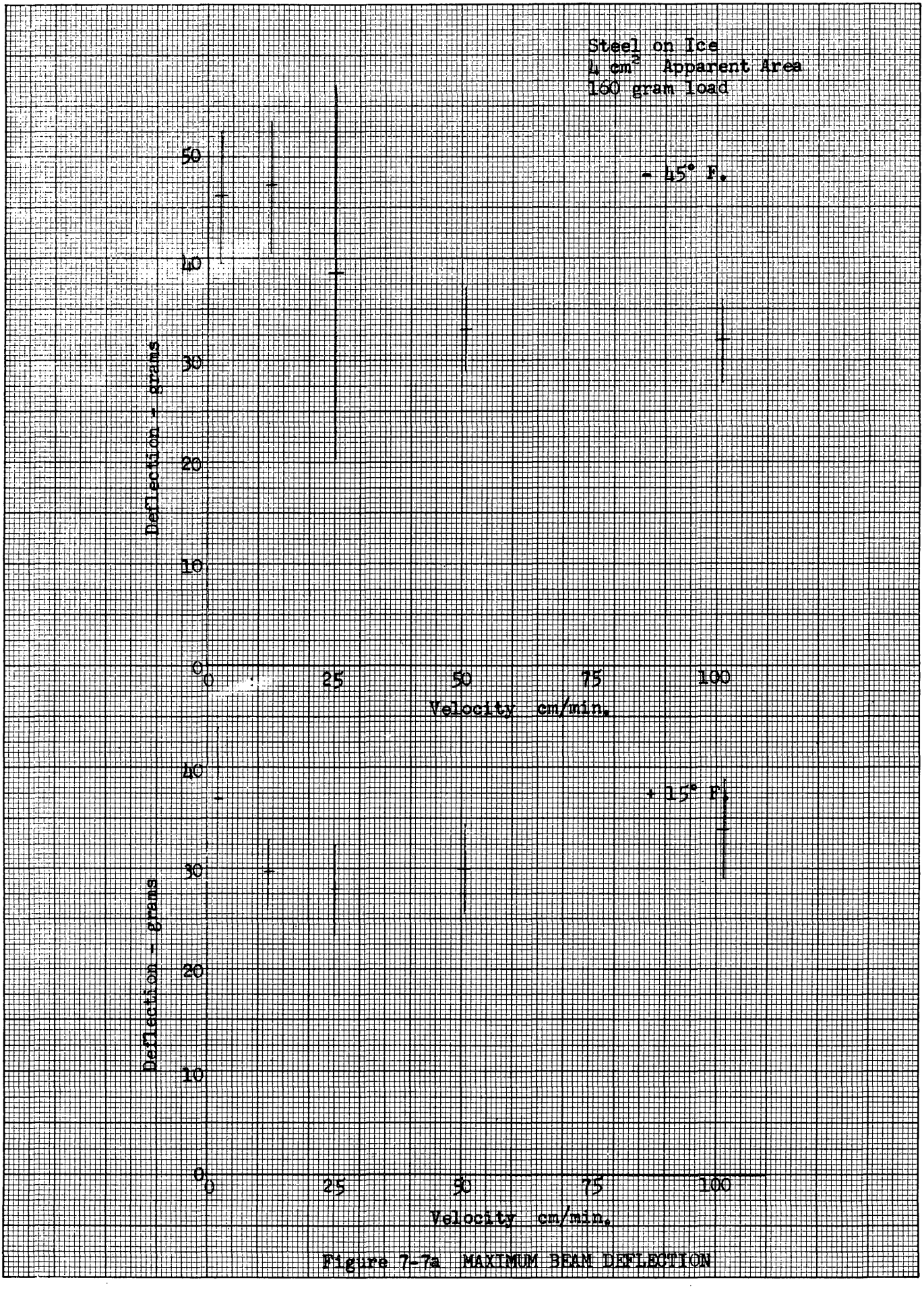

Figure 7-7a MAXIMUM BEAM DEFLECTION

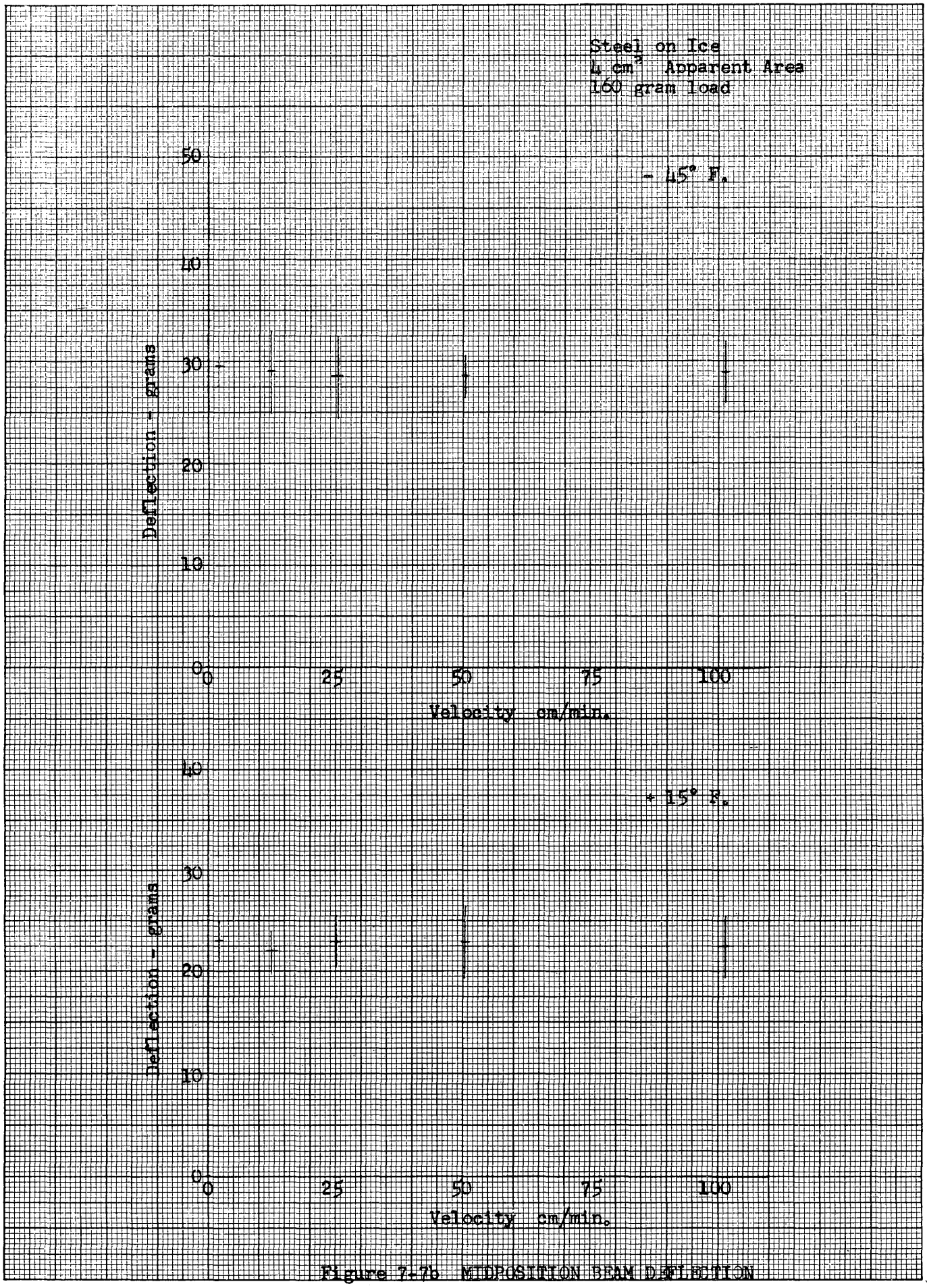

Figure 7-7b MIDPOSITION BEAM DEFLECTION

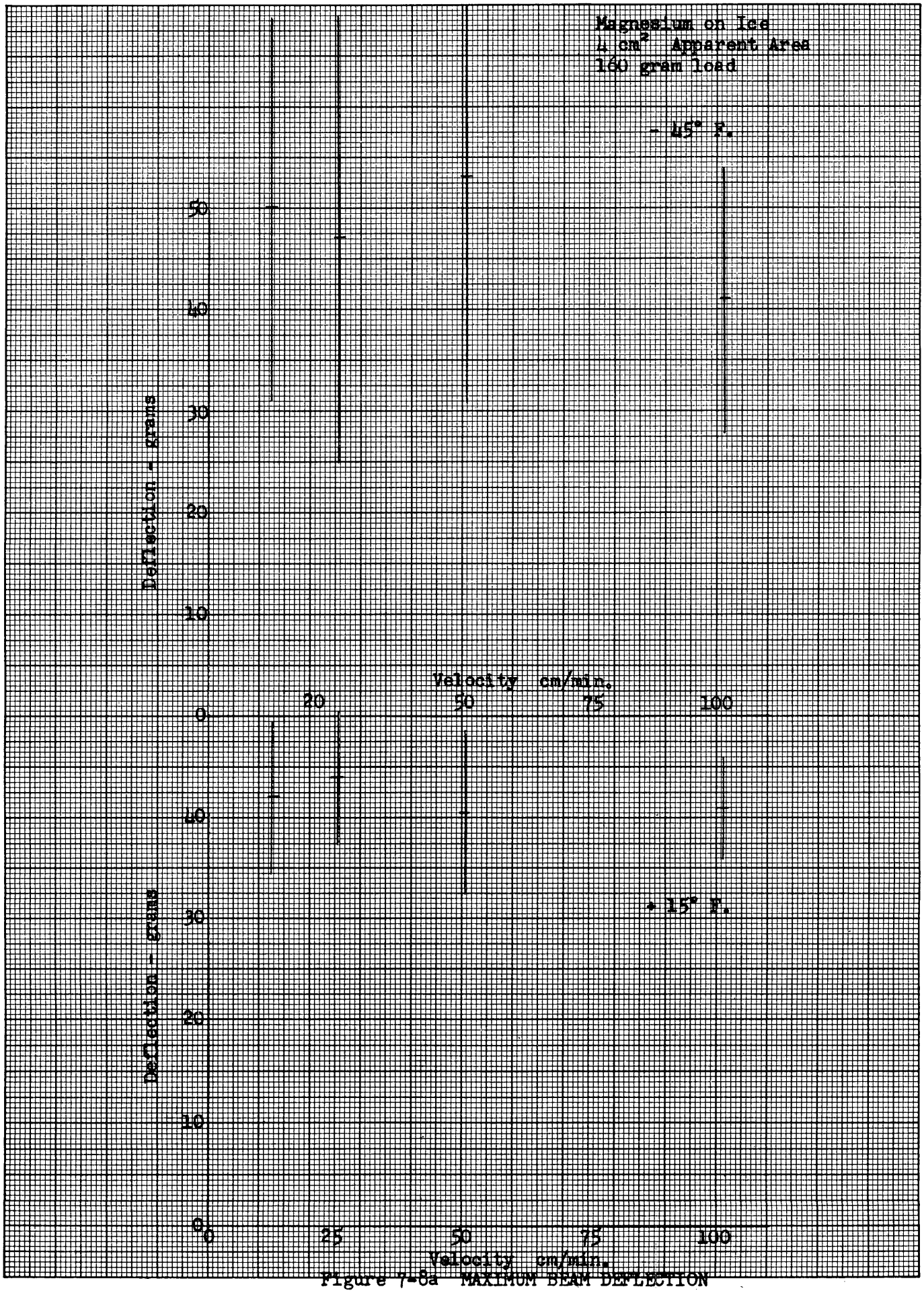

Figure 7-8a MAXIMUM BEAM DEFLECTION

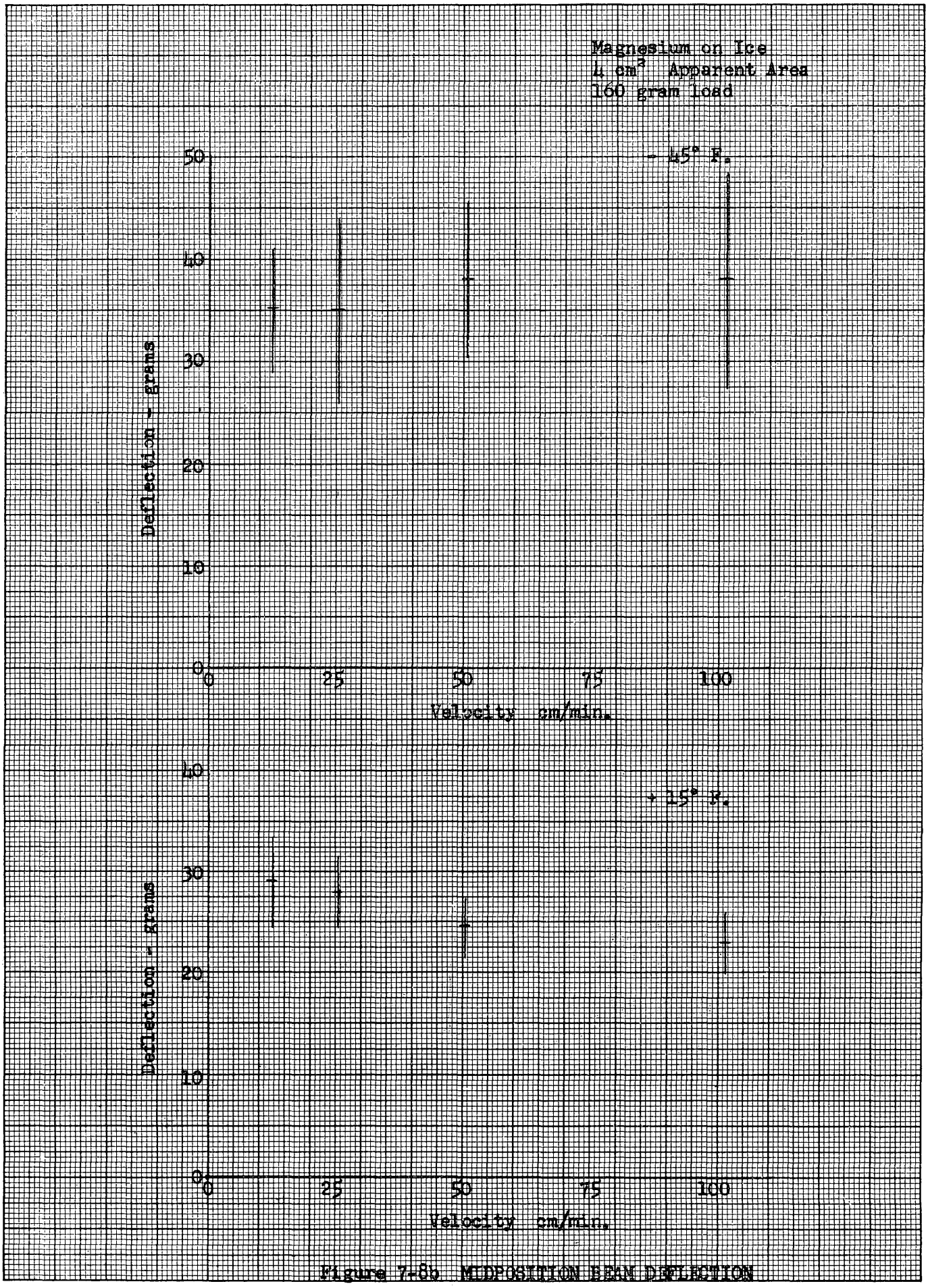

Figure 7-8b MIDPOSITION BEAM DEFLECTION

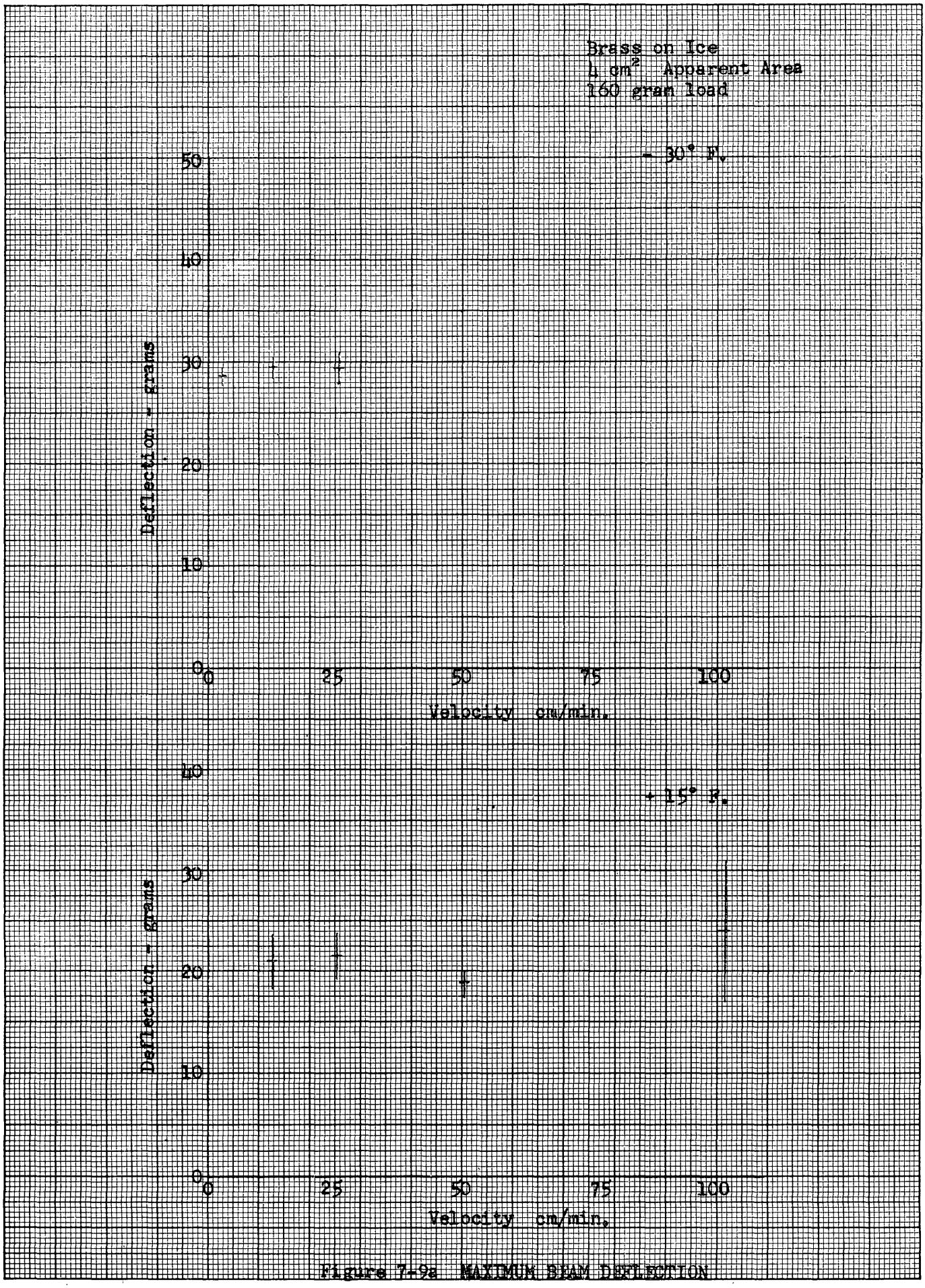

Figure 7-9a MAXIMUM BEAM DEFLECTION

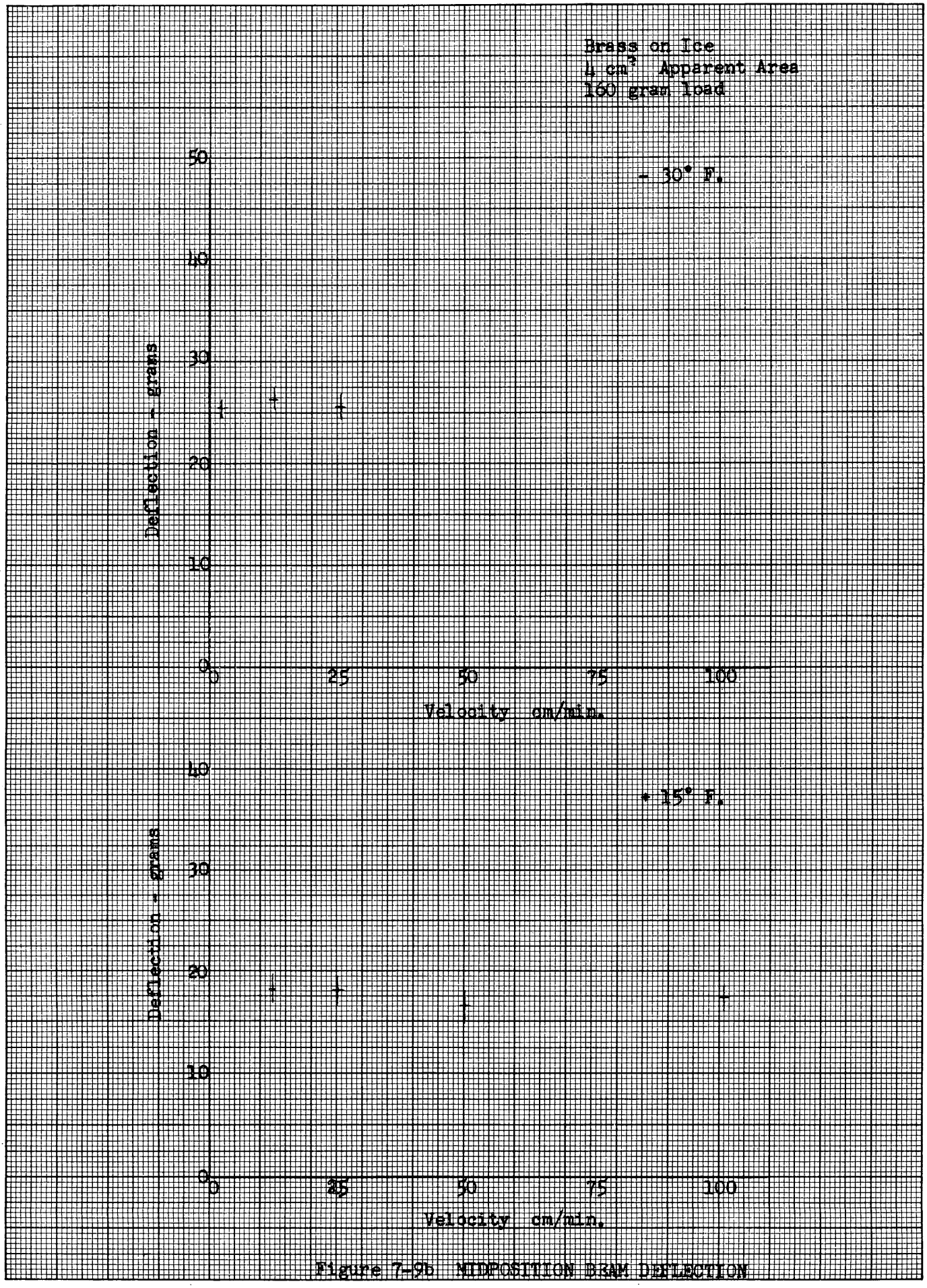

Figure 7-9b MIDPOSITION BEAM DEFLECTION

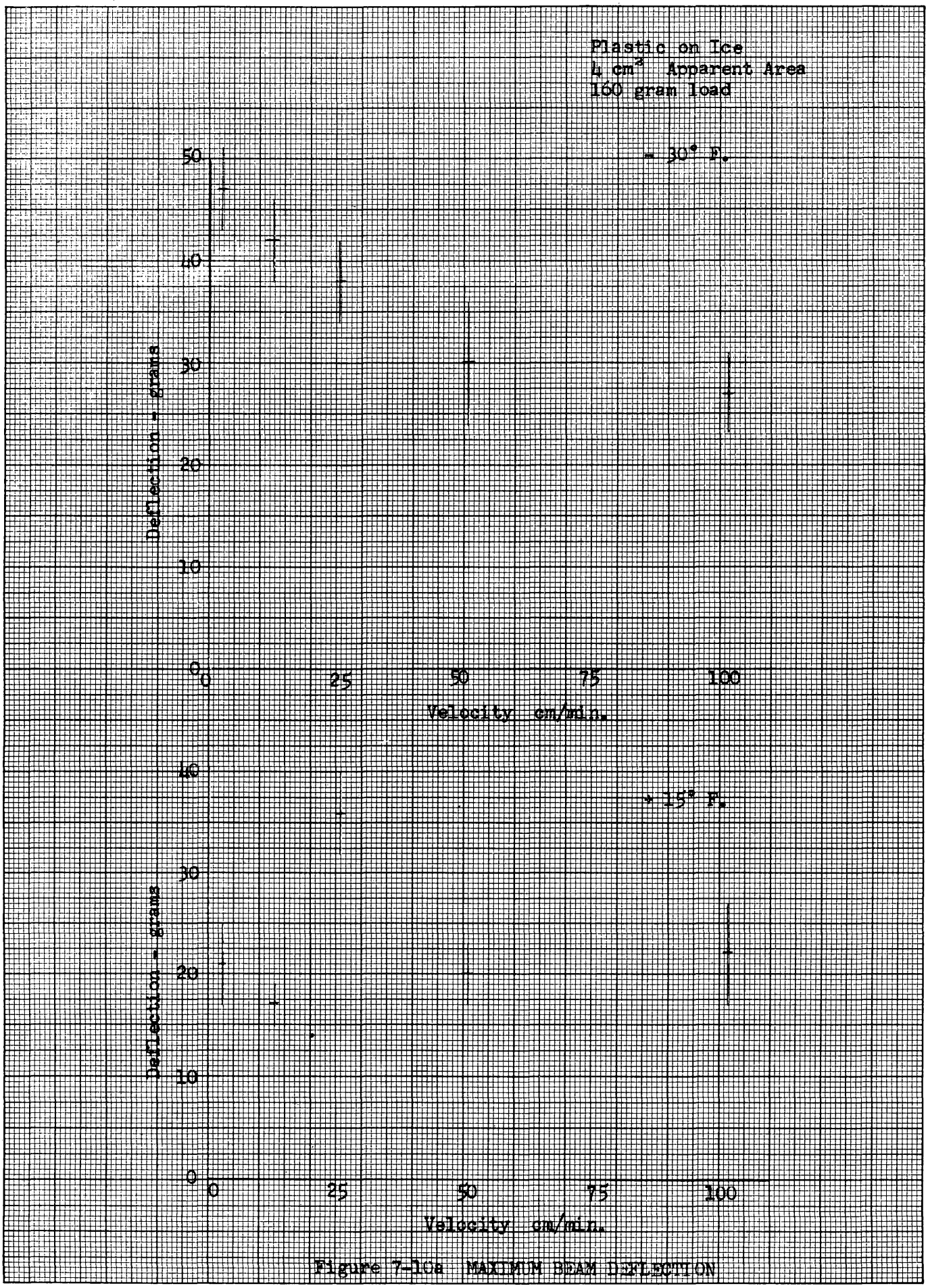

Figure 7-10a MAXIMUM BEAM DEFLECTION

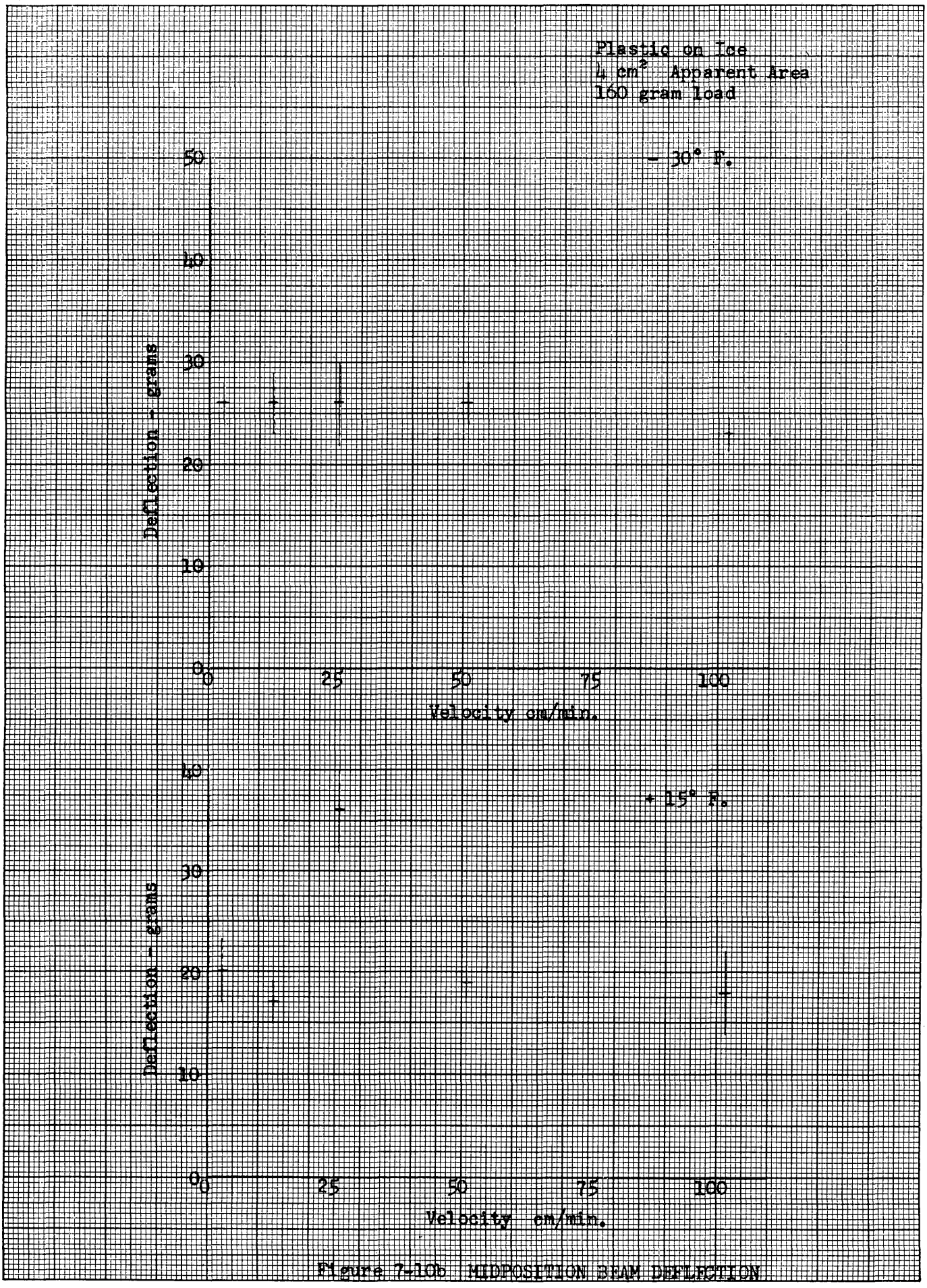

Figure 7-10b MIDPOSITION BEAM DEFLECTION

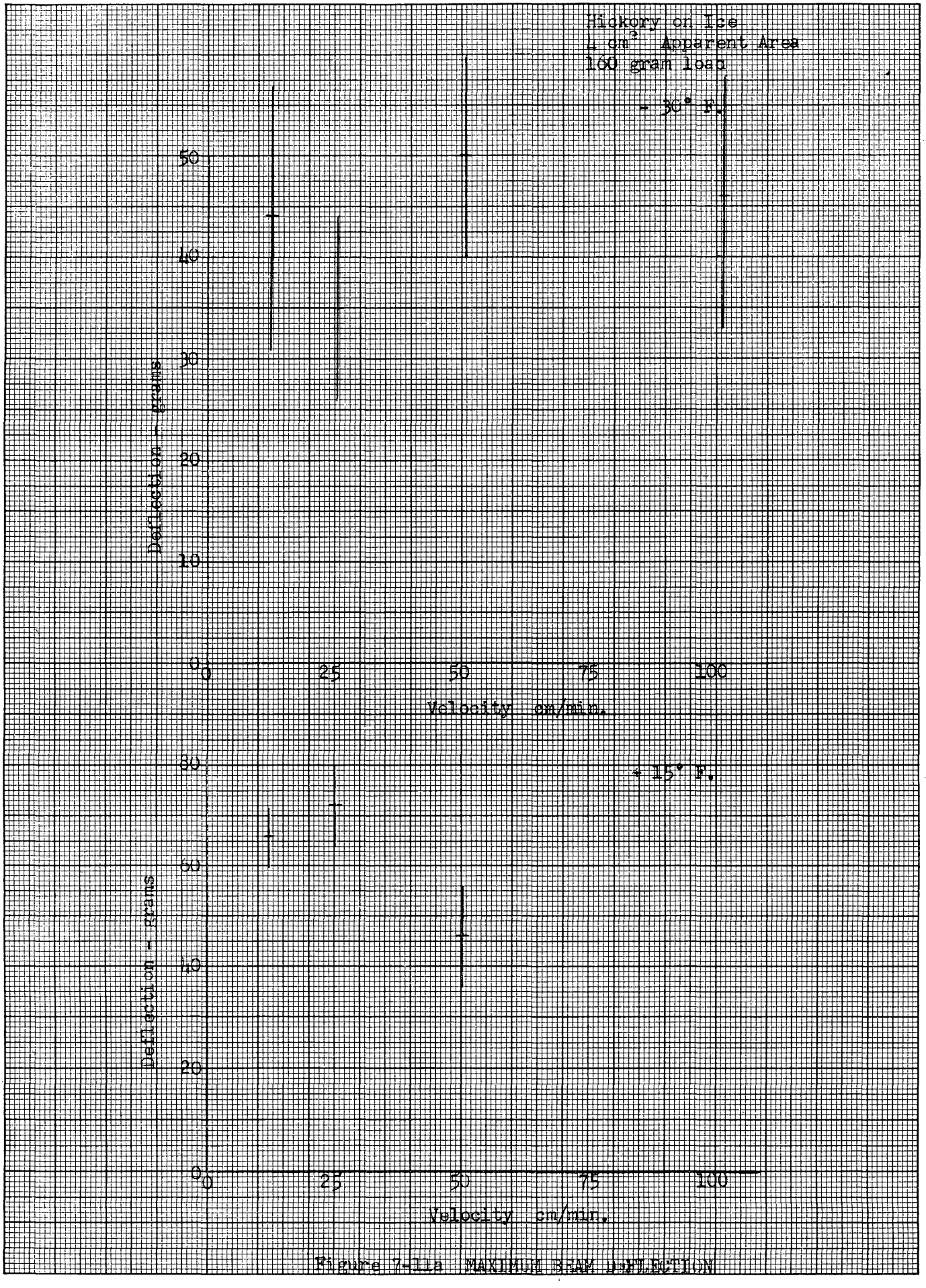

Figure 7-11a MAXIMUM BEAM DEFLECTION

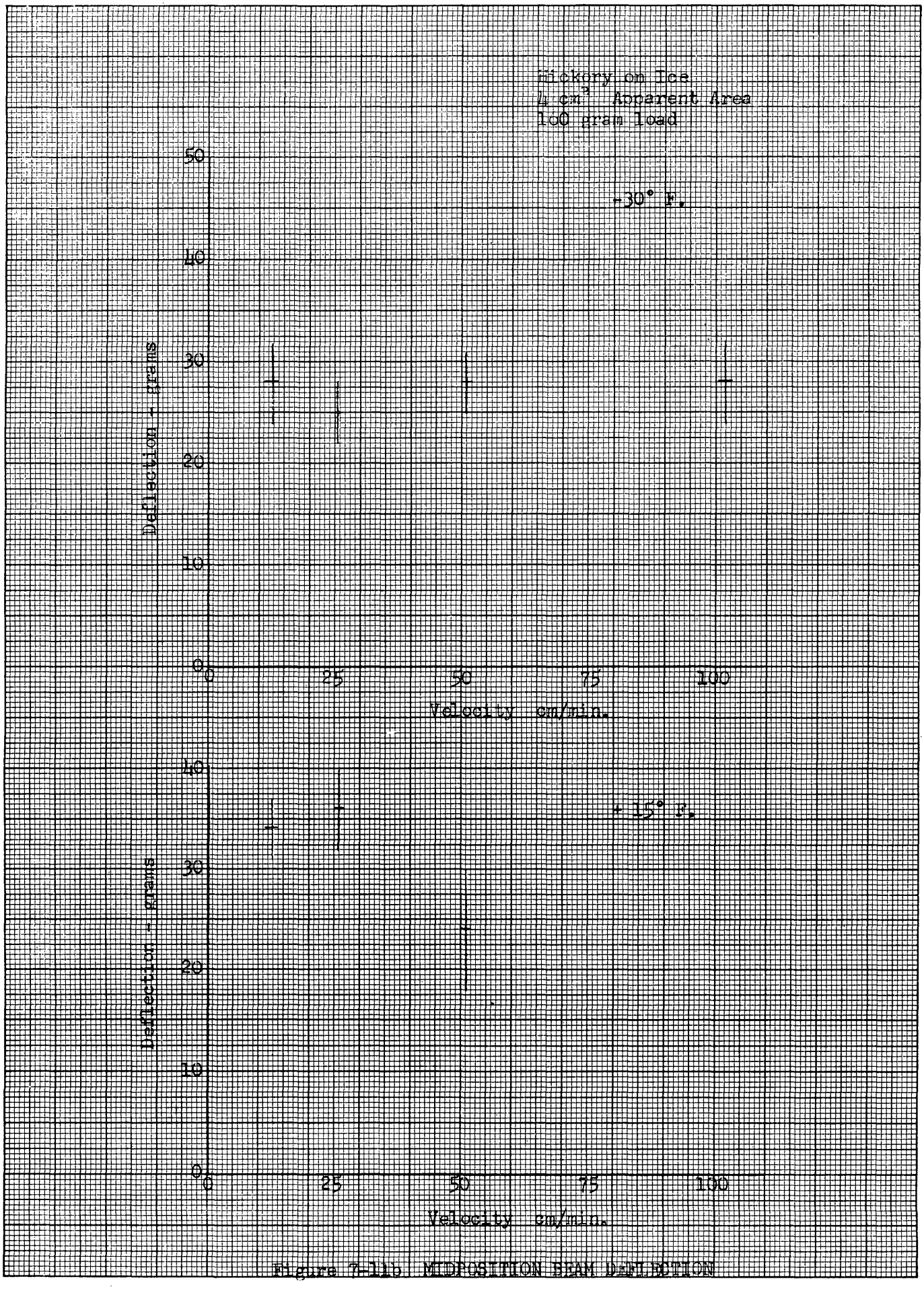

Figure 7-11b MIDPOSITION BEAM DEFLECTION

The graphical plots of the slider midposition versus velocity for steel, brass, plastic, and hickory indicate no change with velocity over the range investigated. This means that the kinetic frictional resistance of these materials is a constant friction of the Coulomb type. The intercept on the vertical axis of the midposition diagrams therefore indicates directly the value of the kinetic friction.

Using an approximate value of the static friction and the value of the kinetic friction from the midposition measurements, the value of $F_s - F_k$ may be determined and compared with $\sqrt{mk}\, v_o$. The resulting values are tabulated in Table 7-5. At the lower velocity the limitation that $F_s - F_k > \sqrt{mk}\, v_o$ held for most materials and the inertial correction term could be calculated in terms of force as $\frac{m}{2} \frac{v_o^2 k}{(F_s - F_k)}$. At higher velocities and for the entire higher temperature set of plastic runs the series of Equation (4-61) is no longer convergent and the approximations of Equation (4-62) cannot be used. For the high velocity runs and the higher temperature plastic runs the quantity $\sqrt{mk}\, v_o$ represents fairly well the inertial influence. Using these values the maximum position was corrected and the static friction determined. Resulting values of the static as well as the kinetic friction for the several materials and temperatures are also listed in Table 7-5.

The tabulated values of static friction forces would indicate that the static friction decreases with velocity. This result may be interpreted in two ways. First there probably is a decrease in the strength of the static bonds due to a shorter time available for plastic flow and

TABLE 7-5

STATIC FRICTION FORCE CORRECTED FOR INERTIA

Temp. °F.	Vel. cm/min.	F_s-F_k gr	$\sqrt{mk}\, v_o$ gr	$\frac{m v_o^2 k}{2(F_s-F_k)}$	F_s gr	F_k gr
			Steel			
- 45°	2.54	16	.15	.001	46	30
	12.7	18	.76	.02	47	29
	25.4	10	1.52	.16	38	28
	50.8	4	3.05	1.00	30	28
	101.6	3	6.1		26	29
+ 15°	2.54	14	.15	.001	37	23
	12.7	8	.76	.03	30	22
	25.4	5	1.52	.25	28	23
	50.8	7	3.05	.67	29	23
	101.6	12	6.1	1.60	32	22
			Magnesium			
-45°	12.7	15	.76	.02	50	35
	25.4	12	1.52	.16	47	35
	50.8	15	3.05	.33	53	38
	101.6	3	6.1		35	38
+ 15°	12.7	13	.76	.02	42	29
	25.4	16	1.52	.12	44	28
	50.8	16	3.05	.30	40	24
	101.6	17	6.1	1.15	40	23
			Brass			
- 30°	2.54	3	.15	.005	28.5	25.5
	12.7	3	.76	.08	29.5	26.2
	25.4	4	1.52	.48	29	25.8
+ 15°	12.7	3	.76	.08	21	18.2
	25.4	3	1.52	.64	21	18.3
	50.8	2	3.05	2.4	16.3	16.5
	101.6	7	6.1		18	17.5

TABLE 7-5 (Continued)

Temp. ° F.	Vel. cm/min.	$F_s - F_k$ gr	$\sqrt{mk}\, v_o$ gr	$\frac{m v_o^2 k}{2 (F_s - F_k)}$	F_s gr	F_k gr
			Plastic			
- 30°	2.54	21	.15	.001	47	26
	12.7	16	.76	.02	42	26
	25.4	12	1.52	.16	38	26
	50.8	6	3.05	.7	29	24
	101.6	4	6.1		21	23
+ 15°	2.54	1	.15		21	20
	12.7	0	.76		17	17
	25.4	0	1.52		35	36
	50.8	1	3.05		17	19
	101.6	4	6.1		16	18
			Hickory			
- 30°	12.7	16	.76	.02	44	28
	25.4	10	1.52	.18	35	25
	50.8	22	3.05	.25	50	28
	101.6	18	6.1	1.5	44	28
+ 15°	12.7	32	.76	.01	66	34
	25.4	36	1.52	.06	72	36
	50.8	22	3.05	.25	46	24

for formation of the bonds. At the high velocities the slider also may not be coming completely to rest and thus not allowing the formation of static bonds. Instead, it may be oscillating around the kinetic position with an amplitude between zero and the maximum amount of the inertia term. It has been shown that in the case of static plus constant kinetic friction, it is possible to nudge or otherwise externally affect the slider motion to obtain a sinusoidal motion of intermediate amplitude. Possibly in the experimental operation of the apparatus the slider was inadvertantly nudged or dampened to the necessary conditions. In this case it would not be correct to subtract the entire value of the inertial quantity from the maximum position. Also in this case the apparent static friction should equal the kinetic friction. As an example, the kinetic friction of steel on ice at - 45° F. and 101.6 cm/min. from Table 7-4 equals 29 grams. The maximum displacement under these conditions is 32 grams. However, the apparent static friction corrected for inertia equals 26 grams, a value lower than the kinetic. Undoubtedly the true static friction is much higher than this and the observed motion is merely a sinusoidal oscillation damped to an amplitude equivalent to 3 grams.

In the case of magnesium on ice a very definite velocity influence may be noted. The friction force appears to decrease with velocity indicating a negative damping constant. Measurements of the slope reveal a damping constant of $c = -4.5$ gr sec/cm. Inserting this value in Equation (4-4) the resulting logarithmic increment would become:

$$d = \frac{-4.5 \times 3.1416}{2\ 1/4 \sqrt{\frac{52}{1/4} - \left(\frac{4.5}{2 \times 1/4}\right)^2}} = -2.5$$

and the correction for the vertical axis intercept equals:

$$x_{max}\ (\frac{d}{4} - \frac{d^2}{16}) = -\ 40\ gr$$

This would indicate a Coulomb resistance equal to:

$$30 - (-\ 40) = 70\ grams$$

Since this value of the Coulomb resistance is considerably greater than the static resistance the application of this approach to the measurement of the kinetic friction constants of magnesium on ice is somewhat questionable.

Several other interesting trends are indicated by the static and kinetic data. For steel, magnesium, brass, and plastic the frictional resistance both static and kinetic decreased as the temperature was increased from - 45° F. and - 30° F. to + 15° F. For the hickory slider, however, the friction increased with an increase of temperature from - 30° F. to + 15° F.

The slider material had several influences upon the frictional characteristics. Of the five materials investigated, the magnesium and the hickory sliders had the highest static friction. These two materials also had the greatest difference between the static and kinetic friction forces. It is interesting to note that hickory and magnesium are the two most common materials used in the construction of personnel skiis. The high static friction of skiis of these materials aids in climbing slopes. The large difference in the static and kinetic friction also leads to less chance of disturbance during the slip portion and thus reduces the possibility of vibration. The negative slope on the kinetic friction vs.

velocity curve of the magnesium slider would indicate that this material would be particularly suited for low kinetic friction applications.

The brass and the plastic sliders according to the data of Table 7-5 present the lowest value of static friction and the least difference between static and kinetic. The static plastic data is somewhat questionable, however, since it may be overcompensated for the inertial effect.

It should be noted that no clear relation may be drawn between the thermal conductivity of the slider materials and the resulting friction.

Hickory, which was just mentioned as having the highest static friction, also had the softest or most easily penetrable surface. This material also had several small grooves in the surface caused by the natural wood grain. It is possible that these grooves might occasionally orient themselves perpendicular to the direction of motion and to create in some manner additional resistance.

The results of the first series of tests were open to some question due to the lack of control of several possible known and unknown variables. Included among these variables are the influence of time upon the structure of the ice and the wearing characteristic of the ice sheet. Thus the ice surface may have changed between the individual tests. It is also possible that the friction differences found between the individual sliders may be due to variables other than those to which the variation is ascribed. Thus the friction difference between two sliders of different material may be due to slight unknown differences in construction rather than to the difference in material.

To enable a check of the reproducibility of the material variation a second series of test runs was performed. For this series the four sliders used in testing static friction reproducibility (Series Twelve measurements described in Chapter VI) were again used. These four sliders included two of steel and two of brass. All steps in the construction of these four sliders were exactly identical and performed concurrently. The basic question to be answered by the second series of kinetic tests was, "Is there a significantly greater difference in the values of the kinetic frictional resistance between ice and sliders of dissimilar material than there is in the values of friction between ice and sliders of the same material?"

Measurements were made corresponding to three carriage velocities at a single load and a single temperature setting for the four sliders. To insure against biasing through the variation of unknown or uncontrolled parameters, the selection of the order of testing of each setting was performed in random fashion. A total of three replicate test runs were made at each test setting. Each replicate was taken in a newly-selected random order. Twenty-five consecutive cycles at each test setting were analyzed and plotted on frequency diagrams. The resulting values of the maximum and midposition values are listed in Table 7-6. From these values a statistical analysis was performed using the analysis of variance. This analysis indicated as shown in Table 7-7 that material has the most significant influence upon both the static and upon the kinetic frictional resistance, the steel sliders presenting a greater frictional resistance than the brass sliders. Individual sliders of each material had no

TABLE 7-6

SERIES TWO FRICTION MEASUREMENTS ON REPRODUCIBILITY OF MATERIAL INFLUENCE

Grams Tangential Resistance

Velocity	Steel				Brass			
cm/	Slider 1		Slider 2		Slider 1		Slider 2	
min.	Stat.	Kin.	Stat.	Kin.	Stat.	Kin.	Stat.	Kin.
	41	19.0	50	25.0	31	20.0	35	17.5
12.7	44	21.5	56.5	25.5	26	18.5	21	16.5
	38	21.0	40	25.0	24.5	20.0	25.5	18.5
	38	18.0	33.5	18.5	20.5	16.0	28.5	18.0
25.4	38.5	21.0	43.5	26.5	24.5	16.5	21.5	17.0
	40.5	2010	36.0	23.0	22	19.0	20	14.0
	31	20.0	42	25.0	22	17.5	29	17.5
50.8	27.5	18.5	31.5	18.5	21	17.0	16	14.0
	27.5	21.0	32	25.0	20.5	18.5	29.5	17.5

TABLE 7-7

Significance of Variables in Series 2

Friction Measurements

Variable	Degrees of Freedom	Tab.'d "F" Value 5% Level Den. =26	Static		Kinetic	
			Computed Ratio	Significance	Computed Ratio	Significance
Material	1	4.22	69.7	Very Sign.	44	Very Sign.
Velocity	2	3.37	8.47	sign.	2.7	Not sign.
Slider Number	1	4.22	3.06	Not sign.	2.58	Not sign.
M x V	2	3.37	21.9	sign.	Small	Not sign.
M x S	1	4.22	2.15	Not sign.	14.4	sign.
V x S	2	3.37	1.09	Not sign.	.13	Not sign.
M x V x S	2	} 26		Not sign.		Not sign.
Random	24					

significant variation. Thus the original question posed was answered by this analysis indicating that the variation attributed to material was correctly assigned.

The variance analysis applied to this data also indicated that velocity is not significant for the kinetic friction although it is significant for the static friction. The velocity independence of the kinetic friction agrees with the results of the first test series for these same two materials and over this same velocity range. Examination of the static friction data of Table 7-6 indicates a general trend towards a decrease in the static friction with an increase in velocity. This result may be interpreted as again indicating a relation between the static bonds and the time of stationary contact. At the higher carriage velocities a shorter time is available for plastic flow and for the formation of the static bonds.

Implication of the "significant" results for the cross products of material time velocity in the case of static friction and of material times slider in the kinetic friction is not understood.

The previously described kinetic friction measurements were performed under comparatively low humidity conditions. Upon completion of the humidity chamber a third set of kinetic measurements were taken under high humidity conditions. In this test series the Theory of Variance was applied to the investigation of the influence of Apparent Contact Area and Load as well as to the previously studied influences of Material and Velocity. The number of test settings of these previously investigated

parameters was increased to three for material and five for velocity. With four area settings and three load settings the total number of experimental combinations equaled 180. Unfortunately time limitations prevented obtaining any replicate measurements.

Table 7-8 illustrates the type of data collected at each experimental point and the method of processing to determine the static and kinetic coefficients of friction. A summary of the static and kinetic coefficients for the 180 parameter combinations is presented in Table 7-9. Results of a preliminary analysis of variance upon the static and the kinetic coefficients of friction are given in Tables 7-10 and 7-11.

The experimental measurements of this test series indicates the following with regard to static friction on ice under high humidity conditions over the investigated range of the variables.

1. Apparent area of contact is very significant.
2. The slider material is also significant at the 5% level.
3. In contradiction to the results of Series 1 and 2 (which applied to low humidity conditions) the velocity variable had no significant influence on the static coefficient of friction on ice.
4. The load also had no significant influence on the static coefficient of friction on ice.
5. The several interactions were insignificant in their influence as compared to the residual.

TABLE 7-8 SAMPLE DATA SHEET
FRICTION ON SNOW AND ICE

Oscillogram Data

Graph Deflection		
Maximum	Midpoint	Minimum
12	7.0	2
13	7.5	2
12	7.5	3
12	7.5	3
11	8.0	5
12	8.0	4
8	8.0	8
11	7.0	3
10	6.5	3
9	6.5	4
7	6.0	5
13	7.0	1
13	6.5	0
12	6.5	1
6	6.0	6
6	5.5	6
7	7.0	7
8	7.5	7
11	6.5	2
14	7.0	0
8	7.0	6
8	6.0	4
9	7.5	6
10	8.5	7
11	8.0	5

Slider type round flat — Code IA4
Temp. +15F — Date, time 4/26/54 1400
Humidity High — Observers V.E. & H.M.
Load 80 gms — Att 2
Carr. Vel. 25.4 cm/min — B.P. 20 LB

Mean Max. G. Def.	10.12
Mean Max. Fric. Force	24.8 gm
Inertia Corr.	neg.
Static Fric. Force	24.8 gm
Static Coeff. of Fric.	0.31
Mean Midpoint G. Def.	7.04
Kinetic Fric. Force	15.6 gm
Kinetic Coeff. of Fric.	0.20

Table 7-9

STATIC AND KINETIC COEFFICIENTS OF FRICTION FOR PARAMETERS OF MATERIAL, AREA, LOAD, AND VELOCITY
(High Humidity Conditions) Upper Values = Static
Lower Values = Kinetic

Material		steel				magnesium				brass			
Apparent Area, cm^2		1/4	1	4	16	1/4	1	4	16	1/4	1	4	16
Load	Velocity												
gm	cm/min.												
80	5.1	.15	.29	.33	.51	.13	.13	.53	.38	.10	.18	.43	.33
		.10	.15	.19	.24	.11	.09	.27	.21	.08	.10	.11	.17
	12.7	.11	.31	.22	.47	.19	.16	.45	.33	.10	.14	.45	.33
		.08	.15	.17	.19	.13	.10	.26	.20	.09	.08	.10	.16
	25.4	.18	.29	.31	.46	.16	.21	.50	.31	.11	.14	.26	.34
		.15	.15	.20	.18	.12	.13	.23	.17	.08	.10	.10	.14
	50.8	.17	.27	.23	.40	.13	.22	.50	.28	.15	.10	.24	.28
		.12	.12	.18	.16	.11	.14	.22	.17	.12	.08	.09	.15
	101.6	.17	.30	.28	.49	.14	.17	.25	.26	.13	.15	.24	.23
		.10	.16	.20	.17	.12	.10	.19	.17	.09	.08	.12	.15
160	5.1	.14	.42	.44	.40	.12	.21	.38	.28	.09	.17	.25	.31
		.10	.13	.16	.18	.10	.10	.22	.19	.07	.12	.15	.17
	12.7	.13	.30	.47	.37	.23	.19	.29	.37	.12	.17	.23	.30
		.09	.14	.14	.14	.12	.10	.18	.18	.07	.10	.12	.15
	25.4	.13	.27	.36	.37	.15	.20	.23	.23	.14	.16	.24	.33
		.09	.11	.17	.13	.11	.09	.15	.14	.10	.11	.13	.15
	50.8	.13	.38	.48	.42	.15	.21	.25	.22	.10	.17	.31	.34
		.09	.11	.11	.14	.11	.11	.13	.12	.08	.12	.13	.14
	101.6	.13	.30	.36	.38	.12	.20	.25	.29	.10	.13	.36	.21
		.10	.14	.11	.14	.10	.12	.16	.17	.06	.11	.14	.16
320	5.1	.14	.36	.48	.32	.10	.25	.51	.31	.12	.16	.33	.27
		.10	.13	.13	.15	.06	.14	.13	.15	.07	.09	.08	.15
	12.7	.15	.33	.39	.36	.10	.26	.39	.31	.12	.19	.28	.25
		.10	.12	.12	.13	.07	.11	.11	.13	.08	.10	.05	.13
	25.4	.14	.39	.47	.42	.10	.27	.50	.31	.13	.15	.39	.25
		.10	.11	.13	.12	.07	.10	.11	.12	.09	.09	.06	.15
	50.8	.15	.38	.43	.41	.10	.29	.50	.31	.12	.16	.31	.29
		.10	.09	.11	.12	.07	.10	.11	.10	.08	.09	.03	.12
	101.6	.12	.47	.44	.44	.13	.31	.44	.17	.10	.17	.35	.31
		.09	.09	.09	.10	.08	.11	.12	.09	.07	.09	.02	.13

Table 7-10

SIGNIFICANCE OF VARIABLES ON STATIC COEFFICIENT OF FRICTION ON ICE FROM SERIES 3 OSCILLATORY MEASUREMENTS

Variable	Sum of Squares	Degrees Freedom	Mean Squares	Computed "F" ratio	Tabulated "F" ratio 5%	Tabulated "F" ratio 1%	Significance
Material	3198	2	1599	3.64	3.05	4.74	Significant at 5%
Area	14,478	3	4826	11.0	2.66	3.90	Very Significant
Load	228	2	114	.259	3.05	4.74	Not Significant
Velocity	131	4	33	.075	2.42	3.43	Not Significant
Residual	7343	167	440				

Table 7-11

SIGNIFICANCE OF VARIABLES ON KINETIC COEFFICIENT OF FRICTION ON ICE FROM SERIES 3 OSCILLATORY MEASUREMENTS

Variable	Sum of Squares	Degrees Freedom	Mean Squares	Computed "F" ratio	Tabulated "F" ratio 5%	Tabulated "F" ratio 1%	Significance
Material	296	2	148	24.7	3.06	4.75	Yes [1]
Area	920	3	307	51.2	2.67	3.91	Yes[1]
Load	533	2	266	44.3	3.06	4.75	Yes[1]
Velocity	88	4	22	3.7	2.43	3.44	Not Excessively
M x A	269	6	45	7.5	2.16	2.92	Yes
M x L	127	4	32	5.3	2.43	3.44	Yes
A x L	232	6	39	6.5	2.16	2.92	Yes
Residual[2]	862	151	6				

[1] This significance may be due either to the interaction or the main effect, or both.

[2] includes insignificant first and second order interactions.

The results of this series of measurements, therefore, agree with the results of Series 14 Static Measurements with respect to the influence of apparent area and material, but disagree with respect to the influence of load and the interactions of material with area and load with area.

Series 3 results also agree with Series 2 Low Humidity Oscillatory Measurements with respect to material but disagree with respect to the influence of velocity.

The preliminary analysis of the kinetic coefficients of friction on ice under high humidity conditions (Table 7-11) indicates the following:

(1) Apparent area of contact is very significant.

(2) Load is also very significant.

(3) Slider material ranks third in significance for the particular set of materials tested.

(4) Velocity also has a significant influence upon the kinetic coefficient although the degree of significance of this variable is much less than that of the first three variables.

(5) The interactions of material with area, material with load, and area with load also have a significance as compared to the residuals.

At the current stage of the statistical development of this problem it is not possible to ascertain whether the indicated influence of material, load, and area is due only to these individual variables or partially due to the interaction effects. Further statistical analysis is required to resolve this question.

It should also be recalled that this analysis was based on only a single set of measurements at each combination of experimental points. For this reason care should be taken not to place more dependence on the experimental results than the situation warrants.

The forces equivalent to the oscillatory mean displacement for the 4 cm^2 sliders of steel, magnesium, and brass are plotted against velocity for several load values in Figures 7-12, 7-13, and 7-14. Mean displacement equivalent force values versus load for several velocity settings are plotted for these same sliders in Figures 7-15, 7-16, and 7-17.

The mean displacement versus velocity curves appear to indicate a decrease of the mean displacement with an increase of the velocity, i.e. a negative damping constant. Examination of the mean displacement versus load curves indicates an increase in the mean displacement with an increase in the load as would be expected from the Second Law of Friction. (Friction Force is proportional to load). It is interesting to note, however, that the mean displacement load relation decreases with higher values of the velocity parameter in the case of steel. For magnesium the slope of the mean displacement-load curves remained more nearly constant over the velocity parameter than the slope obtained for the steel slider.

Assuming a friction function equal to $F_k + c\dot{x}$, one of the functions examined in Chapter IV, the individual componenets should be obtainable from the mean displacement versus velocity and mean displacement versus

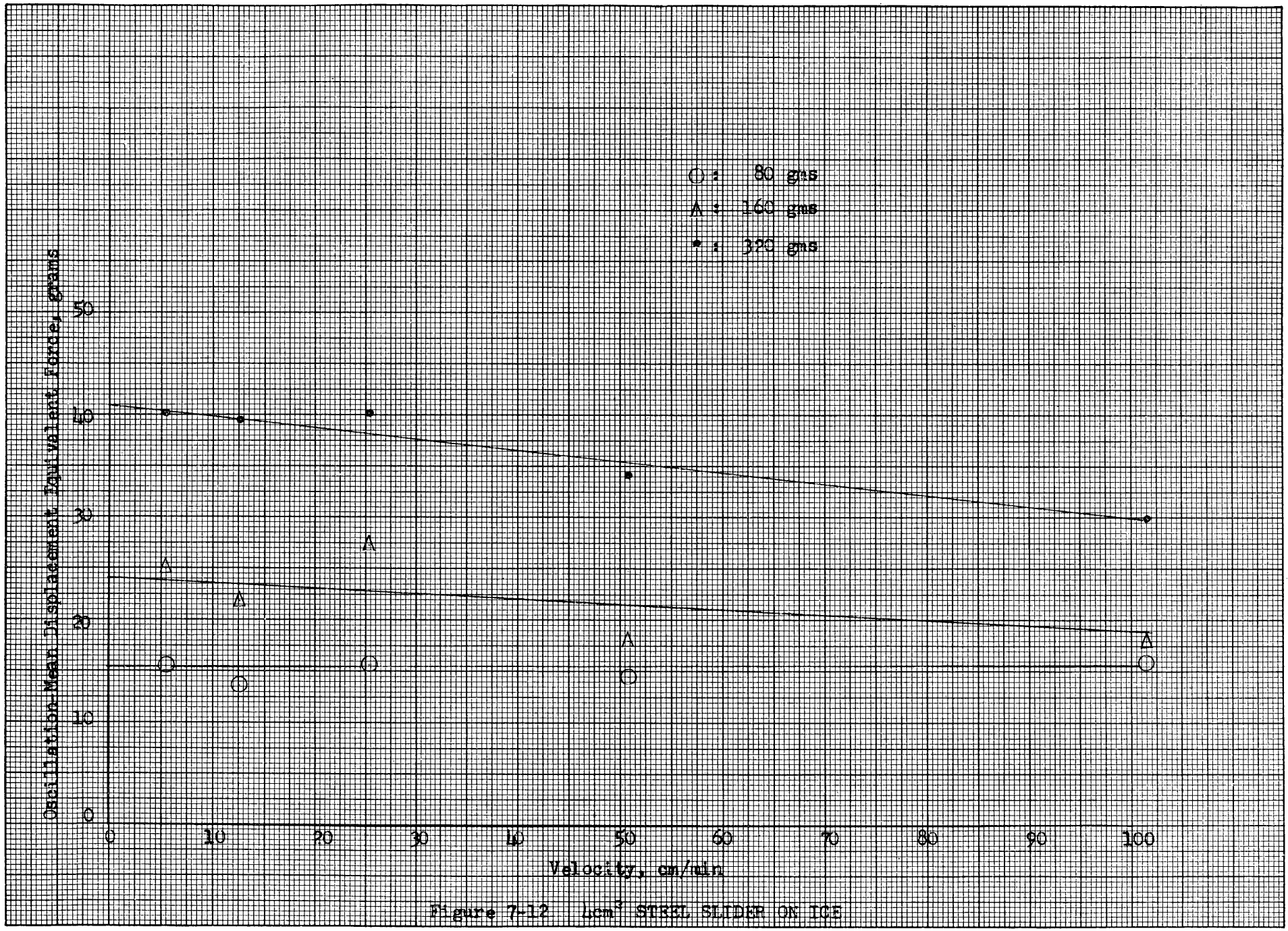

Figure 7-12 $4cm^2$ STEEL SLIDER ON ICE

Figure 7-13 4 cm² MAGNESIUM SLIDER ON ICE

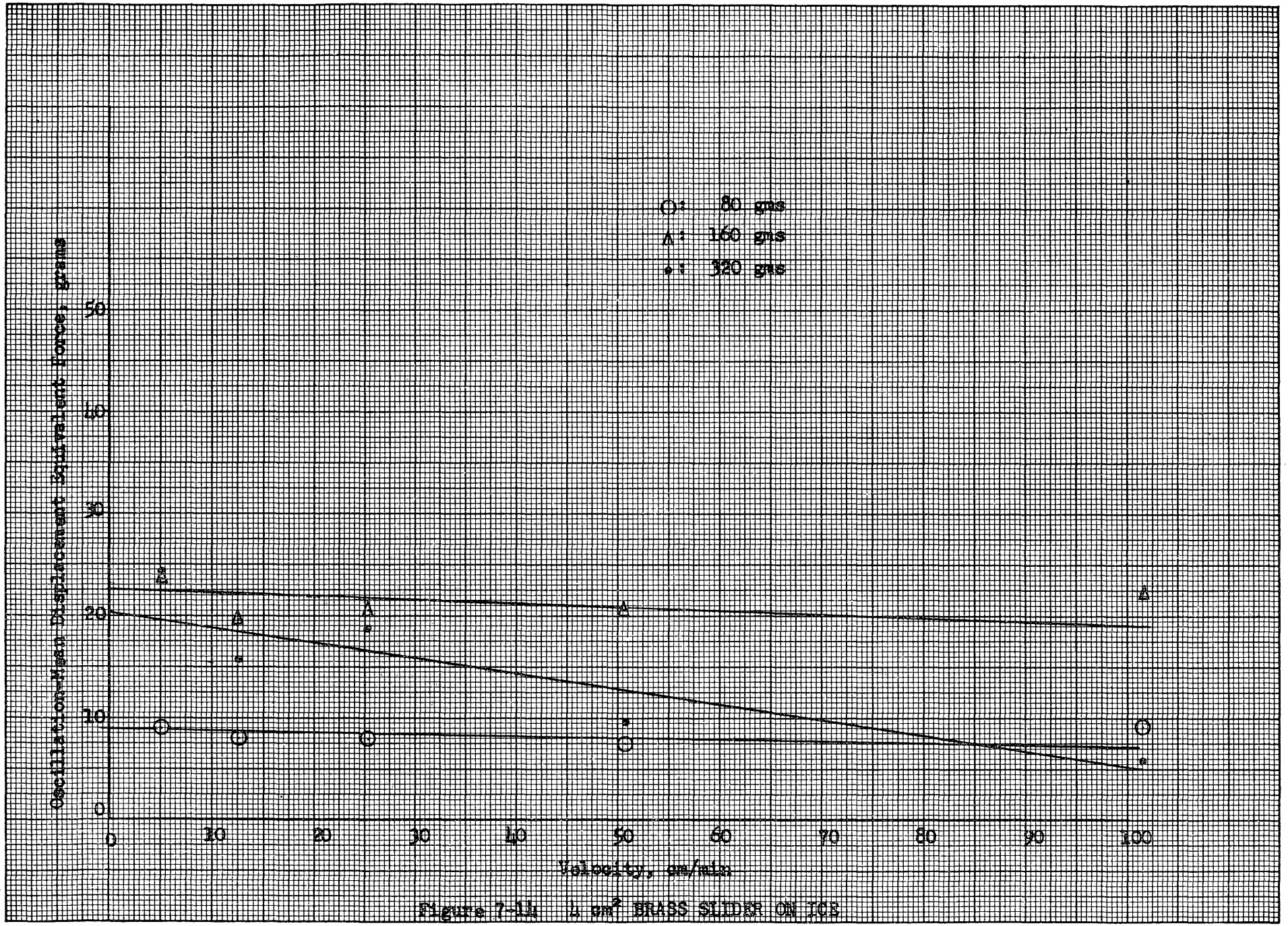

Figure 7-14 4 cm² BRASS SLIDER ON ICE

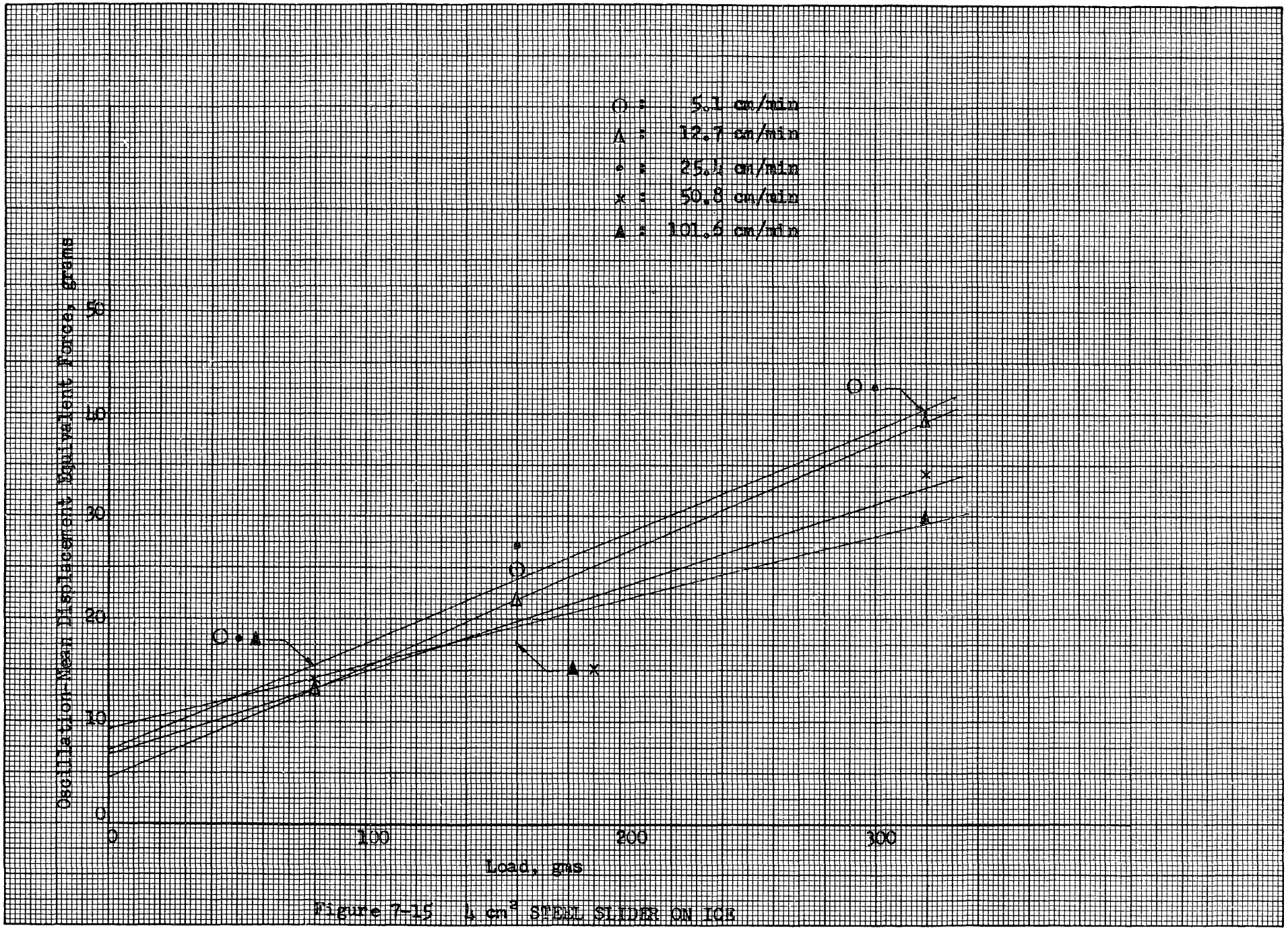

Figure 7-15 4 cm² STEEL SLIDER ON ICE

TABLE 9-3

Calculated Upper Limit for the Fractional Change in Area.

f (cps)	Series 1	Series 2
100	.021 n	.026 n
250	.040 n	.022 n
500	.035 n	.045 n
1000	.011 n	.027 n
1500	.019 n	.017 n
2000	.023 n	.008 n
2500	.023 n	.003 n
Ave.	.025 n	.021 n

Experiment II

Procedure

The promising results of Experiment I supported the use of the proposed method in securing area determinations and other information on the characteristics of the ice-slider surface. Toward this goal the procedures undertaken in Experiment II were more definitive.

The general conditions under which the experiment was performed were essentially the same as in Experiment I.

1. Ambient temperature	- 10° C
2. Slider material	brass
3. Apparent area of slider	4 cm^2
4. Effective area of condenser	4.83 cm^2
5. Thickness of ice dielectric	.5969 cm

The ice was prepared in the wood tray. Attempts to control the formation of the ice such that it would grow from the bottom up met with some difficulty. The low thermal conductivity of the wood delayed the freezing and considerable freezing occurred from the side producing horizontal cylinders of trapped gas. The ice that constituted the dielectric was relatively free of bubbles as the ice was machined to a level below the bubble line.

Measurements of resistance and capacitance of the condenser were taken in the frequency range 7-3000 cps. for each load. The slider was loaded with 214, 412, 611, and 810 gm. in increasing order, care being taken not to disturb the position of the slider on the ice. At the end of

the 810 gm. load run, weights were then removed from the slider and measurements again taken for 611, 412, and 214 gm. loads in that order. The latter procedure was followed to determine whether a mechanical set was taking place. At the end of the 214 gm. run a hot soldering iron was lightly applied to the slider to melt a thin layer of ice at the ice-slider surface and produce a complete freezedown of slider to ice as the layer refroze. Resistance and capacitance measurements were then obtained for the frozen down condition. The slider was then forcibly dislodged. The separation was not at the ice-slider surface but fracture took place in the ice itself indicating essentially a complete freezedown.

Data and Results

Table 9-4 contains the values of resistance of the ice condenser obtained for the loads 214, 412, 611, and 810 gm. under both increasing and decreasing loading conditions. This table also lists the values obtained for complete freezedown. Table 9-5 contains the values similarly obtained for the parallel capacitance for the several different loading conditions together with the freezedown measurements. In Table 9-4 several of the values for the lower frequencies are missing. At frequencies below 50 cps. the bridge output was distorted preventing accurate balancing of the resistance component for the lower frequencies. This fact coupled with the very large resistance at these low frequencies suggests that the values obtained at frequencies below 50 cps. should be discarded. For the freezedown situation sufficiently accurate values were obtained at the low frequencies due to the lower resistance associated with the elimation of surface effects.

Table 9-4

The Resistance of the Ice Condenser

Load	214 gms		412 gms		611 gms		810 gms	Freezedown
f	(a)	(b)	(a)	(b)	(a)	(b)		
7	24.79×10^7	-----	----	123.1×10^7	----	24.62×10^7	61.60×10^7	6.178×10^7
15	24.82	41.05×10^7	24.68×10^7	41.06	24.66×10^7	49.27	----	3.532
25	----	18.96	14.51	18.96	22.43	17.61	18.98	3.389
50	12.41	12.35	24.73?	12.34	13.73	15.43	15.44	2.479
100	9.565	7.501	7.746	7.498	8.255	8.251	7.991	1.692
250	4.034	2.895	2.968	2.765	3.114	2.569	2.679	7.809×10^6
500	1.175	1.047	1.084	1.009	1.035	1.018	1.061	3.788
1000	3.307×10^6	2.95×10^6	3.028×10^6	3.026×10^6	3.03×10^6	3.03×10^6	2.959×10^6	1.497
1500	1.618	1.498	1.515	1.498	1.500	1.482	1.466	.8443
2000	.9989	.9407	.9567	.9501	.9231	.9232	.9261	.5708
2500	.7177	.6809	.6855	.6829	.6765	.6706	.6696	.4338
3000	.5642	.5335	.5441	.5389	.5338	.5325	.5331	.3523

The (a) values were obtained with the increasing loads and the (b) values were obtained with the decreasing loads. All resistances are in ohms.

Table 9-5

The Capacitance of the Ice Condenser

Load f	214 gms (a)	214 gms (b)	412 gms (a)	412 gms (b)	611 gms (a)	611 gms (b)	810 gms	Freeze-down
7	35	37	28	36	37	39	37	118
15	33	31	36	30	33	32	34	76
25	32	31	32	30	31	31	31	70
50	33	32	32	33	32	32	32	65
100	30	31	32	30	32	30	31	61
250	32	30	30	30	30	30	30	40
500	28	28	32	13	30	29	30	55
1000	32	33	12	12	11	12	13	81
1500	10	33	32	9	10	11	12	61
2000	36	9	32	31	10	9	13	38
2500	12	8	36	29	9	8	11	33
3000	31	31	54	56	33	28	31	32

The (a) values were obtained with the increasing loads and the (b) values were obtained with the decreasing loads. All capacitances are in micro-micro farads.

Immediate examination of the data reveals several interesting facts. In Table 9-5 a distinct difference in the magnitude of the capacitance obtained at freezedown compared to the values obtained for the resting situations is evident. This suggests the existence of a surface capacitance which disappeared when the slider was frozen to the surface. Because of the erratic character of the capacitance values, the cause of which was explained in the discussion of Experiment I, the method of least squares was used to obtain a representative value of the capacitance over the entire measured frequency range.

Examination of Table 9-4 reveals a characteristically lower resistance at all frequencies for the freezedown situation suggesting the existence of a resistance associated with surface effects. The difference however between the resting and freezedown resistance at any given load is a function of frequency. This fact rules out the possibility that the surface resistance can consist entirely of a free-ion conductivity that is frequency independent. It may also be seen that the surface resistance represented by the difference between the freezedown and resting resistances decreases with increasing load. As the load increases the contact area certainly cannot decrease. Associating decreasing surface resistance with increasing area, an assumption which was made in Experiment I, now appears justified.

It may also be seen from examination of Table 9-4 that a mechanical set takes place as loads are increased, for as the loads are subsequently removed the resistance does not return to its original value.

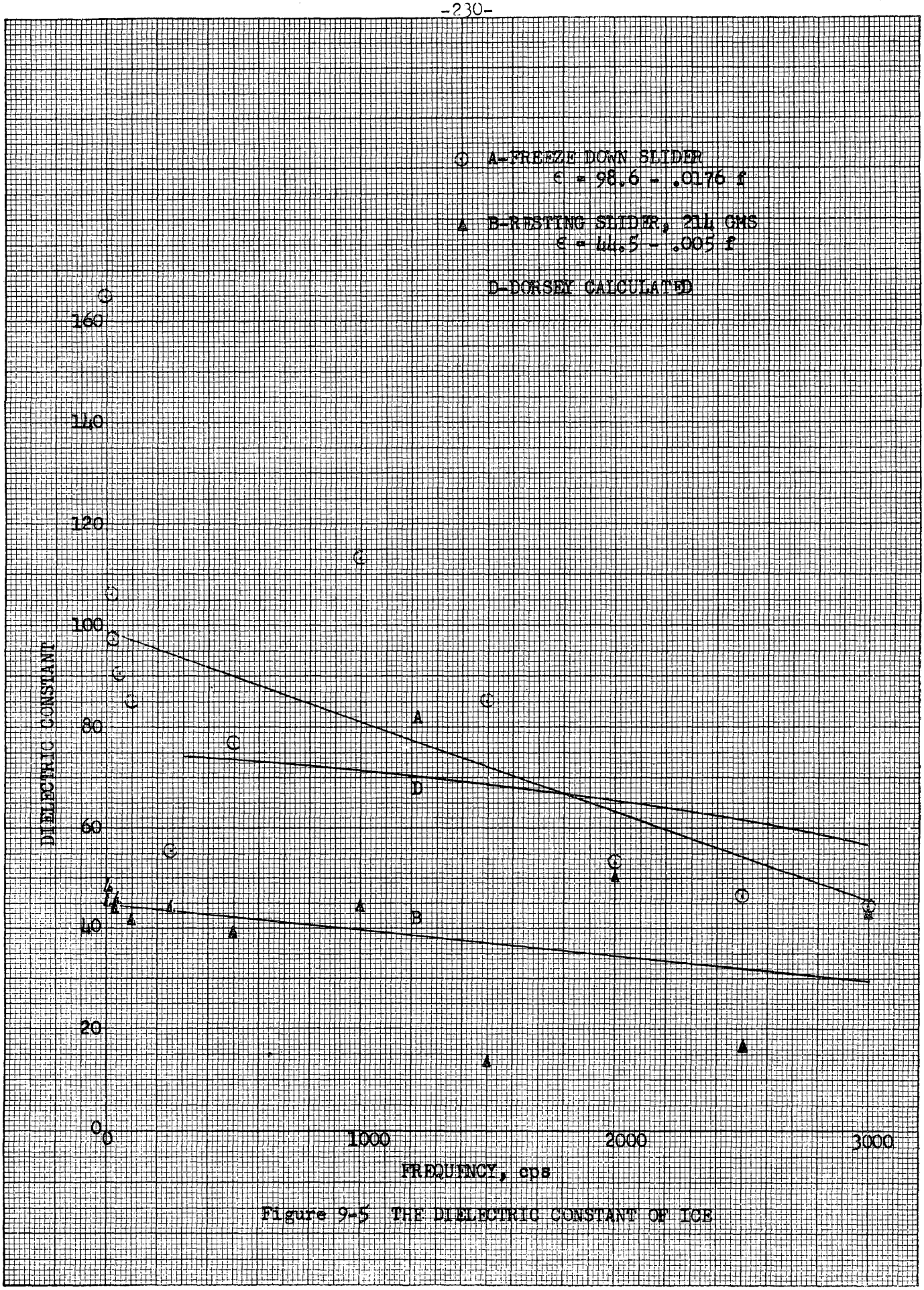

Figure 9-5 THE DIELECTRIC CONSTANT OF ICE

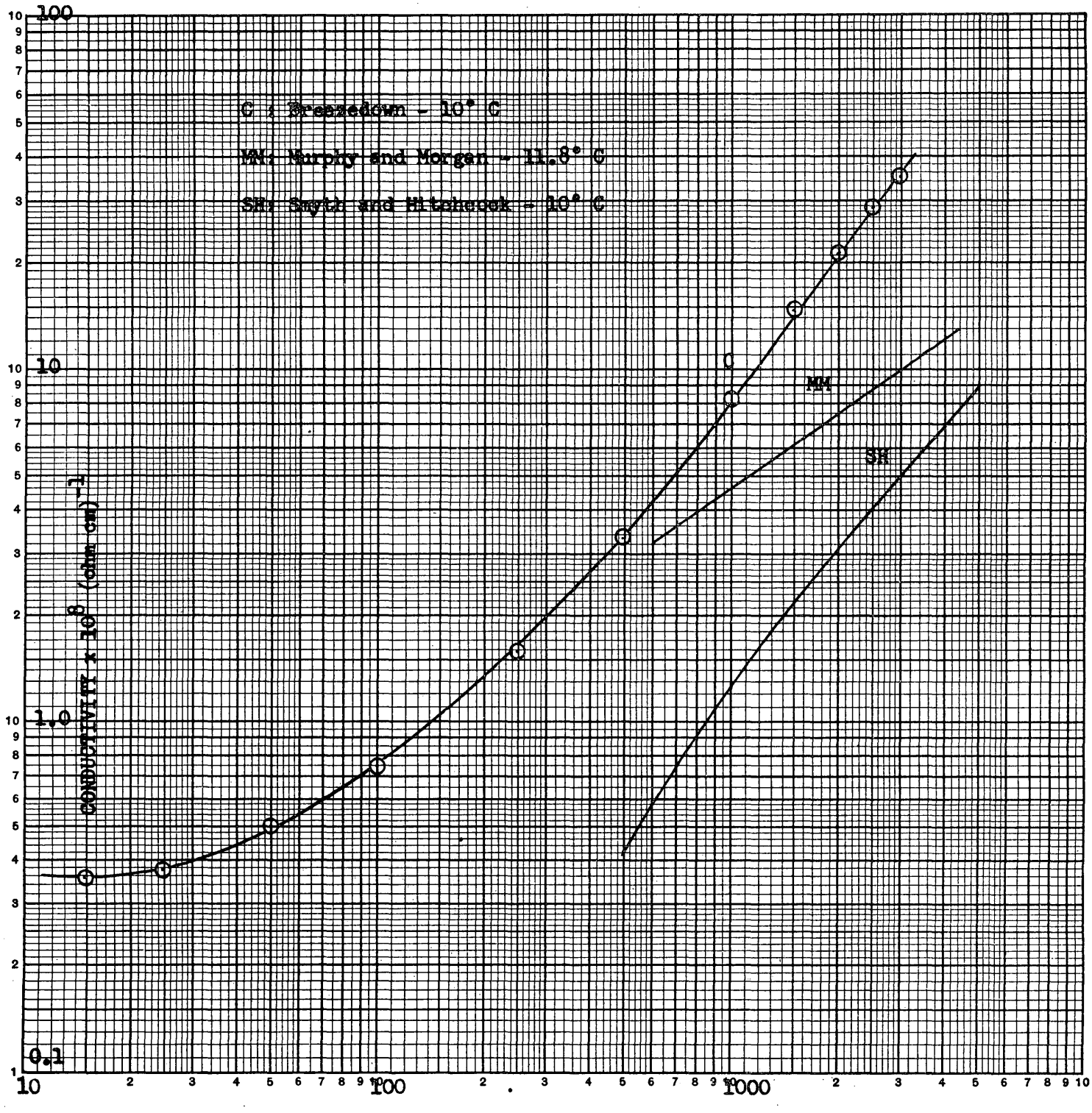

Figure 9-6 CONDUCTIVITY OF ICE

of ice conductivity in the literature. Future work should include measurements on the water from which the ice is obtained.

Estimation of Surface Capacitance

We assume that the capacitance measured under resting conditions, C_R, consists of an ice capacitance, C_F, in series with a surface capacitance, C_S. At freezedown the surface capacitance disappears and the measured capacitance is C_F alone. The surface capacitance is then obtained from the equation

$$C_S = \frac{C_R C_F}{C_F - C_R} \qquad (9\text{-}10)$$

Substituting for C_F, the least square curve of capacitance as a function of frequency obtained from the measured capacitance of the freeze-down slider, and for C_R, the least square curve of capacitance for each of the loaded condensers, C_S, the surface capacitance, as a function of frequency is obtained.

Figure 9-7 indicates the values for surface capacitance as the loads were increased and Figure 9-8 as the loads were decreased. The characteristic feature of all the curves is the constancy of the capacitance out to 1000 cps. at a value of about 55 ± 10 mmf for increasing loads and 52 ± 15 mmf for decreasing loads. No distinctive variation of the surface capacitance with load is apparent, though finer capacitance measurements may later show a dependence on load to exist. The surface capacitance values beyond 1000 cps. should be discarded as inconclusive since the least square approximations for the measured capacitances reduce in accuracy as the frequency is increased.

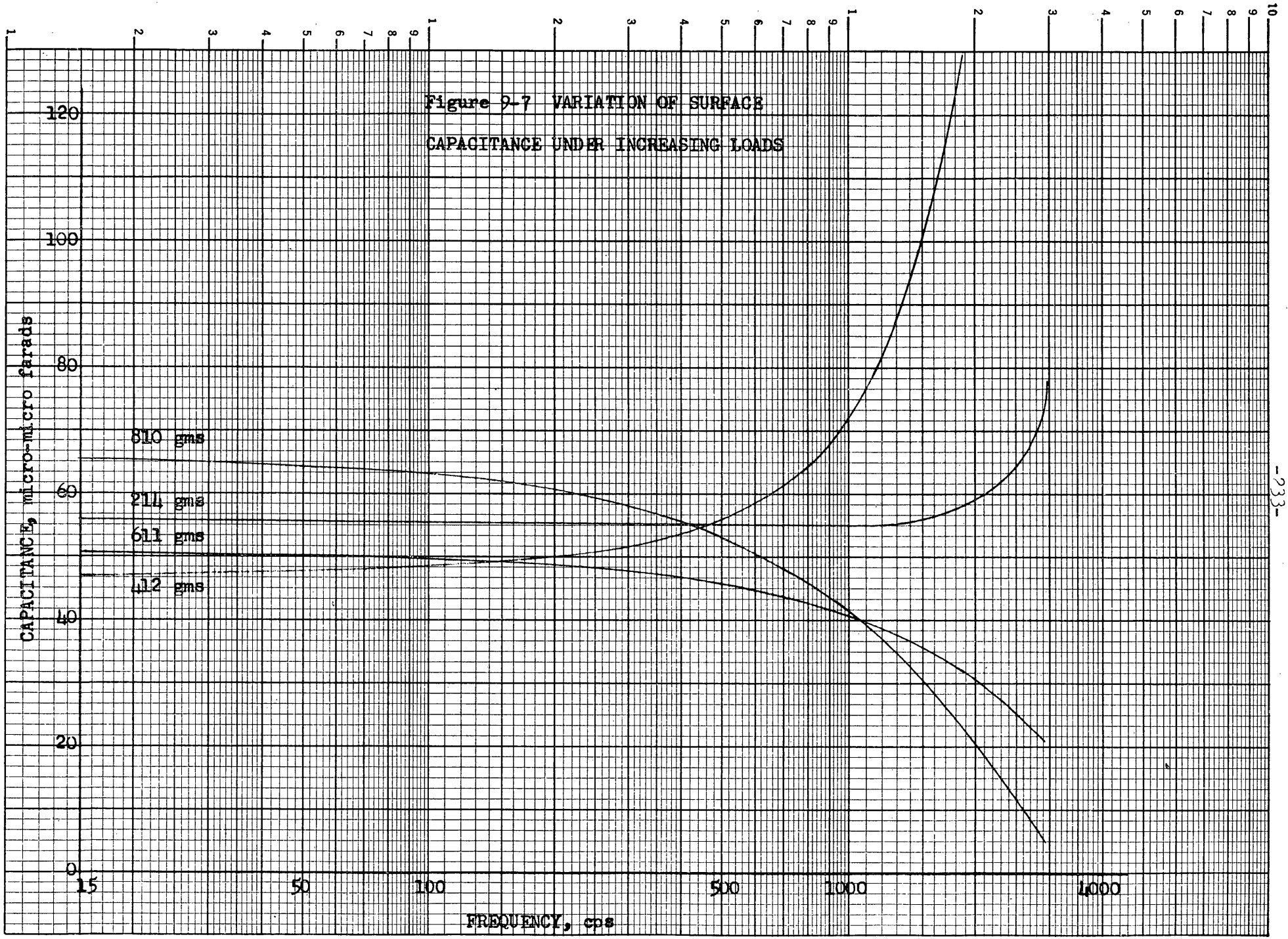

Figure 9-7 VARIATION OF SURFACE CAPACITANCE UNDER INCREASING LOADS

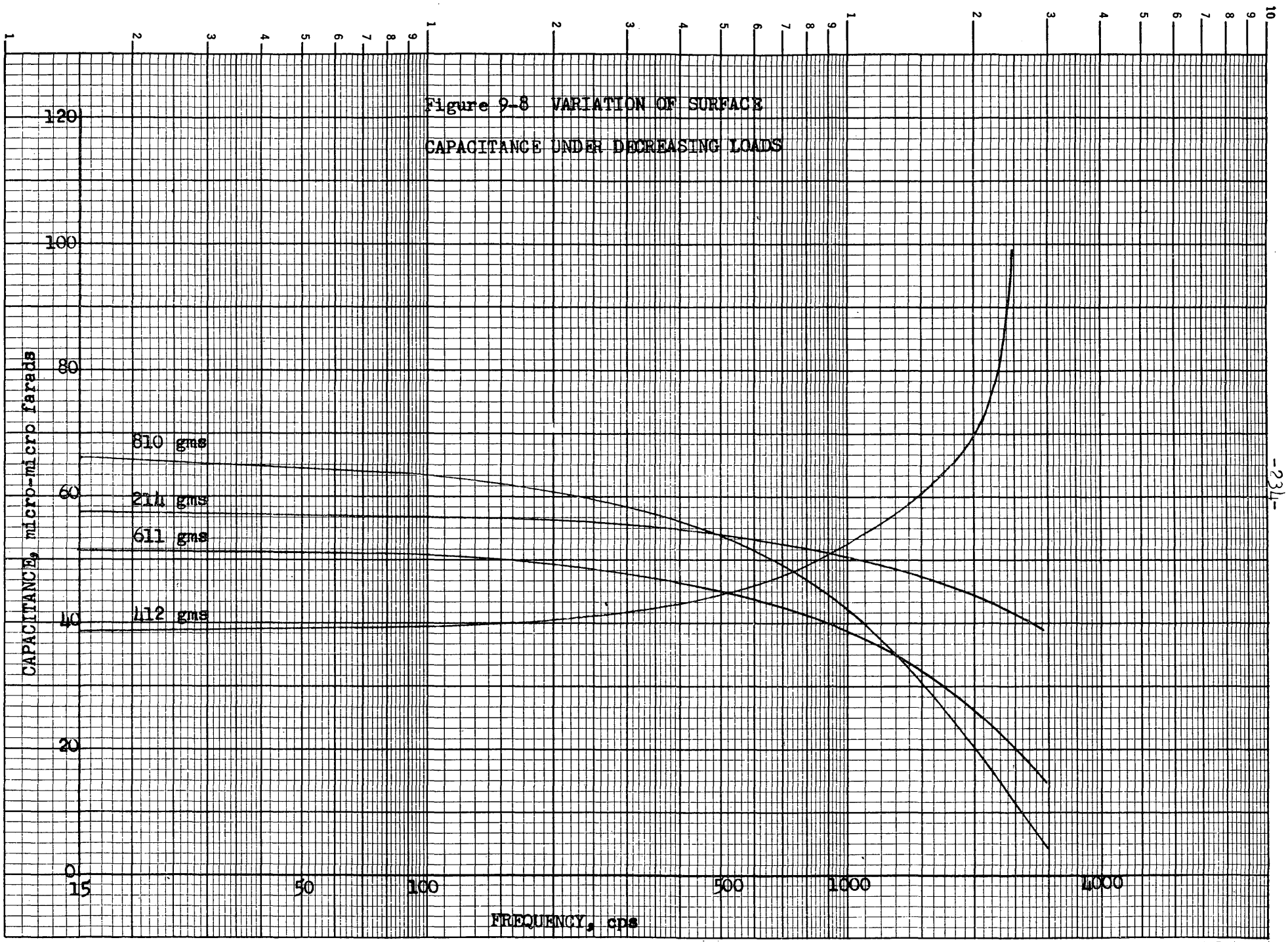

Figure 9-8 VARIATION OF SURFACE CAPACITANCE UNDER DECREASING LOADS

To explain the origin of the surface capacitance, three sources were considered.

1. Formation of a liquid or higher temperature ice film at the surface as a result of dielectric heating.
2. Existence of an air film on the ice slider surface.
3. The existence of a transition film on the ice surface as a result of orientation of H_2O molecules, as postulated by Weyl.[5]

A calculation of the energy lost in the ice revealed that insufficient heat was produced to increase the temperature of the ice and alter the dielectric constant of the surface appreciably. Thus a heating effect was ruled out as a cause for the surface capacitance. An air film to produce a surface capacitance of 55 mmf would have to be 8×10^{-3} cm. thick for an effective capacitance area of 4.83 cm^2. It does not seem conceivable that this large an air film could exist in view of the way the ice surface and the sliders were honed. It is possible, however, that the air bubbles which formed during ice formation may have left some air pockets on the ice surface which were sufficient to give an appreciable contribution to the surface capacitance. Proper evaluation of this possibility awaits improved ice formation using the wood tray together with methods that will permit a pinpointing of the contribution of the air film to the capacitance.

---

[5] Weyl, W. A. (1951) "The Surface Structure of Water and some of its Physical and Chemical Manifestations." Journal of Colloid Science Vol. 6, pp. 389-405.

According to Weyl's Theory, a transition layer forms on the ice surface as the molecules of water make the transition from the bulk structure to the dipole structure (See Appendix B). This strong molecular binding would have the effect of reducing the dielectric constant of the ice surface below that of the interior. This result is supported by Palmer[6], who obtained a dielectric constant of 3 for thin water films bound to clay particles. If we assume a dielectric constant of 3 for the transition layer, it would require a thickness 2.4×10^{-2} cm. for the layer. This value for the thickness of the film is considerably off compared to Weyl's suggestion that it would take a layer of only several hundred molecules to make the transition. Considering that 1000 molecules are necessary for the transition, our value of 2.4×10^{-2} cm. is about 1000 times too large. None of the suggested origins for the surface capacitance seem completely adequate to explain the results obtained. It is believed that a combination of the air film plus the transition layer contribute the most to this surface effect, but definite conclusions must await further experiments. Considering a transition layer as a contributor to surface capacitance requires the absence of this film at the slider-ice surface during complete freezedown. This is possible since the free electrons of the brass slider may have sufficiently neutralized the strong proton forces during the thawing and refreezing which took place as freezedown was obtained. If in addition tin or copper atoms

---

6 Palmer, L. S. (1952) Proceedings of the Physical Society of London Part B Vol. 65, pp. 674-678.

from the brass slider entered the ice surface, they would contribute to the disappearance of the transition film. The fact that in dislodging the slider after the freezedown measurements fracture took place in the interior of the ice supports the contention that the transition layer was absent.

Surface Resistance and Contact Area

It has been remarked that the raw data indicates that irreversible deformation of the ice-metal surface takes place as the slider load increases. Figure 9-9 is a plot of the surface resistance as a function of frequency for increasing loads. A definite decrease in surface resistance as the load was changed from 214 to 412 grams is indicated. Further increase in the load did not produce as consistent a decrease in surface resistance. This suggests that beyond 412 grams the character of the ice-metal surface is unchanged from an electrical point of view.

Figure 9-10 plots the surface resistance for the different loads as they were progressively decreased, and it shows no progressive increase of surface resistance. The changes in surface resistance, Figure 9-9, are not evident in 9-10. The important conclusion to be drawn from these results is that permanent deformation of the ice-slider contact surface takes place with loads of the magnitude here used. This means that elastic contacts are ruled out because they would require similar surface resistance measurements whether loads are progressively increased or decreased. Plastic deformation or actually fracture must therefore take place at the ice-slider surface.

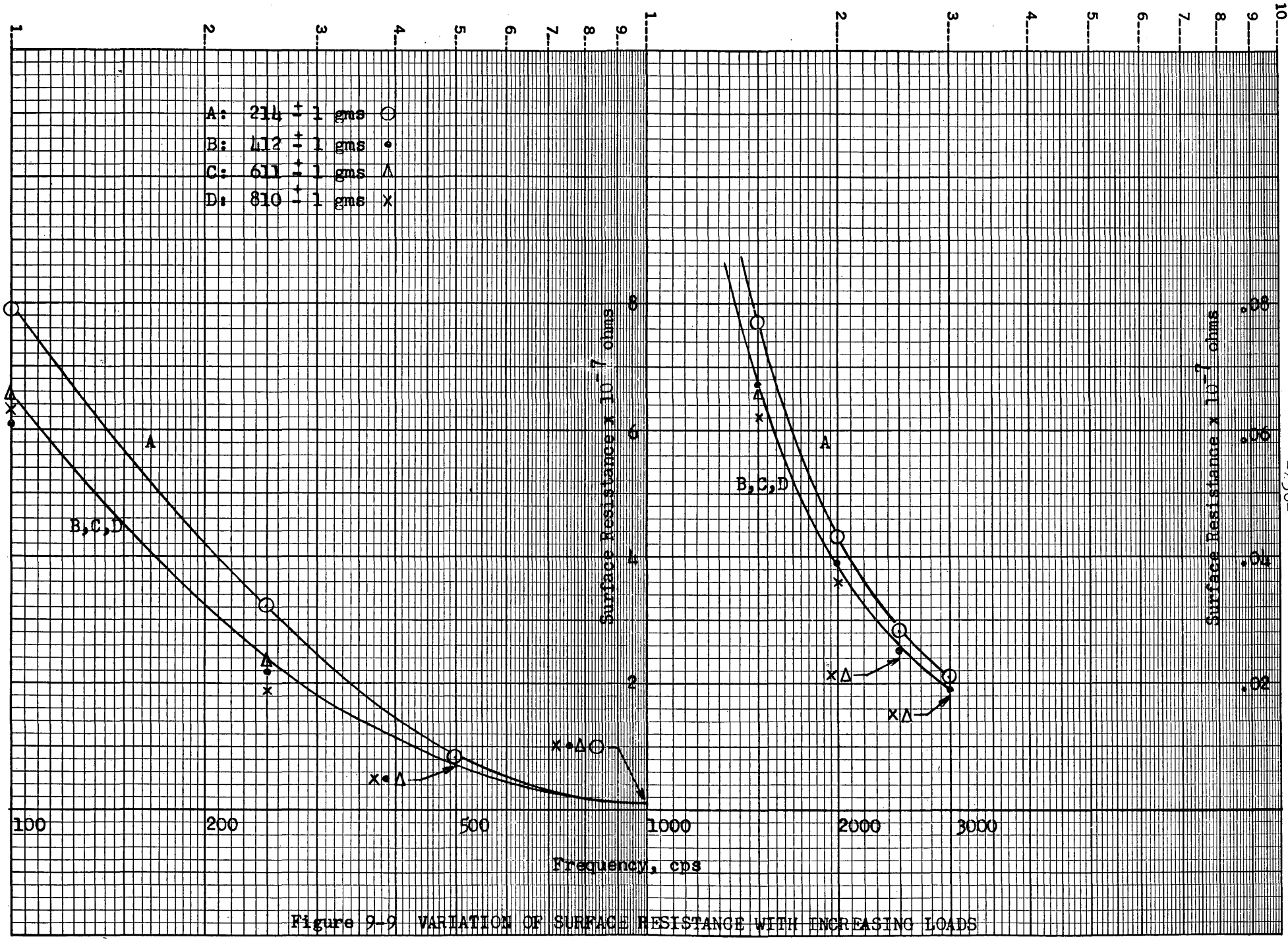

Figure 9-9 VARIATION OF SURFACE RESISTANCE WITH INCREASING LOADS

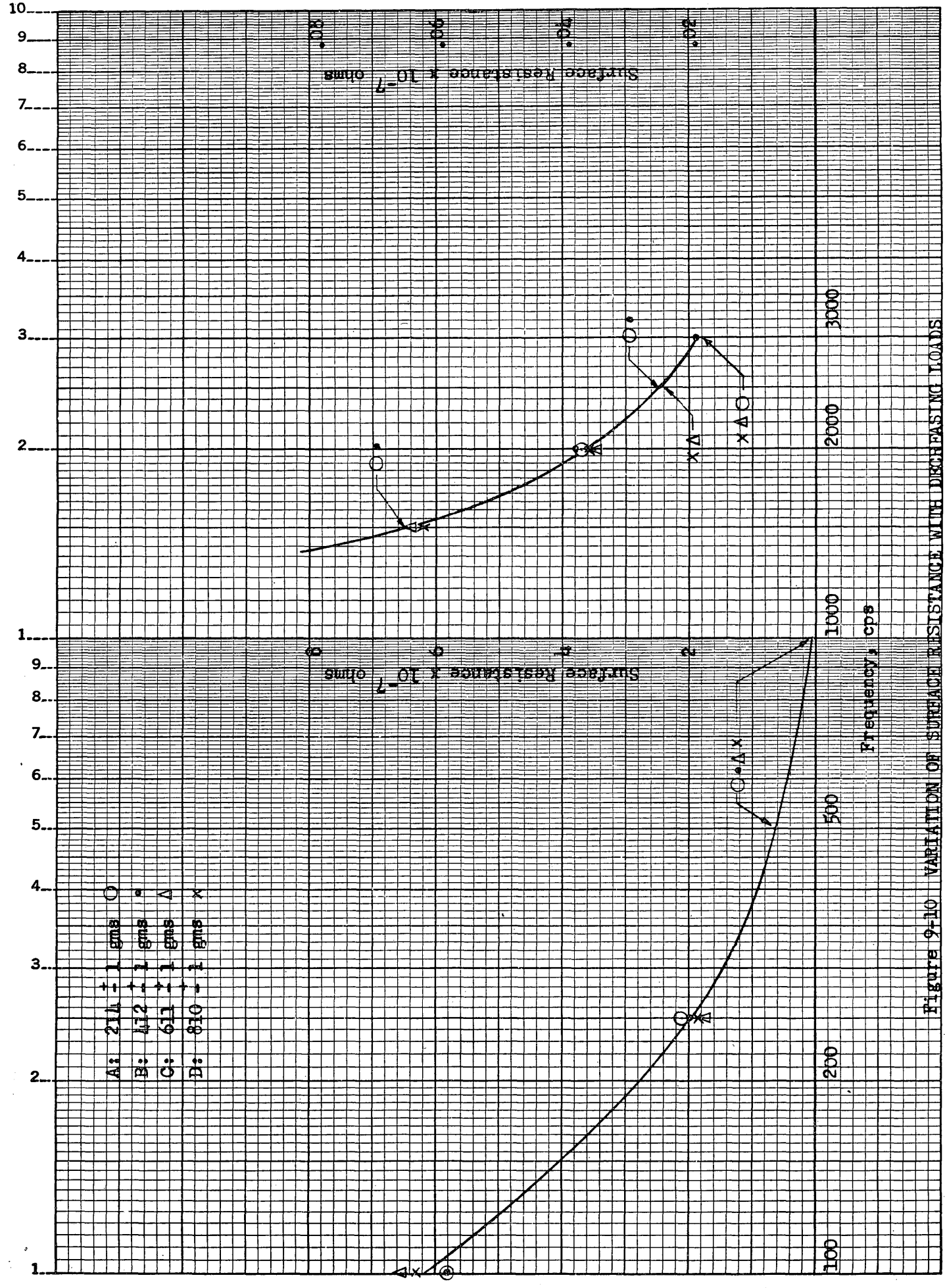

Figure 9-10 VARIATION OF SURFACE RESISTANCE WITH DECREASING LOADS

It might be argued that a time factor may be responsible for this phenomenon. This argument requires that the character of the ice-slider surface changes with time independent of load until some sort of a permanent fix takes place that is subsequently unaltered by load changes. At the present time this alternative explanation has not as yet been ruled out, and is conceivable that both mechanisms are operating. The feeling is that the permanent deformation theory offers a more plausible explanation of the phenomenon. In either case, the importance of these results in understanding friction on ice needs no elaboration and are further studied in Experiments III and IV.

The variation of surface resistance with frequency has already been mentioned and illustrated in Figures 9-9 and 9-10. It was expected from theoretical considerations based on asperity contact between the ice-slider surface that the surface resistance would be frequency independent. These theoretical considerations led to Equation (9-3) for the contact area.

$$A = \frac{\pi \Lambda^2}{16\, n \lambda^2} \qquad (9\text{-}3)$$

Some comment on the usefullness of this equation in view of the experimental results needs to be made. If we assume that the surface resistance is primarily a constriction resistance, the free-ion conductivity must be a frequency dependent quantity. This possibility has already been mentioned in the discussion of Experiment I. Applying this construction of the surface resistance to Equation (9-3) requires a knowledge of this frequency dependent conductivity. Lacking such data the conductivity of the bulk ice obtained in the freezedown measurements was used instead. This conductivity is primarily due to dielectric loss, but it was applied

surface resistance will show no change in value. If permanent deformation does not take place the surface resistance should change, provided aging has not yet had the opportunity to produce the permanent surface.

The variation of surface resistance with frequency has already been mentioned and illustrated in Figures 9-9 and 9-10. It was expected from theoretical considerations based on asperity contact between the ice-slider surface that the surface resistance would be frequency independent. These theoretical considerations led to Equation (9-3) for the contact area.

$$A = \frac{\pi \Lambda^2}{16\, n\lambda^2} \qquad (9\text{-}3)$$

Some comment on the usefullness of this equation in view of the experimental results needs to be made. If we assume that the surface resistance is primarily a constriction resistance, the free-ion conductivity must be a frequency dependent quantity. This possibility has already been mentioned in the discussion of Experiment I. Applying this construction of the surface resistance to Equation (9-3) requires a knowledge of this frequency dependent conductivity. Lacking such data the conductivity of the bulk ice obtained in the freezedown measurements was used instead. This conductivity is primarily due to dielectric loss, but it was applied in the hope its frequency dependence resembled that of the free ion conductivity as postulated. This approach, intuitively weak to begin with, proved fruitless. Equation (9-3) therefore seems of little value at the present time if a frequency dependent free-ion conductivity exists.

A more successful approach to the surface resistance problem is provided by the parallel arrangement of film and asperities discussed in Chapter I. The assumption is made that the measured surface resistance consists of two resistances in parallel. One a frequency independent resistance due to current constriction through the contacting asperities and the other a frequency dependent resistance due primarily to dielectric loss within the surface film.

If we let R be the frequency independent resistance and $\frac{L}{\lambda A}$, the resistance of the film in parallel, then the surface resistance R_s is given by Equation (9-10).

$$R_s = \frac{R \frac{L}{\lambda A}}{R + \frac{L}{\lambda A}} \tag{9-10}$$

L is the film thickness, A its cross sectional area, and λ its conductivity. Solving for R yields:

$$R = \frac{R_s}{1 - R_s \frac{\lambda A}{L}} \tag{9-11}$$

If we assume the surface film obeys Debye's dipole theory the conductivity at any frequency is given by:

$$\lambda = \frac{(e_1 - e_o)\, pf^2}{1.8 \times 10^{12}\, (1 + p^2 f^2)} \quad (\text{ohm cm})^{-1} \tag{9-12}$$

where e_1 is the static dielectric constant, e_o, the dielectric constant at optical frequencies, p the relaxation time, and f the frequency.

Substituting Equation (9-12) into (9-11) gives for R:

$$R = \frac{R_s}{1 - \frac{R_s\,(e_1 - e_o)\,pf^2\,A}{1.8 \times 10^{12}\,(1 + p^2f^2)\,L}} \tag{9-13}$$

If we set:

$$k = \frac{(e_1 - e_o)\,pA}{1.8 \times 10^{12}\,L}\ , \tag{9-14}$$

(9-13) reduces to

$$R = \frac{R_s}{1 - \frac{R_s\,kf^2}{1 + p^2f^2}} \tag{9-15}$$

Since R is frequency independent, Equation (9-15) holds for all frequencies. For any two frequencies, f_a and f_b:

$$R = \frac{R_{sa}}{1 - \frac{R_{sa}\,k\,f_a^2}{1 + p^2\,f_a^2}} = \frac{R_{sb}}{1 - \frac{R_{sb}\,k\,f_a^2}{1 + p^2\,f_b^2}} \tag{9-16}$$

Solving for k we have:

$$k = \frac{R_{sa} - R_{sb}}{R_{sa}R_{sb}} \quad \frac{(1 + p^2\,f_a^2)(1 + p^2\,f_b^2)}{f_b^2 - f_a^2} \tag{9-17}$$

Substituting (9-17) into the first part of (9-16) yields for the frequency independent resistance

$$R = \frac{R_{sa}}{1 - \frac{R_{sa} - R_{sb}}{R_{sb}} \quad \frac{(1 + p^2 f_b^2) f_a^2}{(f_b^2 - f_a^2)}} \tag{9-18}$$

Therefore the surface resistances measured at any pair of frequencies permits a calculation of the static component of the surface resistance if p, the relaxation time is known. Similarly, solving for k in Equation (9-17) permits estimation of the thickness and area of the film if the dielectric constants of the film are known.

Application of this method to the curves of surface resistance as a function of frequency (See Figures 9-9 and 9-10) was done in the following manner. At a given load, surface resistance values of the frequency pairs 50,100; 100, 250; 50, 250 were substituted into Equation (9-18) to yield three values of the frequency independent resistance R, and into Equation (9-17) to yield three values for k. These values were then averaged and substituted into the equation

$$R_s = \frac{\bar{R}}{1 + \frac{\bar{R}\,\bar{k}\,f^2}{1 + p^2 f^2}} \tag{9-19}$$

This equation is the same as (9-10) after the substitutions (9-12) and (9-14) have been made. $\bar{R}$, and $\bar{k}$ are the average of the three values of R and k obtained from the three frequency pairs. Equation (9-19) is then evaluated at each frequency that was studied experimentally to

provide a comparison of the surface resistance calculated from Equation (9-19) with the experimentally determined values. In this way the validity of the interpretation of the surface as two resistances in parallel can be checked. This is admittedly an empirical approach since some of the data must be used to permit evaluation of the theoretical expression for the surface resistance. Close fit therefore between experimental and theoretical values is expected at the frequencies 50, 100, and 250 cps. The behavior of these values at the higher frequencies must test the construction.

In all the calculations the relaxation time was taken as 2×10^{-4} sec. This provides for a transition frequency of 5,000 cps in the anomalous dispersion of the surface film.

The method described was applied to the surface resistance values of the 214 gram, and 412 gram slider (see Figure 9-9) and the 810 gram slider (see Figure 9-10). For the latter slider the values of surface resistance selected were the averages of the values obtained for all four loads during the decreasing test. The reason for this was the apparent constancy of the surface resistance as the loads were removed.

Table 9-6 contains the values of R and k obtained for each frequency pair from Equations (9-17) and (9-18).

From the average values for R and k listed in Table 9-6, the surface resistances from Equation (9-19) were obtained. Table 9-7 lists these calculated surface resistances alongside the experimentally determined values at each frequency. Figure 9-11, 9-12, and 9-13 present the results in graphical form. The curves are from the calculated values, and the

TABLE 9-6

Calculated Values for the Frequency Independent Surface Resistance R, and for k for the (a) 214, (b) 412 and (c) 810 gram Slider.

Frequency Pair	R (ohms)	k (sec^2/ohm)
	(a) 214 gram load	
50,100	1.088×10^8	3.51×10^{-13}
100,250	1.080	3.45
50,250	1.085	3.46
Average	$(1.084 \pm .003) \times 10^8$	$(3.47 \pm .02) \times 10^{-13}$
	(b) 412 gram load	
50,100	1.245×10^8	8.52×10^{-13}
100,250	.914	5.57
50,250	1.155	5.95
Average	$(1.105 \pm .13) \times 10^8$	$(6.68 \pm 1.2) \times 10^{-13}$
	(c) 810 gram load	
50,100	1.610×10^8	10.14×10^{-13}
100,250	1.035	6.68
50,250	1.432	7.13
Average	$(1.359 \pm .22) \times 10^8$	$(7.98 \pm 1.4) \times 10^{-13}$

TABLE 9-7

Calculated and Experimental Surface Resistances for

the (a) 214 gram (b) 412 gram and (c) 810 gram Slider

Frequency	R_s (Calc) ohms	R_s (Exp) ohms
(a) 214 gram load		
50	9.90×10^7	9.93×10^7
100	7.88	7.87
250	3.24	3.25
500	1.05	.796
1000	2.92×10^6	1.81×10^6
1500	1.38	.774
2000	.842	.428
2500	.573	.284
3000	.434	.212
(b) 412 gram load		
50	9.33×10^7	9.86×10^7
100	6.36	6.05
250	1.92	2.18
500	5.73×10^6	7.05×10^6
1000	1.54	1.53
1500	.722	.671
2000	.433	.386
2500	.299	.252
3000	.226	.192
(c) 810 gram load		
50	1.08×10^8	1.14×10^8
100	6.50×10^7	6.12×10^7
250	1.82	1.95
500	.488	.655
1000	.129	.150
1500	$.605 \times 10^6$	$.642 \times 10^6$
2000	.363	.304
2500	.250	.242
3000	.189	.182

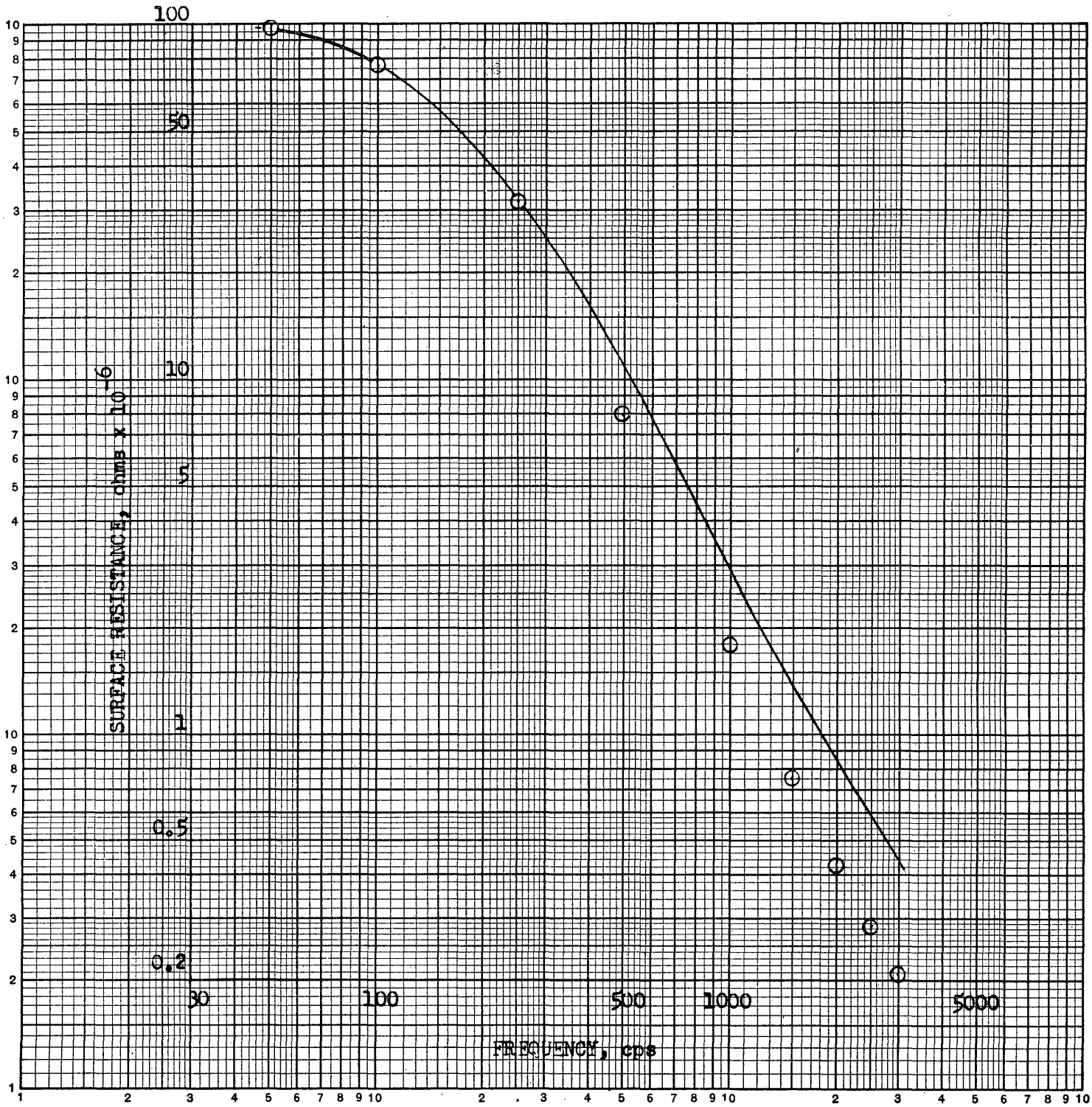

Figure 9-11 CALCULATED AND EXPERIMENTAL

SURFACE RESISTANCES FOR 214 gm SLIDER

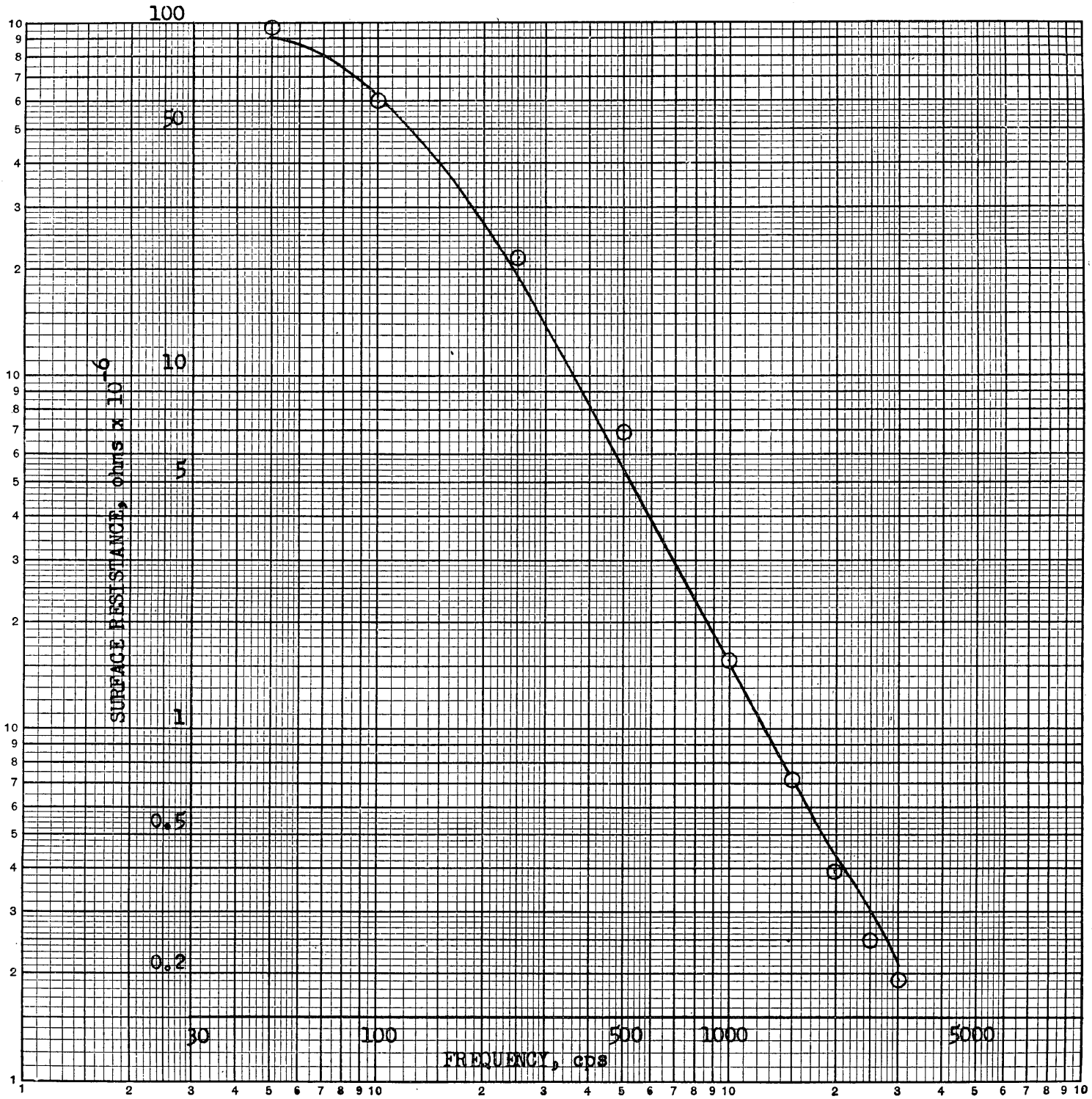

Figure 9-12 CALCULATED AND EXPERIMENTAL SURFACE RESISTANCES FOR 412 gm SLIDER

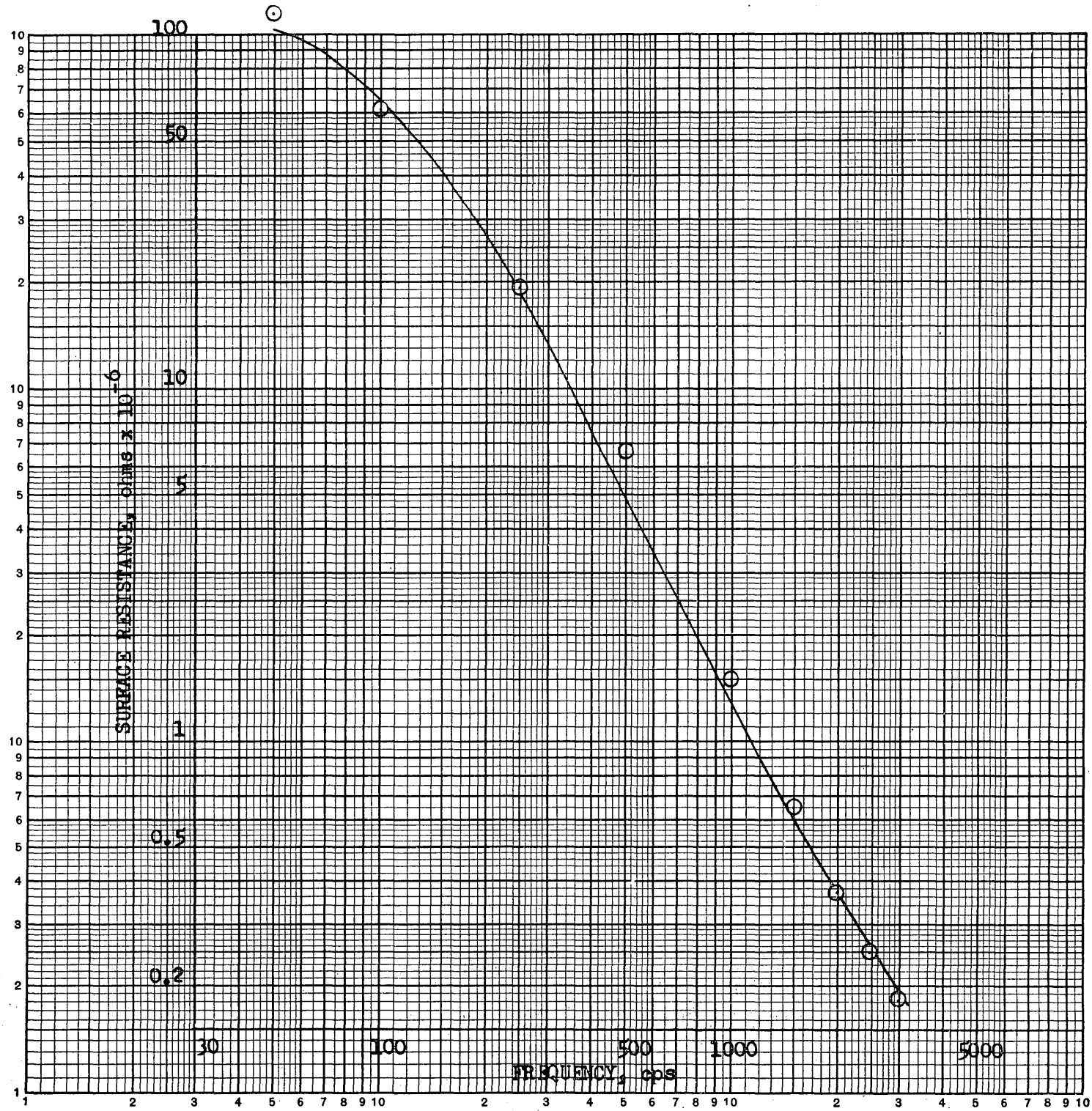

Figure 9-13 CALCULATED AND EXPERIMENTAL SURFACE RESISTANCES FOR 810 gm SLIDER

points indicated are the experimental values.

In the construction of the surface resistance, the frequency independent component, R, is caused by a current constriction through contacting asperities between the ice and slider. Equation (9-3) should therefore apply to this resistance.

$$A = \frac{\pi \Lambda^2}{16\, n\lambda^2} \qquad (9\text{-}3)$$

From Table 9-6 the resistances $(1.084 \pm .003) \times 10^8$, $(1.105 \pm .13) \times 10^8$ and $(1.359 \pm .22) \times 10^8$ ohms are obtained for the 214, 412 and 810 gms loads respectively.

Though the indicated errors produce some overlap these resistance values seem to be increasing. Since $\Lambda = 1/R$, Equation (9-3) requires that the number of asperities decrease with increasing load for certainly increasing the load should not reduce the electrical contact area. A decrease in the number of asperities however does not seem possible. Therefore if the indicated increase in constriction resistance is a real one its explanation must await further study. It should be noted that an electrical contact area calculated from Equation (9-3) need not be the only area of direct contact between ice and slider. The film may also be making contact at certain points and hence be a factor in the frictional force without it necessarily being able to pass a free-ion current.

If we take for the free-ion conductivity the value 0.2×10^{-8} $(\text{ohm cm})^{-1}$ obtained from the freezedown slider at 7 cps, and substitute into Equation (9-3), the electrical contact area in terms of asperity number

for the 214, 412, and 810 gm loads becomes $\frac{4.22}{n}$, $\frac{4.02}{n}$, $\frac{2.66}{n}$, cm^2 respectively. For $n = 50$ the areas are .084, .081, and .053 cm^2. For the purpose of examining the order of magnitude these contact area values give for the coefficient of friction we utilize the formula:

$$F = s A_r = \mu N \tag{9-20}$$

Solving for the coefficient μ we have:

$$\mu = \frac{s A_r}{N} \tag{9-21}$$

where s is the shear strength of ice, A_r the electrical contact area, and N the load. Substituting the shear strength 7040 gm/cm^2 reported in Chapter I, the values of the coefficient of friction for the brass slider for loads of 214, 412 and 810 gms. are 2.8, 1.4, and .4 respectively. This variation in the coefficient is not supported by experimental friction force measurements, and except for the last value, they are too large. No purpose would be served at the present time to correlate these values of the coefficient obtained electrically with friction force measurements until further electrical measurements can be made.

The last piece of information supplied by the surface resistance construction concerns the thickness of the surface film. The value of k from Table 9-6 supplies this information through Equation (9-14)

$$k = \frac{(e_1 - e_o)\, p\, A}{1.8 \times 10^{12}\, L} \tag{9-14}$$

Substituting for the dielectric constant e_1 and e_o, 3 and 2 respectively, for the cross-sectional area 4 cm^2, and for p, 2×10^{-4} the thickness can be calculated. For the 214, 412, and 810 gm slider this yields a surface film thickness of 13, 7, and 6 microns respectively. These values are smaller than the film thickness estimated from the

surface capacitance but are still somewhat larger than Weyl's estimate of the thickness of the transition layer that forms on an ice surface.

EXPERIMENT III

Introduction

Experiment III was set up to resolve further the cause of the permanent deformation phenomenon discussed on page 237. The point was raised that perhaps a time factor was responsible for the permanent structure of the ice-slider and surface and that this caused the surface resistance measurements to remain constant as the loads were successively reduced. Six to seven hours of ice-slider contact has elapsed before decreasing loads were applied. In the experiment to be described, this time interval was reduced to one hour to see if the phenomenon was still present.

Procedure

Bulk capacitor (not surface) resistance measurements were made on 1, 4, and 16 cm^2 steel sliders in the frequency range 50-40,000 cps. for each loading condition. Ice temperatures were maintained at -10.5°C. for all sliders and the thickness of the dielectric was .485 cm, .502cm., and .456cm. respectively, for the 1, 4, and 16 cm^2 sliders.

The sliders were loaded in seccessive order as follows:

	Slider	Load in gms		
1.	4 cm^2	200	800	200
2.	1 cm^2	200	50	
3.	16 cm^2	200	800	200

It took 45 min. to sweep over the entire frequency range at each load. When load changes were made, the ice slider contact was not disturbed. The ice surface was freshly prepared and honed prior to the

measurements on each slider.

Results

Three alternate hypotheses regarding the cause of the apparent stability of the ice-slider contact with decreasing loads were constructed to be tested by the results.

The hypotheses and their expected results are:

A. Permanent deformation with loading does not occur, and aging of the ice slider contact resulting in stability of the contact with decreasing loads does not take place after one hour of contact.

Expected Results

1. Capacitor resistances of the 4 cm^2 condenser decreases when the load is changed from 200 to 800 gms.

2. The resistance of the 1 cm^2 condenser increases when the load is changed from 200 to 50 gms.

B. Permanent deformation with loading does not occur, and aging resulting in stability of contact occurs after two hours of contact.

Expected Results

1. Same as A - 1

2. Same as A - 2

3. The resistance of the 4 cm^2 condenser when the load is changed from 800 to 200 gms does not change.

C. Permanent deformation with loading and/or one hour aging of the contact resulting in stability of contact with decreasing loads occurs.

Expected Results

1. The resistance of the 4 cm^2 capacitor decreases when the load is changed from 200 to 800 gms.

2. The resistance of the 1 cm^2 condenser remains constant when

the load is changed from 200 to 50 gms.

The data for the 1 and 4 cm^2 condensers are given in Table 9-8, and 9-9 respectively. The data for the 16 cm^2 condenser is not included. The resistance trends exhibited by this slider are similar to that of the 4 cm^2 slider and add no additional information.

Figures 9-14 and 9-15 graphically represent this data and are clearly consistent with the expected results of Hypothesis C.

Table 9-8

The Resistance of the 1 cm^2 Condenser

f \ Load	200 gms.	50 gms.
50	5.731×10^6	5.700×10^6
100	4.828	4.831
200	3.965	3.945
500	2.750	2.753
1 000	1.827	1.801
2 000	1.090	1.062
5 000	6.146×10^5	6.102×10^5
10 000	5.761	5.799
20 000	5.500	5.500

All resistances are in ohms.

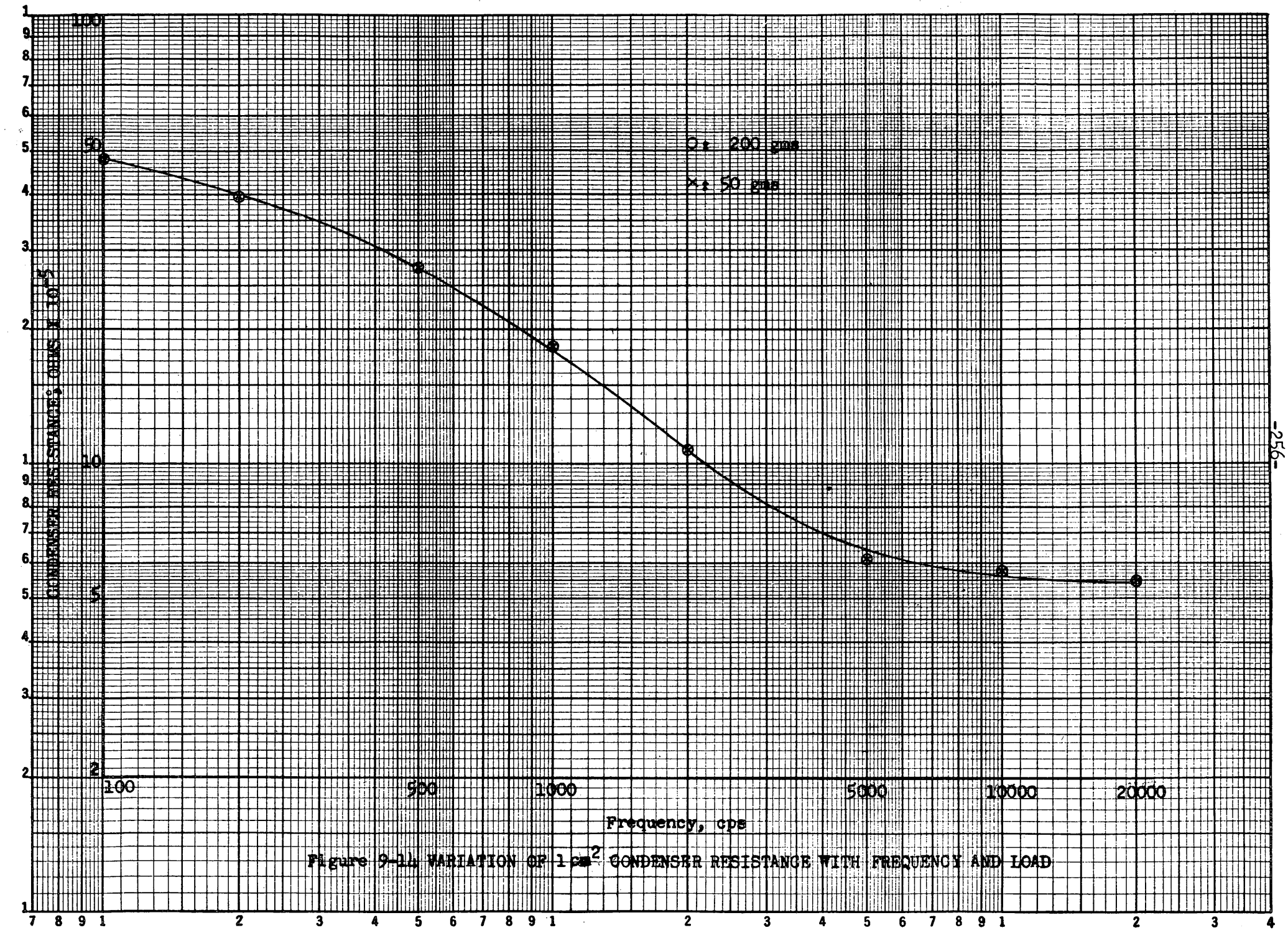

Figure 9-14 VARIATION OF 1 cm^2 CONDENSER RESISTANCE WITH FREQUENCY AND LOAD

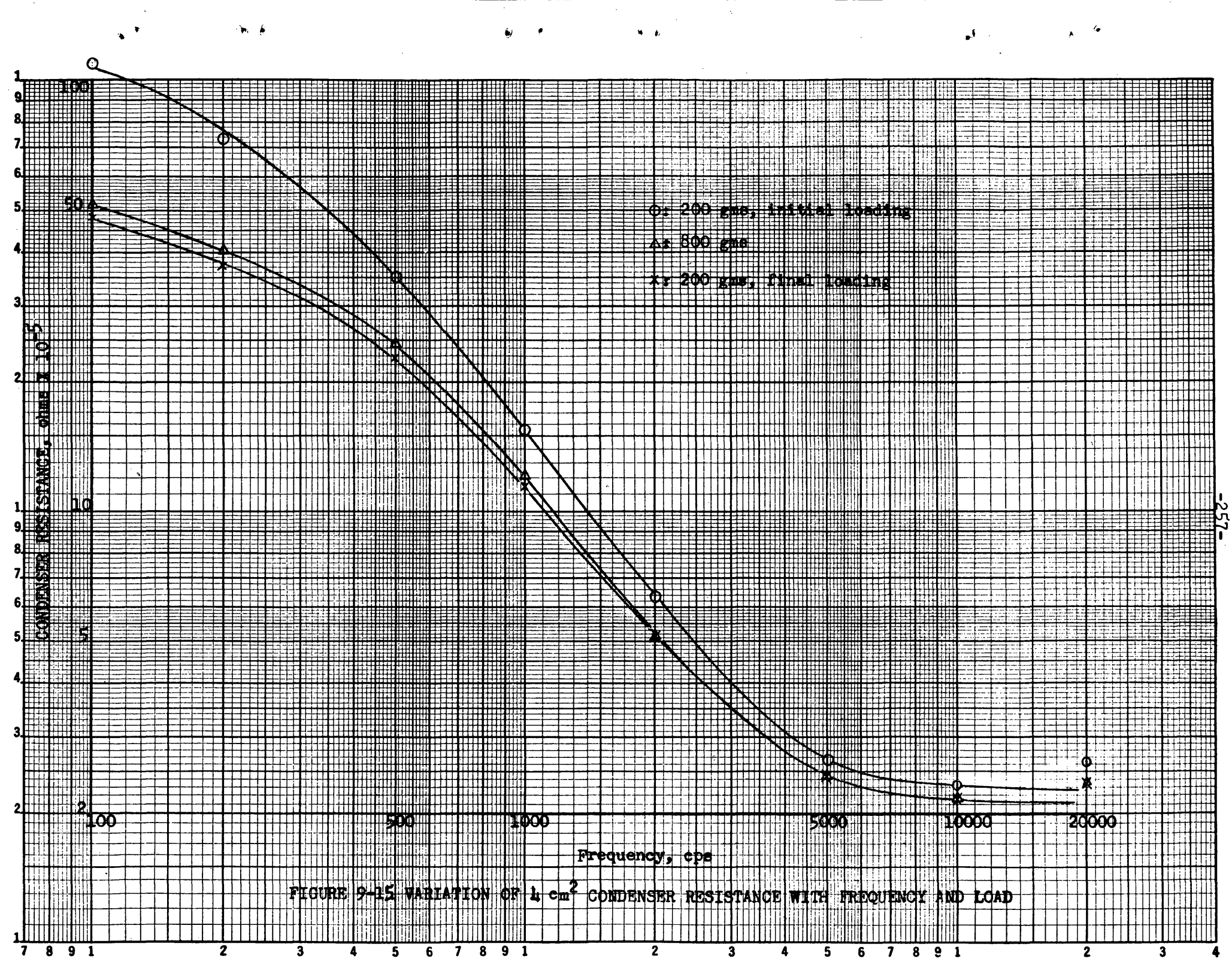

FIGURE 9-15 VARIATION OF 4 cm^2 CONDENSER RESISTANCE WITH FREQUENCY AND LOAD

Table 9-9

The Resistance of the 4 cm^2 Condenser

f \ Load	200 gms	800 gms	200 gms
50	16.04×10^6	6.412×10^6	5.971×10^6
100	11.26	5.194	4.810
200	7.319	4.037	3.717
500	3.554	2.445	2.285
1 000	1.557	1.215	1.158
2 000	6.383×10^5	5.164×10^5	5.128×10^5
5 000	2.675	2.473	2.435
10 000	2.322	2.184	2.173
20 000	2.661	2.356	2.378
40 000	3.150	-----	3.582
50 000	-----	3.150	-----

All Resistances are in ohms.

Experiment III, therefore does not completely resolve the question. We can, at most, say that permanent deformation with loading and/or one hours aging of the ice-slider contact is responsible for the constancy of the contact when subject to decreasing loads.

In the course of the work with the steel sliders, attempts to secure freezedown by touching a soldering iron to the sliders were not successful. In future work a better method to obliterate surface phenomena is needed. Growing the ice such that intimate contact with the condenser plates is secured during the freezing process should be accomplished.

Experiment IV

Introduction

Experiment IV was directed at studying whether the apparent constancy of the ice-slider contact in the face of decreasing loads could be demonstrated by friction force measurements. The concept of slider load was altered to faciliate this study. The terms resting load, normal load, and resting time were introduced to adequately define the condition of an ice-slider contact prior to the determination of the static friction force. Resting time is the length of time the slider is in contact with the ice surface prior to the measurement of the friction force. Resting load is the load on the slider during the resting time period. Normal load is the load on the slider at the instant the friction force measurement is made. Normal load, therefore, need not necessarily equal resting load. In this experiment, friction force measurements were made on two brass sliders of 4 and 16 cm^2 area with resting loads greater than or equal to normal loads.

Procedure

The Linear Path Friction Force Dynammometer was used to measure static friction force. The 4 and 16 cm^2 sliders were subject to the same normal and resting load conditions. The resting time in all cases was one minute. In situations where the resting load was greater than the normal load, the excess load was removed seconds prior to the force measurement. When this was done the ice-slider contact was not disturbed. At each load condition ten measurements were made and averaged and the average mean deviation computed. The results are tabulated in Table 9-10 and plotted in Figures 9-16 and 9-17. The figures indicate that the load history of the ice-slider contact may influence the friction force. Specifically permanent deformation with

TABLE 9-10

STATIC FRICTION FORCE

MEASUREMENTS FOR A RESTING TIME OF ONE MINUTE

(a) Area = 4 cm^2 brass

Resting Load (gms)	Friction Load (gms)	Friction Force (gmf)
80	80	22 ± 8
160	80	19 ± 9
320	80	44 ± 18
640	80	43 ± 16
160	160	36 ± 16
640	640	99 ± 25

(b) Area = 16 cm^2 brass

80	80	23 ± 7
160	80	26 ± 9
320	80	42 ± 29
640	80	42 ± 29
160	160	50 ± 11
320	320	81 ± 21
640	640	240 ± 17

FIGURE 9-16

VARIATION OF STATIC FRICTION FORCE WITH RESTING LOAD FOR 4 cm^2 BRASS SLIDER.

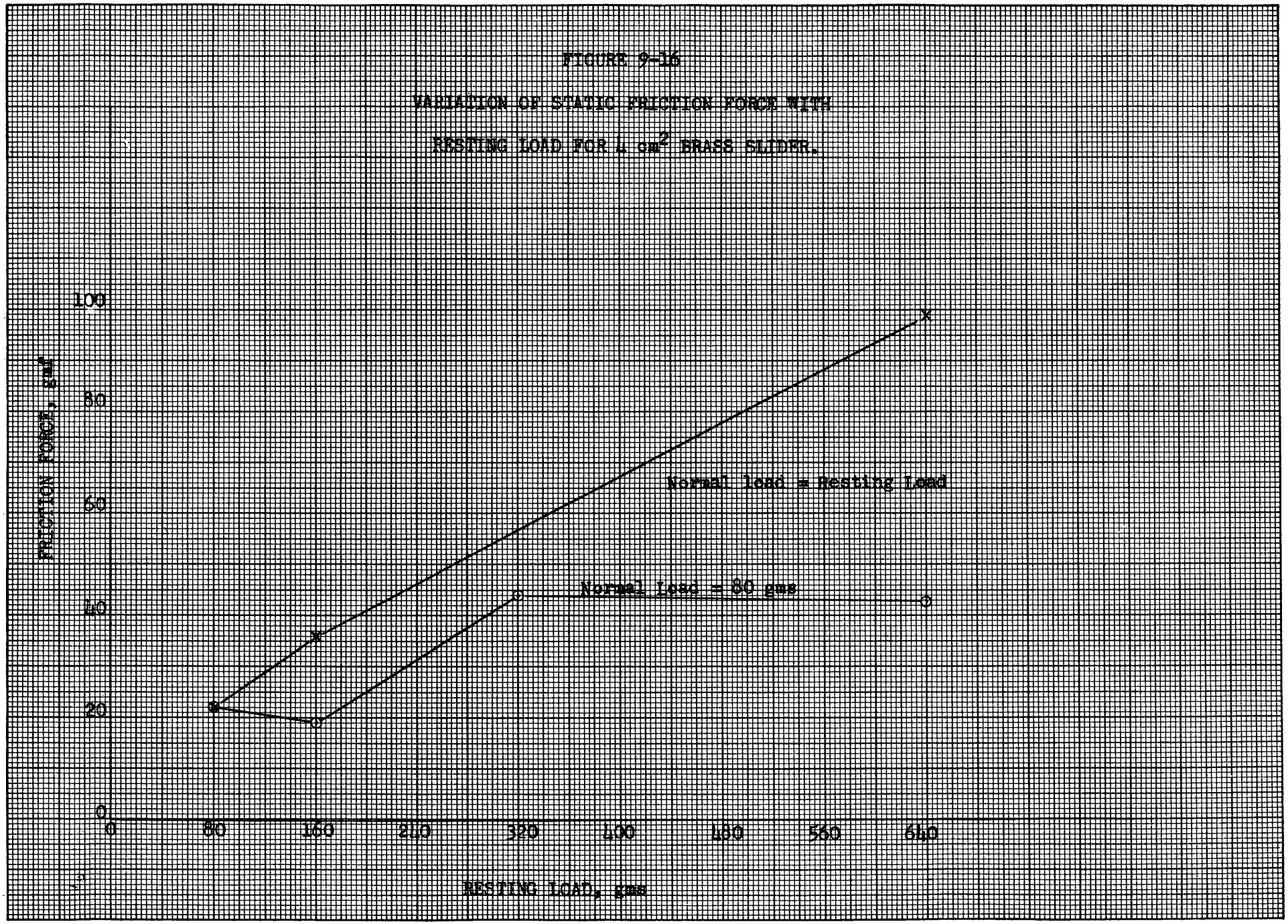

FIGURE 9-17

VARIATION OF STATIC FRICTION FORCE WITH RESTING LOAD FOR 16 cm^2 BRASS SLIDER.

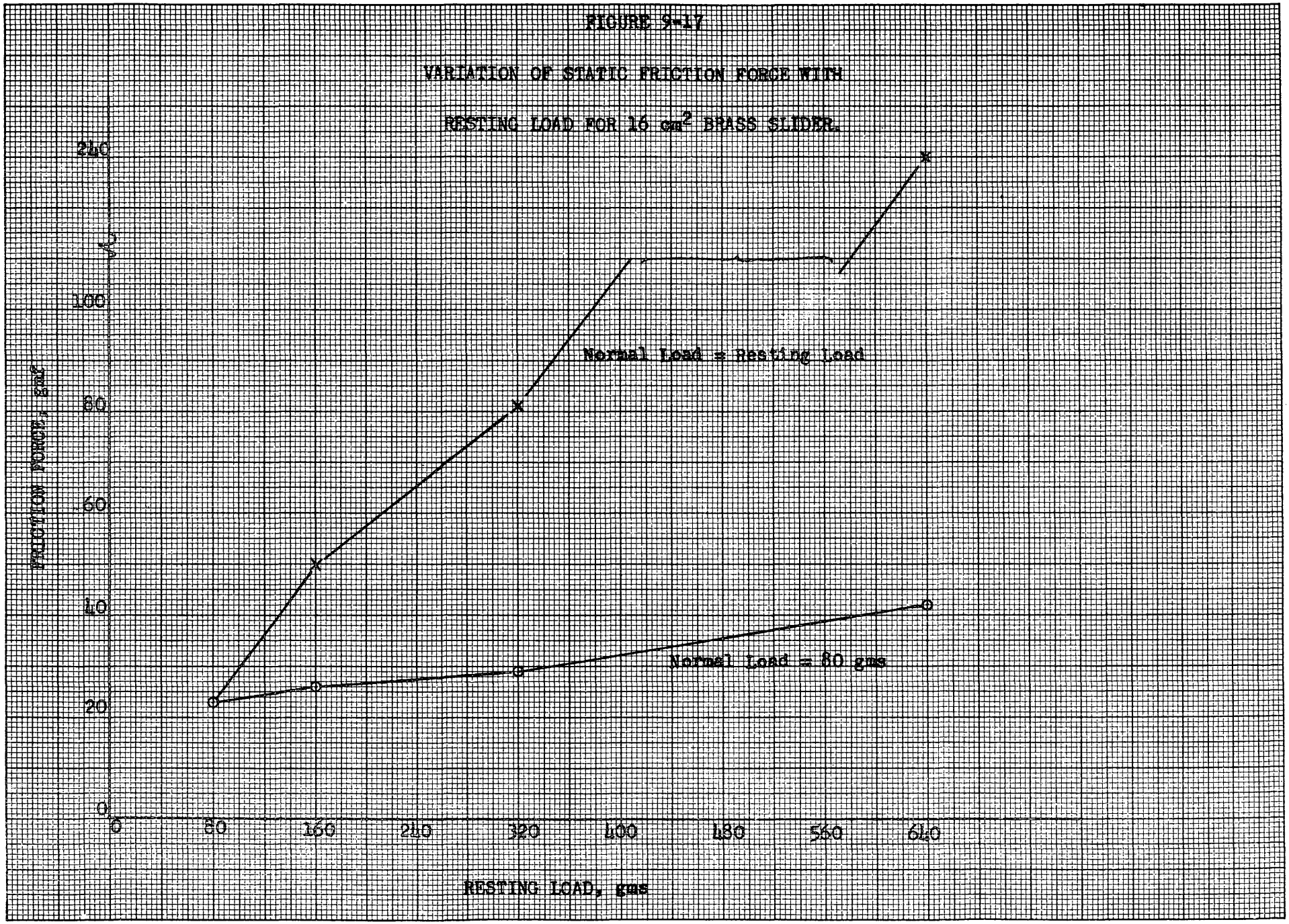

loading appears to occur although some recovery of the surface does take place when the load is reduced. If no recovery took place, the two curves in Figure 9-16 and 9-17 would coincide.

The rather large mean deviation error in the friction force causes overlap which tend to weaken the validity of these conclusions. The introduction of resting load as a variable for statistical analysis to determine whether it is significantly related to the coefficient of friction is easily performed. Future statistical analyses of variance should include resting loads as a variable.

Conclusions

The analysis of the experiments reported here raises several questions which have not been resolved. Nevertheless several important conclusions on the character of the ice-metal slider interface may be made.

1. A definite surface capacitance and surface resistance exists.
2. The surface resistance may be adequately represented by two resistances in parallel, one frequency and load independent and the other frequency and load dependent.
3. Interpretation of the surface resistance as a constriction.
4. The surface from an electrical point of view undergoes permanent deformation with increasing loads. Increasing loads and/or a one-hour aging of an ice-slider contact results in a stability of the contact that is unaltered by decreased loads.
5. The presence of a surface film is indicated.
6. If the resting load (load on slider prior to a friction force measurement) is greater than the normal load (load on slider at

measurement), the measured coefficient of friction is larger than if the resting load equals the normal load.

7. The number of asperities in electrical contact for the sliders investigated have an order of magnitude of 50.

CHAPTER X

RADIOACTIVE TRACER INVESTIGATION OF SURFACE MOVEMENT

CHAPTER X

Radioactive Tracer Investigation of Surface Movement

The discovery and the current availability of radioactive isotope tracers has placed in the investigators' hands a tool for marking and detecting minute quantities of material. This method is outstanding for its sensitivity and its flexibility. This technique is particularly adaptable to the study of such frictional phenomena as the transfer of material between sliding surfaces, and the smearing of material on these surfaces.

As early as 1944 Sakmann, Burwell, and Irvine[1] reported on the investigation of material transfer from a copper beryllium base onto sliders made of various materials to be tested. The copper beryllium used in the base was made radioactive by deuteron bombardment in a cyclotron, and the amount of material picked up by the sliders determined by standard radioactivity detecting instruments.

Subsequent investigators employed a similar technique, but made the sliders radioactive, instead of the base[2-6]. Such investigations were

---

[1] Sakmann, B. W., J. T. Burwell, and J. W. Irvine, (1949) "Measurements of the Adhesion Components in Friction by Means of Radioactive Indicators." Journal of Applied Physics, Vol. 15, pp. 459.

[2] Gregory, J. N. (1946) "Radioactive Tracers in the Study of Friction and Lubrication." Nature, Vol. 157, pp. 443-444.

[3] Rabinowicz, E. and D. Tabor, (1951) "Metallic Transfer between Sliding Metals; an Autoradiographic Study." Vol. A 208, pp. 455-475.

[4] Rabinowicz, E. (1951) "A Study of Metal Transfer During Sliding, Using Radioactive Analysis," Physical Society Proceedings, Vol. 64A, pp. 930-940.

[5] Burwell, J. T. "Radioactive Tracers in Friction Studies." Nucleonics Vol. 1, No. 4, pp. 38-50.

[6] Burwell, J. T. and S. F. Murray (1950) "Radiochromium Plating for Friction Studies," Nucleonics, Vol. 6, No. 1, pp. 34-38.

concerned almost exclusively, however, with the friction of metals.

The purpose of the radioactive tracer studies, in connection with friction on compacted snow, was the examination of two phenomenon. The first phenomenon was the material transfer from the ice surface to the slider, and the second was the material movement on the surface itself. In experiments with metals it has been found that, in the case of a hard material sliding over a softer material, the hard material will pick up a considerable amount of the latter. In addition, the hard slider will disturb the surface of the softer material by moving portions of the surface to a different location. This disturbance is generally termed "scatter." In the current investigation a metal slider was moved over the ice surface. This is a case of a hard material sliding on a soft material. Both "pickup", by the metal slider, and scatter, on the surface, can be expected to take place in this experiment.

To determine the transfer and scatter, experiments were planned in which radioactive material was to be deposited on the ice surface. Sliders were to be drawn over the surface and the effects on the resulting location of the radioactive material determined by autoradiographic and counter techniques.

Several methods were investigated for deposition of the radioactive material upon the ice surface. Among the methods tried were various techniques for grooving or cutting the ice surface by thermal and mechanical means. It was hoped, for example, that a high resistance electrical wire, previously dipped in a radioisotope solution, could be heated by

electrical power to melt a groove and to plant the tracers. This method proved to be unsatisfactory, however, since the water formed has a tendency to run over the edges of the groove and produce an irregularity in the ice surface.

Mechanical cutting of a slot was tried in which a 1/16 inch thick milling cutter was fastened to a 1/4 inch portable electric drill and a groove machined in the ice. A solution containing radioactive material was then deposited in the groove by a pipette. This method proved to produce a good, smooth groove although the problem of smoothing the frozen solution so that it formed a continuous surface with the rest of the ice was not overcome. Due to this difficulty and due to ill-defined autororadiographs, this method of depositing the radioactive material was discarded.

It was finally decided that the most feasible method for deposition of the radioactive material would consist of painting a thin film of a liquid solution of the material on the ice surface. Admittedly this method produces a slight discontinuity on the ice surface, but this irregularity would actually be less than was encountered by the other methods. In the method adopted, a few drops of radioactive solution is deposited on a small paint brush and the brush passed transversely over the ice surface. A smooth line about 3/8 inches wide is formed. Judging from the autoradiographs taken of this line, the radioactive material has been distributed quite evenly in the line.

Another advantage of the painted stripe technique is the increased clarity of the resulting autoradiographs. Since the radioisotope emits

its rays in all directions, a film held at a distance from a distributed region of the radioactive material will detect rays coming from a number of angles. This results in a diffused and ill defined region of blackening on the film. If the film is held close to the radioactive source and if the region of activity is confined to a thin layer, the space angle through which the emitted rays are detected is more restricted and the autoradiographs much better defined.

In the early experiments on this problem, Ca^{45} was used as the tracer. This isotope of calcium has a half life of 180 days; it emits only beta particles, the energy of these particles being in the range of .25 Mev. This is strong enough for detection, even in very dilute solution, and yet weak enough so as not to be too hazardous in handling. Moreover, the isotope is in chloride form which is readily soluble in water. It has a specific activity ranging between 0.2 and 0.4 millicurie per gram; it comes in acid solution of concentration no smaller than 0.01 millicurie per cc, with acidity not exceeding 0.5 N hydrochloric acid. One cc of the original solution was diluted with water to 1000 cc. The resulting solution had a specific activity of no less than 0.01 microcurie per cc, which was readily detectable by a Geiger counter. Initial experiments using the Geiger counter method were not too satisfactory, however, since the region of activity could not be defined closely. Several attempts at obtaining autoradiographs proved futile. At the time it was believed that the energy of the emitted beta-rays (.2 Mev) was too low to blacken the x-ray film.

Due to the low energy of the beta-rays (and conversely their short range) emitted by Ca^{45} and because of the short half-life of this material,

it was decided to procure Co^{60} for tracer material. Co^{60} has a half-life of 5.3 years; emits beta-rays with an energy of .31 Mev and two monochromatic gamma-rays with energies of 1.17 and 1.33 Mev respectively. The gamma-rays have too high an energy level to blacken a photographic film perceptibly, but the beta-rays have energies high enough to give good autoradiographs. The long half-life of Co^{60} (5.3 years) permits the use of a more flexible experimental program.

One millicurrie of Co^{60} was ordered and received from Oak Ridge National Laboratories. The active material was in the form of 0.34 N $CoCl_2$. This solution was mixed with distilled water to give 10 cc of solution with a concentration of 0.1 mc/cc. This solution was not used directly as a tracer solution, but parts of it could be mixed with distilled water to form a solution of any desired concentration. The solution adopted as a tracer has a concentration of 2 microcurries/cc. This was found to produce satisfactory autoradiographs.

The application of the radioactive tracer technique in any particular procedure greatly complicates matters. The necessity for protection against radiation hazards creates a problem out of what would otherwise be a very simple and normal process. Each step requires specific consideration, and sometimes great difficulties must be overcome to insure both accurate and safe operation. Once a substance has been made radioactive all operations must be by remote handling; contaminated instruments must be segregated and handled with care until they have become decontaminated either through time or washing; containers for radioactive materials must be shielded with lead, and all wastes

must be safely stored until the activity is sufficiently low so as to allow their safe disposal, preferably by burial in the ground in some remote spot.

With the above considerations in view, a remote pipetting device was constructed for diluting the original radioisotope solution. (Figure 10-1.) A lead shield was arranged on a stainless steel covered table and a mirror adjusted to enable visual examination of the region behind the shield. (Figure 10-2) With these protective measures the various tracer manipulations could be accomplished with minimum hazard to personnel.

The actual scattering experiments and exposure of the x-ray film for the desired autoradiograph were to be accomplished in a deep-freeze. To prevent contamination of the freezer and to provide personnel protection during scattering experiments, a lead box (Figure 10-3) was fitted inside the freezer.

Unused tracer solutions were stored in a lead covered cabinet and the wastes in a ten-gallon stainless steel milk can wrapped in lead sheeting.

The operations were carefully rehearsed beforehand, using fluorescene dye to simulate radioactive tracers, so as to insure maximum efficiency and safety in technique. Finally, in compliance with federal and local safety requirements, a careful survey of existing facilities was made, so as to procure a location adequate in ventilation, cleaning facilities, sink, running water, and electric power. Protective clothing such as laboratory aprons, gloves and foot-

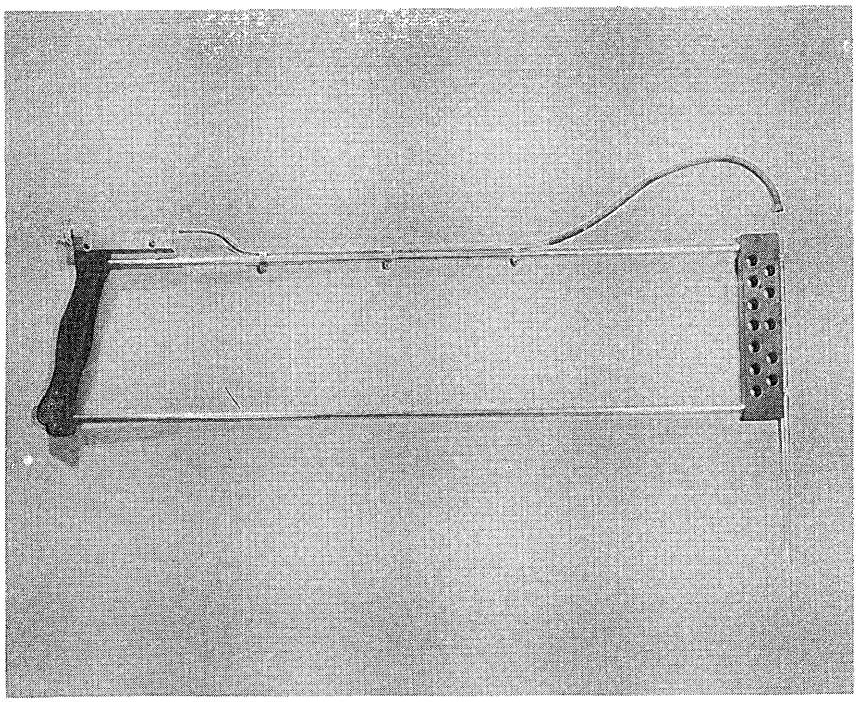

Fig. 10-1 Remote Pipetting Device

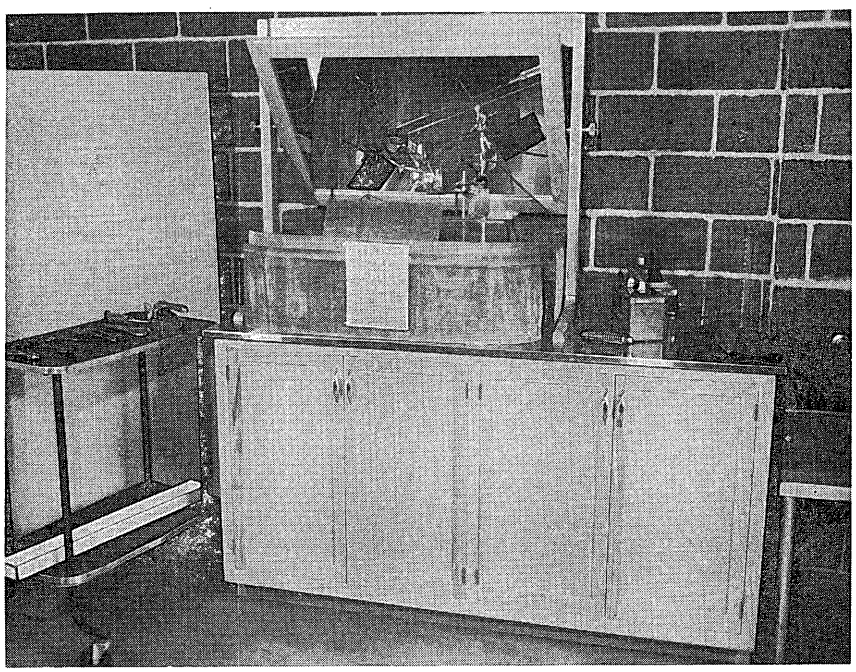

Fig. 10-2 Radioactive Laboratory

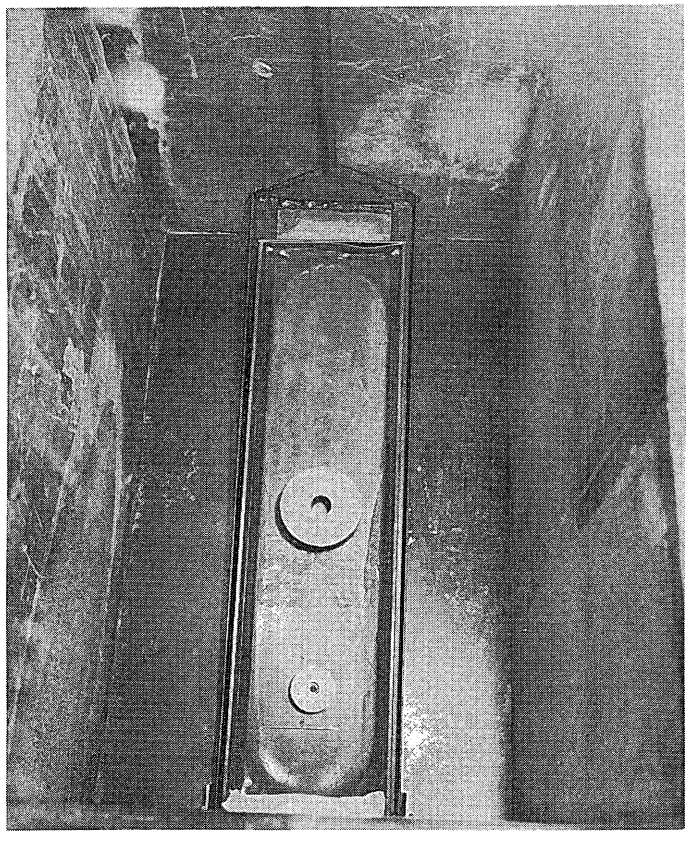

Fig. 10-3

Tilting Apparatus

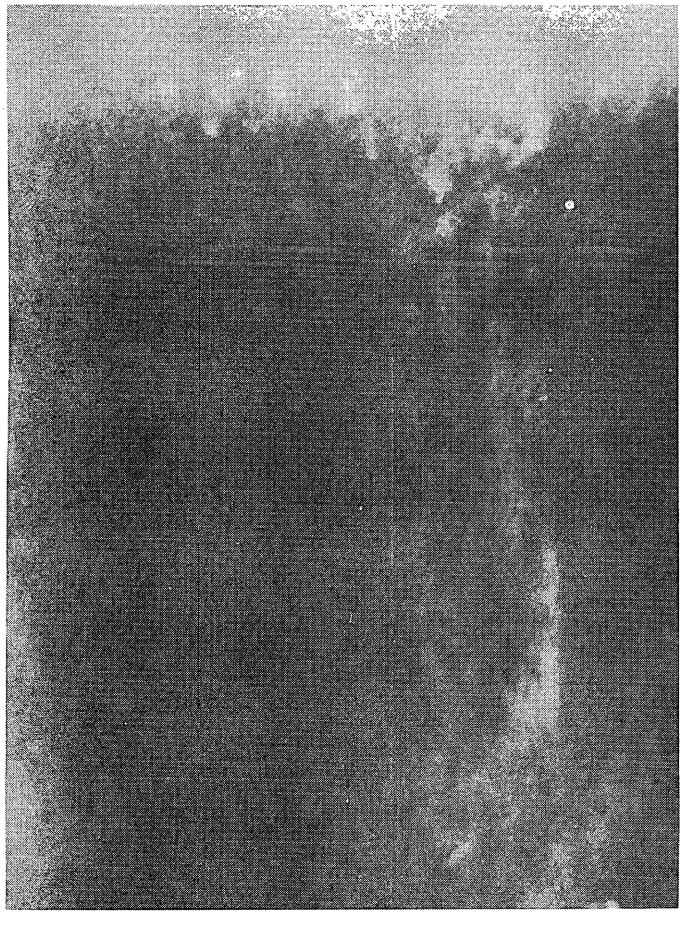

Fig. 10-4

Autoradiograph resulting from passage of loaded steel slider over radioactive stripe.

wear, was also procured, chiefly to guard handlers from internal hazards of radiation.

A series of scattering experiments was made using a tilting table apparatus to initiate slider motion. One end of the tilting table, shown within the lead box in Figure 10-3, was pivoted on a hinge while the other end was lifted by a leather cord. A tray of ice with a radioactive stripe and a test slider placed above the stripe was placed in the tilting table. The table was then lifted until the slider broke away and slipped down over the tracer stripe. Knowing the dimensions of the tray and distance the cord has been raised, it was possible to compute the angle of inclination at the instant of breaking and therefore the static coefficient of friction.

Autoradiographs taken before and after the sliding event indicates the transfer of radioactive material and the resulting scattering.

Despite close examination of the autoradiographs obtained in this manner no material transfer could be detected.

In the above tests however only a single trip was made over the test stripe for each test.

It was next suggested that perhaps passing the slider a number of times over the same path might cause enough material transfer to be detectable. Since the slider moving under the action of gravity down the tilted surface does not necessarily take the same path, it was considered advisable to change the driving method. For this reason and to obtain a remote method for handling the contaminated slider, the linear path frictional force apparatus was utilized for the second series of scattering tests.

The procedure followed in the second series of scattering experiments was as follows:

1. Ice was frozen in a steel tray having the same cross section size and shape as the trays utilized in the regular friction force experiments.
2. The ice surface was machined and honed using the linear path surface machining equipment.
3. A stripe of radioactive material was painted on the surface of the ice.
4. X-ray film was exposed over the ice to determine the initial condition of the radioactive surface.
5. A test slider was drawn over the ice surface using the linear path friction force apparatus. The frictional force was measured simultaneously.
6. After the slider had moved several inches beyond the radioactive stripe, the slider was lifted from the ice surface using the remotely controlled lifting mechanism. The entire apparatus was then returned to the initial position and replaced on the ice.
7. The test slider was drawn in this manner over the ice surface for a total of 15 times.
8. The slider was then removed and x-ray film again exposed to determine the final condition of the radioactive surface.

Figure 10-4 illustrates the final condition autoradiograph resulting from the passage of a steel slider over an ice surface in the manner described above. The spots in a horizontal stripe near the upper part of the picture were caused by the radioactive material remaining in the primary stripe. The spots appearing below this stripe region were undoubtedly caused by material transferred or "scattered" by the steel slider.

It was noted in the course of the "scattering" experiments that scatter could be detected only at temperatures relatively high in comparison with the melting point. At ambient temperatures of 15° F. and below no material transfer could be found.

Another interesting result noted was the relation of the transferred material to the "stick slip" motion of the slide apparatus If the slider came to rest or "stuck" in the region of the stripe, considerable more material was transferred than if the slider passed over the stripe during the "slip" portion of its motion. It was also noted that the scattered material appeared to be deposited chiefly in regions where the slider had been "sticking."

Thus through radioactive experimentation it was established that the ice surface material is actually transferred or scattered during the frictional process. This transfer appeared to occur more readily at higher temperatures. It may also be concluded that a greater amount of transfer may be expected as a result of static friction or adhesion than through kinetic friction.

CHAPTER XI

SUMMARY

CHAPTER XI

Summary

A study was made of the several proposed mechanisms of frictional resistance and the relation of these resistances to the physical properties of the stationary surfaces and the sliders. The influence of the apparatus components and atmospheric conditions upon frictional characteristics was also investigated. Experimental data on the frictional resistance to motion over ice and snow presented by previous investigators as well as the data collected in this project were analyzed in terms of the studied mechanisms and properties.

It was concluded that the resistance to motion over compacted snow and ice is principally a dry friction phenomenon relieved slightly by the presence of a film on the surface. A total frictional resistance composed of the resistance of the surface film in series and in parallel with the resistance created by direct adhesion bonds between the slider and the internal structure appears to best agree with the known experimental facts.

If the snow is capable of further compaction an additional force in the form of a plowing resistance is present.

The amount of internal structure resistance or direct adhesive bonds and the amount of film resistance appears to be dependent upon the time of contact. Thus for very short contact periods such as a slider in continuous motion, the internal structure resistance is negligible and the entire resistance is due to the surface film. The kinetic friction would in this case equal the film resistance. For slightly longer periods of stationary contact, some bonds are formed with the internal structure and the surface

film. Static friction applies to this case. For very long periods of contact time the internal structure bonds increase to a maximum or the film solidifies to form a considerable resistance to motion such as is present under "freezedown" conditions.

Several mechanisms for the production of the surface films on ice have been proposed. These hypothesized mechanisms include (1) Pressure Melting, (2) Frictional Heating, (3) Adsorbed Water Vapor, and (4) Electrical Dipole. Of these four mechanisms, the Frictional Heating and the Electrical Dipole Theories merit special attention since these best correspond to experimental observations. Neither of these theories, however, fully explain all frictional phenomenon on ice and snow.

Consideration has also been given to the mechanical and electrical properties of the surface film. Since the kinetic friction does not display a strong velocity dependence it may be concluded that the film is not viscous in nature. However, since the kinetic friction appears to be a function of the temperature, the slider material, and the area of contact, the surface film is probably related to these parameters.

The principal features of Weyl's Dipole Theory and the application of this theory to friction on ice are outlined in an appendix of this report.

A theoretical analysis has been made of the area of real contact between two rough surfaced bodies. From this analysis it is concluded that under a low ratio of the loading to the mean flow pressure the real area of multiple contact between bodies either elastic or plastic in nature is directly proportional to the first power of the normal applied load. Under this same loading condition it may also be concluded that the real area of contact is independent of the apparent area. However at higher

ratios of the loading to the mean flow pressure, the real area of contact no longer increases linearly with the load but asymptotically approaches the value of the apparent area as a limit.

An analysis was made of the theoretical motion of a sliding block drawn over a stationary plane by a flexible member attached to a moving frame. It was shown that for certain assumed friction functions the resulting motion of the slider is an oscillatory motion made up of sudden forward jerks followed by periods of rest. Methods for the determination of the motion characteristics and the constants of the assumed friction functions from experimental position-time traces of sliders drawn over a stationary base were developed.

Apparatus of the stick-slip variety was constructed for the measurement of the frictional forces between a slider and base as the slider is drawn in a linear path or a cylindrical path. These frictional force dynamometers were enclosed within a humidity chamber which in turn was located within a temperature controlled room. Methods for the remote operation and control of the carriage and slider position and velocity as well as for the recording of the slider position, frictional force, velocity, temperature and other variables were provided.

Experimental data on the static friction of sliders on ice and snow under various conditions of load, apparent area, material, temperature, humidity, and time of stationary contact was obtained.

In the first several test series where the actual static force was measured using a spring balance, the individual test measurements were

found to vary considerably. In order to standardize the time of contact a large number of tests were made in which a known horizontal force was suddenly applied upon a slider after a specific time of stationary contact. The percentage of pullaways at this applied force was counted. In this way the cumulative curve of percentage pullaways versus applied load was determined. From this cumulative curve it was ascertained that the static friction force at a particular setting has a normal distribution around a mean value.

In later test series the influences of several variables were examined by holding all parameters constant except the one under investigation. Tests were made in this manner upon the influence of load, area, velocity, material, and temperature. The resulting data indicated the following trends:

1. Variation with load from 40 grams to 960 grams on 4cm^2 sliders did not appear appreciable.
2. In the load variation tests the phenolic resin (English) bakelite had the highest static coefficient of friction followed in turn by magnesium, brass and steel, with hickory having the lowest coefficient.
3. A decrease in the temperature appeared to consistently increase the static friction force of all materials tested.
4. Static friction force increased slightly with an increase in the apparent contact area.
5. It was difficult to judge from actual data whether the static coefficient at a particular pressure was constant under various combinations of load and apparent area of contact.

6. The kinetic coefficient of friction was lower than the static coefficient and appeared to remain constant over the range of velocities examined.

To provide a better comparism of the influence of the individual parameters and to provide a numerical basis for judging these influences, the later frictional measurements were performed using the statistical methods of the Theory of Variance. Results of these test series may be summarized as follows:

1. Without humidity control and at 15° F sliders of various materials, areas, and loadings were tested for static friction on machined ice. It was found that:

(a) Area variations were the most significant variables.

(b) Material variations were mildly significant.

(c) Sliders of the same material, area, and loading produced essentially the same effect.

2. Without humidity control and at various temperatures, sliders of various materials and areas were tested with constant loading on machined ice. It was found that:

(a) Temperature variations have the greatest effect on the static coefficient of friction.

(b) Area has a large effect but less than that of temperature.

(c) Choice of material has a significant effect but less than that of area.

3. With humidity control at constant temperature (15° F), sliders of various materials, areas, and loadings were tested on compacted snow. None

of the controlled variables were found to be significant with respect to random effects.

4. With humidity control at constant temperature (15° F), sliders of various materials, areas, and loadings were tested on machined ice. It was found that:

(a) Contrary to the results obtained in (1), loading had the greatest effect on the static coefficient of friction.

(b) Area had the next greatest effect.

(c) Material had a significant effect.

An investigation of the frictional characteristics on ice was also made based on the analysis of the intermittent "stick-slip" motion of the sliders. From this analysis the following conclusions were drawn:

1. The oscillatory motion observed compares very closely with the theoretical motion of a sliding body resisted by a high static friction and a lower constant kinetic or Coulomb friction.

2. In the cases in which the kinetic friction is affected by velocity, the damping constant of the velocity dependent term appears to have negative value.

3. There is a decrease in static and kinetic friction between most materials and ice with an increase in temperature from - 45° F and - 30° F to + 15° F. Hickory, however, indicated an increase in friction with an increase in temperature from - 30° F to + 15° F.

4. There is a decrease in the static friction of materials on ice with a decrease in the time of stationary contact.

5. Magnesium and hickory had the highest static friction and the greatest difference between static and kinetic friction of the five materials tested.

6. Brass had the lowest kinetic resistance followed in order by the phenolic resin bakelite, steel, hickory, and magnesium.

7. The surface film on the ice does not act as a viscous substance under the contact region of the studied bodies.

8. Apparent area of contact is a significant factor for both static and kinetic friction under high humidity conditions.

9. For low humidity conditions the carriage velocity has a significant influence upon the static friction (due to time of contact) and little influence upon the kinetic friction. For high humidity conditions the opposite appears true, i.e. little effect on static friction while a significant influence upon the kinetic friction on ice.

10. Under high humidity conditions load had no significant influence on the static friction as determined by the oscillatory method while load does have a significant influence on the kinetic friction.

11. Several interactions between material, area, and load have a significant effect upon static and kinetic friction on ice.

From the several types of friction-time experiments the following conclusions have been drawn:

1. During the time period following a machining operation on an ice surface the friction force decreases indicating a change in the ice surface. This change may be interpreted as the growth of a surface film.

2. The maximum static friction occurring in the stick portion of the intermittent stick-slip motion decreases with an increase in carriage velocity. This has been explained as due to a decrease in the solid structure bonds with a decrease in the time of stationary contact.

3. The kinetic friction appeared to remain constant over the range of velocities investigated.

4. The double and triple slips detected in the Series Three Kinetic measurements indicate that a finite time is required for the formation of the stationary bonds. Merely bringing a slider momentarily to rest is not sufficient to obtain static friction resistance. In addition it is necessary to have the slider remain at rest for a short period of time.

5. Static friction following long periods of stationary rest rose to very high values. This result might be interpreted in terms of the hypothesized liquidlike film as the solidification of the liquidlike film and formation of strong bonds between the solid surface of the slider and the solid interior of the ice slab.

Measurements were made of the electrical resistance and capacitance between an electrode plate frozen within an ice slab and a metal slider drawn over the ice surface. From these measurements the following conclusions were drawn:

1. A definite surface capacitance and surface resistance exists.

2. The surface resistance may be adequately represented by two resistances in parallel, one frequency and load independent and the other frequency and load dependent.

3. Interpretation of the surface resistance as a constriction.
4. The surface from an electrical point of view undergoes permanent deformation with increasing loads. Increasing loads and/or a one-hour aging of an ice-slider contact results in a stability of the contact that is unaltered by decreased loads.
5. The presence of a surface film is indicated.
6. If the resting load (load on slider prior to a friction force measurement) is greater than the normal load (load on slider at measurement), the measured coefficient of friction is larger than if the resting load equals the normal load.
7. The number of asperities in electrical contact for the sliders investigated have an order of magnitude of 50.

Transfer of the ice surface material during the passage of a slider was investigated using radioactive tracer techniques. In this investigation water carrying radioactive cobalt was painted on the surface of the ice. Sliders were drawn over the radioactive stripes and autoradiographs taken before and after the sliding process.

Scatter or transfer of radioactive material from the original stripe location to a new location was detected. It was noted however that the scattering could be detected only at relatively high temperatures. At ambient temperatures of 15° F and below no material transfer was noted.

It was also noted that greater transfer occurred if the slider came to rest over the stripe than if it were in continuous motion over the stripe. Further the scattered material appeared to be deposited in regions where the

slider had been "sticking" during the "stick-slip" motion. From this it may be concluded that a greater amount of transfer may be expected as a result of static friction than through kinetic friction.

The theoretical and experimental work accomplished to date has indicated the necessity for investigation of the following:

1. Friction Force Measurements on ice
   (a) Upon additional materials chosen to characterize certain physical properties such as:
      (i) Hardness
      (ii) Thermal Conductivity
      (iii) Hydrophobic and hydrophilic tendencies
      (iv) Surface electrical characteristics (permanently charged electrets, etc.)
   (b) To determine the influence of the slider edge including outside perimeter, center grooves, etc.
   (c) To determine the influence of slider rigidity and the relation of apparent area to real area under flexible slider conditions.
   (d) To determine the influence of the following parameters upon the static friction during long stationary time conditions (freezedown).
   (e) To determine the change in the kinetic friction during the period following the initial machining of an ice surface (Aging Experiments) and the influence of chemical additives upon the kinetic friction change. These experiments should provide information on the formation of a surface film.

(f) To determine the effect of electrical or thermal energy addition.

2. Electrical Conductivity Measurements

(a) To resolve the question whether aging and permanent deformation are important in altering the character of the ice slider interface.

(b) To examine the surface electrically under a greater variation of slider material, apparent area of slider, load, ice thickness, and frequency. These measurements are important, for each of these variables will affect the relative contribution of the surface to the resistance and capacitance measurements.

(c) To determine the conductivity of the water from which the ice is obtained.

(d) To determine the influence of additives to the ice on the ice-slider interface.

3. Theoretical study of:

(a) The phenomenon of regelation and the correlation of this phenomena with the surface film characteristics.

(b) The physical properties of shear stress and mean flow pressure of the internal ice, the possible means of measuring these properties or determination from other physical properties, and the influence of these properties upon the coefficient of friction.

(c) The interpretation of the interaction effects indicated by statistical analysis of the friction data.

Appendix A

Historical Development of the Classical Laws of Dry Friction

Leonardo da Vinci (1452-1519) appears to be the first man to have systematically investigated the phenomenon of friction. Friction of bodies in contact he divided into four classes:[1,2] fluid on fluid, solid on solid, solid on fluid, and the motion of a wheel in contact with the ground (rolling friction). Regarding the factors affecting the solid on solid class of friction he appears to be remarkably clear for he writes at various times the following items:[1,3]

1. "The resistance created by friction for the movement of weights is separate and remote from this weight."
2. ". . . which movement becomes more difficult in proportion as the smooth surface becomes more scoured and rough."
3. "The friction made by the same weight will be of equal resistance at the beginning of its movement although the contact may be of different breadths or lengths."
4. "Friction produces double the amount of effort if the weight be doubled."
5. "In friction, every body resists with $\frac{1}{4}$ of its weight, assuming a suitable plane with a polished surface."

---

[1] Leonardo da Vinci. The Notebooks of Leonardo da Vinci, (compiled by E. MacCurdy, Reynal and Hitchcock, New York, 1938).

[2] Allan, R. K. (1946) Rolling Bearings, London: Pitman and Sons, Ltd., p. 6.

[3] Palmer, F. (1949) "What About Friction? Part I. Classical Laws," Amer. J. of Phys., Vol. 17, p. 184.

6. "When the inclination of the polished plane enables the body to act with $\frac{1}{4}$ of its weight in the direction of motion, the body is in itself inclined to move downward."

7. "The very rapid friction of two thick bodies produces fire."

These statements express some of the most basic concepts and experimental relations of friction. It is also interesting to note that the apparatus and methods used by da Vinci to experimentally verify his statements are practically identical to the methods used in our present physics classrooms.

Unfortunately the writings and sketches of da Vinci were unpublished and unknown to his contemporaries. The principles discovered by da Vinci thus remained hidden for several hundred additional years.

Guillaume Amontons, a French engineer, appears to be the second man to have systematically studied the causes and relations of frictional phenomenon. Amontons disclosed his findings to the general public through a paper presented to the Royal Academy of Sciences (Paris) in 1699.[4] For this reason the first two laws of friction are generally called Amontons' laws. The following conclusions were reached by Amontons:

(1) Resistance caused by friction is independent of the apparent area of contact.

---

[4] Amontons, G. (1699) "De la Resistance Causee Dans les Machines," Academie de Sciences, Paris, Historie de l'Academie royale des sciences avec les memoires de mathematique et physique, pp. 257-82.

(2) Resistance caused by friction is proportional to the force with which the upper surface presses against the lower.

(3) The resistive force for different surface materials is approximately 1/3 of the normal force.

It was also noted by Amontons that after greasing surfaces the frictional resistance is independent of the nature of the surfaces. He did not distinguish between static friction and kinetic friction nor did he recognize the significance of the angle of repose.

Practically simultaneous with Amontons, the great German mathematician Gottfried Wilhelm von Leibniz published a treatise on friction in the Proceedings of the Berlin Academy. In this treatise he distinguished between sliding friction and rolling friction.[5]

Antoine Parent[6] in 1704 rediscovered the angle of repose.

Leonard Euler[7] in 1748 further discussed the angle of repose, the dependence of friction upon load, and the independence of friction from the shape or extent of surfaces. He also noted that static friction, the force required to start sliding, is greater than kinetic friction, the force required to maintain sliding.

---

[5] Allan, op. cit., p. 7.

[6] Parent, A. (1704) "Memoire qui contient tout ce qui se fait sur les Plans Inclines," Academie des Sciences, Paris, Historie de l'Academie royale des sciences avec les memoires de mathematique et physique, pp. 235-54.

[7] Euler, L. (1750) "Sur le Frottement des Corps Solides," Histoire de l'Academie Royale des Sciences et Belles Lettres, (Berlin, 1748), pp. 122-32.

In 1781 the French scientist, C. A. Coulomb,[8] presented a paper before the Royal Academy of Sciences which verified the observations of Amontons and other previous investigators. Coulomb made a clear distinction between static and kinetic friction and noted that kinetic friction can often be considerably lower than static friction. He also found that Amontons' laws concerning load and contact area applied to both static and kinetic conditions. Coulomb further concluded (sometimes called the Third Law of Friction) that the force of kinetic friction is nearly independent of the velocity. The force of static friction he found to depend upon the length of time during which the surfaces are in contact. Finally, for both kinetic and static friction the force of friction was found to depend upon the nature of the materials in contact and their coatings.

Although Coulomb was not the first to study dry friction, his extensive and well-known work is responsible for our present designation of dry friction as Coulomb Friction. Investigators following Coulomb perfected his crude measuring apparatus into a more precise instrument but contributed very little in the way of new experimental relationships. Thus for the major part of the past two centuries, Coulombs' conclusions have been accepted by scientists and engineers for friction problems.

Coulomb, C. A. (1785) "Theorie des Machines Simples, En Ayant Egard au Frottement de Leur Parties, et a la Roideur des Cordages," Academie des Sciences, Paris, Memoires de Mathematique et de Physique, Vol. 10, pp. 161-332.

APPENDIX B

APPLICATION OF WEYL'S DIPOLE THEORY TO FRICTION ON ICE

Appendix B

Application of Weyl's Dipole Theory to Friction on Ice

The outstanding and obvious characteristic of the ions and atoms which make up the surface of a liquid or a solid is the asymmetrical environment in which they find themselves. This fact forms the basis of Weyl's dipole theory[1]. An attempt will be made in this appendix to explain the formation of the dipole layer together with its implications with regard to friction on ice.

The changes that take place at a nascent surface occur in an effort to reduce the surface free energy of the system. The first step in this reduction consists in the polarization of the surface ions. Figure B-1 represents this schematically in the case of a NaCl crystal. The asymmetry of the environment causes the polarization. The sodium ions on the surface are backed by chlorine ions. This situation causes an increased electron density on the external surface of the sodium ion which decreases the electric field intensity extending outward. Similarly the sodium ions backing up the chlorine ions of the surface increase the electron density of the chlorine ions on the internal surface. This also decreases the strength of the electric field extending outward. As a rule anions are more polarizable than cations[2], therefore, the electric field of the chlorine ions undergo a greater reduction than that of the sodium (Fig. B-1b).

---

[1] Weyl, W. A. (1951) "The Surface Structure of Water and Some of Its Physical and Chemical Manifestations," Journal of Colloid Science, Vol. 6, pp. 389-405.

[2] Fajans, K. (1931) "Chemical Forces and Optical Properties of Substances", McGraw-Hill Book Co., New York.

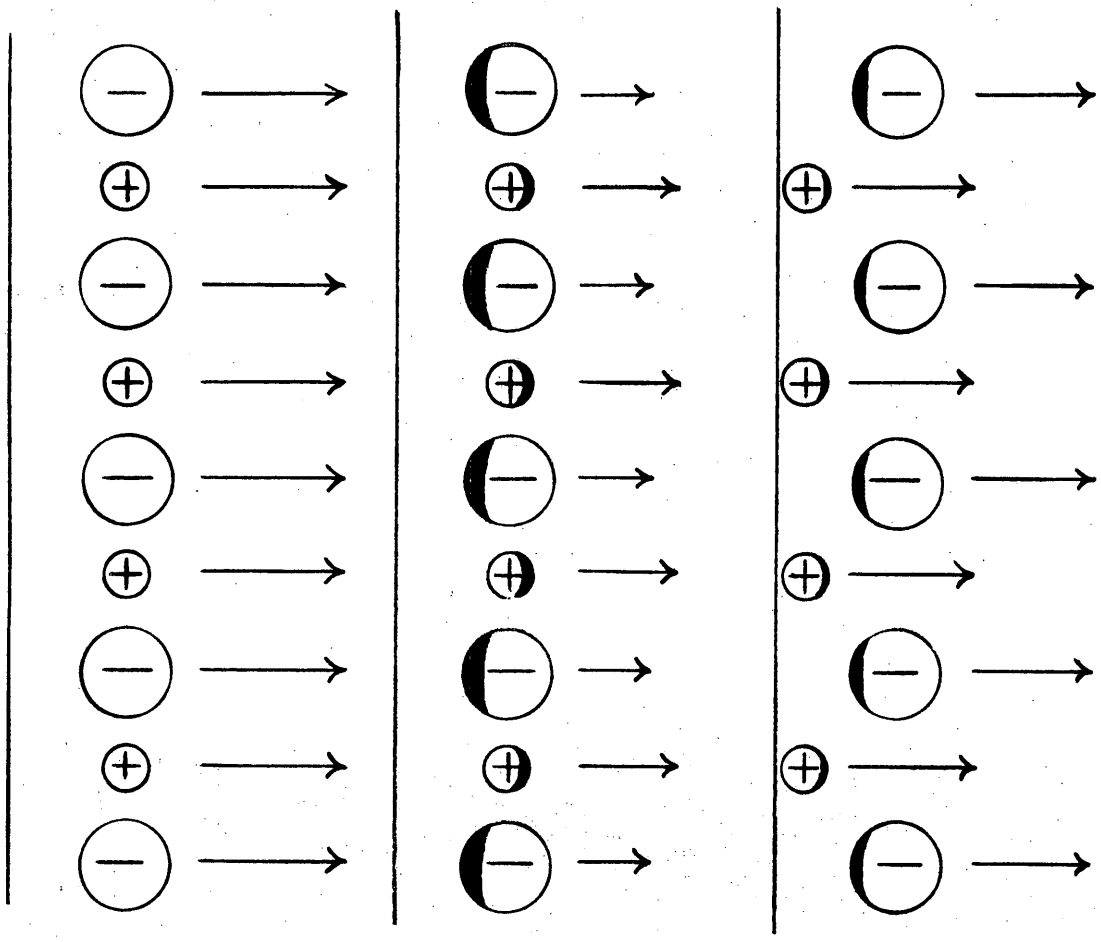

(a)
Nascent Surface

(b)
Polarization of
Surface Ions

(c)
Recession and Partial
Neutralization

Figure B-1

Formation of the Dipole Layer on the Surface

of a NaCl Crystal.

The stronger electric fields that are produced on the inward side of the surface chlorine ions as a result of the polarization, forces the sodium ions to recess into the surface (Fig. B-1c). This recession reduces the degree of polarization of both the sodium and chlorine ions, the former, however, to a greater extent. The net effect is a restoration of the balance or equilibrium of the surface force fields such that the stronger fields of the sodium ions are shielded. The resultant structure simulates a layer of dipoles with the negative charges pointed out from the surface and the positive charges pointed inward. In general terms the changes that undergo at a nascent surface of a solid or liquid result in the more polarizable ions maintained on the outer surface to shield the stronger fields of the less polarizable ions and hence reduce the surface energy.

In the case of water or ice, it is the oxygen ions which enter the outer surface for the proton is not polarizable.

The dipole surface which occurs on water and ice and other crystals is capable of explaining several phenomena. For a description of these phenomena the reader is referred to Weyl's original article and the references cited therein. Some of the experimental facts which are explained by Weyl's transition film theory are ballo-electricity, fluidization of powdered crystals such as MgO, the regelation of ice, and the effervescense associated with the addition of ice to carbonated water. In addition the stability of water droplets in freezing temperatures, the failure of the water droplets associated with fog to coalesce, the seeding of clouds to produce rain, and the chemical phenomena associated with the subjection of water to supersonic vibrations are also explained.

Nakaya and Matsumota[3] have since explained the cohesion of ice spheres in contact on the basis of Weyl's dipole theory.

Certain broad characteristics resulting from the formation of the dipole layer are immediately obvious. In order to make the transition from the bulk molecular structure to the surface dipole layer, a finite distance is required. Thus a transition layer of continuously variable molecular structure is formed on the surface. This layer is in equilibrium with the bulk structure on one side and the vapor phase on the other side if the surface is exposed to the atmosphere. Immediately it follows that the transition layer is a function of the environment of the surface. For example, the size of the transition layer at an ice-metal surface will be different from that at an ice-organic surface. The different results obtained between the passage of an iron wire and an organic string through a block of ice is explained in this manner by Weyl. Similarly two pure blocks of ice brought into contact would freeze together as the transition layer disappears due to the exposure of the film to a symmetrical environment.

Ice because of its more rigid structure requires a greater distance to make this transition than water requires. Furthermore any molecular change which can reduce the surface free energy of the system with a minimum of alteration of the H_2O molecule will reduce the thickness of the layer. For example the addition of a chemical impurity whose ions are

---

Nakaya, V. and Matsumoto, A. (1953) "Evidence of the Existence of a Liquid-like Film on Ice Surfaces," Research Paper 4. Snow, Ice and Permafrost Research Establishment, Corps of Engineers, U. S. Army, Wilmette, Illinois.

more polarizable than oxygen ions will enter the surface. This reduces the amount of molecular rearrangement necessary and hence the thickness of the transition layer.

A proper physical description of the transition layer must contain the hypothesis that a specific set of physical constants can be applicable to the layer only insofar as they represent an average over the layer. This is obvious when we realize that the molecular geometry of the layer is a variable quantity resembling the bulk structure on one side and the dipole structure on the other side.

Confining our discussion to ice and to sliding friction on ice, several deductions may be made which can be tested experimentally. Weyl states that it would take several hundred molecules to make the transition from the bulk structure to the dipole layer. If we consider 500 molecules as being necessary at 0°C for the transition, and take one Angstrom unit as equal to both the diameter of a water molecule and the distance between individual molecules, the thickness of the transition layer must be in the order of 10^{-5} cm. Pure ice therefore exposed to an asymmetrical surface has on its surface a layer which is neither water nor ice, but which should be expected to have more fluid characteristics than ice due to the reduction in rigidity associated with a transition structure.

The low coefficient of friction on ice may have as its cause the presence of this fluid-like layer. Temperature will affect this layer since the thermal agitation of the molecules will affect the distance necessary to make the transition of structure. As the temperature of ice

is reduced, the friction between a perfectly flat slider on perfectly flat ice should increase. The reduced thermal agitation results in a thinner layer of the liquid-like film. The relative humidity of the atmosphere in contact with pure ice should also affect measured frictional forces. In an atmosphere of low relative humidity, sublimation is continually taking place. The transition layer continually is formed anew as the surface molecules leave the surface. This should lead to more erratic friction measurements than those obtained in an atmosphere of high constant relative humidity which permits a more stable and constant transition layer. Friction measurements on ice performed in this laboratory under both low and high temperatures and relatively humidity bear out the above theoretical predictions. (See Chapter VI).

An effect of impurities on the transition layer has already been mentioned. The addition of substances more polarizable than oxygen should reduce the thickness of the layer and hence increase the friction, between a perfectly flat slider and perfectly flat ice. In addition impurities absorbed from the atmosphere or already present in the original water from which the ice was frozen and substances deliberately added to the water may have an effect on friction on ice if we assume a partial chemical basis to the friction process.

Much of what follows is based on several experiments on glass.[4] To be applicable at all to ice some similarity in the molecular structure of glass and ice should be indicated. The molecule of water consists of two hydrogen atoms and one oxygen so orientated in space as to give a resultant dipole structure with centers of positive charge at the two hydrogen atoms

---

Weyl, W. A. (1948) "The Surface Properties of Glasses as Affected by Heavy Metal Ions" Journal of the Society of Glass Technology Transactions, Vol. 32, pp. 247-259.

and centers of negative charge at the oxygen atoms. Thus molecules of water can group together such that the oxygen atoms of two water molecules attach to two hydrogen atoms of a third molecule. The oxygen atom of this molecule can also bond with a hydrogen atom of a fourth molecule. Thus in water or in crystalline ice there exists one oxygen atom between every two hydrogens. This resembles the structure of quartz which has one oxygen between every two silicon atoms.

A chemical explanation for friction would consider the formation of chemical bonds between opposite ions when both materials present ionic surfaces to each other. In the situation of a metal sliding on an ionic surface we may also get compound formation by the passage of single ions from the metal into the ionic surface. If we accept therefore the existence of a chemical basis for friction, then all changes that decrease the number and strength of unsaturated valences of surface ions on ice should decrease the friction.

Molecules or ionic groups that do not exhibit a stable configuration of electrons (incomplete electron outer shells) are strongly deformed in an electric field more so than ions of the noble gas like structure. Doubly charged lead and tin ions fit this requirement. Both of these ions have two electrons in their outer ring. The electric fields of their respective negative ions will concentrate the valence electrons on the surface side of the metallic ion making it appear neutral. The side directed toward the interior will then present a force field similar to the Pb^{4+} or Sn^{4+} ion. The presence of the neutral side will reduce the

chemical reactivity of the surface and hence the friction. $Pb(NO_3)_2$, PbS, and $SnCl_2$ are typical compounds which could be added to the water to study this effect.

To summarize, additives influence friction on ice in two ways, both actions being antagonistic. The more polarizable substances entering the surface reduce the thickness of the transition layer and hence the fluidity of the surface leading to an increase in friction. At the same time fewer unsaturated valence bonds present at the surface reduce the friction by inhibiting chemical combination. Experimental measurements would indicate the predominating influence.

The influence of additives, temperature, and relative humidity on frictional forces was described above for friction between perfectly flat surfaces. Experimental friction measurements however involve contact between relatively rough surfaces. While the effects of additives, temperature, and relative humidity on the transition film holds for rough surfaces also, the transition film itself exerts special effects not present with perfectly flat surfaces.

Friction of a metal slider on ice is similar to the series arrangement described in Chapter I. This description involves a thin layer of soft material completely separating the harder materials of the sliding body and the stationary surface. The thin layer of soft material is the transition layer formed on the ice surface. The phenomena associated with the reduction in film thickness over asperities with increasing load applies as well for the dipole layer. Consider for example the slider in

contact with an ice asperity. As the load increases the fluid transition layer begins to flow, decreasing the thickness of the film at the point of direct contact. As the molecules in the bulk ice under this reduced film layer begin to orient themselves, partial neutralization of the strong proton fields by the slider surface molecules occurs. This makes it unnecessary for the film to recover its original thickness. Therefore, as the load increases, the thickness of the film between the slider and the bulk ice, at the point of contact, progressively decreases. Sooner or later under heavy loads the film is completely squeezed out, the proton force fields are completely neutralized, and no transition film need form. This last situation corresponds to what happens at freezedown (See Chapter IX) and results in the parallel arrangement described in Chapter I. Under heavy loads, therefore, the slider load is supported partially by the bulk ice where the film is squeezed out and partially by the film that persists at other points. The effect of time on the type of load support provided by the ice is described in Chapter 8 and is applicable to the transition film construction of the ice surface.

In Chapter IX the concept of a parallel arrangement of ice, film, and slider is applied to the electrical resistance measurements with good results. The electrical apparatus has been used to good advantage in the investigation of the liquid-like layer due to the difference in the current carrying characteristics of the transition layer and the bulk ice.

APPENDIX C

PREPARATION OF SMOOTH, CLEAR ICE SURFACE

APPENDIX C

PREPARATION OF SMOOTH, CLEAR ICE SURFACE

In the measurement of friction between solid objects and compacted snow it is first necessary to develop techniques which will provide a smooth surface, free from irregularities and subject to reproduction. In order to simplify the initial experiments, an end product of fully compacted snow, namely ice, was chosen for testing. Even with this simplification, a number of problems were encountered in the preparation of a smooth, clear ice surface. In general, the major problems encountered resulted from two basic properties of ice, its air solubility and its volume expansion.

Before discussing the work performed on these problems in the current investigation, it is helpful to examine the previous findings as described by Dorsey.[1]

"Production of Homogeneous Ice

In 1845, C. Brunner described his attempts to produce homogenous ice suitable for use in a determination of the density of ice. On cooling while exposed to the air, carefully boiled-out distilled water takes up so much air that when it is frozen it contains many bubbles, especially in the portion that was the last to freeze. Covering the water with turpentine immediately after boiling kept out the air fairly well, but the ice was then full of cracks. Following a suggestion, which he attributes to F. C. Achard, he exposed one side of the vessel, containing the water to be frozen, to a low temperature and the opposite to a temperature above 0°C. The ice so formed contained some air bubbles, but not nearly so

---

[1] Dorsey, N. E. (1940) Properties of Ordinary Water Substance in All Its Phases, Reinhold, Publ. Corp., New York, pp. 414-417.

many as that formed in the usual manner. He found that selected river-ice was much superior to any ice he succeeded in freezing in the laboratory.

L. Dufour boiled-out and froze water in a Torricellian vacuum, air pressure not over 0.5 mm. The ice contained a few very small bubbles. It was opalescent and very homogeneous. He states that the opalescence was not due to air, but to the crystalline structure of the ice, or to internal crevices.

R. Bunsen introduced boiled-out distilled water into one arm of a U-tube initially filled with air-free mercury. The water was introduced while hot, was boiled in the tube, and the tube was then sealed so as to exclude all air. The water was frozen gradually from the top downward. Thus, he obtained a cylinder of ice that was entirely (vollig) free of air-bubbles, and that was equal to the best crystal glass in clearness and transparency.

G. Forbes used the same procedure, and stated: "The ice formed was quite uniform, very clear, and when cloven by planes perpendicular to the plane of freezing, split easily, showing the crystalline structure with great clearness."

G. Quincke stated that by repeated fractionations, by means of freezing and thawing, the ice becomes ever purer and purer, and the crystals large, but that he had never succeeded in obtaining ice that was not an aggregate of many crystals. The removal of air by alternate freezing and rapid thawing had been described, and the method seems to have been used by Duvernoy nearly 40 years before.

A. Leduc introduced hot, boiled-out distilled water into an exhausted vessel, and froze it progressively from the bottom to the top. The upper portions contained bubbles. Even after three such freezings <u>in vacuo</u>

there were small bubbles in the portion last frozen. A fourth freezing appeared to produce no further improvement. Likewise, G. Bode has stated that neither the boiling-out of distilled water nor its repeated freezing in a vacumn is sufficient to insure a clear sheet of ice.

H. Hess stated that by slow, long-continued freezing, very homogeneous ice-sheets may be formed on the water in large reservoirs. On thawing, these sheets break up into vertical, columnar pieces."

1. Problem of Air Solubility

As previously stated the first problem in the preparation of ice is presented by the air solubility of water. Liquid water, the practically universal solvent, carries a considerable amount of air in the dissolved state. In the frozen state, however, the solubility is much lower. Thus as the water freezes the dissolved air originally contained in the water becomes concentrated in the unfrozen liquid, and ultimately this liquid becomes saturated with air. At this point the dissolved air begins to leave the water as bubbles. In an ice sheet this point is quite apparent as a plane of bubbles appears at a level distance below a region of clear ice. As the water continues to freeze, more air escapes and joins the previously formed bubbles. In addition to this, the volume expansion of the ice squeezes the bubble region pushing the bubble ahead of the forming ice plane. The bubble leaves as a track, a long air tube in the ice indicating, incidentally, the direction of ice growth. The photographs of Figures C.1 and C.2 illustrate this phenomenon.

The bubbles and honeycombed structure can be prevented by several methods such as by allowing the bubbles to escape or by preventing the remaining liquid from ever reaching the air saturated state.

River water flowing under an ice layer effectively solves this problem in nature. By carrying bubbles to open regions in the ice, the

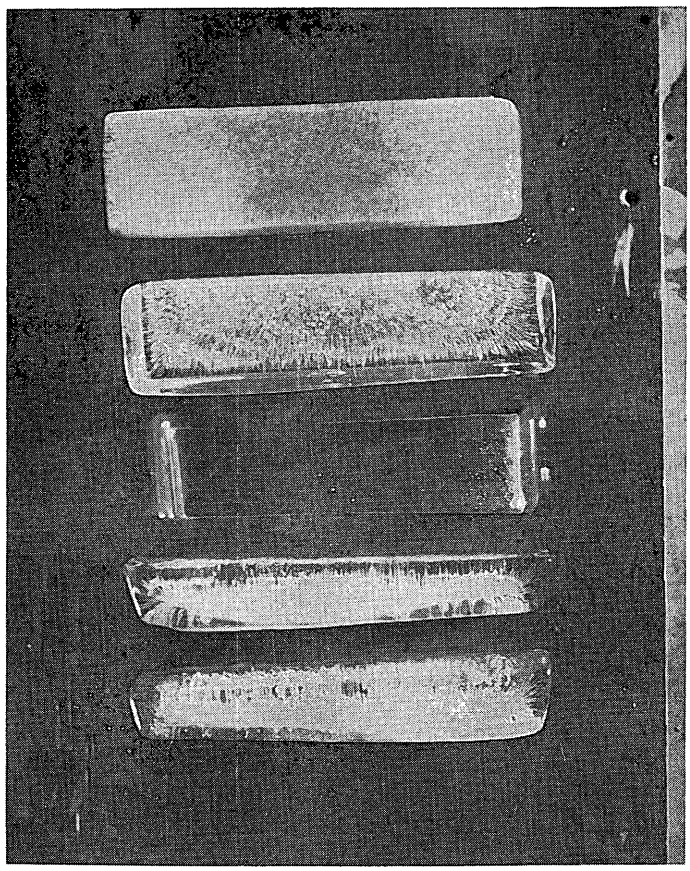

Fig. C-1 Bubble Formation in Ice

Upper Two Specimens

Top view of regularly frozen ice demonstrating cloudy appearance due to formation of bubbles.

Middle Specimen

Top view of clear ice frozen by special process.

Lower Two Specimens

Cross section views of ordinary ice showing plane at which bubbles first appear and bubble tracks.

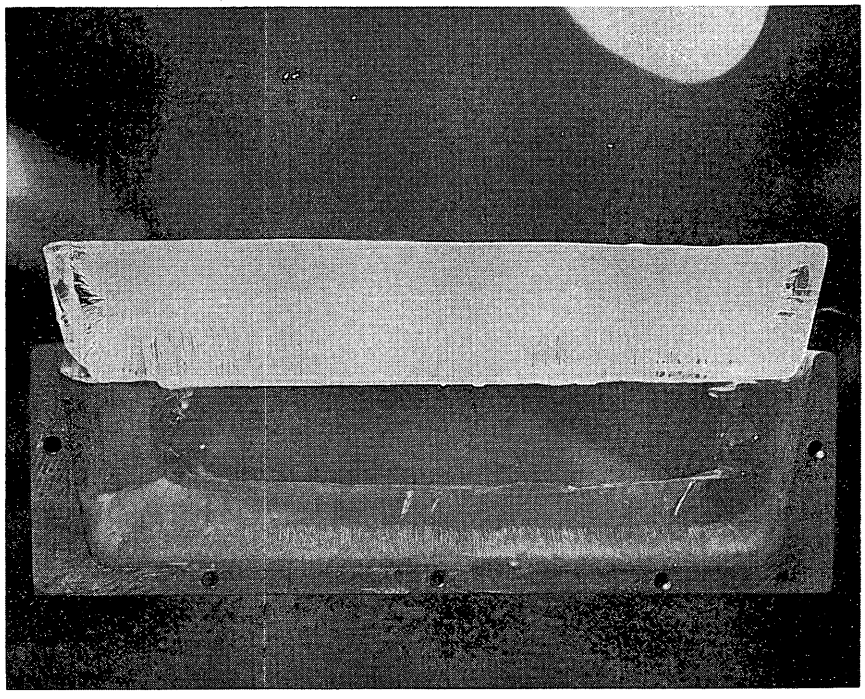

Fig. C-2 Cross section comparison of ordinary and specially prepared ice.

Top Specimen is ordinary ice containing air tubes formed by expanding ice forcing air bubbles ahead of plane of freezing.

Lower Specimen is ice frozen by special process. This view is actually an end view of the ice tray with end plate removed, a region where the special process is not completely effective. Filaments at the bottom of the clear ice were formed at intersection of tray and cover plate and do not occur in the body of the ice. Top portion of this ice illustrates clear ice obtainable.

bubbles are allowed to escape, and by changing the water in contact with the ice the freezing water is prevented from becoming air saturated. If properly controlled in the laboratory, this method could probably be used to prevent bubble formation. However, as the liquid region shrinks below the ice layer, it becomes more difficult to move water in the available space.

Several methods of eliminating or reducing the dissolved air have been experimentally investigated in this project.

a. Vibration of water during freezing:

Water was vibrated while freezing in an attempt to dislodge air bubbles from the freezing water as the bubbles formed. A low energy level vibration of about 60 cps was used. Small regions of ice which were clearer than the surrounding area were obtained by this method. The energy level and frequency used were probably both too low. L. Bergmann[2] states that gases in a supersaturated liquid progress toward the nodes of vibration when the liquid is subjected to ultrasonic vibrations. The gases evidently form into bubbles and rise to the surface. It would seem possible to use such a technique; since air bubbles in ice are caused by a supersaturated condition of the unfrozen water. The surface of the freezing water should be kept liquid so that the air bubbles can be scarified from the water. Frequencies with a small wave length should probably be used so that a sufficient number of nodes of vibration would be present to degas the liquid throughout.

b. Use of a clear section of an ice surface:

It was noted that the bottom 1/8" of a 1" frozen ice section was

---

[2]Bergman, L. (1938) Ultrasonics, John Wiley & Sons, Inc., New York.

generally clear ice, with but few air bubble formations present. It would be possible to machine an ice surface down to this level and produce an area of clear ice. The suggested procedure described later enables the formation of a deeper section of bubble free ice for machining.

c. Freezing water previously placed under a vacuum:

Water was evacuated in a jar to 27 inches of mercury and agitated to bring out the absorbed air. The jar was sealed and the water frozen. Air bubbles still were present, although in much smaller numbers than ice formed from untreated water.

d. Rapid freezing of supercooled water:

Although the rapid freezing of supercooled water might possibly entrap the air along grain boundaries rather than in bubbles, the practical difficulties in producing supercooled water deterred investigation of this technique.

e. Freezing a tray of water under a temperature gradient:

A temperature gradient was obtained by placing a metal tray of water in the cold box and covering it with an insulation board. Nichrome heater wires attached to the underside of the insulation board supplied heat to prevent the top water surface from freezing. Cold air blown by fans upon the underside of the tray set up a subfreezing temperature in the lower portion of the ice tray. Freezing was initiated and progressed from the bottom of the pan. This allowed the air bubbles to escape to the water surface as freezing progressed. Since the top surface is open it was also possible to replenish the air saturated water with fresh low air content water.

2. Problem of Volume Expansion

As water is cooled, its specific volume contracts until temperature

of 4°C is reached. Below this point the specific volume expands and as the liquid freezes to ice the specific volume increases considerably more. One explanation of this phenomenon attributes the expansion to the increased formation of the larger molecules of trihydrol, $(H_2O)_3$, even though the individual molecules in the mixture of hydrol, dihydrol, and trihydrol continue to decrease in size as the temperature decreases.[3]

In the customary type of freezing, the less dense material rises to the top and freezes on the upper surface. If the container is sufficiently large, the ice will float above the liquid and rise gradually and uniformly as more water freezes upon the undersurface. In a container such as a refrigerator ice tray, however, ice first forms along the sides of the tray. This first formed ice expands in volume and squeezes the remaining water to the center usually causing it to overflow at the top. As the ice continues to freeze toward the center, more and more water is pushed out the center causing a distinct bulge in the top central surface.

The action is further complicated by the usual procedure of exposing the water surface to a low temperature atmosphere. As top surface of the last overflow of water freezes over, a volume of liquid is trapped inside which, upon freezing, is restricted in its expansion, causing large stresses and a cracking action.

The following methods for obtaining level ice have been studied:

(1) Procurement of ice from a large surface region such as a lake or river.

(2) Freezing ice practically instantaneously throughout.

(3) Allowing lateral motion by providing flexible sides for the material trays.

---

[3] Schmidt, E. (1949) Thermodynamics, Oxford University Press, London, pp. 187.

(4) Controlling crystal growth direction sufficiently well so that the ice will form on definite planes and rise as a unit with volume expansion.

(5) Smoothing a previously formed uneven ice surface by application of surface heating.

(6) Machining the uneven surface actually formed down to a smooth, level surface.

In the attempt to form smooth level ice artifically, several experimental techniques were tried:

a. Vibration of liquid during freezing:

It was hoped that vibration would prevent crystallization of the surface until the entire body of water froze. Jarring a tray of water with a vibrator slowed down the freezing process but did not prevent formation of a humped surface.

b. Control of direction of ice formation

Direction growth control was attempted in several ways:

(i) By exposing a very thin sheet of water to the freezing region. In the thin sheet, lateral crystal growth did not have time to form and the resulting surface was comparatively smooth.

(ii) By placing compressible insulation in the freezing tray. It was expected that heat would not be conducted rapidly through the insulation material and that the ice would only form from the upper and lower surfaces. Expansion of the ice into the region of collapsible insulation was expected to prevent bulging surfaces. In operation, this technique was only partially successful. Ice did form outward from the insulation material, indicating a greater flow of heat through the insulation than through the remaining water. Expansion of the ice into the insulation

material was not sufficient to prevent bulging of the top surface.

(iii) By freezing ice from the lower surface upward. This method proved fairly satisfactory in preventing undesired expansion.

c. Smoothing of the top surface by melting a small layer of ice:

In applying this technique an ordinary iron was used to iron down the bumps. It was found that too high an "ironing" temperature or excessive application of the iron melted too much water and bumps were reformed upon refreezing. Also since the surface tension of water is considerably greater than that of ice, water formed during melting tended to pull together and form globules on the ice surface. Upon freezing, these globules further roughened the surface.

Remote melting of the ice surface using infrared lamps was also attempted. Again, the heat of the lamps tended to melt the top projections, the resulting water drops pulled together, and the ice became even more rough than previously.

d. Machining a large ice sample down to the required levelness and smoothness:

Machining of the ice surface down to the desired shape and smoothness was attempted and proved feasible. Since ice is very abrasive, it is difficult to keep a milling cutter sufficiently sharp to produce a smooth surface. In exploring this technique, it was found necessary to design a special milling cutter to shave the ice. In addition to the shaving process, it was found feasible to hone the ice to remove tool marks. During later refinement of the surface smoothness, great care must be taken to prevent excess heat and consequent melting of the surface.

In spite of its disadvantages, machining is judged to be the most practical method of producing a smooth, level surface.

3. Volume Contraction at Low Temperatures

Low temperature operation presented another problem in the preparation of ice. As the temperature was lowered, the ice expanded and then contracted setting up large thermal stresses. Before reaching the desired temperature the ice would crack or shatter. It was, therefore, necessary to provide a flexible container in which the ice could expand or contract as a unit.

Several methods for obtaining this flexibility were tried. A sand bed on the bottom and sides was one method investigated. Water filling the pores between the sand grains would freeze with the remaining water, making the entire mass a large rigid body bounded by the steel tray. Water also soaked into sponge rubber giving the same result for sponge rubber sides. Harder rubber becomes very rigid at the low temperatures desired.

A method was finally found, however, which proved satisfactory. In this method the bottom of the tray is first coated with vaseline to prevent direct adhesion of the ice crystals to the steel bottom and thus allow shifting along the bottom. Strips of Biltrite, rigid insulation board, are placed along the tray sides. This insulation does not allow excessive penetration of water and retains its flexibility at low temperatures. Water frozen in this container is able to expand and contract without setting up the stresses which would result in shattering of the ice.

4. Method Utilized in the Preparation of Smooth, Homogeneous Ice Surface

The following procedure for freezing clear homogeneous ice has been found to be satisfactory:

1. Distill water - removes majority of solid impurities.
2. Place water under vacuum and vibrate, this removes the larger portion of dissolved air.
3. Siphon water into material tray at atmospheric pressure--prevents excessive reentry of air.
4. Place material tray in cold region with circulation of coolant over bottom of tray.
5. Place electrical resistance heater over air space above tray. Heater maintains temperature of top surface above freezing, allowing the ice to freeze from bottom surface upward.
6. Before the unfrozen liquid above the ice becomes saturated with air, replace the remaining liquid with fresh water having a lower percentage of dissolved air. This process may be accomplished by a continual flow of water over the surface of the ice or by simply removing and replacing at definite time intervals. For an original depth of 2 centimeters of water being frozen at -4°C, a change every three hours and discard of the remaining water after nine hours is recommended.

Since solid impurities are also rejected during freezing, the first formed ice is more pure than that which freezes last. Replacing the unfrozen liquid thus

serves to remove any remaining solid impurities along with dissolved air.

In this procedure the vacuum and agitation tend to remove a considerable amount of the dissolved air. Freezing from below allows access to the unfrozen liquid and aids in the escape of bubbles should any be formed. Replacing the water keeps the air content below the saturation state. Discrete changes of water are advocated over continous flow since temperature gradients in the quiescent water are easier to maintain than in flowing water.

Mechanical smoothing of the top surface requires several machining steps. In addition to large scale cutting for removal of the major bumps, it is necessary to carefully hone the surface to remove the tool marks.

For the Linear Path Dynamometer, a special milling and honing machine has been designed and constructed. The milling head of this machine is designed to carry a cutting tool at several different positive and negative rake angles. Connected to the other end of the shaft is a 1/20 HP electric motor and speed reduction unit which drives the tool holding head and cutting tools at a uniform rate. Frame, motor, reduction unit, coupling, and cutter head are illustrated in Figure C.3.

Additional surface smoothing is obtained from a honing tool. Four of these tools are mounted in the cutter head and revolved over the previously machined ice surface. Cross hatching of the honing tool provides the necessary cutting edges and the space for absorbing the ice chips. These

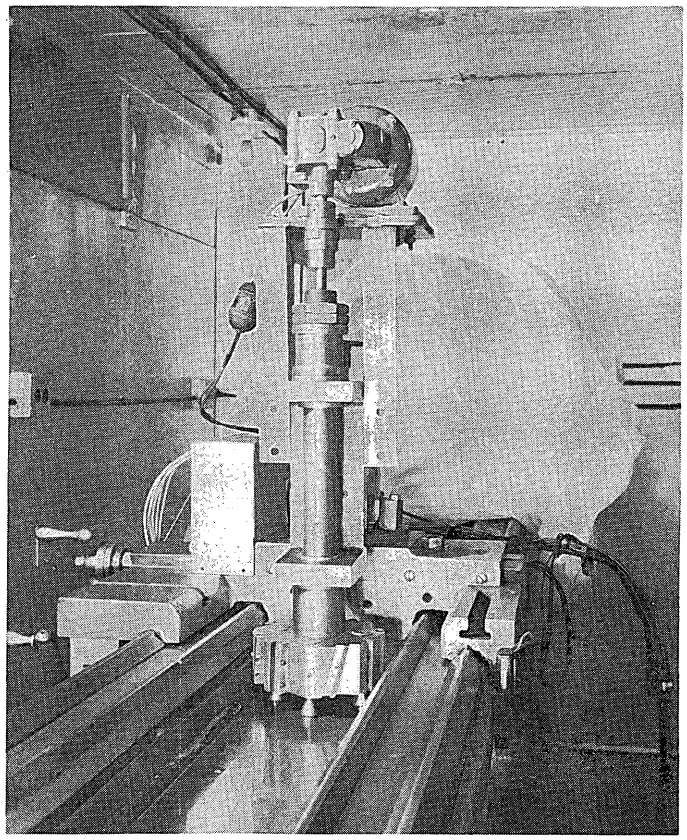

Fig. C-3 Linear Path Machining and Honing Apparatus

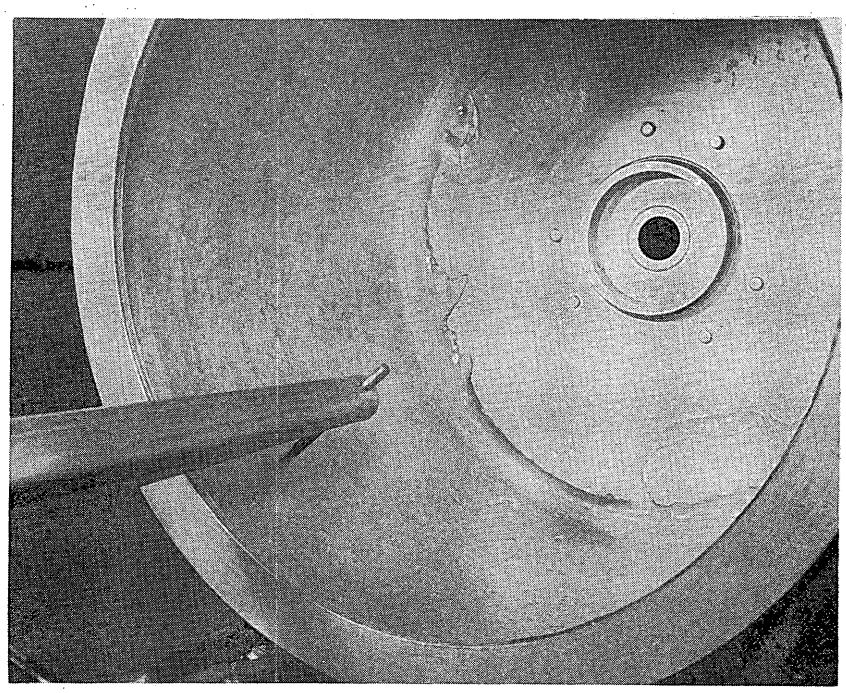

Fig. C-4 Cylindrical Path Machining

tools remove any remaining tool marks on the ice surface. Spring loading in the vertical direction and freedom of the tool to pivot around a conical point and socket joint provide sufficient independence of motion and position to present a random shaving edge for a honing action.

Freezing of ice in the drum of the Cylindrical Path Friction Force Dynamometer has also presented special problems. The method of heating the top surface while cooling from the bottom is not too applicable in this case.

Another freezing method was found to be fairly satisfactory for this particular apparatus. Distilled and vacuum processed water is placed in the bottom of the drum while the drum is slowly rotated. The water forms a pool in the bottom of the drum bounded by the rear wall, the front ring and the curved drum sides. The drum rotating through this pool picks up a thin film of water. During the remainder of the drum revolution, the film freezes and the surface is able to pick up another film layer on its next pass through the water bath. The resulting ice layer is surprisingly clear since the dissolved air is always free to escape and the air concentration never builds up to the saturation level.

One other problem does arise with this freezing method. Since the water in the bottom pool in the drum is cooled, there is a tendency for an ice layer to form on the surface of this water. Agitation of the water by the rotation of the drum prevents the formation of a solid surface but crystal groups do form. These crystal groups floating near the edge of the pool are picked up by the emerging drum surface and freeze to the drum surface. The small bumps formed by the crystal groups act as the nucleous for large projections on the ice surface. These projections sometimes grow to better than a centimeter above the remaining surface.

Machining of the ice surface to remove the projections is accomplished through the use of a specially designed boring bar bolted directly to the carriage cross feed (Figure C.4) At the far end of the boring bar shaft, an adjustable tool holder supports a collet type extension tool bit at approximately a 45° angle to the horizontal. Movement of the cross feed brings the tilted cutting tool into contact with the ice layer at the correct cutting angle.

Experience has shown that a very fine feed is necessary to produce the desired surface smoothness. Following the machining operation, an aging time is required to allow the machined ridges to flow slightly and smooth themselves. It has also been noted that over a long period of time the ice in the cylindrical drum has an extensive and detrimental flow. If the cylinder is allowed to remain stationary for a period of time, the ice will flow from the drum top to the drum bottom, thus enlarging the ice thickness at the bottom and changing the curvature within the drum. It is therefore necessary to periodically machine the interior of the stationary surface or to keep the drum continually moving.

The problem of avoiding the shattering of the ice in the cylindrical drum under low temperature operation has not as yet been solved.

Snow is prepared for testing in the linear path apparatus in the following manner: Following a snow fall, the snow to be used is examined for its physical characteristics. A quantity of snow is then sifted into a tray, filling the tray uniformly to a depth greater than the tray sides. A straight edge is then used to remove the surplus above the tray sides. Next a flexible masonite sheet slightly smaller than the tray dimensions is placed on the snow. This masonite sheet is loaded uniformly to a pressure of approximately 3 p.s.i. The masonite

sheet,in turn, transmits the loading to the snow compacting the snow evenly. The filling and compaction process is repeated twice resulting in a compacted snow surface approximately 1 1/4 inches in depth. The smooth masonite sheet pressed against the snow forms a smooth snow surface which requires no further machining.

APPENDIX D

A BRIEF DESCRIPTION OF THE ANALYSIS OF VARIANCE

Appendix D

A Brief Description of the Analysis of Variance

Suppose we have N values of a random variable having two classifications. For instance it might be supposed that one is endeavoring to determine what, if any, variation different makes of lathes have on various machinists' outputs. An experimental study would be set up in which each operator would work on each machine for a certain length of time, the choice of which operator works on what machine being a completely random choice, except that for all work periods after the first the choice would preclude any man working twice on the same lathe.

In addition to the above, we may further assume that each man does work on each machine a certain number of times, each work period being called a "replicate". Hence we have P machines (columns), Q operators (rows), and R periods (replicates).

The results may be tabulated below:

		Machine				
		1	2	3	...	P
Operator	I	a_{11} b_{11} ⋮ R_{11}	a_{21} b_{21} ⋮ R_{21}	a_{31} b_{31} ⋮ R_{31}		
	II	a_{12} b_{12} ⋮ R_{12}	a_{22} b_{22} ⋮ R_{22}			
	III					
	⋮					
	Q					

We shall refer to each tabulated item as x_{ijk} where $i = 1,2,\ldots,P$; $j = 1,2,\ldots,Q$; and $k = 1,2,\ldots,R$. Also for a particular row and column, all observations (or replicates) constitute a "cell".

Consider the very hypothetical case where each machine has the same effect in equal degree on each operator and where each machine performs identically, and each operator is equally proficient and does perfect work. If this be the case, then each value of x_{ijk} representing man-machine output would be the same and the difference represented by $\sum_{i=1}^{P}\sum_{j=1}^{Q}\sum_{k=1}^{R}(x_{ijk} - \bar{X})^2$ would be zero. Here $\bar{X}$ is the average of all the values of :

$$\bar{X} = \frac{\sum x_{ijk}}{N}$$

In other words each observation is equal to the average.

In an actual situation, the above would not be true and we must seek some explanation.

We make a few assumptions regarding the populations from which these samples are drawn. We assume that the populations from which each observation x_{ijk} was drawn has a normal distribution with standard deviation σ, and a mean made up of the sum of four parts: (i) a basic mean of μ; (ii) a constant value for each column, p_i; (iii) a constant value for each row, q_j; (iiii) an "interaction" term, I_{ij}. μ is the same for all cells, P_i is the same for all cells in $i^{\underline{th}}$ column, q_j is the same for all cells in the $j^{\underline{th}}$ row, and I_{ij} is the same for all observations in a particular cell.

We may illustrate the above by considering our machines and operators example. Machine 2 may have the longitudinal feed clutch in an unusually

easy-to-use position. As a result each machinist on lathe 2 does more work than he does on any other machine. This is a form of column or p_i effect. Now operator 3 has had a year more experience than any other operator. Hence any machine he works on will enable him to produce more than any other operator. This represents a row or q_j effect. Further, suppose some of the machinists each own a share of stock in a machine tool company, each share representing a different company. If the results of these tests being carried on will influence the purchase of lathes, these share-holding operators will try to make that machine represented by their stock look outstanding. They will perform (or attempt to do so, at any rate) better on these particular lathes than on the others. This improved output will not be reflected equally on a machine, nor equally by an operator, but only for a particular man-machine combination. This is a form of interaction.

We may write out a 2 x 3 design in the light of the above as follows:

	1	2
I	$\mu + p_1 + q_1 + I_{11}$	$\mu + p_2 + q_1 + I_{21}$
II	$\mu + p_1 + q_2 + I_{12}$	$\mu + p_2 + q_2 + I_{22}$
III	$\mu + p_1 + q_3 + I_{13}$	$\mu + P_2 + q_3 + I_{23}$

We refer back now to the sum of squares mentioned earlier, $(x_{ijk} - \bar{X})^2$. If the above is not zero, there must be some factors which cause the discrepancy. These factors we have given as column effect, row effect, and interaction. Another effect not previously mentioned is "residual" or "error". This value takes into account all

effects not accounted for by the other three. Included might be instrument error and observation error.

Basically speaking, in analysis of variance we break down the above sum of squares, known as the fundamental sum of squares, or fundamental sum, into its components. This is:

$$\sum_{i=1}^{P}\sum_{j=1}^{Q}\sum_{k=1}^{R}(x_{ijk}-\bar{X})^2 = \underbrace{\sum\sum\sum(\bar{X}_i-\bar{X})^2}_{\text{Column Effect}} + \underbrace{\sum\sum\sum(\bar{X}_j-\bar{X})^2}_{\text{Row Effect}} + \underbrace{\sum\sum\sum(\bar{X}_{ij}-(\bar{X}_i-\bar{X})-(\bar{X}_j-\bar{X})-\bar{X})^2}_{\text{Interaction Effect}}$$

$$+\underbrace{\sum\sum\sum(x_{ijk}-\bar{X}_{ij})^2}_{\text{Residual}}$$

This is trus inasmuch as the cross products always are zero when the summation is carried out.

We call the total, column, row, interaction, and residual E, A, B, C, and D, respectively, and set up the following table.

Source of Variation	Sum of Square	degree of freedom	Mean of squares	F ratio	Significant
between columns	A	P - 1	A/ (P-1)		
between rows	B	Q - 1	B/ (Q-1)		
interaction	C	(P - 1) (Q - 1)	C/ (P-1)(Q-1)		
residual	D	N - PQ	D/ (N - PQ)		
Total	E	N - 1			

The values of A, B, C, etc. are calculated from the basic equation.

The degree of freedom column needs some explanation. Suppose we have three billiard balls. We may choose a first ball completely at random. From the remaining two we can again pick a second random ball. However, now there remains no choice, we can only choose the third ball as the remaining one. So for three balls, we choose two at random, or we had (3 - 1) = 2 degrees of freedom in our choice. Hence for P machines we have P - 1 degrees of freedom, etc.

The mean of squares represents a χ^2/ degrees of freedom distribution for we assumed that the random variable was distributed normally. Hence this also is a measure of the ratio S^2 / σ^2 where S is the sample deviation and σ the population deviation.

The F ratio is now used to compare the mean of squares of column and row effects with that of interaction or residual pooled with interaction. Initially the mean of squares for interaction is divided by that of residual. This in effect gives us

$$F = \frac{S \text{ interaction}}{S \text{ residual}} = \frac{S_c}{S_d}$$

since we had previously assumed equal σ's, and since S^2 / σ^2 possesses a χ^2/d.f. distribution. The resulting value of F is compared with a previously established value at some level of significance. If the calculated value is larger than the established value, we say that interaction is significant. This basically implies that the means of the cells, when column and row effects have been removed, are more disperse than one would expect for samples from the same population. The hypothesis that all I_{ij}'s are zero is not acceptable.

Interaction may be due to the following:

(a) Depending on the significance level, we shall get interaction indicated even though none exists. The percentage of times that this will occur is equal to the significance level.

(b) Interaction may actually exist; i.e., effects are produced by acting together that wouldn't be produced separately.

(c) There are influencing factors not included in the tests that should be considered.

(d) The samples are not randomly drawn.

If interaction is significant, similar F ratio comparisons are then made between column mean of squares and interaction mean of squares, and also between mean of squares of row and interaction. Significance here implies that all p_i's or all q_j's are not zero.

If interaction is not significant, it is a common practice to add the sum of squares and degrees of freedom for the interaction term and the residual, and form a new mean of squares. This new value is used for comparison as previously with the row and column means. The idea here is that if interaction is not significant, it is in reality additional residual.

The above discussion has dealt with two variables with replication, while this report deals with experimental designs having three variables with replication. The basic ideas presented here are still involved, and except for additional work in computation, nothing new exists.

APPENDIX E

A MODIFIED FORD AND REYNOLDS ALTERNATING CURRENT BRIDGE

APPENDIX E

A Modified Ford and Reynolds Alternating Current Bridge

Introduction

The modified Ford and Reynolds alternating current bridge (See Fig. 9.1) is designed to measure the resistance and pure capacitance that must be placed in parallel in order to obtain an exact equivalence of an ice condenser.[1] The functional value of the various features of the bridge will be presented in this appendix along with the development of the contact area equations obtainable from surface resistance measurements.

Theory

Balance is secured first with the ice condenser out of the circuit, Switch S_1 being open. At balance the following relation holds:

$$\frac{R_1}{R_2} = \frac{Z_{AD}}{Z_{CD}} \qquad \text{(E-1)}$$

where $$\frac{1}{Z_{AD}} = \frac{1}{R_3} + j\omega C_{AD} \qquad \text{(E-2)}$$

and $$\frac{1}{Z_{CD}} = \frac{1}{R_4} + j\omega C_3 \qquad \text{(E-3)}$$

Since $R_1 = R_2$

$$\frac{1}{R_4} + j\omega C_3 = \frac{1}{R_3} + j\omega C_{AD} \qquad \text{(E-4)}$$

With S_1 closed, balance is again secured with the new values R_4' and C_3' on the variable precision resistance and capacitance respectively. We therefore have

$$\frac{1}{R_4'} + \frac{1}{R_x} + j\omega(C_3' + C_x) = \frac{1}{R_3} + j\omega C_{AD} \qquad \text{(E-5)}$$

---

[1] Ford, W. A. and Reynolds, S. T. (1933) "Alternating current bridges for measurements of electrical insulating materials", Gen. Elec. Rev., Vol. 36, pp. 99-105.

From equations (E-4) and (E-5) it follows that

$$C_x = C_4 - C_4' \qquad \text{(E-6)}$$

$$\frac{1}{R_x} = \frac{1}{R_4} - \frac{1}{R_4'} \qquad \text{(E-7)}$$

and the capacitance and parallel resistance of the ice condenser is determined independent of a knowledge of the frequency or the accuracy of the stated values of the other components.

Shielding principles

In constructing a bridge one always runs the risk of introducing unintentional electric and magnetic couplings between various components of the network. These are represented by leakage conductances and capacitances joining the branches of the network to one another or connecting branches to earth. Hence when balance is secured, it must involve these undesired coupling effects and thus cause inaccuracy. The purpose then of a shielding system is to make inter- and earth-admittances definite in magnitude, independent of the position of the network or of the observer, and at the same time to modify the distribution and location of these admittances so that their effect on the accuracy of the bridge balance is as small as possible. In a bridge based on a substitution principle, the important thing is that residual and stray impedances are definitely located and kept constant during both balances.

In a capacitance bridge of the type used, magnetic coupling is negligible and is limited only to the direct influence of the source upon the detector. Proper isolation of source from the bridge is secured through the General Radio doubly shielded bridge transformer, T_1.

The shielding technique here as shown in Figure 9.1 fixes all stray capacitances from point A and stray inductances from the secondary of the transformer and places them across the bridge from point A to C where they do not disturb the balance.

Electric coupling is taken care of as follows: The doubly shielded resistance R_1 and R_2 fix the stray capacitances from the inner shield to ground and place these capacitances in parallel with the detector from B to D where they cannot affect bridge balance. All other leads not at ground potential are shielded to fix their stray capacitance to ground. This elaborate shielding construction is confined to the main bridge arms, namely, those containing the resistances R_1, R_2, R_3, and R_4. The guard circuit elements, those containing the resistances R_5 and R_7 in their respective arms, and the phase selective bridge components do not require elaborate shielding to perform their function as long as they are suitably decoupled from the main bridge arms.

These shielding arrangements proved satisfactory. There is no stray pickup from the atmosphere, and no inherent undesirable effects apparent in the components to disturb good and accurate bridge balance.

Ice condenser and guard circuit

Area measurements are significant if they can be properly correlated with frictional force measurements. For this reason the measurements were taken under the same conditions that frictional force measurements were taken. To this end, one desires to make measurements on the same ice that is used for frictional force measurements. Furthermore, we want the contact between ice and slider during area measurements to duplicate force measurement conditions. This is accomplished by having the ice and slider ground and honed by the same methods used in force

measurements. Loading conditions are duplicated by the same apparatus assembly.

To satisfy these conditions the condenser (Figure E. 1) has been constructed. Schematically it may be represented as in Figure E. 2. G is the guard ring encircling the slider S that maintains parallel electric lines of force from S to the Plate P. The capacitance C_x and the resistance R_x are what is measured. To guarantee that this is what our bridge does determine, the guard circuit arms identified by the resistances R_5 and R_7 are added to the bridge. Its function is to maintain the slider and guard ring at the same potential though electrically disconnected. When this is done, the capacitance C_p is eliminated as a factor in the bridge balance and the capacitance C_x is placed across the bridge arm CD. The capacitance C_g is thrown across theguard circuit arm. This insures that the difference in the reading of the variable condenser C_3 and the variable resistance R_4 are due only to capacitances and conductances between the slider S and the plate P.

In operation the plate P is placed in the ice tray, water is allowed to freeze over it, and the resulting ice is honed. The slider and guard ring unit is then laid on top of the ice. The slider is loaded as desired and measurements taken.

Balance, detection, and accuracy

For simplicity let us diagramatically represent the bridge and guard circuits as in Figure E. 3. All components except those mentioned above associated with the ice condenser are here lumped together.

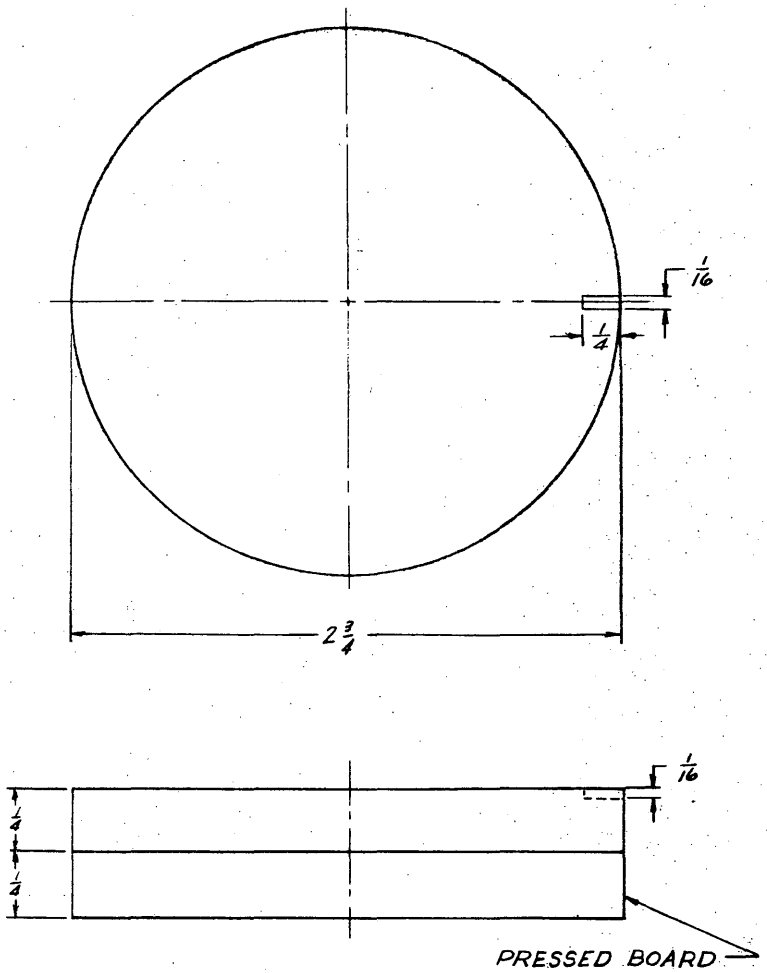

PLATE

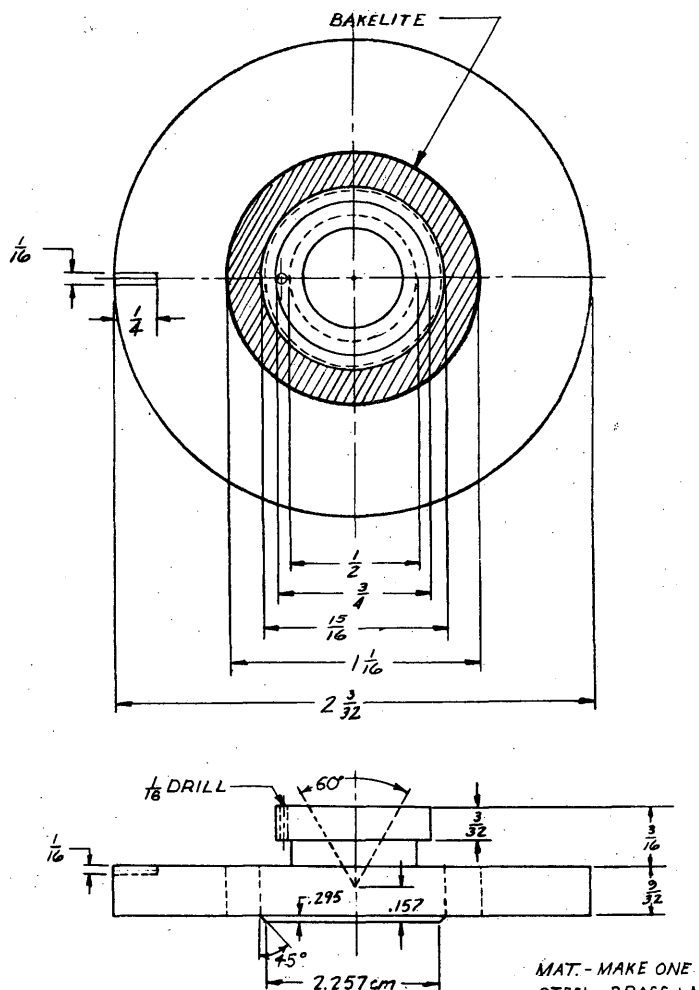

MAT. - MAKE ONE EACH OF STEEL, BRASS & MAGNESIUM

SLIDER AND GUARD RING

FIG. E.1

E-5

ICE CONDENSER SLIDER, GUARD RING & PLATE		
NO SCALE	DN. BY J.L.S.	BE105
MAT. AS NOTED	3-26-53	

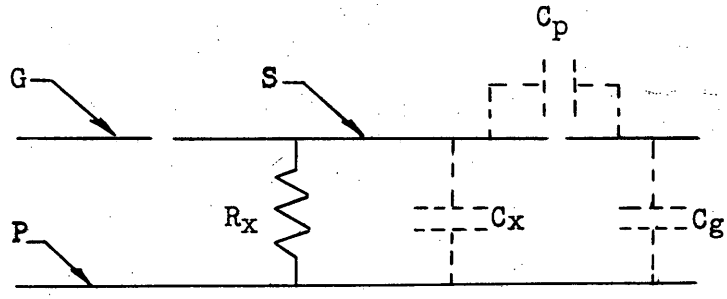

Figure E.2

SCHEMATIC OF ICE CONDENSER

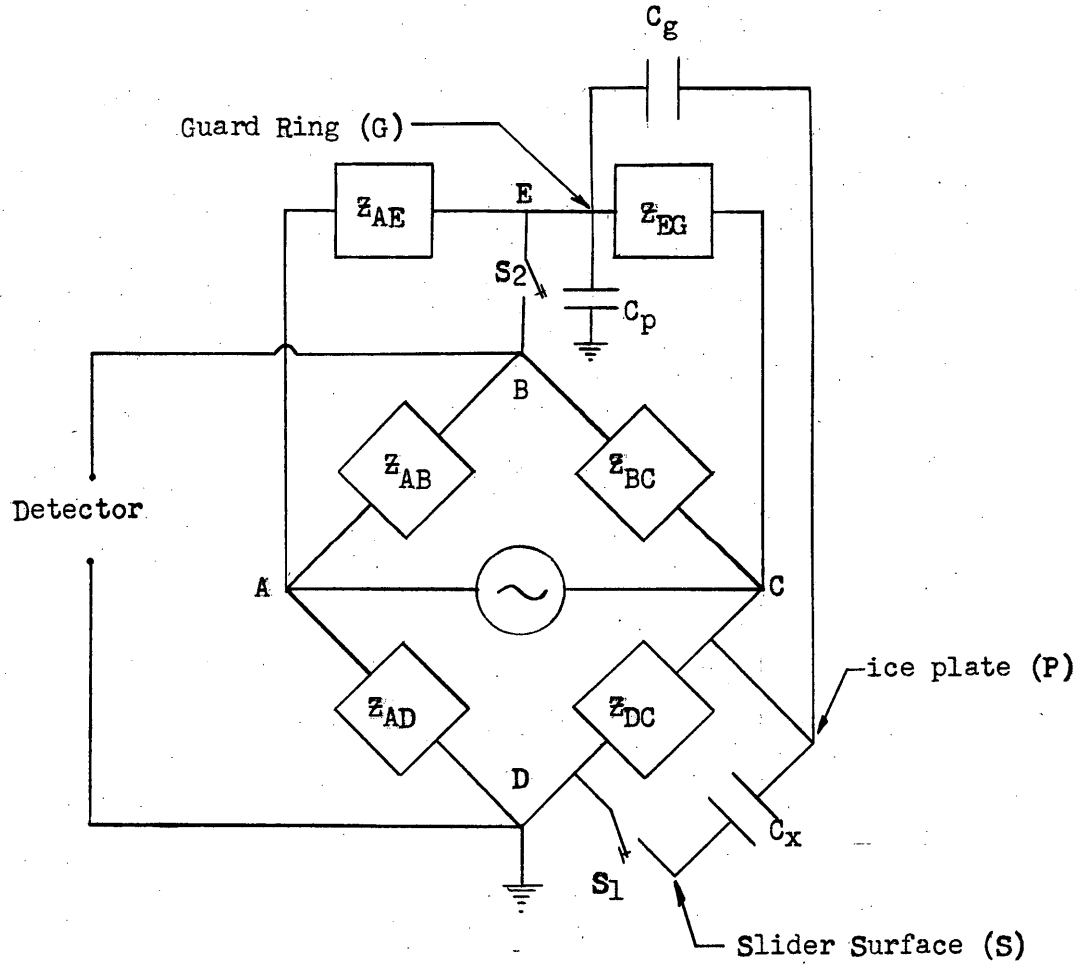

FIGURE E.3

DIAGRAMATIC REPRESENTATION OF BRIDGE AND GUARD CIRCUITS

It was previously mentioned that it was necessary to bring the guard ring G and slider surface S to the same potential to eliminate C_p from figuring in the balance. To this end at balance, it is required that points E, B, and D are brought to the same potential.

The steps in the securing of bridge balance:

1. With switch S_1 and S_2 open, adjust R_4 and C_3 in Z_{DC} until balance is obtained.
2. Close switch S_2 and adjust R_7 and C_7 until guard circuit balance is obtained.
3. Repeat steps 1 and 2 as many times as is necessary to obtain bridge and guard circuits in simultaneous balance.
4. Close switch S_1 and repeat the above procedure.

The determination of the balance point of the bridge circuits utilizes a principle outlined by Lamson[2]. The method permits the determination of whether the resistance or capacitance is out of balance, and allows one to balance either component independent of the other.

The bridge output is placed on the vertical plates of a Dumont 208-B oscilloscope. The sinusoidal sweeping voltage of the bridge input oscillator O_r is applied through a transformer T_2 to the horizontal plates. When the bridge is unbalanced, the pattern becomes an ellipse whose major axis tilts from the horizontal. Normally the adjustment of either bridge control alters both the tilt of the ellipse and the size

2 Lamson, H. W. (1939) A New Null Detector for AC Impedance Bridges, Radio Exp., XIII (II).

of its minor axis.

Selectivity in the balancing is accomplished by varying the phase relation between the bridge output and the oscillator input to the horizontal plates. When the proper phase adjustment is obtained, variation in capacitance will vary only the tilt of the ellipse and the resistive component will control only the width of the semi-minor axis. Changing the phase of the sweeping voltage by 90° will reverse the effect of the two controls.

In this manner the direction of off balance is obtained by noting the character of the ellipse, and furthermore, calibration for how much off balance can be secured. Sudden changes in the capacitive or resistive component of the test ice condenser can be immediately observed and the change recorded.

Figure E. 4 is a diagram of the phase shifting network in use, and Figure E. 5 of the voltage diagram appropriate to this circuit.

If R_8 is much greater than $\frac{1}{\omega C_8}$, C_{AC} is about 180° out of phase with C_{BD}. If $\frac{1}{\omega C_8}$ is much greater than R_8, the phase change is negligible.

For comparable values of R_8 and $\frac{1}{\omega C_8}$, the phase change φ equals 2θ where θ is given by the expression: $\tan \theta = \omega C_8 R_8$. Since R_8 has a maximum vlaue of one megohm, the phase change can be altered from 0° - 120° at a frequency of 1000 cps.

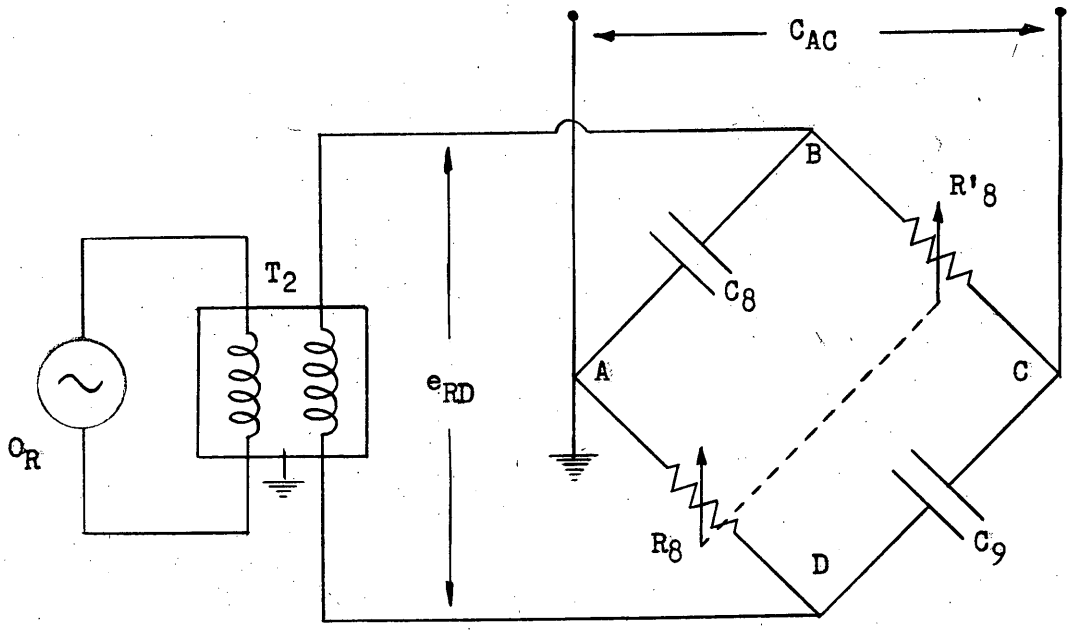

$R_8 = R'_8 = 1$ meg. pot.

$C_8 = C_9 = 1500\ \mu\mu f.$

FIGURE E.4

PHASE SHIFTING NETWORK

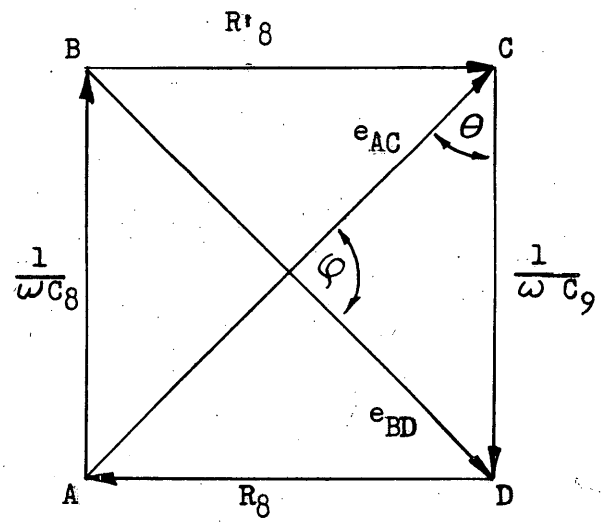

FIGURE E.5

VOLTAGE DIAGRAM FOR PHASE SHIFTING NETWORK

Test experiments on the bridge indicate that capacitance changes of .5 $\mu\mu$f. and conductance changes of 10^{-11} $(\text{ohms})^{-1}$ can be measured by the bridge.

Determination of contact area from impedance measurements

On the assumption that a slider placed on an ice surface is supported only by a finite number of asperities, contact area can be determined from surface resistance measurements. As free ion current flows from ice to slider and back, it must be constricted as it passes through the asperities making direct contact between slider and ice. This constriction introduces a spreading resistance which depends on the electrical conductivity of the slider, the ice and the area of the asperities.

For a given asperity of area, small compared to the size of the electrode, this spreading resistence is given by

$$R_s = \frac{1}{4a\lambda_s} + \frac{1}{4a\lambda_i} \qquad \text{(E-8)}$$

where a is the radius of the asperity and λ_s, λ_i the electrical conductivity of slider and ice respectively. For a metallic slider $\lambda_i \gg \lambda_s$, so that we may write

$$R_s = \frac{1}{4a\lambda_i} \qquad \text{(E-9)}$$

If we assume the slider surface is supported on n equal bridges of radius a, the total contact electrical conductance Λ due to n parallel spreading resistances is

$$\Lambda = 4an\lambda_i \qquad \text{(E-10)}$$

The total contact area $A = n\pi a^2$, may then be expressed in terms of the measured electrical conductance;

$$A = \frac{\pi \Lambda^2}{16\, n \lambda_i^2} \qquad \text{(E-11)}$$

Equation (7-9) is limited in application because of uncertainties in the true conductivity of ice λ_i and in the number of asperities n, other than there are at least three supports on which the slider rests.

The electrical conductance Λ is obtained from the difference in the effective resistance of the ice condenser when the two capacitor plates are frozen to the ice and when only one plate is frozen to the ice while the other is resting on the ice surface. λ_i, the true conductivity of the ice can be determined from resistance measurements at low frequency when the two plates are frozen to the ice, and from the results of other investigators.

This method may be correlated to frictional force measurements to yield information about the number of asperities in contact. If we assume that the frictional force F is related to the shear stress, then

$$F = s\, A \qquad \text{(E-12)}$$

where A is the real contact area, and s, the shear stress.

From equations (E-11) and (E-12), we may write

$$n = \frac{s \pi \Lambda^2}{16 \lambda_i^2 F} \qquad \text{(E-13)}$$

BIBLIOGRAPHY

1. Adam, N. K. (1938), Physics and Chemistry of Surfaces, London: Oxford University Press.

2. Allan, R. K. (1946), Rolling Bearings, Pitman and Sons, Ltd., London.

3. Amontons, G. (1699), "De la Resistance Causee Dans les Machines," Academie de Sciences, Paris, Historie de l'Academie royale des sciences avec les memoires de mathematique et physique, pp. 257-82.

4. Anonymous, (1953), "Frictional Properties of Polytetrafluoroethylene," Scientific Lubrication, Vol. 5, pp. 17-18.

5. Anonymous, (1951), "Friction as a Function of Temperature," Engineer, Vol. 192, pp. 118-119.

6. Archard, J. F. (1953), "Contact and Rubbing of Flat Surfaces," J. of Appl. Phys., Vol. 24, No. 8, pp. 981-88.

7. Armi, E. L., J. L. Johnson, R. C. Mackler, and N. E. Polster. (1947), "Application of the sliding thermocouple method to the determination of temperature at the interface of a moving bullet and a gun barrel," J. Appl. Phys., Vol. 18, pp. 88-94.

8. Armour Research Foundation of Ill. Inst. Tech. (1951), "Investigation of Sliding Friction," Chicago, Ill. 32 pp. 14 supp. plates.

9. Arnold-Alabieff, V. L. (1936), "The External Friction of Ice," Transactions of the Meetings of the International Commissions of Snow and of Glaciers, Association Internationale D'Hydrologic Scientifique Bulletin No. 23, pp. 537-61.

10. Baker, H. D., Claypoole, W., and D. D. Fuller. (1952), "Further Developments in the Measurement of the Coefficient of Friction," Proceedings of the First U. S. National Congress of Applied Mechanics, Ann Arbor, Michigan: Edward Brothers, Inc., pp. 23-29.

11. Barnes, H. T. (1928), Ice Engineering, Montreal: Renour Publishing Company, 364 pp.

12. Barwell, F. T. (1950), "Some Aspects of Research on Friction and Wear," Institution of Shipbuilders in Scotland, Vol 95, Part 2, pp. 64-100.

13. Beare, W. G., and F. P. Bowden. (June 6, 1935), "Physical Properties of Surfaces, Part I: Kinetic Friction," Philosophical Transactions of the Royal Society of London, Vol. A 234 pp. 329-54

14. Beeck, O. et al. (1951), "The Fundamental Aspects of Lubrication," Annals of the New York Academy of Sciences, Vol. 53, Art. 4, pp. 753-994.

15. Beeck, O. (1941), "The Physical Aspects of Boundary Lubrication," J. Appl. Phys. Vol. 12, pp. 512-518.

16. Beeck, O., J. W. Givens and A. E. Smith. (1940), "On the Mechanism of Boundary Lubrication," Proc. Roy. Soc. Vol. A 177, pp. 90-102.

17. Beilby, G. (1921), Aggregation and Flow of Solids, London: Macmillan Company, p. 197.

18. Bell, A. E. (1948), "Theory of Skating," Nature, Vol. 161, pp. 391-402.

19. Belser, R. B. (1954), "Frictional Adhesion of Metal to Glass, Quartz, and Ceramis Surfaces," The Rec. of Scientific Instruments, Vol. 25, No. 9, pp. 862-864.

20. Berer, J. H., and R. Schnurmann. (1948), "Rate of Wear in the Region of Validity of Amontons' Law," Nature, Vol. 161, p. 728.

21. Bernal, J. D. and R. H. Fowler. (1933), "The structure of ice -- a theoretical discussion of the dielectric constants of ice and water; a theory of water and ionic solution, with particular reference to hydrogen and hydroxyl ions," J. of Chem. Phys. Vol. 1, pp. 522-26.

22. Bezer, H. J. and R. Schnurmann. (May 8, 1948), "Rate of Wear in the Region of the Validity of Amontons' Law," Nature, 161:728.

23. Bikerman, J. J. (1949), "Effect of Surface Roughness on Rolling Friction," J. of Appl. Phys. Vol. 20, No. 10, pp. 971-75.

24. Bikerman, J. J. (1948), "Mechanism of Friction and Lubrication," Lub. Eng., Vol. 4, No. 5, pp. 208-14.

25. Bikerman, J. J. (1944), "Surface Roughness and Sliding Friction," Rev. Mod. Phys., Vol. 16, No. 2, pp. 53-68.

26. Bikerman, J. J. (1941), "Friction and Adhesion," Phil. Mag. Vol. 32, pp. 67-76.

27. Bikerman, J. J. (1939), "On the Formation and Structure of Multilayers," Proc. Roy. Soc. Vol. A. 170, pp. 130-144.

28. Bikerman, J. J., and E. K. Rideal. (1939), "A Note on the Nature of Sliding Friction," Phil. Mag., Series 7, Vol. 27, p. 687.

29. Bisson, E. E. (1953), "The Influence of Solid Surface Films on the Friction and Surface Damage of Steel at High Sliding Velocities," Lubrication Engineering, Vol. 9, No. 2, pp. 75-77, 100-101.

30. Bisson, E. E., and R. L. Johnson. (1950), "NACA Friction Studies of Lubrication at High Sliding Velocities," Lub. Eng., Vol. 6, No. 1, pp. 16-20.

31. Bjerrum, Niels. (1952), "Structure and Properties of Ice," Science, Vol. 115, pp. 385-90.

32. Blodgett, K. B., and I. Longmuir. (1939), "Built-up Films of Barium Stearate and Their Optical Properties," Phys. Rev. Vol. 51, pp. 964-982.

33. Blok, H. (1940), "Fundamental Mechanical Aspects of Boundary Lubrication," J. Soc. Aut. Eng., Vol. 46, pp. 54-68.

34. Blok, H. (1937), "Theoretical Study of Temperature Rise at Surfaces of Actual Contact under Oiliness Lubricating Conditions," Gen. Discussion of Lubrication and Lubricants, Inst. of Mech. Engs. Vol. 12, pp. 222-235.

35. Born, M. (1939), "Thermodynamics of Crystals and Melting," J. Chem. Phys. Vol. 7, p. 591.

35. Bowden, F. P. (1954), "Friction of Non-Metallic Solids," J. Inst. Petroleum, Vol. 40, No. 364, pp. 89-101.

36. Bowden, F. P. et al. (1952), "A Discussion on Friction," Proc. Roy. Soc. Vol. A 212, pp. 439-520.

37. Bowden, F. P. (1950), "Friction," (Royal Institution Address), Nature, Vol. 166, pp. 330-34.

38. Bowden, F. P. (1950), "Frictional Properties of Porous Metals Impregnated with Plastic," Research Vol. 3, pp. 147-48.

39. Bowden, F. P. (1950), "Frictional Properties of Porous Metals Containing Molybdenum Disulphide," Research, Vol 3, pp. 383-4

40. Bowden, F. P. (1948), "Importance of Chemical Attack in Lubrication of Metals," J. of Inst. of Petroleum, Vol. 34, No. 297, pp. 654-58.

41. Bowden, F. P. (1945), "The Influence of Surface Films on the Friction, Adhesion, and Surface Damage of Solids," Nature, Vol. 156, pp. 97-101.

42. Bowden, F. P., J. N. Gregory, and D. Tabor. (1945), "Lubrication of Metal Surfaces by Fatty Acids," Nature, Vol. 156, pp. 97-101.

43. Bowden, F. P. (1944), "The Physics of Rubbing Surfaces," J. and Proc. of the Roy. Soc. of New South Wales, Vol. 78, pp. 187-219.

44. Bowden, F. P. and L. Leben. (1940), "The Friction of Lubricated Metals," Phil Trans. Vol. A 239, pp. 1-27.

45. Bowden, F. P. and L. Leben. (1939), "The Nature of Sliding and the Analysis of Friction," Proc. Roy. Soc. Vol. 169, pp. 371-91.

46. Bowden, F. P. and L. Leben. (1938), "The Nature of Sliding and the Analysis of Friction," Nature, 141:691.

47. Bowden, F. P. and L. Leben. (1937), "General Discussion on Lubrication and Lubricants," Institution of Mechanical Engineers, Group IV: Properties and Testing, p. 40.

48. Bowden, F. P., L. Leben, and D. Tabor. (1939), "The Sliding of Metals, Frictional Fluctuations, and Vibration of Moving Parts," The Engineer, Vol. 168, pp. 214-17.

49. Bowden, F. P., and T. P. Hughes. (1939), "The Mechanism of Sliding on Ice and Snow," Proc. Roy. Soc. Vol. A 172, pp. 280-98.

50. Bowden, F. P. and T. P. Hughes. (1939), "The Friction of Clean Metals and the Influence of Adsorbed Gases," Proc. Roy. Soc. Vol. 172, pp. 263-79.

51. Bowden, F. P. and T. P. Hughes. (1938), "Friction of Clean Metals and the Influence of Surface Films," Nature, Vol 142, pp. 1039-40.

52. Bowden, F. P. and T. P. Hughes. (1937), "Physical Properties of Surfaces, Part IV: Polishing, Surface Flow, and Formation of Beilby Layer," Proc. Roy. Soc. Vol. A 160, pp. 575-87.

53. Bowden, F. P., A. J. W. Moore, and D. Tabor. (1943), "The Ploughing and Adhesion of Sliding Metals," J. Appl. Phys. Vol. 14, pp. 80-91.

54. Bowden, F. P. and E. K. Rideal. (1928), "On the Electrolytic Behavior of Thin Films, The Area of Catalytically Active Surfaces," Proc. Roy Soc. Vol. A 120, p. 80.

55. Bowden, F. P. and K. E. W. Ridler. (1936), "The Surface Temperature of Sliding Metals, The Temperature of Lubricated Surfaces," Proc. Roy. Soc. Vol. A 154, pp. 640-56.

56. Bowden, F. P. and M. A. Stone. (1946), "Visible Hot Spots on Sliding Surfaces." Experientia, Vol. 2, pp. 186-8.

57. Bowden, F. P., M. A. Stone, and G. K. Tudor. (1946), "Hot Spots on Rubbing Surfaces and the Detonation of Explosives by Friction," Proc. Roy. Soc. Vol. A 188, pp. 329-349.

58. Bowden, F. P. and D. Tabor. (1950), The Friction and Lubrication of Solids, Oxford: Clarendon Press, 337 pp.

59. Bowden, F. P. and D. Tabor. (1949), "Seizure of Metals," Proc. Mech. Eng. Vol. 160, No. 3, pp. 380-3.

60. Bowden, F. P. and D. Tabor. (1944), "Friction and Lubrication," Annual Reports on Progress in Chemistry, Chemical Society of London. Vol. 41, pp. 5-15.

61. Bowden, F. P. and D. Tabor. (1943), "The Lubrication by Thin Metallic Films and the Action of Bearing Metals," J. Appl. Phys. Vol. 14, pp. 141-151.

62. Bowden, F. P. and D. Tabor. (1943), "The Ploughing and Adhesion of Sliding Metals," J. Appl. Phys. Vol. 14, pp. 80-91.

63. Bowden, F. P, and D. Tabor. (1942), "Mechanism of Metallic Friction," Nature, Vol. 150, pp. 197-199.

64. Bowden, F. P. and D. Tabor. (1939), "The Area of Contact Between Stationary and Between Moving Surfaces," Proc. Roy Soc. Vol. A 169, pp. 391-413.

65. Bowden, F. P. and J. E. Young. (1951), "Friction of Clean Metals and the Influence of Adsorbed Films," Proc. Roy. Soc. Vol. A 208, pp. 311-25.

66. Bowden, F. P. and J. E. Young, (1951), "Friction of Diamond Graphite and Carbon and the Influence of Surface Films," Proc. Roy. Soc. Vol. A 208, pp. 444-45.

67. Bowden, F. P. and J. E. Young. (1950), "Influence of Interfacial Potential on Friction and Surface Damage," Research Vol. 3, pp. 235-37.

68. Bowden, F. P. and J. E. Young. (1949), "Friction and Adhesion of Clean Metals," Nature, Vol. 164, p. 1089.

69. Bowers, R. C. and W. C. Clinton. (1954), "Mechanoelectronic Transducer System for Recording Friction with a Stick Slip Machine," Rev. Sci. Instruments, Vol. 25, pp. 1037-8.

70. Bowers, R. C., W. C. Clinton, and W. A. Zisman. (1953), "Effect of Halogenation on Frictional Properties of Plastics," J. Appl. Phys. Vol. 24, No. 8, pp. 1066.

71. Bowers, R. C., W. C. Clinton, and W. A. Zisman. (1953), "Frictional Behavior of Polyethylene, Polytetrafluorethylene and Halogenated Derivatives," Lub. Eng. Vol. 9, pp. 204-308, 218-219.

72. Boyd, J. and B. P. Robertson. (1945), "Friction Properties of Various Lubricants at High Pressures," Trans. ASME, Vol. 67, pp. 51-9.

73. Brewington, G. P. (1951), "Comments on Several Friction Phenomena," American J. Phys. Vol. 19, pp. 357-58.

74. Bridgman, P. W. (1944), "Flow and Fracture," Metals Tech. TD. 1782.

75. Bridgman, P. W. (1938), "Reflections on Rupture," J. Appl. Phys. Vol. 9, pp. 517-528.

102. Conant, F. S., J. C. Dum, and G. M. Cox. (1949), "Frictional Properties of Tread-type Compounds on Ice," Indus. and Eng. Chem. Vol. 41, No, 1, pp. 120-26.

103. Coulomb, C. A. (1785), "Theorie des Machines Simples, En Ayant Egard au Frottement de Leur Parties, et a la Roideur des Cordages," Academie des Sciences, Paris, Memoires de Mathematique et de Physique, Vol. 10, pp. 161-332.

104. Dacus, E. N., F. F. Coleman, and L. C. Roess. (1944), "A New Experimental Approach to the Study of Boundary Lubrication," J. Appl. Phys. Vol. 15, pp. 813-824.

105. Dalton, D. (1878), "Railway Brakes," Engineering, Vol. 26, pp. 153-54.

106. Dance, J. B. and D. J. Norris. (1948), "Structure of Abraded Surfaces," Nature, Vol. 162, p. 71.

107. Davies, J. M. (1951), "The Influence of Roughness and Oxidation on Wear of Lubricated Sliding Metal Surfaces," Annals of the New York Academy of Sciences, Vol. 53, Art. 4, pp. 919ff.

108. Deeley, R. M. (1908), "The Viscosity of Ice," Proc. Roy. Soc. Vol. A 81, pp. 250-59.

109. de Fleury, R. (1953), "Etude de l'usure comparee des materiaux soumie au frottement," Revue d l'A luminium, Vol. 30, No. 203, pp. 341-5.

110. Den Hartog, J. P. (1947), Mechanical Vibrations, New York: McGraw-Hill Book Company, 473 pp. (Self-excited Vibrations, pp. 346-405; Relaxation Oscillations, pp. 439-48).

111. Denny, D. F. (1953), "The Influence of Load and Surface Roughness on the Friction of Rubber-Like Materials," Proc. Phys. Soc. B. Vol. 66, pp. 721-727.

112. Derjaguin, B. (1934), "External Friction," Zeitschrift fur Physik, Vol. 88, pp. 661-75.

113. Desch, C. H. (1945), "The Part of Chemical Reactions in the Phenomena of Friction and Wear," Comm. Tech. Etats et Proprietes Surface Metaux, pp. 235-6.

114. Dokos, S. J. (1946), "Sliding Friction Under Extreme Pressures," Trans. Am. Soc. of Mech. Engrs. Vol. 68, pp. A 148- A 156.

115. Dorsey, N. E. (1940), "Sliding Friction of Ice," Properties of Ordinary Water Substance in all its Phases, New York: New York: Reinhold Publ. Corp., p. 428.

116. Dreyer, C. W. (1950), "Comparative Ski Tests for Liaison Type Aircraft," Headquarters Air Material Command, Memo Report.

117. Dudley, B. R. and H. W. Swift. (1949), "Frictional Relaxation Oscillations," Phil. Mag. Vol. 40, No. 307, pp. 849-61.

118. Erikson, R. (1949), "Friction of a Runner on Snow and Ice," SDA Reports, No. 34-35.

119. Ernst, H. and E. M. Merchant. (1940), "Surface Friction of Clean Metals -- A Basic Factor in the Metal Cuting Process," Proc. of the M.I.T. Special Summer Conferances on Friction and Surface Finish.

120. Euler, L. (1750), "Sur le Frottement des Corpe Solides," Histoire de l'Academie Royale des Sciences et Belles Lettres, (Berlin, 1748), pp. 122-32.

121. Ewald, P.P., T. Posch, and L. Prandtl. (1930), The Physics of Solids and Fluids, London: Blachie and Sons, Chapter II.

122. Fabian, O. (1877), "Uber Dehnbarkeit und Elastizitat des Eises," Carl's Report d Phys. Vol. 13, pp. 447-452.

123. Faraday, M. (1933), Faraday's Diary, Vol. IV, London: G. Bell and Sons, Ltd.

124. Faraday, M. (1860), "Note on Regelation," Proc. Roy. Soc. London: Vol. 10, pp. 440-450.

125. Feng, I-Ming, (1952), "Metal Transfer and Wear," J. Appl. Phys. Vol. 23, p. 1011.

126. Finch, G. L. (1951), "The Boundary Layer," Brit. J. of Appl. Phys. Supplement No. 1. (Physics of Lubrication), pp. 34-5.

127. Finch, G. I. (1950), "Sliding Surface," Phys. Soc. Proc. Vol. 63B, pp. 465-83. See also Vol. 63A, pp. 785-803.

128. Finnie, I. and M. C. Shaw. (1954), "The Friction Process in Metal Cutting," ASME Paper, No. 54--A--108. Presented before ASME Annual Meeting, New York, Nov. 1954.

129. Fisher, J. C. and J. H. Hollomon, (1947), "A Statistical Theory of Fracture," Trans. AIME, Vol. 171, p. 546.

130. Föppl, L. (1936), "Beanspruchen von Schiene und Rad beim Anfahren und Bremsen," Forschung auf dem Gebeite des Ingenieurueesens, Vol. 7, No. 3, pp. 141-147.

131. Forbes, J. D. (1858), "On Some Properties of Ice Near its Melting Point," Proc. Roy. Soc. (Edinburgh)

132. Forbes, J. D. (1846), "On the Conversion of Néve into Ice," Thirteenth Letter on Glaciers, section 2.

133. Gemant, Andrew. (1950), "External Friction of Solids," Frictional Phenomena, Brooklyn: Chemical Publishing Company, Chapter XX, pp. 411-31.

134. Geniesse, J. C. (1951), "Bearings, Lubricants, and Lubrication, A Digest of 1950 Literature," Mech. Engr. Vol. 72, No. 9, pp. 892-896.

135. Geniesse, J. C., and H. A. Hartung. (1954), "Bearings, Lubricants, and Lubrication, A Digest of 1953 Literature," Mech. Engr. Vol. 76, No. 9, pp. 739-747.

136. Geniesse, J. C., and H. A. Hartung. (1953), "Bearings, Lubricants, and Lubrication, A Digest of 1952 Literature," Mech. Engr. Vol. 75, No. 10, pp. 801-808.

137. Geniesse, J. C., and H. A. Hartung. (1952), "Bearings, Lubricants, and Lubrication, A Digest of 1951 Literature, Mech Engr. Vol. 74, No. 11, pp. 885-892.

138. Cheorghiu, V. G. (1948), "New Methods of Measuring Friction," Engineers' Digest, (British ed.), Vol. 9, No. 11, pp. 367-68.

139. Gliddon, C. (1922), "Investigation into the Effect of Weather Conditions on the Friction of Sleigh Runners on Snow," Canadian Air Force Report.

140. Godfrey, D. and E. E. Bisson. (1952), "NACA Studies of Mechanism of Fretting (Fretting Corrosion) and Principles of Mitigation," Lub. Engr. Vol. 8, pp. 241-243, 262-263.

141. Godfrey, D. and E. C. Nelson. (1952), "Oxidation characteristics of molybdenum disulfide and effect of such oxidation on its role as a solid film lubricant." NACA TN 1882

142. Good, J. N. and D. Godfrey. (1947), "Changes found on run-in and scuffed surfaces of steel chrome plate and cast iron," NACA TN 1432.

143. Goodzeit, Carl L., A. E. Roach, and R. P. Hunnicutt. (1954) "Frictional Characteristics and Surface Damage of Thirty-Nine Different Elemental Metals in Sliding Contact with Iron," ASME Paper, No. 54--A--53. Presented before ASME Annual Meeting, New York, Nov. 1954, 7 pages.

144. Gortler, H. (1948-49), "Reibungswiderstand Einer Schwach Gewellten, Langs Angestromten Platte," Archiv fur Mathematick Vol. 1, pp. 450-53.

145. Gough, V. E. (1953), "Simple Direct Reading Friction Meter," J. Soc. Instr. Vol. 30, pp. 345-349.

146. Gould, G. G. (1951), "Determination of Dynamic Coef. of Friction for Transient Conditions," Trans. ASME Vol. 73, p. 649.

147. Gould, G. G. (1951), "Determination of Dynamic Coef. of Friction for Transient Conditions," Machine Design Vol. 23, pp. 153-54.

148. Gregory, J. N. (1946), "Radioactive Tracers in the Study of Friction and Lubrication," Nature, Vol. 157, pp. 443-4.

149. Griffith, (1921), "The Phenomena of Rupture and Flow in Solids," Phil. Trans. Roy. Soc. (London), Vol. 221A, p. 163.

150. Grodzinski, P. (1951), "The Effect of Lubrication on Friction, Wear and Abrasion," Brit. J. Appl. Phys. Supplement No. 1, (Physics of Lubrication) pp. 86-90.

151. Grotsch, C. and E. Plake. (1938), "Determination of the Coefficient of Friction of Steel on Steel at High Velocities," Jahrb. deut. Luft fahrtforsch. Abt. II, pp. 345-49.

152. Gwathmey, A. T. and H. J. Leidheiser and G. P. Smith, (1948), "Influence of Crystal Plane and Surrounding Atmosphere on Some Types of Friction and Wear Between Metals," NACA Tech. Note No. 1461. p. 37.

153. Haiken, S., L. Lissovsky, and A. Solomonovich. (1940), J. Phys. (USSR) Vol. 2, pp. 253.

154. Haiken, S., L. Lissovsky, and A. Solomonovitch, (1939) "Studied Elastic Conditions in Surface Friction," J. Phys. (USSR) Vol. 1, p. 455.

155. Hardy, W. B. (1936), Collected Works. London, Cambridge University Press.

156. Hardy, W. B. (1920), "Static Friction - II," Phil. Mag. Series 6, Vol. 40, pp. 201-210.

157. Hardy, W. B. (1920), "Some Problems of Lubrication," Nature, Vol. 106, pp. 569-72.

158. Hardy, W. B. and I. Doubleday. (1922), "Boundary Lubrication- The Paraffin," Proc. Roy. Soc. (London) Vol. A100, pp. 550-574.

159. Hardy, W. B. and I. Doubleday. (1922), "Boundary Lubrication- The Temperature Coefficient," Proc. Roy. Soc. Vol. A101, pp. 487-92.

160. Hardy, W. B. and J. K. Hardy. (1919), "Note on Static Friction and on the Lubricating Properties of Certain Chemical Substances," Phil. Mag. Series 6, Vol. 38, No. 223, pp. 32-48.

161. Hargis, C. D. (1922), "The Viscosity and Rigidity of Ice," Phys. Rev. Vol. 19, pp. 526-27.

162. Harkins, W. D., G. Jura, and E. H. Loeser. (1946), "Surface of Solids XVI. Adsorbed Films of Water and Normal Heptane on the Surface of Graphite," J. of the Amer. Chem. Soc. Vol. 68, pp. 554-7.

163. Heaton, J. L., J. R. Bristow, G. Wittingham, and T. P. Hughes. (1942), "Frictional Properties of Bearing Metals," Nature, Vol. 150, p. 520.

164. Henniker, J. C. (1949), "The Depth of the Surface of a Liquid," Rev. Mod. Phys. Vol. 21, pp. 322-341.

165. Herrenden Harker, G. F. (1940), "Relaxation Oscillations," Amer. J. Phys. Vol. 8, pp. 1-22.

166. Hertz, H. (1882), "Uber die Beruhang fester elasticher Korper," J. fur die reine und angewandtl Mathematik," Vol. 92, pp. 156-71.

167. Hirst, W. and J. K. Lancaster, (1954), "Influence of Oxide and Lubricant Films on Friction and Surface Damage of metals," Proc. Roy Soc. Vol. 223, No. 1154, pp. 324-338.

168. Holloman, H. H. and C. Zener, (1949), "Conditions of Fracture of Steel," Metals Tech. TP 1782.

169. Holm, R. (1948), "Calcuation of the Temperature Development in a Contact Heated in the Contact Surface, and Application to the Problem of the Temperature Rise in a Sliding Contact," J. Appl. Phys. Vol. 19, pp. 361-66.

170. Holm, R. (1946), Electric Contacts, Stockholm: Hugo Gerbers Forlag, 398 pp.

171. Holm, R. (1944), "Frictional Force with Respect to Actual Contact Surface," National Advisory Committee for Aeronautics," Technical Memo No. 1074, 8pp.

172. Holm, R. (1941), Die technische Physik der elektrischen Kontakte, Berlin: Julius Springer.

173. Holm, R. (1941), "Beitrag zur Kenntnis der Reibung," Wiss. Veroff. Siemens-Werk. p. 68.

174. Holm, R. (1938), "Uber die auf die wirkliche Beruhrungsflache bezogene Reibungskraft," Wiss. Veroff. Siemens-Werk, Vol. 17, No. 4.

175. Holm, R., Guldenpfenning, F., E. Holm, and R. Stormer, (1931), "Metallic Contacts," Wissenschaftliche Veroffentlichungen aus dem Siemens-Konzern. Vol. 10, pp. 20-64.

176. Holm, R. and B. Kirschstein. (1936), "Uber das Haften zweier Metallflachen aneinander im Vakuum und die Herabsetzung des Haftens durch gewisse Gase." Wiss Veroff. Siemens-Werk, p. 122.

177. Hopkins, W. (1845), "On the Motion of Glaciers," Phil. Mag. Series 6, Vol. 47, pp. 303-6.

178. Hoppler, F. (1941), "Die Plastizitat des Eises," Kolloid Zeitschrift, Vol. 97, pp. 154-60.

179. Howell, H. G. (1953), "Laws of Static Friction," Textile Res. J. Vol 23, pp. 589-91.

180. Hughes, T. P. and G. Whittingham, (1942), "The Influence of Surface Films on the Dry and Lubricated Sliding of Metals, Trans. Faraday Soc. Vol. 38, pp. 9-27.

181. Hultberg, S. O. (1948), Foreningen for Skidiopningens Framjande i Sverige, pp. 153-163.

182. Hummel, O. H. (1949), "Uber den Verschleiss bei Gleitender Reibung," Zeit.fur Mettallkunde, Vol. 40, No. 10, pp. 356-71.

183. Hunter, M. C. (1944) "Static and Clinging Friction of Pivot Bearings," Engineering, Vol. 157, No's 4074 and 4075. pp. 117-20, 138-40.

184. Institute of Physics, (1951), "Physics of Lubrication," London: Brit. Jour of Appl. Phys. Supplement No. 1.

185. Jacob, C. (1912), "Friction," Annalen der Physik, Vol. 38, No. 1, pp. 126-48.

186. Jenkin, C. F. and W. N. Thomas. (1924), "Damped Vibrations," Phil. Mag. Series 6, Vol. 47, pp. 303-6.

187. Jentzsch, H. (1950), "Uber den Einfluss von Metallen auf d. Reibungswert von Schmiermitteln," Erdol und Kohle, Vol. 3, pp. 124ff.

188. Johnson, R. L., D. Godfrey and E. E. Bisson, (1950), "Friction of surface films formed by decomposition of common lubricants of several types," NACA TN 2076.

189. Johnson, R. L., D. Godfrey and E. E. Bisson, (1948), "Friction of Solid Films on Steel at High Sliding Velocities," NACA Tech. Note No. 1578, 65 pp.

190. Johnson, R. L., M. D. Peterson and M. A. Seikert, (1951), "Friction at High Sliding Velocities of Oxide Films on Steel Surfaces Boundary Lubricated With Stearic Acid Solutions," NACA Tech. Note No. 2366.

191. Johnson, R. L., M. A. Swikert and E. E. Bisson, (1951), "Preliminary investigation of wear and friction properties under sliding conditions of materials suitable for cages of rolling-contact bearing," NACA TN, No. 2384.

192. Johnson, R. L., M. A. Swikert, and E. E. Bisson, (1947), "Friction at High Sliding Velocities," National Advisory Comm. for Aero -- Tech. Note No. 1442, 35 pp.

193. Joly, J. (1886), "The Phenomena of Skating and Professor J. Thomson's Thermodynamic Relation," Scientific Proc. Roy. Dublin Soc. (N. S.) Vol. 5, pp. 453-454.

194. Kaidanovskii, N. L. (1949), "The Nature of the Mechanical Autovibrations Produced in Dry Friction," Zhurnal Tekhnicheskai Fisiki, Vol. 19, pp. 985-96.

195. Kaidanovskii, N. L. and S. E. Haykin. (1933), "Mechanical Relaxation Oscillations," Zhurnal Tech. Phys. USSR, Vol. 3, No. 1, pp. 91-109.

196. Kamm, W. I. E. (1947), "Vehicles in Snow and Bog," Air Material Command Tech. Rep. F-Tr-2132-ND

197. Kimball, A. L. (1929), "Vibration Damping, Including the Case of Solid Friction," Trans. Soc. Mech. Engrs. Vol. 51, Part I, p. APM227.

198. King, R. F. and D. Tabor. (1953), "The Effect of Temperature on the Mechanical Properties and the Friction of Plastics," Proc. Phys. Soc. Vol. 66, No. 405B, pp. 728-736.

199. Klein, G. J. (1950), "Aircraft Ski Research Canada," Nat'l Res. Council of Canada Rep. No. MM-225.

200. Klein, G. J. (1947), "The Snow Characteristics of Aircraft Skiis," Nat'l Res. Council of Canada, Division of Mechanical Engineering, Aeronautical Report Ar-2, Ottawa, 19 pp.

201. Klein, G. J. (1938), "The Snow Performance of Aircraft Skiis," Nat'l Res. Council of Canada, NRC. No. 722, Ottawa, (mimeographed). 20 pp.

202. Klemencic, A. (1940), Forschung Ingwes, Vol. 11, p. 108. (from Morgan et al. J. Appl. Phys. Vol. 12, p. 745.)

203. Kobeko, P.P., Shishkin, N. E., F. I. Marvey, and N. S. Ivanova, (1945), "Deformation of an Ice Cover Under Moving Loads," Physics, Technical Institute, Academy of Sciences, USSR. Lenigrad. (In Russia.)

204. Kraft, J. M. (1945), "Effect of Surface Friction of High Speed Penetration," Paper presented at meeting of American Physical Society, Minneapolis, Minnesota. (Naval Research Laboratory).

205. Kragelskii, I. V., and E. M. Shevetsova. (1950), "Types of Process of Deterioration in Friction Conditions," Doklady Akademii Nauk, USSR, Vol. 75, No. 5, pp. 681-3.

206. Landsberg, K. E. (1869), "Uber die Physikalischen Vorgange bei der gleitenden Reibung fester Korper," Ann. d. Physik und Chemie, Vol. 121, pp. 283-306.

207. Lane, T. B. (1951), "Scuffing Temperatures of Boundary Lubricant Films," Brit. J. of Appl. Phys. Supplement No. 1, (Physics of Lubrication), pp. 35-8.

208. Langmuir, I. (1934), "Mech. Prop. of Monomolecular Films," J. Franklin Institute, Vol. 218, No. 2, pp. 143-171.

209. Langmuir, I. (1920), "The Mechanism of the Surface Phenomenon of Flotation," Trans. Faraday Society, Vol. 15, No. 3, pp. 62-74.

210. Lavrov, U. U. (1947), "The Temperature Dependence of Ice Viscosity," J. of Tech. Phys., Vol. 17, pp. 1027-1034.

211. Lecuir-Chaumeton, and H. Bilde, (1950), "Chemical Transformations Caused by the Action of Friction During Grinding at Ambient Temperatures," Academie des Sciences--Comptes Rendus, Vol 231, pp. 477-9.

212. Levtskii, M. P. (1949), "The Temperature of Surface Friction of Solids (Theoretical Error in Bowden's Work.)" J. Tech. Phys., USSR, Vol. 19, pp. 1010-14.

213. Lewis, C. R. (1952), "Surface Finish--Its Effect on Wear," Society of Automotive Engineers, New York.

214. Lincoln, B. (1952), "Frictional and Elastic Properties of High Polymeric Materials," Brit. J. of Appl. Phys., Vol. 3, p. 1260.

215. Locks, H. B. (1950), "The Nature of Friction: The Phenomena of Wear and Boundary Lubrication," Metal Industry, pp. 303-5. and 323-4.

216. Lodge, A. S. and H. G. Howell, (1954), "Friction of Elastic Solids," Proc. Phys. Soc. Vol. 67, No. 410 B, pp. 89-97.

217. Lowey, F. J. (1948), "Powdered-metal Friction Material," Mech. Eng., Vol. 70, pp. 869-75.

218. Ludwik, P. (1924), Uber die Bedeutung der Elastizitatsgrentze, Bruchdehaung und Kerbzahigkeet, Ztsch. Metellkunde, Vol 16, pp. 207-212.

219. MacFarlane, J. S. and D. Tabor. (1950), "Relation Between Friction and Adhesion," Proc. Roy. Soc., (London), Vol. A202, p. 244.

220. Macky, Wallace A. (1928), "On Quantitative Measurements in Frictional Electricity," Proc. Roy. Soc. London, Vol. A119, p. 107.

221. Marcelin, A. (1950), "Friction of Wear in the Physics of Surfaces," J. de Physique et le Radium, Vol 12, pp. 1A-16A.

222. Marcelin, A. (1950), "L'usure en Relation avec les Regimes du Frottement," Revue Generale de Mechanique, Vol. 34, No. 14, pp. 67-75.

223. Marcelin, A. (1949), "Le Frottement Elementaire," Revue de Mettalurgie, Vol. 46, No. 1, pp. 27-35.

224. Marcelin, A. (1948), "Niveaux de Frottement," Acedemie des Sciences -- Comptes Rendus, Vol. 226, No. 20, pp. 1584-5.

225. Maslov, E. N. (1950), "Friction Coefficient in Sliding and Scratching of Metals," J. Tech. Phys., (USSR), Vol 20, pp. 888-91.

226. McAdam, D. J., Jr. (1944), "The Technical Cohesive Strength of Metals in Terms of the Principal Stresses, Metals Tech., TP1782.

227. McConica, T. H. (1951), "Aircraft Ski Performance," American Ski Company Report, WADC TR 52-19.

228. McConica, T. H. (1950), "Sliding on Ice and Snow," American Ski Company Report to Res. and Devel. Div. Office QM Gen., U. S. Army, (mimeographed).

229. McConica, T. H. (1948), "Friction on Snow," American Ski Company Report to the Research And Development Division, Office of the Quartermaster General, U. S. Army. (mimeographed).

230. McConnell, J. C. (1881), "On the Plasticity of an Ice Crystal," Proc. Roy. Soc. Vol. 49, p. 323.

231A. McConica, T. H. (1953), WADC TR 53-153.

231B. McConica, T. H. (1952), WADC TR 52-318.

232. McFarlane, J. S. and D. Tabor. (1950), "Relation Between Friction and Adhesion," Proc. Roy. Soc., Vol. A 202, pp. 244-53.

233. McFarlane, J. S. and D. Tabor. (1950), "Adhesion of Solids and Effect of Surface Films," Proc. Roy. Soc., Series A, Vol. 202, No. 1069, pp. 224-43.

234. Menter, J. W. (1951), "A Study of Boundary Lubricant Films by Electron Diffraction," Brit. J. of Appl. Phys. Supplement No. 1, (Physics of Lubrication), pp. 52-54.

235. Menter, J. W. and D. Tabor. (1951), "Orientation of Fatty Acid and Soap Film on Metal Surfaces," Proc. Roy. Soc., Vol. A 204, pp. 514-24.

236. Merchant, M. E. (1940), "The Mechanism of Static Friction," J. Appl. Phys., Vol. 11, No. 3, p. 230.

237. Mindlin, R. D. (1949), "Compliance of Elastic Bodies in Contact," J. Appl. Mech., Vol. 16, pp. 259-268.

238. Mindlin, R. D., W. P. Mason, T. F. Osmer, H. Deresiewicz. "Effects of an Oscillating Tangential Force on the Contact Surfaces of Elastic Spheres," Proc. of the First U.S. Nat'l Congress of Applied Mechanics, pp. 203-208.

239. Minnesota, University of, Engineering Experiment Station. (1951) "Review of the Properties of Snow and Ice," SIPRE Report 4, H. T. Mantis (ed.), Snow, Ice, and Permafrost Res. Est., Corps of Eng., U.S. Army.

240. Minnesota, University of, Inst. of Tech., Mech. Engg. Dept., (1953), "Progress Report II, Friction on Snow and Ice," Snow, Ice, and Permafrost Res. Est., Corps of Eng., U.S. Army. 144 pp.

241. Minnesota, University of, Inst. of Tech., Mech. Engg. Dept., (1952), "Progress Report I, Friction on Snow and Ice," Snow, Ice, and Permafrost Res. Est., Corps of Eng., U.S. Army, 186 pp.

242. Mitinsky, A. (1948), "A Fundamental Considerations Regarding Friction," Metal Progress, Vol. 53, p. 102.

243. Moore, A. C. (1951), "The Adsorption of Lubricant Films, A Study of Radioactive Tracers," Brit. J. of Appl. Phys., Supplement No. 1, (Physics of Lubrication) pp. 54-7.

244. Moore, A. J. W. (1948), "Deformation of Metals in Static and Sliding Contact," Proc. Roy. Soc. Vol. A195, p. 231.

245. Moore, A. J. W. and W. J. Tegart. (1951), "Rupture of Oxide Films During Repeated Sliding," Australian Journal Scientific Research, Series A. pp. 181-4.

246. Morgan, F., M. Muskat, and D. W. Reed. (1949), "Friction of Dry and Lubricated Surfaces," Lubrication Eng., Vol. 5, No. 2, pp. 75-82, 103.

247. Morgan, F., M. Muskat, and D. W. Reed. (1941), "Studies in Lubrication X, Friction Phenomenon and the Stick-Slip Process," J. Appl. Phys. Vol. 12, pp. 743-52.

248. Morghen, I. (1949), "Research into Boundary Lubrication," Engineers' Digest. Vol. 10, No. 7, p. 232.

249. Morphy, H. (1913), "The Influence of Pressure on the Surface Friction of Ice," Phil. Mag., Series 6, Vol. 25, pp. 133-24.

250. Moseley, H. (1871), "On the Mechanical Impossibility of the Desent of Glaciers by Their Weight Only," Phil. Mag. Series 4, Vol. 42, pp. 138-49.

251. Nagusu, Hideo. (1950), "Statistical Features in Static Friction," J. Phys. Soc. of Japan, Vol. 6, No. 2, pp. 123-24.

252. Nakaya, U., and A. Matsumoto. (1953), Evidence of the Existence of a Liquidlike Film on Ice Surfaces, Research Paper 4, Snow, Ice, and Permafrost Research Estab. Corps of Engineers, U. S. Army, Wilmette, Illinois.

253. Nakaya, U., M. Tada, Y. Sekido, and T. Takano. (1936), "The Physics of Skiing: the Preliminary and General Survey," J. of Faculty of Sciences, Hokkaide University, Series 2, Vol. 19, pp. 265-87.

254. Nansen, F. (1898), Farthest North. London, George Newnes, Vol. 1.

255. National Research Council of Canada, (1947), "Proceedings of 1947 Conference on Snow and Ice," Tech. Memo. No. 10. Assoc. Comm. on Soil and Snow Mechanics.

256. Nicol, H. (1950), "Some Interesting Points on Lubrication," Trans. of the Institute of Marine Engineers, pp. 342-50.

257. Niven, C. D. (1954), "The Effect of High Loading on the Kinetic Friction of Ice," Can. J. of Phys., Vol. 32, pp. 782-789.

258. Oechlin, Max. (1936), "Kriechschnee und Schneekohasion," Transactions of Meetings of the International Commissions of Snow and of Glaciers, Association Internationale D'Hydrologic Scientifique, Bulletin No. 23, pp. 721-22.

259. Osgood, W. R. (1939), "The Sliding of Metals," The Engineer Vol. 168, p. 426.

260. Pallin, H. N. (1945), "Resistance to Sliding in Skiing," Föreningen för Skidirpningens Framjande i Sverige.

261. Palmer, F. (1951), "Friction," Scientific American, Vol. 184, pp. 54-58.

262. Palmer, F. (1949), "What About Friction?" Amer. J. of Phys., Vol. 17, pp. 181-87, 327-42.

263. Papenhuyzen, P. J. (1938), "Wrijvingsproeven in verband met het slippen van autobanden," De Ingenieur, Vol. 53, pp. v75-v81.

264. Parent, A. (1704), "Memoire qui contient tout ce qui se fait sur les Plans Inclines," Academie des Sciences, Paris, Histoire de l'Academie royale des sciences avec les memoires de mathematique et physique, pp. 235-54.

265. Parker, R.C. (1949), "Frictional Behavior of Engineering Materials," Engineering, Vol. 167, No. 4336, 4337, pp. 193-96, March 4, pp. 217-19, March 11.

266. Parker, R. C., W. F. Farnworth and R. Milne. (1950), "Variation of Coefficient of Static Friction with Rate of Application of Tangential Force," Proc. of the Inst. of Mech. Eng. Vol. 163, (War Emergency Proc. No. 59), pp. 176-84.

267. Parker, R. C. and D. Hatch. (1950), "Static Coefficient of Friction and the Area of Contact," Phys. Soc. Proc., Vol. 63B, pp. 185-97.

268. Perutz, M. F. (1947), "Report on Problems Relating to the Flow of Glaciers," J. of Glaciology, Vol. 1, No. 2, pp. 47-51.

269. Perutz, M. F. and G. Seligman, (1939), "A Crystallographic Investigation of Glacier Structure and the Mechanism of Glacier Flow," Proc. Roy. Soc. (London), Vol. 172, pp. 335-60.

270. Peterson, J. W. (1950), "Charging by Sliding Friction in Controlled Atmospheres," (In its Final Report on Static Electrification, TIP U14411, Septber 2, 1947-August 31, 1950,) Berkely, California University.

271. Pfaff, F. (1875), "Versuche uber die Plastizitat des Eises Ann. d. Phys. Vol. 155, pp. 169-174.

272. Pfalzner, P. M. (1950), "On the Friction of Various Synthetic and Natural Rubbers on Ice," Canadian J. of Res. Vol. F 28, pp. 468-89. (N.R.C. No. 2260).

273. Pfalzner, P. M. (1947), "The Friction of Heated Sleigh Runners on Ice," Can. J. of Res. Vol. F 25, pp. 192-95, (N.R.C. No. 1510).

274. Pognting, J. H. (1881), "Change of State:Solid - Liquid," Phil. Mag. Series 5, Vol. 12, pp. 32-48.

275. Pomey, J. (1948), "Friction and Wear," NACA Tech. Memo. 1318. Translation of "Le Frottement et l'Usure" Office National d'Etude et de Recherches Aeronautiques Rapport technique No. 36. Travaux Groupment Francais pour le Development des Recherches Aeronautiques (GRA). 108 p.

276. Poncelet, E. F. (1946), "Nature of Strength and Failure in in Brittle Solids," Colloid Chemistry, Vol.6, pp. 77-88.

277. Prandtl, L. (1928), "Ein Gedankenmodell zur kinetischen Theorie der festen Korper," Z. angew. Math. und Mech. Vol. 8, pp. 85-106.

278. Rabinowicz, E. (1954), "Boundary Friction of Very Well Lubricated Surfaces," Lub. Eng. Vol. 10, No. 4, pp. 205-8.

279. Rabinowicz, E. (1951), "An Investigation of Surface Damage Using Radioactive Metals," Brit. J. Appl. Phys., (Physics of Lubrication), Supplement No. 1, pp. 82-5.

280. Rabinowicz, E. (1951), "A Study of Metal Transfer During Sliding, Using Radioactive Analysis," Phy. Soc. Proc., Vol. 64A, p. 939-40.

281. Rabinowicz, E. (1951), "The Nature of the Static and Kinetic Coefficients of Friction," J. Appl. Phys. Vol. 22, pp. 1373-79.

282. Rabinowicz, E., B. G. Rightmore, C. E. Tedholm, and R. E. Williams. (1954), ASME Paper, No. 54-lub.-2 for meeting Oct. 18-20. 7 pp.

283. Rabinowicz, E. and D. Tabor, (1951), "Metallic Transfer Between Sliding Metals: an Autoradiographic Study," Proc. Roy. Soc. Vol. A208, pp. 455-75.

284. Rankin, J. S. (1926), "The Elastic Range of Friction," Phil. Mag. Vol. 2, pp. 806-816.

285. Reynolds, O. (1901), "On the Slipperiness of Ice," Papers on Mechanical and Physical Subjects, Cambridge University Press Vol. 2, pp. 734-38.

286. Roach, A. E., C. L. Goodzeit, and R. P. Hunnicutt. (1954) "Scoring Characteristics of Thirty-Eight Different Elemental Metals on High-Speed Sliding Contact with Steel," ASME Paper No. 54--A--61. Presented before ASME annual meeting, New York, Nov. 1954, 10 pp.

287. Roth, F. L., R. L. Driscoll and W. L. Holt. (1942), "Frictional Properties of Rubber," Journal of Research of the National Bureau of Standards, Vol. 28, pp. 439-62.

288. Rowell, H. S. (1922), "Note on the Analysis of Damped Vibrations," Phil. Mag., Series 6, Vol. 44, pp. 951-53.

289. Sack, (1946), "Extension of Griffith's Theory of Rupture to Three Dimensions," Proc. Phys. Soc. (London), Vol. 58, p. 729.

290. Saibel, E. (1947), "A Thermodynamic Theory of the Fracture of Metals," Am. Inst. Mining Met. Engrs. Tech. Publ. No. 2131.

291. Saito, R. (1949), "Physics of Fallen Snow," The Geophysical Magazine (Japan) Vol. 19, (1-2) pp. 1-56.

292. Sakmann, B. W., J. T. Burwell, Jr., J. W. Irvine, Jr., (1944), "Measurements of the Adhesion Component in Friction by Means of Radioactive Indicators," J. Appl. Phys., Vol. 15, p. 459.

293. Sakman, B. W., N. Grossman, and J. W. Irvine Jr., (1947), "A Study of Metal Transfer Between Sliding Surfaces," NACA TN 1355, 14 pp.

294. Salmonovich, A. E. (1950), "Dry Friction and Electric Contact at Small Displacements," J. Exp. Theor. Phys., USSR, Vol. 20, pp. 647-60.

295. Sampson, J. B., F. Morgan, D. W. Reed, and M. Muskat. (1943), "Friction Behavior During the Slip Portion of the Stick-Slip Process," J. Appl. Phys. Vol. 14, p.696.

296. Savage, R. H. (1951), "Physically and Chemically Adsorbed Films in the Lubrication of Graphite Sliding Contacts," Annals of the New York Academy of Sciences. Vol. 53, Art. 4.

297. Savage, R. H. (1948), "Graphite Lubrication," J. Appl. Phys., Vol. 19, No. 1, pp. 1-10.

298. Schallamack, A. (1953), "Surface Condition and Electrical Impedance in Rubber Friction," Phys. Soc. Proc., Vol. 66, No. 406B, pp. 817-825.

299. Schallamack, A. (1952), "Elementary Aspects of Rubber Abrasion," Engineering, Vol. 173, p. 218.

300. Schmoltz, G. (1936), "Technische Oberflachenkunde," Blok "Bound Lub." p. 223, Berlin.

301. Schnurmann, R. (1951), "The Electrostatic Component of the Force of Friction," Brit. J. of Appl. Phys., Supplement No. 1, (Physics of Lubrication), pp. 62-8.

302. Schnurmann, R. (1942), "Amonton's Law, 'traces' of Frictional Contact, and Experiments on Adhesion," J. Appl. Phys. Vol. 13, pp. 235-45.

303. Schnurmann, R. (1941), "Experiments on the Temperature Coefficient of Static Friction," Proc. Phys. Soc., Vol. 53, pp. 538-46.

304. Schnurmann, R. (1941), "Contact Electrification of Solid Particles," Proc. Phys. Soc. London, Vol. 53, pp. 547-53.

305. Schnurmann, R. (1939), "The Sliding of Metals," The Engineer, Vol. 168, p. 278.

306. Schnurmann R., E. Warlow-Davies, (1942), "The Electrostatic Component of the Force of Sliding Friction," Proc. Phys. Soc. (London), Vol. 54, pp. 14-27.

307. Scott, J. M. (1933), The Land that God Gave Cain, London: Chatte and Windus.

308. Seligman, G. and F. Debenhan. (1943), "Friction on Snow Surfaces," Polar Record, Vol. 4, No. 25, pp. 2-11.

309. Shaw, P. E. (1930), "The Nature of Friction," Proc. Roy. Soc. Vol. A 128, pp. 628-39.

310. Shaw, P. E. (1930), "Frictional Electricity," Phil. Mag., Series 7, Vol. 9, pp. 577-583.

311. Shaw, P. E. and R. F. Hanstock. (1930), "On the Surface Strain and Relaxation for Unlike Solids, Triboelectricity and Friction," Proc. Roy. Soc. (London), Vol. A 128, pp. 480-87.

312. Shaw, P. E. and E. W. Leavey, (1930), "Friction of Dry Solids in Vacuum," Phil. Mag., Vol. 10, pp. 809-22.

313. Shchedrow, V. S. (1947), "Molecular Theory of Friction," Zhurnal Tekhnicheskei Fiziki, Vol. 17, No. 5, pp. 537-42.

314. Sherwood, R. S. (1951), "The Mechanism of Dry Friction," Iowa Eng. Exper. Sta., Report No. 6.

315. Shooter, K. V. and P. H. Thomas. (1949), "Frictional Properties of Some Plastics," Research, Vol. 2, pp. 533-35.

316. Shugarts, W. W. (1953), "Measuring Friction at High Speeds," J. Franklin Inst., Vol. 256, pp. 187-189.

317. Simon, I., H. O. McMahon and R. J. Bowen. (1951), Dry Metallic Friction as a Function of Temperature Between 4.2° K and 600° K," J. Appl. Phys., Vol. 22, No. 2, pp. 177-84.

318. Sinclair, David. (1954), "Frictional Vibrations," ASME PAPER Presented before ASME Annual Meeting, New York, Nov. 1954, 8 p. No. 54-A-46.

319. Smith-Johannsen, R. (1951), "Surfaces Having Low Adhesion to Ice," U.S. Patent No. 2, 575, 141.

320. Soderberg, N. (1932), "Investigations of Ski Friction," I.V.A.'s Flygte Kniska Kommittee Rep. No. 1. Stockholm.

321. Stanton, T. E. (1923), Friction. London: Longman's Green and Company.

322. Stevens, J. S. (1899), "Some Experiments in Molecular Contact," Phys. Rev., Vol. 8, pp. 49-53.

323. Strang, C. D. and C. R. Lewis. (1949), "On Magnitude of Mechanical Component of Solid Friction," J. Appl. Phys., Vol. 20, No. 12, pp. 1164-7.

324. Strelkov, S. P. (1933), "The Proud Pendulum," Zhurnal Tech. Phys. USSR, Vol. 3, pp. 563-73.

325 Tabor, D. (1945), "The Frictional Properties of Some White Metal Bearing Alloys; The Role of the Matrix and the Hard Particles," J. Appl. Phys., Vol. 16, pp. 325-37.

326. Tabor, D. (1941), "Desorption or 'Surface Melting' of Lubricant Films," Nature, Vol. 147, pp. 609-10.

327. Tabor, D. (1940), "Effect of Temperature on Lubricant Films," Nature, Vol. 145, p. 308.

328. Tarrant, A. G. (1954), "Measurement of Friction at Very Low Speeds," Engineer, Vol. 198, No. 5143, pp. 262-263.

329. Taylor, N. W. (1947), "Mechanism of Fracture of Glass and Similar Brittle Solids," J. Appl. Phys., Vol. 18, p. 943.

330. Tegart, W. J. M. (1949), "Friction and Wear of Metallic Surfaces," Australian Engineer, pp. 58-68.

331. Thomas, S. (1930), "Vibrations Damped by Solid Friction," Phil. Mag., Series 7, Vol 9, pp. 329-45.

332. Thomson, J. (1861), "Note on Professor Faraday's Recent Experiments on Regelation," Proc. Roy. Soc. (London), Vol. 11, pp. 198-204.

333. Thomson, J. (1859), "On Recent Theories and Experiments Regarding Ice at or Near its Melting Point," Proc. Roy. Soc. (London) Vol. 10, pp. 152-;60.

334. Thomson, J. (1857), "On the Plasticity of Ice as Manifested in Glaciers," Proc. Roy. Soc. (London), Vol. 8, pp. 455-58.

335. Thomson, J. (1849), "Theoretical Considerations on the Effect of Pressure in Lowering the Freezing Point of Water," Trans. Roy. Soc. of Edinburgh, Vol. 16, pt. 5. also in Cambridge and Dublin Math Journal Nov. 1850, Vol. 5, p. 248.

336. Thomson, W. (1858), "Remarks on the Interior Melting of Ice," Proc. Roy. Soc. (London), Vol. 9, pp. 141-143.

337. Thomson, W. (1858), "On the Stratification of Vesicular Ice by Pressure," Proc. Roy. Soc. (London), Vol. 9, pp. 209-13.

338. Thomson, W. (1850), "The Effect of Pressure in Lowering the Freezing Point of Water Experimentally Demonstrated," Proc. of the Roy. Soc. of Edinburgh, Vol. 15, also in Phil. Mag., Vol 37, pp. 123-127.

339. Thorpe, R. E. and R. G. Larsen, (1949), "Antiseizure Properties of Boundary Lubricants," Ind. and Eng. Chem. Vol. 41, p. 938.

340. Thyssen-Bornemisza, S. (1948), "Oscillatory Sliding Friction," Microtecnic, Vol. 2, No. 6, pp. 254-62, Vol. 3, No. 1, pp. 22-33.

341. Tingle, E. D. (1951), "The Importance of Surface Oxide Films in the Friction and Lubrication of Metals," Trans. Faraday Soc. Vol. 46, pp. 93-102.

342. Tingle, E. D. (1948), "Fundamental Work on Friction, Lubrication and Wear in Germany During The War Years," Inst. Petrol. J. Vol. 34, No. 298, pp. 743-74.

343. Tingle, E. D. (1947), "Influence of Water on the Lubrication of Metals," Nature, Vol. 160, p. 710.

344. Tomlinson, G. A. (1929), "A Molecular Theory of Friction," Phil. Mag., Vol. 7, pp. 905-39.

345. Tomlinson, G. A. (1927), "The Rusting of Steel Surfaces in Contact," Proc. Roy. Soc. Vol. A 115, pp. 472-83.

346. Tyndall, J. (1858), "On Some Physical Properties of Ice," Proc. Roy. Soc., Vol. 9, p. 76.

347. Umstaetter, H. (1947), "Oiliness and Boundary Phase Friction," (Am. ed.), Vol 4, No. 12, pp. 570-2. Engineers' Digest

348. Underwood, A. F. (1940), "Some General Aspects of Rubbing Surfaces," Proceedings of the Special Summer Conference on Friction and Surface Finish Massachusetts Institute of Tech. Cambridge, Mass., pp. 5-12.

349. Van der Pol, B. (1926), "Relaxation Oscillations," Phil. Mag., Series 7, Vol. 2, pp. 978-92.

350. Wakefield, W. E. (1938), "The Efficiency of Logging Sleighs for Pulp Wood Operations in Different Types of Terrain," Forest Products Laboratories of Canada

351. Weinberg, B. (1938), "Mechanical Properties of Ice," Trans. of the Internatl. Comm. of Snow and Glaciers, Internatl. Assoc. of Scientific Hydrology, Bull. No. 23, Riga, pp. 509-36.

352. Weinberg, B. (1936), "An Attempt at a Program of Theoretical and Experimental Investigations of the Properties of Snow and Ice," Trans. of the meetings of the International Commissions of Snow and of Glaciers. Association Internationale D'Hydrologic Scientifique Bulletin No. 23, pp. 537-61.

353. Weinberg, B. "The Role of Regelation in the Condensation of the Snow Cover," Transactions of the Meetings of the International Commissions of Snow and of Glaciers, Association Internationale D'Hydrologic Scientifique, Bulletin No. 23, pp. 493-508.

354. Wells, J. H. (1929), "Kinetic Boundary Friction," The Engineer, Vol. 147, pp. 454-56.

355. West, A. C. (1953), "Friction and Boundary Lubrication," Lub. Eng., Vol. 7, pp. 211-217.

356. Weyl, W. A. (1951), "Surface Structure of Water and Some of its Physical and Chemical Manifestations," J. of Colloid Science, Vol. 6, pp. 389-404.

357. Weyl, W. A. (1950), "The Role of Ionic Deformation in Surface Chemistry," Trans. of the New York Academy of Science, Series II, Vol. 12, pp. 245-57.

358. Weyl, W. A. (1948), "Friction Phenomena Involving a Glass Surface; the Surface As Affected by Heavy Metal Ions," J. Soc. Glass Tech. Vol 32, pp. 253-56.

359. Weyl, W. A., D. D. Enright and L. R. Sanders, (1949), "Surface Polarization and Wettability of Inorganic Substances by Water," J. Appl. Phys., Vol. 20, p. 1011.

360. Weyl, W. A. and E. C. Marbee. (1949), "Some Mechano-Chamical Properties of Water," Research, Vol 2, p. 19.

361. White, H. S. and D. Zie. (1951), "Static Friction Tests with Various Metal Combinations and Special Lubricants," J. of Research of the National Bureau of Standards, Vol. 46, pp. 292-298.

362. White, M. L. (1949), "Dynamical Friction," Astrophysics, pp. 159-63.

363. Whitehead, J. R. (1950), "Surface Deformation and Friction of Metals at Light Loads," Proc. Roy. Soc. Vol. 201, No. 1064, pp. 109-24.

364. Whittaker, E. J. W. (1947), "Friction and Wear," Nature, Vol. 159, p. 541.

365. Wilkinson, C. S. Jr., (1953), "Study of Factors Affecting Friction of Tread Compounds on Ice," India Rubber World, Vol. 128, No. 4, pp. 475-481.

366. Winter, G. and N. S. Grace, "The Influence of Chemical Rubbers on Winter Driving," India Rubber World, Vol. 126, No. 5, pp. 633-635.

367. Wilson, J. T., and J. M. Horeth. (1948), "Bending and Shear Tests on Lake Ice," Trans. of Amer. Geophy. Union, Vol. 29, pp. 909-12.

368. Wooster, W. A. and G. L. McDonald. (1947), "Smears of Titanium Metal," Nature, Vol 160, p. 260.

369. Zener, C. (1945), "Fracture Stress of Steel," Rev. Mod. Phys. Vol. 17, p. 20.

370. Epprecht, G.W. (1954) "Current Fluctuation Phenomena in Current Carrying Sliding Contacts," J. Appl. Phys. Vol. 25, pp. 1473-1480.

371. Inaho, Y. (1941) "Angle of Kinetic Friction of Snow," Seppyo, Vol. 3, pp. 303-307. Transl. by C.A. Meyer and Co. Inc. SIPRE Transl. 42, Jan. 1955.

372. Kuroda, M. (1942) "Resistance of Snow to a Sledge," Seppyo, Vol. 4, No. 8, pp. 229-234. Transl. by C. A. Meyer and Co., Inc. SIPRE Translation 36, Feb. 1955.